UNIVERSITY OF SOUTHAMPTON

SCHOOL OF MEDICINE

Peptoid Modification of Therapeutic Agents to Enhance Topical Drug Penetration

By

Pawan Kumar

Thesis for the degree of Doctor of Philosophy

November 2008

ABSTRACT

Topical agents have been used by doctors and dermatologists for many decades to treat a variety of skin diseases. Systemic agents are also widely used to treat skin disorders because of the limited number of topical preparations and the poor absorption of these systemic drugs through the stratum corneum, the main barrier layer of the skin. To enhance the topical delivery of drugs many techniques have been developed including physical, chemical and cell-penetrable peptides based approaches. The main limitation of physical techniques (microneedle, electroporation and iontophoresis) is that delivery of the compound is restricted to a limited surface area of the body. Chemical penetration enhancers, although widely used, are not able to deliver many molecules, particularly compounds with a molecular weight >500 dalton. Cell penetrable peptides (CPP) such as penetratin, Tat and transportan can be used to deliver a range of compounds into cells *in vitro* but there is limited information on their ability to transport molecules across the stratum corneum into skin. We have developed a novel carrier molecule (polypseudolysine; PPL), and have investigated whether this compound has the ability to transport compounds into cells and skin. Initially, alpha-melanocyte stimulating hormone (αMSH) was selected as a cargo molecule. Later, a 19mer antisense oligonucleotide (ON) targeting the translational start site of the tyrosinase gene and a peptide nucleic acid (PNA) also targeting the tyrosinase gene were selected as cargo.

The results in this thesis show that αMSH conjugated to PPL can bind to the MC1R receptor and stimulate pigmentation of melanoma cells, suggesting that the function of αMSH is not affected when attached to PPL. The antisense results demonstrated that 15merPNA-SS-PPL and 12merPNA-PPL significantly inhibited αMSH-induced pigmentation of B16F10 melanoma cells whereas PNA alone did not. In addition, ON-PPL also suppressed the increase in tyrosinase activity induced by αMSH. Confocal microscopy showed that αMSH-PPL and separately PNA-PPL compounds internalised in a range of cell lines, but αMSH and PNA without the carrier molecule did not penetrate into cells to a similar extent. *Ex vivo* skin penetrations studies performed in a Franz diffusion chamber demonstrated the penetration of fluoresceinated forms of αMSH-PPL and separately PNA-PPL into the skin and various other epithelial barriers (eyes, ileum and colon). The preliminary results indicate that PPL has the potential to be used as a

carrier molecule to deliver agents into skin and possible also into other epithelial organs.

Table of contents **Page number**

Table of contents **Page number**

Table of content **Page number**

Table of content **Page number**

Table of content **Page number**

Lists of figures and tables

DECLARATION OF AUTHORSHIP

I declare that the thesis entitled "**Peptoid Modification of Therapeutic Agents to Enhance Topical Drug Penetration"** and the work presented in it are my own. I confirm that:

- This work was done wholly or mainly while in candidature for a research degree at this University,
- Where any part of this thesis has previously been submitted for a degree or any other qualification at this university or any other institution, this has been clearly stated,
- Where I have consulted the published work of others, the source is always given. With the exception of such quotation, this thesis is entirely my own work,
- Where I have quoted from the work of others, the source is always given. With the exception of such quotations, this thesis is entirely my own work;
- Where the thesis is based on work done by myself jointly with others, I have made clear exactly what was done by others and what I have contributed myself
- I have acknowledged all the sources of help.

List of published abstract

- **Polypseudolysine (PPL) enhances topical antisense delivery.** P Kumar, C. Pickard, M.A. Fara, M. Bradley, P.S.Friedmann and E.Healy **– [Abstract]** *Journal of Investigative Dermatology* (2007). **127: s53.**

- "**Polypseudolysine (PPL), a carrier molecule based approach to transport agents into skin".** P Kumar, M.A. Fara, M. Bradley, P.S.Friedmann and E.Healy**– [Abstract]** *Journal of Investigative Dermatology* (2007). **127: s48**

- **"Cell penetrable peptide based delivery of oligonucleotide antisense/peptide nucleic acid (PNA) directed against tyrosinase".** P Kumar, C. Pickard, M.A. Fara, M. Bradley, P.S.Friedmann and E.Healy **– [Abstract]** *British journal of dermatol*ogy (2007). **156:p1105**.

- **"Peptoid modification of αMSH to enhance penetration into skin".** P Kumar, M.A. Fara, M. Bradley, P.S.Friedmann and E.Healy **– [Abstract]** *British journal of dermatol*ogy (2006). **155:p237**.

- **"Cell penetrable peptoid based transdermal penetration".** P Kumar, M.A. Fara, M. Bradley, P.S.Friedmann and E.Healy – **[Abstract]** *Journal of Investigative Dermatology* (2006). **126:s19.**

Signed: Pawan Kumar

Date: 10th of November 2008

Acknowledgements

I would like to acknowledge and thank my supervisors Professor Eugene Healy and Professor Peter Friedmann for their kind support and supervision. I would also like to thank our collaborators Professor Mark Bradley, Dr Stifun Mitto and Mario Antonio Fara for providing the novel compounds that were tested in this study. I am also grateful to Dr Chris Pickard, Dr Fethi Loafi, Dr Samantha Robinson and Dr Sandie Dixon for their assistance and support during my time carrying out this work. I would also like to acknowledge Dr Myron Christodoulides and Dr John Heckels for their supervision and assistance in generating some of the *S aureus* results. I would like to thank Prof. Andrew Lotery and Dr Catherine Joarney for assistance in labelling of eye penetration pictures. I would also like to thank Dr Scott Hans for helping me to analyse data in this thesis. I would like to thank all my other colleagues within Dermatopharmacology and the IIR research division for their support and help, and also my wife Reeta, Dr. S.N. Prasad (uncle), my father and mother for their support and encouragement during this period. I dedicate this thesis to Dr. S.N.Prasad (uncle) and my parents whose courage and support has been a great help to me.

Abbreviation

ACTH – Adrenocorticotrophic Hormone

ATP – Adenosine triphosphate

ASP – Agouti signalling protein

BMV – Brome mosaic virus

BNF – British national formulary

BSA – Bovine serum albumin

CFU – Colony forming unit

CPP – Cells penetrable peptide

CO_2 – Carbon dioxide

CPM – Count per minute

CRE – cAMP responsive element

CREB – cAMP responsive element binding proteins

cAMP – cyclic Adenosine mono phosphate

DCT – Dopachrome tautomerase

DHI - 5,6-dihydroxylindole

DHICA –5,6-dihydroxylindole-2-carboxylic acid

dH_2O – Deionised water

Da - Dalton

DMSO –Dimethyl sulfoxide

DNA – Deoxyribose nucleic acid

DNP – 2'-O-(2,4-dinitrophenyl)

DOPA – 3,4 –dihydroxyphenylalanine

DOPE – Dioleylphosphosphatidylethanolamine

DOTMA – N-[1-(2,3-dioleoyloxy)propyl]-N,N,N-trimethylammonium chloride

DOTAP – N-[1-(2,3-dioleoyloxy)propyl]-N,N,N-trimethylammoniummethyl sulphate

EDTA – Ethelenediamine tetra acetic acid

FACs – Fluorescence activated cell sorting (also known as flow cytometer)

FBS – Foetal bovine serum

FHV – Flock house virus

GFP – Green fluorescent protein

GTP – Guanosine triphosphate

HIV – Human immunodeficiency virus

HRP – Horseradish peroxidase

HSP70 – Heat shock protein 70

ICAM-1 – Intracellular adhesion molecule-1

IL – Interleukin

IFNγ – Interferon gamma

ITN – Iodotetrazolium chloride

LDH – Lactate Dehydrogenase

LPS - Lipopolysacchride

LTT – Lymphocyte transformation test

MAP – Model amphipathic peptide

MBTH – Methyl-benzothiazolinonehydazone

MC-R – Melanocortin Receptor

MC1R – Melanocortin 1 Receptor

ml – Millilitre

mRNA – Messenger RNA

αMSH – alpha melanocyte stimulating hormone

MTX – Methotrexate

NaOH- Sodium hydroxide

NDP-αMSH - Nle^4, $D\text{-}Phe^7$-α-melanocyte stimulating hormone

NF-kB – Nuclear factor- kappa B

OCA – Oculocutaneous albinism

ON – Oligonucleotide

PAGE – Polyacrylamide gel electrophoresis

PBMC – Peripheral blood mononuclear cells

PBS – Phosphate buffer saline

PFA - Para formaldehyde

PHA-P - Phytohemagglutinin

PKA – Protein kinase A

PKC – Protein kinase C

PNA – Peptide nucleic acid

POMC – Pro-opiomelanocortin

PPL – Polypseudolysine

PS – Phosphorothionate

PTFE – Polytetrafluoroethylene

RNA – Ribose nucleic acid

SCID – Severe combined immunodeficiency

SK-SD – Streptokinase - streptodornase

SI – Stimulation index

SOD – Superoxide dismutase

siRNA – Small interference RNA

TBS – Tris buffered saline

TGF-β – Transforming growth factor beta

Tm – Thermal melting temperature

TNF-α – Tumour necrosis factor alpha

TRP-1 – Tyrosinase related protein 1

TRP-2 – Tyrosinase related protein 2

dsDNA – Double strand DNA

ITN - Iodotetrazolium chloride

MITF – Microphthalmia transcription factor

UV – Ultraviolet

UTR – Untranslated region

VEGF – Vascular endothelial growth factor

μ - Micron

μl – Microlitre

Chapter 1; Introduction

1.1 Skin barrier

The skin is an important multicellular tissue of the body which is involved in thermoregulation, protection, metabolic functions and sensation. It protects our body from a vast array of pathogens, chemicals and UV induced DNA damage. It is comprised of two layers, the outer epidermis and the inner dermis (Haake *et al.* 2001).

The outermost layer, the epidermis contains mainly keratinocytes but also has melanocytes, which synthesise melanin pigment, and Langerhans cells which are part of the cutaneous immune system. The epidermis is further subdivided into four layers. These layers are (arranged from the inner surface to the outer surface) the basal layer, the stratum spinosum (suprabasal layer), the stratum granulosum and the stratum corneum (Haake *et al.* 2001). In the basal layer keratinocytes proliferate and upon leaving the basal layer the cells start to differentiate. At the stage of reaching the stratum corneum final differentiation occurs in which cells have become dead cells called corneocytes. In the stratum granulosum there are two types of granules, one of which give this layer its name (keratohyaline granules) and the other which is important for the lipid component of the stratum corneum. Keratohyalin granules are basophilic, irregularly shaped structures without an outer membrane (Manabe & O'Guin 1992). Lamellar granules are small organelles which contain stacks of lipid lamellae composed of phospholipid, cholesterol and glucoceramides (Wertz & Downing 1982). At the stages of late differentiation, the lamellar granules are thought to fuse with the plasma membrane of the granular cell and discharge their content into the intercellular space. Lamellar granules also secrete acid hydrolases which break down phospholipids and transform glucosylceramide to

ceramide, the main lipid constituent accounting for 45-50% of the lipids of the stratum corneum. It is the ceramide and free fatty acid components of the stratum corneum that allow for tight lateral packing and the formation of a highly ordered gel phase membrane domain which imparts less fluidity and less permeability to the stratum corneum than the cell membrane of living cells (Madison 2003). The barrier function role of lipids in the stratum corneum is clear from the increased transepidermal water loss following removal of the stratum corneum lipids by solvent extraction (Grubauer *et al.* 1989).

The dermis plays an important role in the mechanical support, thermoregulation and supplying metabolites and oxygen to the epidermis and dermis. It is divided into two layers, the superficial papillary layer and the deeper reticular layer. The fibroblast is the principal cell type of the dermis and synthesises collagen, elastin and ground substance which give the support and elasticity to the skin (Haake *et al.* 2001). In dermis, cells of innate immunity (Dendritic cells, macrophages, mast cells) and adaptive immunity (T and B lymphocytes) component also present, which play an important role in cutaneous immune response against bacterial or viral antigen.

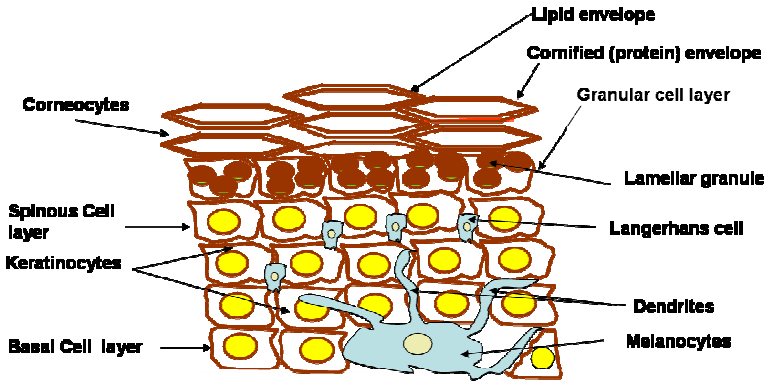

Figure 1.1 Structure of epdermis. Diagram of human epidermis showing different cell layers. The melanocytes are pigment producing cells in the epidermis and transfer melanin to adjacent keratinocytes through dendritic processes. Langerhans cells are part of the cutaneous immune system.

1.2 Skin Pigmentation

Melanocytes are pigment producing cells in the epidermis with long dendritic processes to enable the transfer of melanin into adjacent keratinocytes where it determines skin colour. Melanoblasts are precursors of melanocytes and arise from the neural crest and migrate during embryogenesis through the mesenchyme to the ear, retina, leptomeninges and to the epidermis and hair follicle (Haake *et al.* 2001). In the epidermis a single melanocyte transfers melanin to approximately 36-40 adjacent keratinocytes and this grouping is referred as the epidermal–melanin unit (Fitzpatrick & Breathnach 1963; Haake *et al.* 2001). The melanocytes synthesise the melanin pigment within membrane bound organelles called melanosomes (Seiji *et al.* 1963).

Melanosome transfer increases after exposure to UVR and in the presence of the hormone alpha-melanocyte stimulating hormone (αMSH) produced by the melanocytes and the keratinocytes (Virador *et al.* 2002). The size and the distribution of the melanosomes within keratinocytes varies according to the skin type with larger melanosomes present in dark skinned individuals (Szabo *et al.* 1969). Melanocytes synthesise two types of melanin pigment, a brown black eumelanin and a red yellow phaeomelanin (Hunt *et al.* 1995). The melanosome shape varies between ellipsoid (eumelanin) and spherical (phaeomelanin) according to the type of melanin produced (Kono *et al.* 1984). The biochemical pathway for the synthesis of melanin is shown in figure 1.2. Tyrosinase is a key enzyme in the production of both types of melanin, as evidenced by the fact that humans and animals lacking functional tyrosinase are albino, i.e without pigment (Kwon *et al.* 1987). Similarly, tyrosinase activity is higher in skin from negroes than in Caucasian skin (Fitzpatrick 1965; Pomerantz & Ances 1975).

Variation in eumelanin and phaeomelanin content between individuals and across populations is responsible for the normal variation in skin and hair colour (Thody *et al.* 1991; Hunt *et al* 1995). The difference in the number of melanocytes at similar body sites between individuals from different races is negligible, although the density of epidermal melanocytes varies slightly between skin sites (Szabo 1954). Dark skinned individuals have more eumelanin compared to the subjects with lighter skin (Hunt *et al.* 1995).

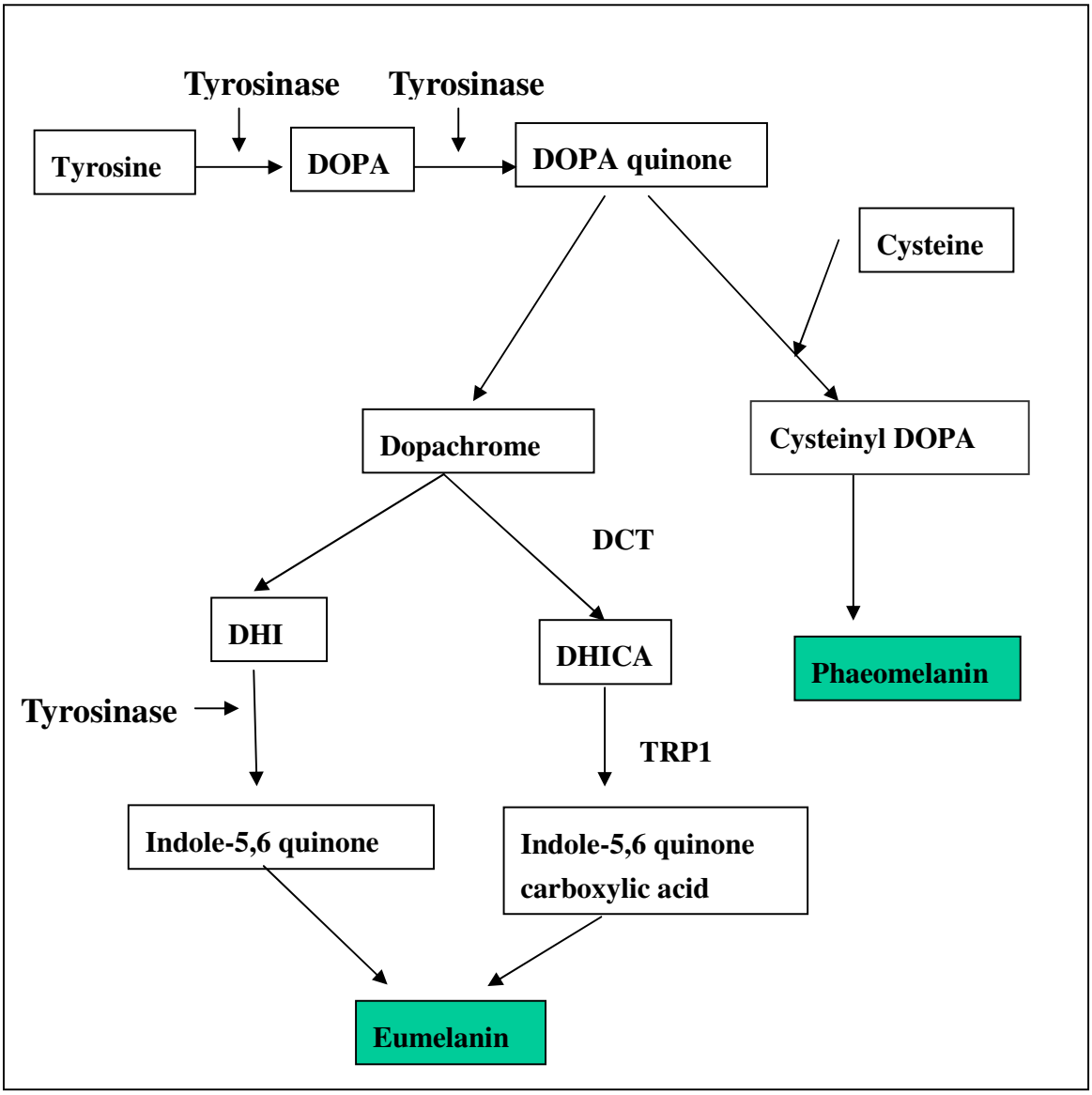

Figure 1.2. Melanin biosynthesis pathway. Diagram of melanogenesis pathway from tyrosine to eumelanin (the brown / black pigment) and to phaeomelanin (the red /yellow pigment). The enzyme tyrosinase catalyses the conversion of tyrosine to 3, 4 dihydroxyphenylalanine (DOPA), DOPA to DOPAquinone and 5,6-dihydroxylindole (DHI) to indole-5,6 quinone. In the eumelanin pathway, DOPAquinone is converted to DOPAchrome which become isomerised to 5,6-dihydroxyindole-2-carboxylic acid (DHICA) via the enzyme DOPAchrome tautomerase (DCT). DHICA is oxidized by tyrosinase-related protein 1 (TRP1) to brown eumelanin. Alternatively, DOPAchrome is isomerised to 5,6-dihydroxyindole (DHI) which is converted to black eumelanin via tyrosinase. Phaeomelanin is generated from DOPAquinone via a separate pathway in which DOPAquinone incorporates cysteine residues (Nordlund & Boissy 2001).

Normal human skin pigmentation is a genetically complex process; approximately 4-5 different genes are responsible for phenotypic variation in skin colour (McEvoy *et al.* 2006). Polymorphisms in the human melanocortin 1 receptor (*MC1R*) gene have been shown to be responsible for some of this variation, resulting in fairer skin type (Valverde *et al.* 1995). Recently, it has been suggested that the human ortholog of a gene (*SLC24A5*) associated with a pigment alteration in zebrafish, plays an important role in human skin pigmentation. This gene is highly conserved in African and East Asian populations, whereas a variant allele is reported in European populations with lighter skin pigmentation (Lamason *et al.* 2005). Other genes such as the *P* gene (the human homologue of the murine pink-eyed dilution gene), beta-defensin gene (a defensin mutation leads to black coat colour of dog) and the agouti signalling protein (*ASP*) may also play an important part in the variation of pigmentation between individuals but further research is necessary to confirm this finding (Wilson *et al.* 1995; Orlow & Brilliant 1999; Kanetsky *et al.* 2002, Candille *et al* 2007).

1.3 Ultraviolet radiation and its effects on skin

Ultraviolet radiation (UVR) is part of the electromagnetic spectrum with a wavelength range of 10nm to 400nm., It is divided into UVA (400nm - 320nm), UVB (320nm – 290nm), UVC (290nm – 200nm), and vaccum / extreme UVR below 200nm (Diffey 1991). Solar radiation is the main source of UVR in the earth's atmosphere, in which UVR comprises of 5% of total solar radiation (Diffey 2004). However, the upper atmosphere absorbs most of the shorter wavelengths of UVR and the main proportion of UVR that reaches the earth's surface on a sunny summer's day is UVA (94%, depending

on altitude) which penetrates deep into the skin, whereas the UVB component (6%) is mainly absorbed by the epidermis (Diffey 2002; Kadekaro *et al.* 2003). UVR stimulates skin pigmentation (also referred as sun tanning), epidermal hyperplasia, vitamin D synthesis, and causes erythema, immunosuppression and skin cancer (Friedmann & Gilchrest 1987; Gilchrest *et al.* 1999; Diffey 2004). Initially, UVB was considered as the main culprit for the development of skin cancer, including melanoma, but Setlow *et al* proposed that UVA may be the primary cause of solar radiation induced melanoma based on results in a xiphophorus fish model (Setlow *et al.* 1993). The risk of developing melanoma relates to skin type, with skin type I or II individuals (who tan poorly) being more susceptible than people with darker skin types (table 1.0) (Fitzpatrick 1988; Agar & Young 2005). UVB is able to induce the formation of DNA photoproducts (cyclobutane pyrimidine dimers and 6,4-photoproducts) which lead to mutation and skin cancer development if inadequately repaired (Gilchrest *et al.* 1999). It has been suggested that generation of reactive oxygen species and double strand breaks are mainly responsible for UVA related skin cancer production, but Mouret *et al* recently reported that UVA can also generate cyclobutane pyrimidine dimers (but not 6,4-photoproducts), so this may be an alternative mechanism through which UVA may lead to the development of melanoma and non-melanoma skin cancer (Mouret *et al.* 2006).

Table 1.0. Human skin types. Classification of human skin types on the basis of acute and chronic responses to solar radiation (Fitzpatrick 1988; Dubin N *et al* 1989; Bliss JM *et al* 1995).

Skin types	Skin colour	Tanning ability	Cancer susceptibility
I	White	Very poor	High
II	White	Poor	High
III	White	Good	Moderate
IV	Olive	Very good	Low
V	Brown	Very good	Very low
VI	Black	Very good	Very low

The protective response of skin against UVR-induced DNA damage includes melanogenesis and upregulation of DNA repair enzymes (Friedmann & Gilchrest 1987; Eller *et al.* 1997; Tadokoro *et al.* 2003). Many commercially available sunscreen lotions can protect from UVR-induced DNA damage (Freeman *et al.* 1988). Most sunscreens contains organic chemicals (e.g. oxybenzone, para-aminobenzoic acid and cinnamates) which absorb UVR (Rosen 1999). In addition, some sunscreens contain opaque material like titanium oxide and/or zinc oxide, thus protecting through the reflection of UVR (Rosen 1999). Many sunscreens work by a combination of absorption and reflection as a result of containing both types of ingredients, however, sunscreens often do not offer 100% protection against sun damage and some individuals can become allergic to some of the active ingredients (e.g benzophenone) contained in sun lotions (Lautenschlager *et al.* 2007). αMSH and its analogues may have potential to be used as tanning agents in order to protect against UVR-induced DNA damage, for example, αMSH and melanotan-1/NDP-αMSH (a superpotent αMSH analogue which was developed at the University of

Arizona), can stimulate tanning of human skin (Dorr *et al.* 2000; Lerner and McGuire 1961).

1.4 Cutaneous immunity

The skin is a site where potentially harmful organisms like bacteria, viruses, parasites and fungi might enter the body. Thus, in the skin, the stratum corneum is the first line of defence against invasion by these organisms (Cruz 2001b). However, microorganisms can enter through the skin when epidermal integrity is lost following mechanical, physical, biological or chemical injury. Fortunately, the skin has a second line of defence in the skin immune system. Like elsewhere in the body, the cutaneous immune system is divided into the innate immunity (Langerhans cells, macrophages, mast cells) and adaptive immunity (T and B lymphocytes) components. Non-specific immunity against invading microorganisms includes phagocytosis of pathogens by macrophages and inflammatory responses by tissue mast cells which release histamine and other mediators which increase the blood flow to the affected area and cause infiltration of fluid and white blood cells (Gordon *et al.* 2001). Langerhans cells in the epidermis participate in the initiation and elicitation of specific immune responses by acting as antigen presenting cells which present antigen (usually in the form of processed peptides) to T cells (Salmon *et al.* 1994; Cruz 2001). Other skin antigen presenting cells include dermal dendritic cells and dermal macrophages (Valladeau & Saeland 2005). In human skin, the vast majority of T cells are located in the dermis and it is thought that the skin is a major reservoir of T cells in the body (Clark *et al.* 2006). In the case of the first exposure of Langerhans cells to the antigen, the Langerhans cells migrate to the local lymph nodes and prime “naïve” T

cells at that site, but during subsequent exposure with the same antigen the Langerhans cells can present the antigen to memory effector T cells in the dermis. Macrophages and Langerhans cells further regulate T cell mediated responses by secreting specific cytokines, including IL-1, TNF-α, IL-6 and IL-8 (Sauder *et al.* 1984; Lore *et al.* 1998). Keratinocytes also produce TNF-α to enable Langerhans cells to migrate to the local lymph nodes. In addition, keratinocytes produce antimicrobial peptides (e.g β defensin) (Harder *et al.* 1997) and express toll like receptors which recognise microorganism components (DNA, RNA, LPS etc) and lead to initiation of signalling cascades important in the generation of cytokines, chemokines, antimicrobial peptides and upregulation of costimulatory and adhesion molecules involved in the innate and adaptive immune responses (Song *et al.* 2002; Baker *et al.* 2003; Pivarcsi *et al.* 2003; Mempel *et al.* 2003). Many skin diseases (e.g psoriasis, eczema etc) are linked to alterations in the skin immune system, and a variety of topical and systemic drugs which target the immune system are frequently used to treat these disorders (Lebwohl *et al.* 2004; Lowes *et al.* 2007).

1.5 Topical drug delivery

There are a number of diseases which can affect the normal function of the skin, including diseases of the epidermis and the dermis, and a variety of drugs can be administered systemically (oral, intra-muscular, intra-venous) or less frequently topically through the skin to treat these disorders (British National Formulary). However, there are potential problems associated with the systemic administration of drugs for skin diseases, including inadequate therapeutic concentration of drugs in the target tissue and the

potential for systemic adverse effects. Topical drug delivery offers certain advantages over systemic routes. For example, compared to orally administered drugs, it avoids digestion within the gastrointestinal system and bypasses the detoxification metabolism in the liver. Topical drug delivery also has the potential for sustained and controlled drug release at the target tissue site. In spite of the advantages of topical delivery, only a small percentage of drugs can be delivered in this way due to the barrier properties of the skin as a result of the presence of the stratum corneum (Ranade 1991).

There are three proposed pathways of drug absorption through the skin (Barry 2002). These routes are the 1) intercellular in which drug absorption occurs via lipid domains between the corneocytes, 2) transcellular where diffusion of drugs takes place across the corneocytes and lipid matrix and 3) appendagial in which the drug enters via the hair follicles and eccrine glands. The appendages (hair follicles and sweat ducts) cover only 0.01 to 0.1 % of the total surface area of the stratum corneum and the efficiency of the drug absorption by this route is unclear. In the intercellular route, diffusion takes place through the lipid lamellae; this is proposed to be the main pathway of diffusion of hydrophobic drugs. In the transcellular route, diffusion occurs through both the keratinocytes and lipid lamellae; this is proposed to be involved in the diffusion of polar drugs (Scheuplein 1967).

Topical drugs are usually dissolved in various types of bases (ointment, cream, hydrogel and lotion) with additives that can enhance their penetration (e.g. sulfoxide, azone, pyrrolidone). The topical delivery of certain therapeutic agents in some solvent formulations have been used successfully for several decades, for example topical steroids have been used to treat skin diseases since 1952 (Sulzberger & Witten 1952).

However, at present it is still a challenge to deliver many drugs topically so that they can permeate the stratum corneum at levels or rates that achieve significant therapeutic effect (Williams & Barry 2004).

1.6 Drug penetration into skin

Penetration of drugs or compounds into skin or cells depends mainly upon the molecular weight and hydrophobicity of the compound. Hydrophobicity is calculated from the octanol-water partition coefficient (Kow), which is the ratio of the concentration of a compound/chemical in octanol and in water at equilibrium and at a specified temperature. Kow values of many organic chemicals range from 10^{-3} to 10^{7}, where a compound with a low Kow value (less then 10) is hydrophilic and a high Kow value (greater than 10^{4}) is hydrophobic (Moss *et al.* 2002). The lipophilicity nature of the stratum corneum allows the restricted diffusion of highly lipophilic (Kow $>10^{5}$) compounds. In addition, the compound must have sufficient hydrophilicity to traverse through the epidermis to the dermis (Moss *et al.* 2002). The ability of a compound to diffuse into the skin can be determined by Fick's law which indicates that $J = -D(\delta c/\delta x)$, where J is the rate of transfer/ unit area of the surface (i.e the flux), D is the diffusion coefficient, C is the concentration of the diffusing substance and X is the spatial co-ordinate measured normal to the section.

1.7 Other Epithelial Barriers

1.7.1 The Gut

In the gastrointestinal tract, absorption of molecules or nutrients from the lumen of the

gut to its outer surface (lamina propria) mainly takes place in the small intestine and colon. This transport is highly regulated because of the presence of various layers and structures within the gut epithelium, including the microvilli, the glycocalyx, the mucus layer, the intercellular tight junction and the extracellular basement membrane (Siccardi *et al.* 2005). The transport of nutrients, ions, amino acids, vitamins and sugars across the gut epithelium involves an active mechanism in which various transporter protein families participate (Stenberg *et al.* 2000). The diffusion of small lipophilic molecules (less the 500 dalton) tends to be by the transcellular route (Maxton *et al.* 1986), whereas small hydrophilic molecules (200-400Da) tend to diffuse through the paracellular route which is regulated by tight junctions (Artursson *et al.* 1993). The digestion of foodstuff by gastric juice, bile salts and pancreatic enzymes ensures that the nutrients and other molecules are available for absorption within the intestine. Therefore, the delivery of drugs and therapeutic molecules via the intestine, and to the intestine itself, requires a protective covering on the drug to prevent its degradation from the gastric juice. However, successful delivery of proteins, peptides and oligonucleotides through an oral route to target a gastrointestinal disease is still a major challenge.

1.7.2 The Eye

Ocular diseases which affect the anterior part of the eye (cornea, conjuctiva, sclera and anterior uvea) are mainly treated by eyedrops. Because of rapid drainage (tears and systemic absorption) and the presence of the outer corneal barrier, only less then 5 % of the applied dose actually reaches the intraocular tissue. On the other hand, diseases in the posterior segment of the eye (retina, vitrous chroid) are targeted by intravenous or

intravitreal delivery of drugs because of the poor permeability of the drugs across the eye barriers (Urtti 2006). The commonly used ocular eyedrops in clinics are generally lipophilic compounds of small molecular weight (Tamilvanan & Benita 2004). More recently, oligonucleotide and antibody-based approaches have been developed for the treatment of eye diseases such as macular degeneration and cytomegalovirus-induced retinitis. Fomivirsen sodium (ISIS pharmaceutical) is an antisense oligonucleotide which is approved for the treatment of cytomegalovirus induced retinitis but delivery of this and other antisense compounds into the eye requires intravitreal injection (Kurreck 2003).

1.7.3 The Lungs

The pulmonary tract is composed of the conducting region and the respiratory region. The nasal cavity, nasopharynx, bronchi and bronchioles form the conducting region, whereas the respiratory region mainly comprises of alveoli, where gas exchange takes place (Uchenna Agu *et al.* 2001). To treat diseases in the pulmonary system, direct delivery of drug to the lung is prefered to oral delivery because of rapid onset of action, less systemic side effects and requirement for low doses. However, the delivery of drugs into the lungs is affected by the presense of mucociliary clearance, respiratory mucous, alveolar epithelium, basement membrane and respiratory enzymes (Uchenna Agu *et al.* 2001). Aerosol formulation is the most commonly used method to deliver drugs into the lung; this consists of small liquid droplets or solid particles in a gaseous suspension. The size of the aerosol particles must be 1μm-5μm for an efficient delivery of drug (Uchenna Agu *et al* 2001).

1.8 Models used to investigate drug penetration

Topical drug penetration studies using human skin obtained from cosmetic surgery, punch biopsy or cadavers are a well-established and validated *in vitro* system to evaluate drug penetration (Schmook *et al.* 2001; Wagner *et al.* 2001). Skin from other animals (rats, mice, pigs, and monkeys) has also been employed as an alternative for human skin in these studies, among them rat and pig skin are commonly used because of the similar barrier characteristics of their stratum corneum to that of humans (Bronaugh & Maibach 1985; Scott *et al.* 1986; Sekkat *et al.* 2002). Indeed, pig's ear skin is morphologically and histologically very similar to human skin, for example in terms of the epidermal thickness and lipid composition (Jacobi *et al.* 2007). In addition, both active and passive drug diffusion characteristics of human and porcine skin are comparable (Dick & Scott 1992; Sekkat *et al.* 2002).

The main drawback of some animal skin models is their higher permeability than human skin and the stringent regulations for the use of animals in drug delivery studies. Therefore, other non-animal drug delivery models (such as various skin substitutes/artificial skins, bioengineered human skin, polymeric membrane, shed snake skin, and epidermal lipidic bilayers) have been developed to provide an alternative system for drug delivery investigations (Asbill *et al.* 2000; Megrab *et al.* 1995). Skin substitutes are mainly subdivided into epidermal and full thickness types. The commercially available epidermal skin substitute (EpiEthic), in which keratinocytes are grown over a polycarbonate filter, is morphologically similar to human epidermis (Netzlaff *et al.* 2005). The EpiSkin has been marketed by L'Oreal as a full thickness skin substitute in which keratinocytes are laid over artificially constituted dermis (made up of

bovine and human collagen) (Netzlaff *et al.* 2005). Both skin substitutes (EpiEthic and EpiSkin) are structurally and biochemically similar to human skin, therefore they have been used for testing the irritancy and penetration of chemicals, but one concern is that they seem to be more permeable than normal human skin (Ponec *et al.* 2000; Faller & Bracher 2002; Lotte *et al.* 2002; Netzlaff *et al.* 2005).

1.9 Methods to enhance drug delivery

Several techniques have been developed to assist the delivery of drugs and compounds into cells and in some cases into skin. These approaches to enhance delivery are briefly reviewed here.

1.9.1 Physical methods – Microinjection, Electroporation, Pulsed microjets and Iontophoresis.

In microinjection techniques a solution of DNA/RNA is injected into a cell through a fine microcapillary needle (Gordon *et al.* 1980), but the main drawback of this technique is that the delivery is restricted to single cells. In the electroporation technique a transient aqueous pore is created in the lipid bilayer of the cell membrane by the application of short (microseconds to milliseconds) electrical pulses (Prausnitz *et al.* 1993), but the need for a high voltage and limited delivery are the main drawbacks to using this technique for skin diseases (Mehier-Humbert & Guy 2005). However, iontophoresis, whereby low voltage electrical current is used to enhance delivery of polar drugs across the stratum corneum, has been employed successfully to treat post operative pain with fentanyl hydrochloride (Mayes & Ferrone 2006). In addition, a modification of microinjection,

where nanolitre volume pulsed microjets allow entry of drugs into skin, has recently been reported and may have benefits for delivery of certain drugs (Arora *et al.* 2007).

1.9.2. Supersaturation - Binary solvent system, Ternary solvent system

The concentration of drug at the site of application can be increased after evaporation of the volatile component in the drug mixture, making the solution on the skin a supersaturated solution (Kondo *et al.* 1987). In the binary solvent system, enhancement of percutaneous penetration is achieved by the combination of a volatile vehicle and non-volatile vehicle, whereas in the ternary solvent system, a mixture of volatile/non-volatile-hydrophile/non-volatile-lipophile solvent system is used (Kondo *et al.* 1987). Although supersaturation can improve penetration of some drugs into skin, supersaturated states are thermodynamically unstable and may precipitate out of the solution and crystallise on extended storage (Finnin & Morgan 1999).

1.9.3. Metabolic/ biochemical enhancers

Metabolic/biochemical enhancer systems are based on the inhibition of the epidermal synthesis of key lipid constituents (ceramide, cholesterol and free fatty acids). It has been shown that the fatty acid synthesis inhibitor 5-(tetradecyloxy)-2-furancarboxylic acid, the cholesterol synthesis inhibitor fluvastatin and cholesterol sulphate separately increase the absorption of lignocaine through the stratum corneum (Tsai *et al.* 1996). However, the amount of drug delivered by using these techniques is still limited because the barrier properties of the stratum corneum do not change to a large degree at the concentrations suitable for use in humans (Brown *et al.* 2006).

1.9.4. Chemical penetration enhancers

Chemical penetration enhancers are pharmacologically inactive agents (in that they differ pharmacologically to the drug in the cream or ointment) but can interact with components of the stratum corneum (Marjukka Suhonen *et al.* 1999). Chemical penetration enhancers include dimethylsulfoxide (DMSO), azones, pyrrodilones, glycol, alcohols and alkanols and enhance permeation by altering the barrier properties of the skin (Marjukka Suhonen *et al.* 1999). They are used in many topical drug preparations but there are many side effects associated with potent chemical enhancers including irritant dermatitis secondary to reduced barrier function of the skin (Kligman 1965; Jungbauer *et al.* 2001; Williams & Barry 2004). Information on selected chemical penetration enhancers is included in table 1.1.

Table 1.1 Chemical penetration enhancers. Examples for chemical penetration enhancers and side effects associated with them.

Chemicals	Mode of action	Side effects	References
DMSO	Reacts with lipid component of stratum corneum.	Irritant; high concentration (>60%) can cause erythema and wheal on skin and can denature some proteins.	(Kligman 1965)
Azones	Unknown; may interact with lipid domain of stratum corneum.	Irritant, but less toxic then DMSO.	(Williams & Barry 2004)
Pyrrodillone	Alters the solvent nature of lipid membrane and create reservoir of drugs within the skin	Causes erythema of the skin.	(Jungbauer *et al.* 2001)

1.9.5. "Delivery in an envelop" – viral and liposomal delivery systems

Drugs and therapeutic compounds can be packaged in viral envelops (e.g. adenovirus) or spherical lipid structures called liposomes. Indeed, the enzyme T4 endonuclease has been admininstered topically using liposomes (Yarosh *et al.* 2001). Risks associated with the

use of viral vectors are the possibility for immune responses to expressed viral proteins (which may kill the cell that is producing the therapeutic gene effect) and for insertional mutagenesis caused by random integration of viral genes into the host genome (Pfeifer & Verma 2001). The similarities of the cationic lipids in liposomes to cellular membrane lipids in terms of physical and chemical properties offer advantages for drug delivery, but the major drawback of the liposomal based gene delivery is the poor transfection efficiencies *in vivo* (Rao & Gopal 2006).

1.10 Cell penetrable peptide based drug delivery

In 1967, Ryser observed that mixing polylysine or other positively charged peptides with proteins greatly increased the internalisation of those proteins (Ryser 1967). In 1988, it was reported that Tat, a nuclear transcription activating protein of Human Immunodeficiency Virus (HIV), can cross cell membranes without seeming to adversely affect normal cell function (Frankel & Pabo 1988; Green & Loewenstein 1988). Later it was noted that the homeodomain of the Anntenapedia transcription factor (*Dorsophilla spp*) crosses the plasma membrane (Joliot *et al.* 1991). To date, many peptide sequences with an ability to cross cell membranes and deliver cargo molecules into cells have been discovered. These observations have opened up new approaches for potential drug delivery, in that cell-penetrable peptides (CPPs) can carry cargo molecules (drugs, proteins, and oligonucleotides) into cells and some have been reported to be capable of transporting cargo molecules into skin (see table 1.2).

Table 1.2. Examples of some common CPPs, which have been reported to deliver various conjugated cargo *in vitro* (Cells).

Carrier	Cargo	Delivery into cell types/ skin	Functional effects observed	Topical delivery into skin	References
Tat and penetratin	Oligonucleotide against p-glycoprotein	NIH 3T3	Gene inhibition	No	(Astriab-Fisher *et al.* 2000)
Tat	Ovalbumin	E.G7- Ova cell line	Antigen presentation	No	(Moy *et al.* 1996)
Tat	srIkappaBalpha protein	HeLa cell and Jurkat T cells	Inhibition of NFkB	No	(Kabouridis *et al.* 2002)
Tat	Nanoparticle	HeLa cells (Radiolabelled detection of conjugate inside cells)	No	No	(Bhorade *et al.* 2000)
Penetratin	CD44 derived phospho peptide	RPM-MC cells	Blocking of CD-4 mediated cell migration	No	(Peck & Isacke 1998)
Penetratin	ICAM-1 peptides	Lewis rat brain microvascular EC line (GP8/3.9)	Inhibition of trans-endothelial lymphocyte migration	No	(Greenwood *et al.* 2003)
Penetratin and transportan	PNA against gelanin receptor	Bowes cells	Gene inhibition	No	(Pooga *et al.* 1998)
Polylysine	Reporter plasmid	COS-1, BHK and 3T3	β-Gal expression	No	(Sosnowski *et al.* 1996)
Polylysine	Horseradish peroxidase (HRP)	Fibroblast (Detection of HRP inside cells.)	No	No	(Ryser *et al.* 1982)
Polylysine	HRP and serum albumin	Fibroblast (Radiolabelled detection of conjugated compounds)	No	No	(Shen & Ryser 1978)
Polylysine	Methotrexate	Chinese hamster ovary cell line (Intracellular detection of methotrexate)	No	No	(Ryser & Shen 1980)
Polyarginine	No cargo	Jurkat T cells (Cellular uptake comparison of fluorescein-linked polyarginine with other polycationic peptide)	No	No	(Mitchell *et al.* 2000)

Carrier	Cargo	Delivery into cell types	Functional effects	Topical delivery into skin	References
Polyarginine, Tat, penetratin, SynB3	Peptide nucleic acid (PNA)	pLuc705HeLa	Evaluation of CPPs for intracellular delivery of PNA by detection of fluorescence inside cells	No	(Bendifallah *et al.* 2006)
Transportan	Double-stranded oligonucleotide NkappaB decoy	Rat Rinm5F insulinoma cells	Inhibition of IL-1β induced NFkappaB activation	No	(Fisher *et al.* 2004)
Transportan	Biotinyl group	Melanoma cell (Fluorescence observed inside cells)	No	No	(Pooga *et al.* 1998)
Transportan	GFP, avidin-TRITC	BRL and COS-7 cells (Fluorescence observed inside cells)	No	No	(Pooga *et al.* 2001)
Transportan and penetratin	siRNA	COS-7, C166-GFP and EOMA-GFP cells (Fluorescence observed inside cells)	No	No	(Muratovska & Eccles 2004)
D and L SynB1 and SynB2, Penetratin	NBD and TAMARA-fluorophore	K562 (Endocytotic localisation of fluorophore)	No	No	(Drin *et al.* 2003)
VP-22	GFP	COS-7 cells (Detection of fusion protein inside cells)	No	No	(Derer *et al.* 1999)

Table 1.3. Examples of some common CPPs, which have been reported to deliver various conjugated cargo *in vivo*.

Carrier	Cargo	Delivery into cell types	Functional effects	Topical delivery into skin	References
Tat	Tyrosinase related protein 2	Specifically targeted dendritic cells	Antigen presentation	No	(Shibagaki & Udey 2003)
Tat	β-galactosidase	*In vivo* by intra-peritoneal injection (Fluorescence observed in different tissues)	No	No	(Schwarze *et al.* 1999)
Tat	Lipolytic peptide (GKH)	Skin (Mice) (Skin penetration)	No	Yes	(Lim *et al*. 2003)
Tat	Superoxide dismutase	Skin (Mice) (Ginsenoside enhances skin penetration of Tat-SOD)	No	Yes	(Kim *et al*. 2003)
Tat	Catalase and superoxide dismutase	Skin (Mice) (Skin penetration)	No	Yes	(Jin *et al*. 2003)
Penetratin	Interferon-γ	Skin (Mice) (Skin penetration)	No	Yes	(Lee *et al.* 2005)
Penetratin	Antigenic peptide (OVA)	Tape stripped skin (Mice)	Epicutaneous immunisation	Yes	(Schutze-Redelmeier et al. 2004)
Polylysine	Superoxide dismutase (SOD)	Skin (Mice) (Increase viability of paraquat treated fibroblast and detection of SOD in skin by anti-SOD antibody)	No	Yes	(Park *et al.* 2002)
Polyarginine	Cyclosporine A	Skin (Mice and grafted human skin)	Inhibition of inflammation and transdermal detection of fluorescein-linked cyclosporine.	Yes	(Rothbard *et al.* 2000)
Polyarginine	Tumour antigen derived peptide	Subcutaneous injection polyarginine conjugated peptide	Antigen presentation	No	(Mattner *et al.* 2002)

Carrier	Cargo	Delivery into cell types	Functional effects	Topical delivery into skin	References
Polyarginine	Hemagglutinin epitope	Skin (Skin delivery)	No	Yes	(Robbins *et al.* 2002)
VP-22	GFP	Neuron (Expression of GFP observed in neuron, retina etc)	No	No	(Kretz *et al.* 2003)

Table 1.3. Examples of some common CPPs, which have been reported to deliver various conjugated cargo *ex vivo*.

Carrier	Cargo	Delivery into cell types	Effects	Topical delivery into skin	References
Tat and YARA	Peptide (P20)	Skin (Pig) (Skin penetration comparison)	No	Yes	(Lopes *et al.* 2005)
Penetratin	Caveolin-1	Microvessels endothelial cells	Inhibition of microvessels permeability.	No	(Zhu *et al.* 2004)
Polyarginine	Hydrophilic macromolecule (dextran)	Excised rabbit nasal epithelium (Paracellular delivery)	No	No	(Ohtake *et al.* 2003)
Polyarginine	PKCepsilon	Isolated cardiac myocytes	Reduced ischaemic damage	No	(Chen *et al.* 2001)

1.10.1 Penetratin

Homeoproteins are a class of transcription factors that bind to the DNA and play a role in multiple biological processes (Gehring *et al.* 1990). It has been shown that the DNA binding domain (homeodomain) of the *Drosophila* transcription factor Antenapedia crosses the cell membrane (Joliot *et al.* 1991). Furthermore, investigations have revealed that the third helix of the three helices homeodomain is responsible for translocation through biological membranes (see figure 1.3); this 3rd helix has been named penetratin (Derossi *et al.* 1994; Derossi *et al.* 1996).

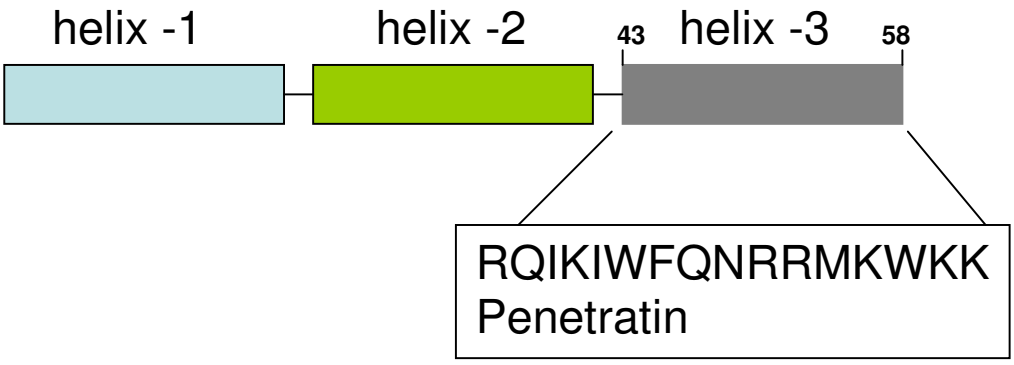

Figure 1.3. DNA binding domain of antenapedia. DNA binding domain of anntenapedia consists of three alpha helices. The 16 amino-acid sequence of the third helix, named penetratin, has been shown to contain the membrane translocating property.

The homeodomain of antennapedia was the first CPP reported to deliver a cargo molecule (C terminus of Rab3, a small GTP binding protein) into myoblast and neuronal cells (Perez *et al.* 1992). Since then penetratin has been shown to deliver a vast array of molecules, including proteins, peptides and oligonucleotides into various types of cells (as shown in table 1.2). Tryptophans at position 48 and 56 of the penetratin sequence seem to plays an important role in the transport across the cell membranes as evidenced by a decrease in the translocation efficiency when this amino acid is replaced with phenylalanine (Letoha *et al.* 2005). In comparison to other CPPs (Tat, polyarginine and transportan), penetratin showed a better cellular uptake and less toxicity in an *in vitro* cell culture-based investigation (Jones *et al.* 2005). However, in another study which evaluated the ability of different CPPs to deliver PNA, penetratin was found to have the least or minimal activity (Bendifallah *et al.* 2006). One study to date has indicated an ability of penetratin to deliver cargo into intact skin, however, it is unclear how good penetratin is at performing this role because the single paper failed to report on reproducibility and showed only one image to indicate penetratin mediated transport of

interferon-γ into skin as detected by an anti-interferon-γ antibody (Lee *et al.* 2005).

1.10.2. Tat

Tat is a transcription-activating factor of HIV varying from 86-101 amino acids in length depending on the viral strain (Dingwall *et al.* 1989; Rusnati *et al.* 2000). Tat binds to the trans-acting response element of the viral RNA to activate the viral promoter and is composed of several functional domains, namely the acidic region, DNA binding region, the core region and the basic region (see figure 1.4; (Vives *et al.* 1997).

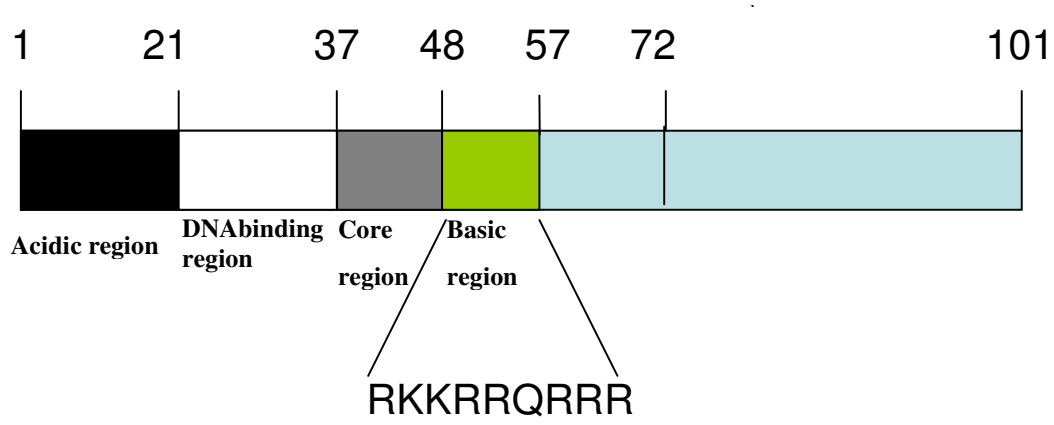

Figure 1.4. Structure of Tat protein. Structure of tat protein consists of acidic region, DNA binding region, core region, basic region and C terminal region. It is the amino acid sequence in the basic region, which is responsible for internalisation.

It is the arginine rich basic region (amino acids 49-57), which is responsible for the internalisation of Tat (Futaki 2005; Al Taei *et al.* 2006). In this part of the Tat amino acid sequence, there are six arginine and two lysine molecules, which impart a highly basic and hydrophobic character to the Tat protein. Deletion of the arginines from this part of the sequence resulted in a significant decrease (up to 80%) in cell penetration (as observed by reduced cellular fluorescence) (Wender *et al.* 2000). Like penetratin, Tat has

been shown to deliver a large number of compounds *in vitro* and *in vivo* (table 1.3). However, Tat is a short polypeptide of viral origin and can act as a powerful transactivator of gene expression and several studies have shown that Tat protein upregulates several cytokines including IL-2, IL-6 and TGF-β which may restrict usage of the Tat protein as a CPP for drug delivery in humans (Zauli *et al.* 1992; Zauli *et al.* 1993; Scala *et al.* 1994; Westendorp *et al.* 1994; Westendorp *et al.* 1995).

1.10.3 Polyarginine

A number of studies have been carried out with arginine rich carriers to investigate the cell penetration ability of these compounds; for example Tat, flock house virus coat protein, brome mosaic virus (BMV) gag protein and HIV-1 Rev protein, each of which contains more than 5-6 arginine residues in their amino acid sequence, have been examined in this way (Futaki *et al.* 2001). Interestingly internalisation of polyarginine seems highly dependent on the number of arginine residues in the sequences (Wender *et al.* 2000a; Futaki *et al.* 2001), with efficient internalisation observed with a longer chain length of more than 4 arginines. The chain length of polyarginine for optimum transport was found to be in between 5-11 amino acids, with octa-arginine and nona-arginine shown to translocate most efficiently (Mitchell *et al.* 2000; Suzuki *et al.* 2002). Polyarginine has been reported to be capable of delivering proteins, peptides, oligonucleotides and PNAs into various cell lines (table 1.3) and has been documented as being able to transport cyclosporine and hemagglutinin epitope into skin (Rothbard *et al.* 2000; Robbins *et al.* 2002).

1.10.4 Transportan

Transportan is a chimeric peptide (27 amino acids in length, see figure 1.5) generated from the fusion of the first twelve amino acids of the N-terminus of galanin (a neuropeptide which modulates gastric smooth muscle activity) and the 14 amino acids of the wasp venom peptide, mastoparan, with an additional lysine linker between the two peptides (Pooga *et al.* 1998).

It has been reported that internalisation of transportan is not inhibited by low temperature (4^0C), but the transduction kinetics of transportan in some cases are faster than those of Tat and penetratin (Lindgren *et al.* 2000). Transportan has been reported to translocate proteins and PNAs *in vitro* into various cell lines (see table 1.3). However, transportan may generates undesirable effects due to its ability to lower GTPase activity and because of the distribution and function of galanin and its receptor in the nervous system (Kask *et al.* 1997).

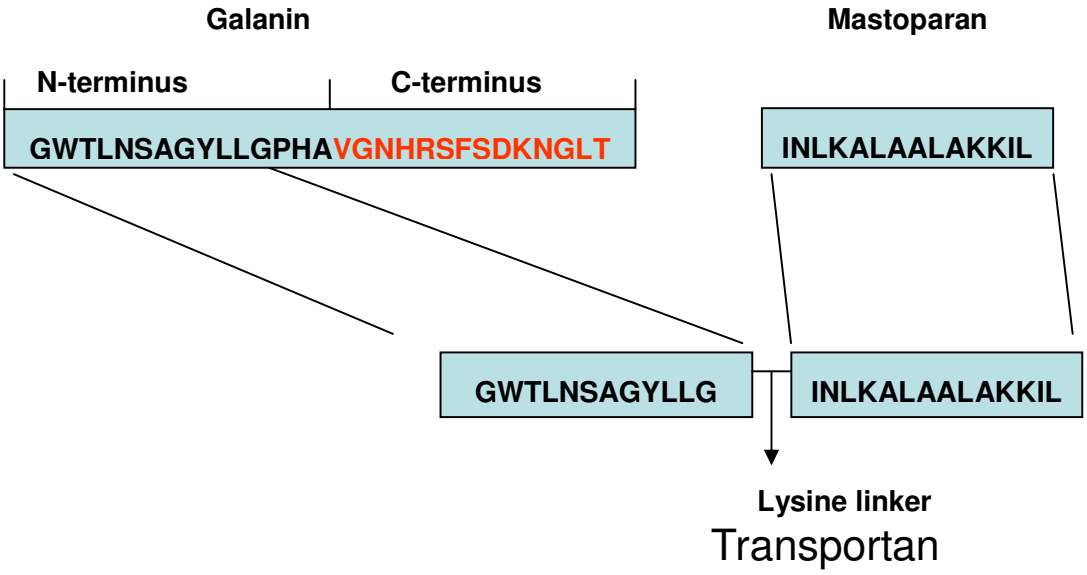

Figure 1.5 Structure of transportan. Amino acids sequence of transportan, derived from first 12 amino acids of the neuropeptidide, galanin, and all amino acids sequence of the wasp venom peptide, mastoparan, linked by a lysine linker.

1.10.5 Polylysine / Poly-L-lysine

Poly-L-lysine (L optical isomer of lysine) can facilitate the delivery of methotrexate, serum albumin and horseradish peroxidase into various cell lines (Shen & Ryser 1978; Ryser & Shen 1978; Ryser *et al.* 1982). Poly-D-lysine (D optical isomer of lysine) has also been shown to transport methotrexate into cells and seems to do so more efficiently then poly-L-lysine, possibly because it is more resistant to protease degradation (Shen & Ryser 1979). The size of poly-L-lysine used in the studies to date has ranged from 3.1 to 130kDa, but it has been reported that an increase in chain length of poly-L-lysine greater than 10 lysine residues increases the toxicity of compounds (Lv H *et al* 2006). In one study, poly-L-lysine demonstrated more efficient transport of β-galactosidase in comparison to polyarginine and Tat (Mai *et al.* 2002). Moreover, poly-L-lysine has been reported to enhance the penetration efficency of superoxide dismutase into cells and into skin (Park *et al.* 2002). Although most studies have noted little toxicity with poly-L-lysine, the degranulation of mast cells by poly-L-lysine has been observed, and could lead to inflammation if used *in vivo* (Church *et al.* 1991).

Other CPPs which have been used to deliver compounds into cells include VP22 (derived from herpes simplex virus), PEP-1 consisting of a hydrophobic and a lysine rich nuclear localization signal and model amphipathic peptide (MAP) (Oehlke *et al.* 1998; Morris *et al.* 2001). Most of the work carried out with commonly used CPPs has been done *in vitro* with few *in vivo* studies performed. To date, very few CPPs capable of transporting molecules into skin have been identified; these include polyarginine, Tat, penetratin and poly-L-lysine (Rothbard *et al.* 2000; Park *et al.* 2002; Lee *et al.* 2005).

1.11 Mechanisms of translocation of cell-penetrable peptides

Translocation across the cell membrane by CPPs takes place through an unidentified mechanism. Two main possibilities exist, that is through endocytosis or via direct passage across the cell membrane. Some early studies (before 2002) have suggested endocytosis of the CPP as the major mechanism based on inhibition of internalization at 4^0C and the reduction in cellular entry in the presence of inhibitors of endocytosis (Vives 2003; Lundberg *et al.* 2003). However, other later studies have suggested that direct penetration through the cell membrane is more relevant because of a lack of effects of temperature alteration and energy dependence mechanisms in CPP translocation (Mitchell *et al.* 2000; Thoren *et al.* 2003). The lack of entry of certain CPP into membrane bound organelles such as mitochondria supports endocytosis as a possible means of cellular entry but it should be kept in mind that different CPPs may get into cells by different mechanisms and it is possible that the some CPPs could enter into different cell types by different mechanisms (Ross & Murphy 2004). Regarding direct penetration into cells by CPPs, there are a few hypotheses as to the exact interaction between CPPs and the cell membrane, including the formation of micelles, the carpet model and the formation of pores. In the former, the CPP causes the membrane to invert into itself so that lipid capsule (micelle) is formed within the membrane and following the trafficking of the micelle across to the opposite side of the membrane, it discharges the CPP with its cargo molecule (Derrosi *et al* 1996; Lundberg & Langel 2003). In the carpet model, the interaction between the CPP and the membrane lipids allows the CPP to glide with the membrane lipids from the outer to the inner face of the membrane (Pouny *et al* 1992; Lundberg & Langel 2003). In the pore model, the CPPs form a membrane pore, similar to

a connexin channel, through which the CPP and cargo passes (Lundberg and Langel 2003). For those CPPs which have been reported to carry cargo molecules into skin, no group to date has addressed whether similar mechanisms of penetration would apply in skin or whether alternative additional transport mechanisms are likely to be relevant.

1.12 A novel new carrier molecule: - Polypseudolysine (PPL)

In collaboration with the Department of Chemistry in the University of Southampton and subsequently with the members of the same group when they moved to Edinburgh, a novel carrier molecule, polypseudolysine (PPL) was developed. This molecule, according to the chemists, is comparatively easy to synthesize and is stable / relatively resistant to degradation. Pseudolysine is structurally different from lysine in that the chain length is slightly longer plus the carbon side chain is linked to an amino group instead of a methyl group as per figure 1.6.

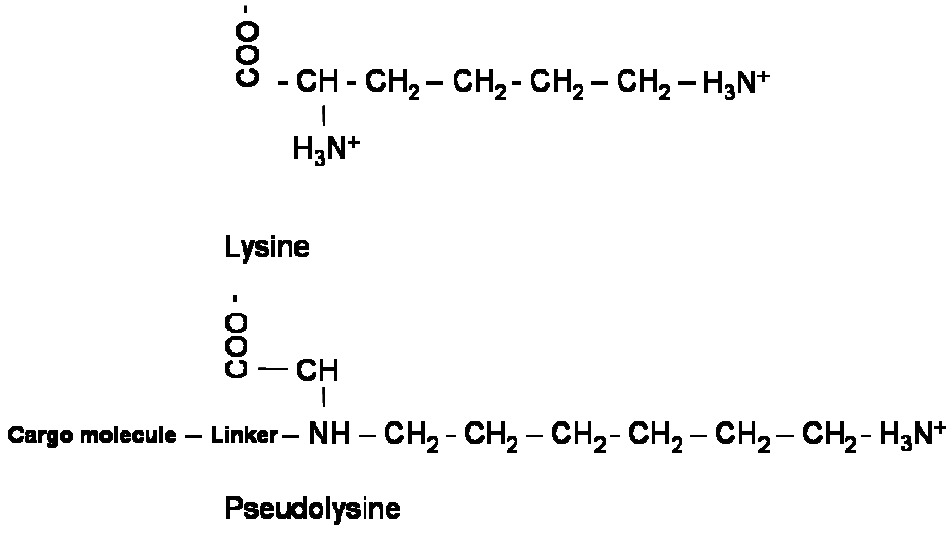

Figure 1.6. Structure of lysine and pseudolysine. The chain length is longer in pseudolysine and the carbon chain is linked to the amino group. The site of cargo molecule attachment also showed in figure.

Both lysine and pseudolysine are positively charged basic molecules at certain physiological condition. PPL consists of seven pseudolysines in which the nitrogen closest to the COO- group of one pseudolysine is covalently bound to the COO- group of the next pseudolysine and the $(CH_2)_6$-NH_2 of each pseudolysine branches off as a side-chain. The cargo molecules used in this thesis were αMSH and antisense compounds targeting tyrosinase and the structures for each compound are shown in the appendix.

1.13 αMSH

αMSH is a tridecapeptide (Ac-Ser-Tyr-Ser-Met-Glu-His-Phe-Arg-Trp-Gly-Lys-Pro-Val-NH_2) derived from the cleavage product of the preprohormone, propiomelanocortin (POMC) peptide. Other cleavage products of POMC are adrenocorticotropic hormone (ACTH), ß- and γ-melanocyte-stimulating hormone, ß-lipotropic hormone and ß-endorphin (see figure 1.7) (Hadley & Haskell-Luevano 1999).

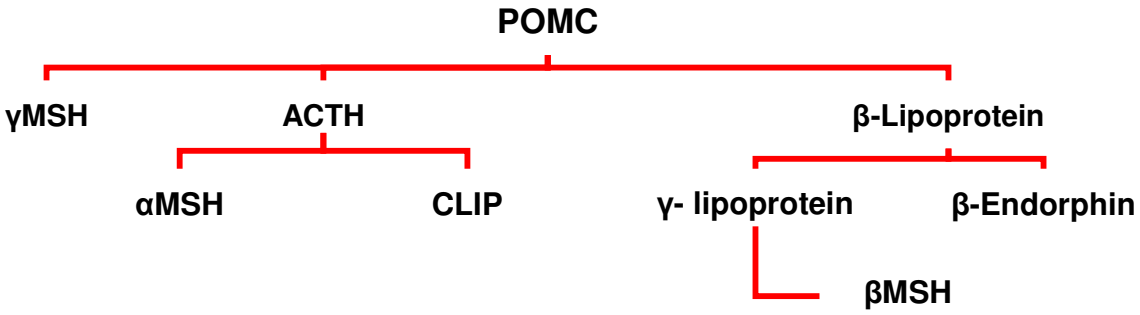

Figure 1.7. POMC derivatives. Synthesis of αMSH and related peptides from POMC.

1.13.1 αMSH and pigmentation

αMSH can stimulate pigmentation (tanning) in human skin (Lerner & McGuire 1961) and could have a potential use as a treatment for post-inflammatory hypopigmentation

and / or inducing a protective tan in some people prior to sun exposure (Barnetson *et al.* 2006). In addition, αMSH has anti-inflammatory and immunomodulatory roles and could have the ability to be employed for skin diseases in which inflammation plays a predominant role (Lipton & Catania 1997; Getting 2002; Donnarumma *et al.* 2004; Cooper *et al.* 2005).

The pigmentary action of αMSH is mediated through the melanocortin 1 receptor (Mc1r / *MC1R*) (Chhajlani and Wikberg 1992; Mountjoy *et al.* 1992; Gantz & Fong 2003)**.** MC1R is a 7 transmembrane G-protein coupled receptor, and is one of five separate melanocortin receptors. These include the ACTH receptor (MC2R), melanocortin-3 (MC3R), melanocortin-4 (MC4R) and melanocortin-5 receptors (MC5-R) (Gantz *et al.* 1993; Roselli-Rehfuss *et al.* 1993; Vamvakopoulos *et al.* 1993; Gantz *et al.* 1994). Both αMSH and ACTH bind to MC1R with the same affinity and activate the receptor (Suzuki et al 1996). As a result of MC1R activation, the activity of tyrosinase, the rate-limiting enzyme in melanin synthesis, is increased and skin pigmentation is promoted by a complex series of reactions in which tyrosine is transformed into a mixture of eumelanin (black) and pheomelanin (yellow) pigment which determines skin colour (Prota & Thomson 1976; Thody *et al.* 1991).

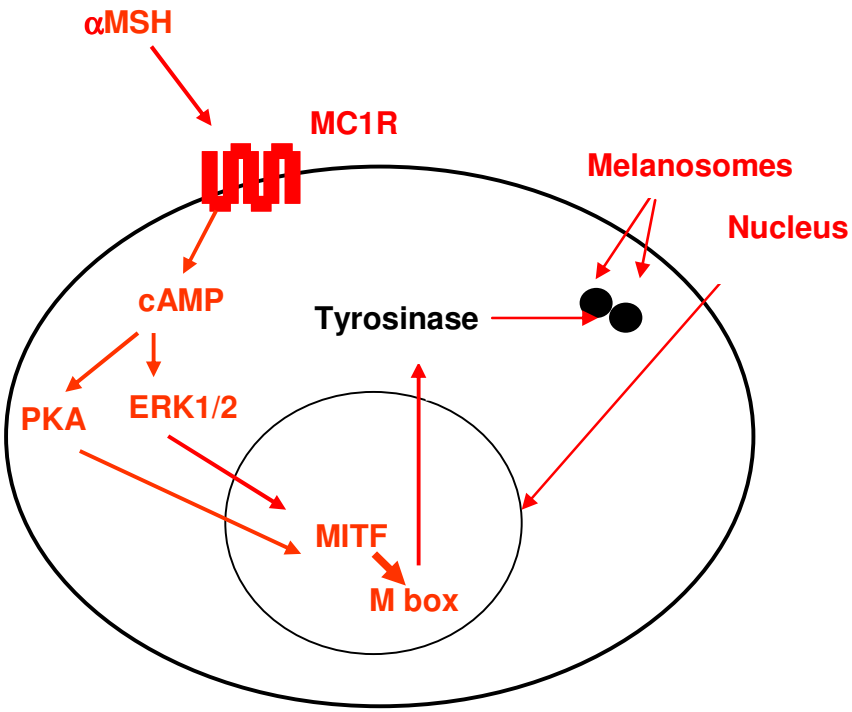

Figure 1.8. MC1R signalling cascade. αMSH binds to MC1R and activates cAMP resulting in activation of protein kinase A (PKA) and MAPkinase signalling pathways, causing microphthalmia (MITF) gene expression. MITF subsequently binds to the promoters (M box) of tyrosinase, TRP1 and TRP2, the synthesised tyrosinase, TRP-1 and TRP-2 then migrates to the melanosomes (in figure only shown tyrosinase) and catalyses the pigmentation reaction (Del Marmol & Beermann 1996).

αMSH and its superpotent analogue Nle4,D-Phe7-alpha-MSH (NDP-αMSH) do not seem capable of penetrating the stratum corneum and entering into skin (J Coyne & E Healy, unpublished data). However, topical application of NDP-αMSH induces a darkening of mouse hair (Hadley *et al.* 1987). It has been reported that topical NDP-αMSH does not penetrate into the skin of rats, thus although the exact mechanism was not investigated in the NDP-αMSH and mouse hair darkening study, it seems likely that the stratum corneum of mice is much thinner than rat skin.

1.13.2 αMSH and anti-inflammatory effects

αMSH mediates its anti-inflammatory function by downregulating proinflamatory cytokines (IL-1, IL-6 and TNF-α) and upregulation of IL-10 (Martin *et al* 1991 Bhardwaj *et al* 1996; Eves *et al.* 2006). In addition, αMSH can inhibit TNF-α induced upregulation of ICAM-1, which plays an important role in controlling immunological and inflammatory reactions by coordinating the intercellular interaction between T lymphocytes and other cells (Hedley *et al.* 1998). Furthermore, αMSH can suppress NF-kB activation induced by various inflammatory agents (Manna & Aggarwal 1998) and can inhibit TNF-α and hydrogen peroxide activated glutathione peroxidase activity (a key enzyme important to ameliorate oxidative stress) (Haycock *et al.* 2000).

1.13.3 αMSH and antimicrobial activity

Many natural antimicrobial peptides, for example defensins and cathelicidins are an important component of the innate immune system and form part of the first response against invading microbial agents (Hancock 2001). In fact, more than 500 different antimicrobial peptides are produced in many tissues/cell types of a range of animal and plant species (Hancock & Scott 2000). The presence of αMSH in the mucosal barrier of the gastrointestinal tract and in the skin means that it could be encountered by many organisms invading into these tissues (Catania & Lipton 1993; Cutuli *et al.* 2000; Catania *et al.* 2006). Indeed, many investigations have suggested that αMSH has antimicrobial effects. For example, αMSH and its terminal peptide (KPV) showed inhibitory activity against *Staphylococus aureus* and *Candida albicans* at a wide range of concentrations including at the normal plasma concentration (picomolar) of αMSH (Catania *et al.* 2000;

Catania *et al.* 2006). Furthermore, a recent study has shown that αMSH reduces the internalisation of *Staphylococcus aureus* in human keratinocyte cell lines (Donnarumma *et al.* 2004). However, the ability of αMSH to kill *Staphylococus aureus* is low in comparison with penicillins and so αMSH alone would not be a useful exogenous treatment for infections with this organism.

1.14 Antisense agents

Oligonucleotides (ONs), small interference RNA (siRNA) and peptide nucleic acids (PNA) are examples of some commonly used antisense agents which interfere with gene function. ONs are small single stranded DNAs which, upon internalisation, bind to the complementary strand of DNA / RNA to inhibit gene expression (Stephenson & Zamecnik 1978). For an antigene application, an ON must enter the cell nucleus, bind to the target strand of DNA thereby inhibiting transcription (McShan *et al.* 1992). However, for an antisense strategy the ON forms a duplex with a specific mRNA sequence in the cytoplasm and then prevents its translation (Stephenson & Zamecnik 1978; Braasch & Corey 2002). The efficacy of an ON depends upon its design. The length and ratio of purine and pyrimidine bases in its structure are critical factors for an optimum efficacy. For example selective inhibition of mutant Ha-ras mRNA expression by a ON was correlated with ON length in which those less than 15 nucleotides in length showed less activity, and ONs larger than 14 nucleotides gave good inhibition (Monia *et al.* 1992). Furthermore, Flanagan *et al* showed that a decrease in length of an ON from 13mer to 9mer significantly reduced (from 54 % to 10%) the luciferase enzyme activity in a tetracycline-responsive promotor (Flanagan *et al.* 1996). PNA is a DNA analogue, first

developed by Nielson and co-workers in 1991, in which the deoxyribose sugar and phosphate backbone is replaced by a peptide backbone (uncharged N-(2-aminomethyl)-glycine) to which the purine / pyrimidine bases are attached by methylenecarbonyl linkers; figure 1.9 (Nielsen *et al.* 1991).

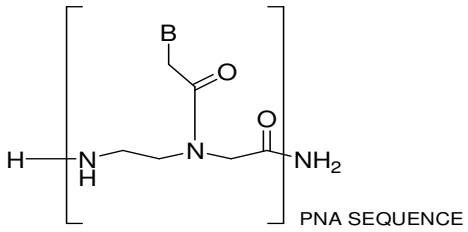

Figure 1.9. Structure of PNA. PNA is a DNA analogue in which the phosphate deoxyribose backbone is replaced by uncharged N-(2-aminomethyl)-glycine. B is nucleotide base.

The most commonly used target site for the antisense activity of ONs or PNA is the translational start region of the mRNA. For example, Sun *et al* showed that a PNA targeted to the translational start site, or to a sequence nearby to this site, of the *n-Myc* oncogene resulted in maximum inhibition of proliferation of IMR32 (human neuroblastoma) cells, whereas a PNA against the middle of the coding region caused no inhibition (Sun *et al.* 2002).

A pharmacokinetic study has suggested that an ON has very short plasma half-life (30 minutes to 1 hour) following intravenous injection into mice (Agrawal *et al.* 1991). During systemic administration the ON localises to the liver, kidney, bone marrow and the spleen to a greater extent compared to other organs and the primary mechanism of ON clearance is via tissue metabolism and cleavage by nucleases (Temsamani *et al.* 1992; Yu *et al.* 2001). Although the urinary elimination of ON is not the principal pathway for its clearance, its excretion in urine seems dose dependent, which is evident

by a study performed by Yu *et al*, where an increase in urinary excretion of ON from 3 to 29% was observed after 24 hours when an intravenous dose of ON in mice was increased from 5 to 50mg/kg (Yu *et al.* 2001). Furthermore, the tissue distribution of an ON following intraperitonial or subcutaneous injection is similar to that following intravenous injection, however the plasma concentrations of an ON are higher when given intravenously (Agrawal *et al.* 1995). As compared to unmodified ON, PNA seems to be a more stable compound, and its binding affinity to a complementary DNA sequence was reported to be two fold higher than for a ON (Nielsen *et al.* 1991). A study by McMohan *et al* reported that 2 hours after intraperitoneal injection into rat, PNA was detected (amount in decreasing order) in the kidney, liver, heart, brain and spleen and 90% of the dose was recovered from urine as unchanged PNA after 24 hours of injection (McMahon *et al.* 2002). Unmodified negatively charged ONs and non-charged PNAs are not able to penetrate the cell membrane and skin (Chan *et al.* 2006), therefore a variety of delivery techniques (eletroporation, liposomes and CPPs) have been employed to enhance cellular (and skin) uptake (Pooga *et al.* 1998; Hamilton *et al.* 1999; Shammas *et al.* 1999). Although, CPPs have been shown to be able to deliver PNA into various cells (see table 1.3), to date no one has investigated the ability of a CPP to transport PNA into skin.

1.15 Tyrosinase

Tyrosinase is a key enzyme for the biosynthesis of melanin, and is encoded by the tyrosinase gene which is located at the c locus of mouse chromosome 7 and chromosome number 11 in the human (Barton *et al.* 1988). Tyrosinase plays an important role in visible colour of the skin and hair (Kwon *et al.* 1988). For example, a mutation in this

gene results in a lack of pigmentation (albino phenotype), whereas introduction of a functional tyrosinase gene into fertilized eggs of albino mice rescues the albino phenotype (Kwon *et al.* 1987; Beermann *et al.* 1990). Albino mice have a normal life span (similar to wild type mice), however loss of tyrosinase function is associated with visual abnormalities including an underdeveloped central retina and an abnormal pattern of connections between the eyes and the brain. The tyrosinase enzyme plays an important role in normal retinal development as confirmed by a tyrosinase transgenic animal model which exhibited a correction of all visual abnormalities associated with the albino phenotype (Gimenez *et al.* 2004). Oculocutaneous albinism type 1 (OCA1) in humans is caused by a loss of function mutation in the tyrosinase gene and is further subdivided into OCA1A, characterised by no tyrosinase or inactive tyrosinase with an absence of pigment from birth which continues throughout life (Halaban *et al.* 2000; Giebel *et al.* 1991), and OCA1B showing different levels of ocular and cutaneous pigment depending on the rate of partial activity of the tyrosinase enzyme (Giebel *et al.* 1991). More than 100 mutations of the tyrosinase gene have been reported to associate with albinism, in which missense mutations are very common (Giebel *et al.* 1991). In the normal wild type pigmentation phenotype, following synthesis and post synthesis modification in the endoplasmic reticulum, the tyrosinase enzyme migrates through the trans-golgi network to the melanosome, where melanin synthesis takes place. In OCA1, the trafficking of tyrosinase from the endoplasmic reticulum to the melanosomes is disrupted and immature tyrosinase is retained in the endoplasmic reticulum (Halaban *et al.* 2000).

A number of natural (flavonoids, kojic acid) and synthetic (captropril, hydroquinone, arbutin, aloesin) tyrosinase inhibitors exist, some which can depigment cells *in vitro* and

some which can reduce skin colour *in vivo* (Solano *et al.* 2006). However, hydroquinone is cytotoxic, arbutin contain a hydroquinone moiety in its structure which may cause toxicity over long term use and the *in vivo* efficacy of kojic acid is still under investigation (Kasraee *et al.* 2004). Targeting tyrosinase using an antisense approach could potentially be used to decrease mammalian pigmentation *in vivo* because Boonanuntanasarn *et al* showed that injecting morpholino oligonucleotides (targeted to the translational start site of tyrosinase) into trout embryos resulted in a significant decrease in tyrosinase activity and reduced levels of pigmentation in the skin and eye (Boonanuntanasarn *et al.* 2004).

1.16 Aims of this study

Based on the relative scarcity of topical agents for skin diseases, and based on the reported ability of some CPPs to carry cargo molecules into skin, the ability of PPL to transport agents into cells and skin has been investigated in this thesis. The ability of this carrier molecule to deliver molecules across other epithelial barriers was also analysed in this thesis. Specifically the aims were

1) To determine whether PPL could carry a hormone peptide, αMSH, into cells, skin and through other epithelial barriers (gut, eyes and trachea).

2) To examine whether the covalent addition of PPL to αMSH affects the function of αMSH.

3) To investigate whether PPL could transport antisense molecules targeted against tyrosinase into cells, skin and across other epithelial barriers.

4) To identify whether PPL-conjugated anti tyrosinase agents could inhibit melanin

pigmentation.

Chapter 2: Materials and Methods

2.1 Chemical compounds, synthesis and purity

For this project, chemical synthesis and conjugation of αMSH and antisense compounds with PPL was carried out in collaboration with Prof Mark Bradley (initially in the the Department of Chemistry, University of Southampton and later in the Department of Chemistry, University of Edinburgh). The αMSH compounds used are as follows – for detailed structure see appendices.

1. αMSH-PPL[98] (see A.1.6 in appendix)
2. Fluorescein-αMSH-PPL[98] (see A.1.7 in appendix)
3. αMSH-PPL[99] (see A.1.8 in appendix)
4. αMSH-PPL[99]-Fluorescein (see A.1.9 in appendix)
5. Fluorescein-αMSH (see A.1.2 in appendix)
6. αMSH (see A.1.1 in appendix)

The PPL molecule was linked to αMSH in two different ways using two different linkers, therefore these compounds were given separate names, PPL[98] and PPL[99]. In the case of PPL[99], a lysine molecule was used to link αMSH to the PPL, whereas PPL[98] linked to αMSH using a 6-aminohexanoic acid linker. In addition, fluorescein molecule was linked to N-terminal of αMSH in case of Fluo-αMSH-PPL[98], whereas in αMSH-PPL[99]-Fluo it was linked to PPL. The following PNA and ON compounds were used to target the translational start sites of the tyrosinase mRNA – for detailed structure see appendices.

1. PNA; including 15mer, 12mer and 9mer PNA (see A.1.12 in appendix)
2. 15mer PNA-S-PPL, where S is a sulphide linker (see A.1.18 in appendix)

3. 15merPNA-SS-PPL, where SS is a disulfide linker (see A.1.17 in appendix)
4. 15mer PNA-M-PPL, where M is a maleimide linker
5. 19merON (see fig 4.1 in chapter 4)
6. 19merON-S-PPL (see A.1.11 in appendix)
7. 19merON-SS-PPL (see A.1.10 in appendix)
8. PNA-PPL; including 15mer, 12mer and 9mer PNA directly linked to PPL (see A.1.14 in appendix)
9. Fluo-PNA; including 15mer, 12mer and 9mer PNA (see A.1.13 in appendix)
10. Fluo-PNA-PPL; including 15mer, 12mer and 9mer PNA directly linked to PNA (see A.1.15 in appendix)

All the compounds used in this study were synthesized (initially in the Department of Chemistry, University of Southampton and later in the Department of Chemistry, University of Edinburgh) using solid phase chemistry and further purified by high performance liquid chromatography (HPLC) by Antonio M Fara as a part of his doctoral thesis (Submitted at University of Ediburgh). Some of this work has been published (Fara MA et al 2006).

2.2 Cell lines

The following cell lines were used in the investigations; - S91 Cloudman mouse melanoma cell line (American type culture collection, ATCC), B16F10 mouse melanoma cell line (kindly gifted by Dr. Dott Bennett, United kingdom), B16G4F mouse melanoma cell line (kindly gifted by Prof. Alex Eberle, Switzerland) which is amelanotic, B16UWT-3 which is a human MC1R transfected B16G4F cell line (transfection carried

out by Dr Sam Robinson), RPMI 7951 human melanoma cell line (ATCC), HaCaT human keratinocyte cell line (kindly gifted by Norbert Fusenig), HEK-293 human embryonic kidney cell line (kindly gifted by Dr. Paul Lambden, Southampton) and HT1080 human fibrosarcoma cell line (kindly gifted by Dr. Markus Bohm, Germany).

2.3 Cell culture

S91, B16G4F, B16F10, HaCaT and HEK-293 cells were cultured in Dulbecco's Modified Eagle Medium (DMEM) (Invitrogen, Paisley,UK) with 10% heat inactivated foetal bovine serum (FBS) (Invitrogen, Paisley,UK), 2mM L-Glutamine, 100 U/mls penicillin and 100 µg/mls streptomycin at 37^0C and 5% CO_2. Whereas the B16UWT-3 cell culture medium and conditions were the same as the above, geniticin (1.5 mg/mls) was added in order to prevent any untransfected cells proliferating; geneticin is an analogue of neomycin and is commonly used for selection of cells which have been transfected with DNA containing a neomycin resistance plasmid. HT1080 cells were cultured in similar conditions as above except that Roswell Park Memorial Institute (RPMI-1640) medium (Invitrogen, Paisley,UK) was used instead of DMEM.

Once the cells reached 60-70% confluency they were dissociated from the flask ($75cm^2$) using 2mls of non-enzymatic 1x cell dissociation solution prepared in Hanks' balanced salt solution (containing EDTA, glycerol and sodium citrate, without calcium and magnesium; Sigma-Aldrich, Dorset, UK). Complete medium (cell culture medium with FBS and antibiotics) was added to the subsequent cell suspension and the solution transferred into 15mls falcon tubes. Cell counts were performed using a haemocytometer. In some experiments with fluorescein labelled compounds, cells were dissociated with

0.05% trypsin-0.02% EDTA solution (Invitrogen, Paisley, UK) because trypsin is more effective in removing non-internalised, surface bound fluorescencent compound (Mai *et al.* 2002); trypsin is a proteolytic enzyme which in combination with the chelating agent EDTA (which removes divalent cations such as calcium and magnesium) dissociates the cells from flasks and wells.

For storage of cells at -80^{0}C, following dissociation with non-enzymatic cell dissociation solution, the cell suspension was centrifuged at 120 x g for 5 minutes to pellet the cells. The supernatant was discarded and the cell pellet (from 75cm^2 flask) was dissolved in 1mls FBS containing 10% DMSO (Sigma-Aldrich, Dorset, UK). Cells were stored in 500µl aliquots at -80^{0}C.

2.4 Melanin assay

S91 cells were seeded at 4 x 10^4 cells per well in 6-well plates. The compounds were added to triplicates wells and the plates incubated for 5 days at 37^{0}C. Cell numbers were counted on the 5th day of culture following detachment with cell dissociation solution. The cells were transferred into 1.5ml ependroffs and centrifuged at 800 x g for 5 minutes. Supernatants were discarded and the cell pellets containing the intracellular melanin were dissolved in 200 µl of 0.1N NaOH. The suspension from each eppendorf was then transferred into a single well of a flat bottomed 96-well plate. The melanin content was determined spectrophotometrically at 450nm and 500nm and compared against a series of dilutions of standard mushroom melanin (Sigma-Aldrich, Dorset, UK) in 0.1N NaOH.

2.4.1 Melanin assay for antisense investigation

B16F10 cells were seeded at 2 x 10^4 cells per well in 12-well plates. Cells were treated with the tyrosinase antisense compounds in the presence or absence of αMSH (10^{-10}M) for 48 hours. The remaining protocol for the assessment of the intracellular melanin was the same as for the pigmentation assay above.

2.5 Ligand binding assay

B16UWT-3 cells were seeded in 96-well plates at 4 x 10^4 cells per well and incubated at 37^0C overnight to allow the cells to attach to the wells. The following day, the cells were washed with 1 x binding buffer (see solutions section in appendix), and incubated for 2 hours at room temperature with 50µl of binding buffer containing 15,000 count per minute of ^{125}I-NDP-αMSH (Nle^4, D-Phe^7-α-melanocytes stimulating hormone), and a series of incremental concentrations of unlabelled ligand for competition binding assays. The cells were washed twice with 200µl of ice cold binding buffer and lysed using 100µl of 0.1 N NaOH. The lysates were transferred to tubes containing 900µl of 0.1N NaOH. Radioactivity was counted using an auto-Gamma Counter (Packard Bioscience Ltd., UK) and the data analysed using the Graphpad package (Graphpad Software, Inc. San Diego, USA).

2.6 Fluorescence and Confocal microscopy

2.6.1 Fixed cells

To ensure a similar level of cell confluency at the time of addition of the investigational compounds, cells were seeded at 1 x 10^5 cells per well for 3 hours exposure to the compounds or 5 x 10^4 cells per well for 24 hours exposure. Cells were seeded onto poly-

L-lysine (1% w/v) (Sigma-Aldrich, Dorset, UK) coated coverslips (16mm), which had been placed into each well of 12-well plates, and incubated overnight at 37^0C with 5% CO_2. The following day the culture medium was removed and cells were washed twice with PBS prior to being incubated with the various concentrations of the investigational compounds for the desired time points. Following treatment with the test compounds, the culture medium was taken off and the cells washed twice with PBS. Cells were fixed with 4% paraformaldehyde (PFA) for 7 minutes. The PFA was removed and 50mM of ammonium chloride was added for 10 minutes to stop fixation followed by two washes with PBS. Coverslips containing fixed cells were inverted onto 100µl of the nuclear counterstain TO-PRO-3 (diluted 1 in1000) (Invitrogen, Paisley, UK) on a sheet of parafilm and incubated at room temperature for 5 minutes. The coverslips were then washed twice (cell side up) in a clean well of a 12-well plate with PBS, before being mounted onto a slide (with cells facing downward) containing a small drop of vectashield (Vector Laboratories, Ltd Peterborough, UK) which is a transparent non-fluorescent mountant with fluorophore protective action (the latter prevent the samples from photo bleaching as a result of exposure to a light source). Each coverslip was sealed to the glass slide using clear nail varnish which was applied to the edge of the cover slip. Cells were visualized on a Leica SP2 laser scanning confocal microscope or by fluorescence microscopy. Confocal images were captured at different magnifications (40x, 63x and 100x) with resolution 1024 x 1024 pixels and 400Hz laser speed. Three dimensional (3D) images were generated by capturing individual cross sections every 1µm (4 repeat scan, setting Airy 1) throughout the Z plane of the samples . The middle image of the Z series

was selected for evaluation of penetration. The excitation and emission spectra of fluorescein was 488 and 530nm respectively.

2.6.2 Live cells

Cells were seeded at a density of 1 x 10^5 cells on poly-l-lysine coated coverslips in the wells of a 12-well plate and incubated overnight at 37^0C with 5% CO_2. The following day cells were treated with fluorescein labeled compounds for a required time. After exposure to the compounds for a desired time point, cells were washed three times with PBS and immediately analysed for penetration using a water immersion lens (50x magnification) on a Leica SP2 laser scanning confocal microscope.

2.7 Toxicity investigations

2.7.1 Lactate dehydrogenase assay

Cell cytotoxicity was determined using a lactate dehydrogenase (LDH) kit (Roche Applied Bioscience, East Sussex, UK). LDH is a stable cytosolic enzyme which is released upon cell lysis or from leaky cells. Cells were seeded at 2 x 10^4 cells per well in 96-well plates and incubated overnight at 37^0C with 5% CO_2. After overnight incubation the culture medium was taken off and cells washed twice with PBS to remove the LDH released during the incubation period. The test compounds in fresh culture medium were added to triplicate wells for the desired time points. Triplicate wells were also set up for background control (culture medium, no cells), low control (cells, but no investigational compound) and high control (cells with 100µl of 1% Triton X-100 (to kill all the cells)). Following exposure to the test compounds, 100µl of supernatant from each well was

transferred into an optically cleared flat bottom 96-well plate. The LDH reaction mixture was prepared; this contained a dye solution (iodotetrazolium chloride (ITN) and sodium lactate) and the catalyst (Diaphorase/NAD^+). 100µl of this LDH reaction mixture was added to the wells containing the cells and the plate was incubated for 30 minutes at room temperature in the dark. The plate was then read at 490nm using an ELISA plate reader (spectra Max 340 pc, Molecular device, UK) to obtain the released LDH values for the cells under investigation. The cytotoxicity result was calculated from the LDH values as follows:

$$\% \text{ Cytotoxicity} = \frac{\text{Experimental value} - \text{low control}}{\text{High control} - \text{low control}} \times 100$$

2.7.2 Flow cytometry (FACS) analysis for dead cells

Cells were seeded at 1x 10^5 cells per well in 6-well plates and incubated overnight. The following day cells were treated with different concentrations of the investigational compounds for various time points. Following treatment, the culture medium was removed and cells washed twice with PBS. Cells were dissociated with 0.05% trypsin-0.02% EDTA solution and after detachment, fresh culture media containing FBS was added to stop the trypsin reaction. Cells were washed twice in PBS and pelleted at 170 x g for 5 minutes. The cell pellets were dissolved in 300µl of FACS buffer (see solutions section in appendix) and 5µl (50µg/mls) propidium iodide was added; propidium iodide, a red fluorescence nuclear dye which is excluded by live cells, was used to detect dead cells within the whole population. Cells (10,000 events) were analysed using a Becton

Dickinson FACS caliber flow cytometer. The excitation and emission spectra of propidium iodide was 488 and 617nm respectively.

2.7.3.Toxicity analysis following ultraviolet radiation (UVR)

Cells were seeded at 1 x 10^5 cells per well in 6-well plates and cultured until they reached 60-70% confluency. Cells were then pretreated with different concentrations of the test compounds and incubated overnight at 37^0C. The following day culture medium was removed and kept in separate ependroffs, the cells were then washed twice with PBS and irradiated with UVR (735mJ/$cm^2$of UVR) in 1ml PBS using a TL12 lamp (emitting a broad spectrum (280-360nm) of UVB and UVA). After UVR irradiation, the cells were washed with PBS and the same culture medium (in which cells were grown before UV irradiation and containing the same investigational compound) added back into the respective wells. The cells (10,000 events) were further incubated for either 4 hours or 24 hours before carrying out the toxicity analysis using propidium iodide as a marker of cell death as per section 2.7.2.

2.8 Quantification of half life of fluorecsceinated compounds *in vitro*

To assess the half life of the fluoresceinated compounds within cells, cells were incubated with the fluorophore conjugated compound for 3 hours. Following this, the culture medium was removed, the cells washed twice with PBS, and then placed into fresh media for various time points (3 hours – 24 hours). At the end of each time point, cells were washed twice with PBS and dissociated with 0.05% trypsin-0.02% EDTA solution. The dissociated cells were transferred into FACS tubes, washed twice with PBS and pelleted at 170 x g for 5 minutes. The cell pellets were resuspended in 300µl of FACS buffer (see

solutions section in appendix) and analysed (10,000 events) for fluorescence using a FACS caliber (Becton Dickinson). FACS data were analysed using Win MDI5.8 computer software (Variety House Software, Inc). The excitation and emission spectra of fluorescein was 488 and 530nm respectively.

2. 9 FACS analysis to determine presence of the compounds

Cells were seeded at 1 x 10^5 cells per well in 6-well plates and incubated overnight to allow the cells to attach. The fluorescein labelled compounds were added to the cells for various time points. Following this treatment, cells were washed twice with PBS and dissociated with 0.05% trypsin-0.02% EDTA solution. The cells were transferred to FACS tubes and analysed as per section 2.8. The excitation and emission spectra of fluorescein was 488 and 530 respectively.

2.10 Lymphocyte transformation test (LTT)

2.10.1 Isolation of peripheral blood mononuclear cells (PBMC)

Venous blood from healthy volunteers was collected in vacutainer tubes containing tri-potassium EDTA (BD Biosciences, Oxford UK). To isolate PBMCs, 10ml of venous blood was layered onto 10mls of lymphoprep (Axis-Shield, Cambridgeshire, UK). Tubes were centrifuged at 500 x g for 20 minutes. Following centrifugation the intermediate (middle layer) "buffy" coat containing the PBMCs was transferred to another tube and diluted in 5 volumes of PBS. Cells were washed twice in ice cold PBS by centrifugation at 170 x g for 7 minutes. The PBMC pellet was resuspended in RPMI 1640 medium (Invitrogen, Paisley, UK) enriched with L-glutamine and supplemented with 5% heat-

inactivated human AB serum (Sigma-Aldrich, Dorset, UK), 100 U/mls penicillin, 100 µg/mls streptomycin, and 1% sodium pyruvate (Invitrogen, Paisley, UK)

2.10.2 PBMC / lymphocyte proliferation (LTT) assay

1.4 x 10^6 cells/ml per well were seeded into 48-well plates and incubated with various concentrations of the investigational compounds (in triplicate wells). By way of a positive control PBMCs were also stimulated by the addition of the streptococcal antigen mixture, streptokinase-streptodornase (SK/SD; 0.5/0.125 U/mls) (Phoenix Pharmaceuticals, Karlsrule, Germany) or phytohemagglutinin (PHA-P; 4µg/mls) (Sigma-Aldrich, Dorset, UK). Cells were cultured for 6 days during challenge with SK/SD or for 3 days during challenge with PHA-P. Lymphocyte proliferation was assessed by the incorporation of ^{3}H-thymidine which was added for last 6 hours of the culture period. Proliferation was quantified using a gamma scintillation counter and expressed as count per minute (cpm).

2.11 *Ex vivo* skin penetration assay using a Franz diffusion chamber

In this study a home office licence was not required to use mouse skin as it was collected after killing (schedule 1 killing), which was carried out under home office regulations. Regarding the pig skin, there was no ethics required as we used skin from pigs that had been euthanased for other reasons. Human skin was collected after surgical removal under approval of generic trust ethics committee to the Dermatopharmacology department, covering excess tissue which would otherwise be disposed of.

Special minaturised Franz diffusion chambers were obtained through Dr Marc Brown, King's College London; his group have studied the penetration of schistosomiasis into skin and thus he had links with an in-house technician who manufactured Franz diffusion

chambers (Bartlett *et al* 2000). The Franz diffusion system is composed of two parts, the upper donor compartment and the lower receptor compartment. In order to set up a Franz' chamber experiment, cell culture medium (DMEM) was added to the receptor compartment. To hold the skin tightly in the chamber, two polytetrafluoroethylene (PTFE) coated rubber rings of 6mm diameter with a small hole (2.5mm) in the centre and two rubber 'O' ring (6mm diameter) were prepared; note that the PTFE rings are generally resistant to a wide variety of chemicals and are used to prevent leakage around the side of the skin and contamination of the lower compartment. Skin (6mm diameter) was placed in between the two PTFE rings, with the epidermal surface facing towards the donor chamber. The donor and recipient chamber were held together by two springs, one on each side (see figure 2.0). The fluorescinated compounds were added (20µl) to the donor compartment, i.e. onto the outer epidermal surface of the skin. Note that skin from mice and pigs was excised and used immediately following euthanasia; however, human skin was kept in physiological saline for up to 4 hours during transport from the dermatology department in the Royal South Hants hospital to the laboratory in Southampton General Hospital.

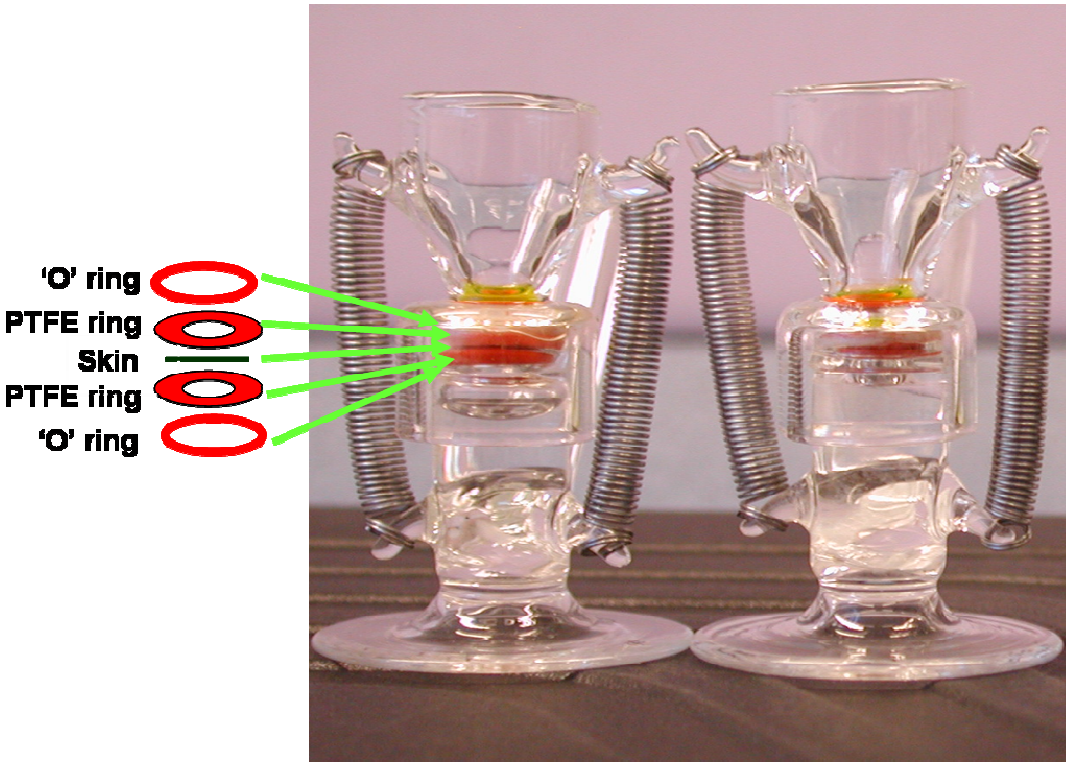

Figure 2.0 Franz's diffusion chamber set up. The Franz's diffusion chamber skin penetration system consists of two parts, the upper donor chamber and the lower recipient chamber. Skin (with the epidermis facing towards the donor chamber) was mounted in between two polytetrafluoroethylene (PTFE) coated rubber rings and 'O' rings as shown in the figure. Fluoresceinated compounds were added to the donor chamber.

Because of the limited size of the hole in the PTFE rings, the diffusion of the investigational compound takes place only in the central exposed area of the skin, by moving through the epidermis and into the dermis (i.e. from the donor chamber towards the recipient chamber). After treatment with the investigational compounds, the skin samples were washed three times with PBS before gently removing from the chamber and then bisected vertically. One half of skin was snap-frozen in liquid nitrogen for cryosection and the other half was fixed in 4% PFA (3 hours) for paraffin embedding. Following paraffin embedding, 4μm sections of skin were cut on a microtome and air

dried on aminopropyltriethoxysilane (APS)-coated slides at 37^0C for 24 hours. Sections were then deparaffinised by two changes of xylene (5 minutes each), transfered to 100% ethanol for 5 minutes and then 70% ethanol for 5 minutes. After evaporation of ethanol, the skin section were then mounted in Vectashield and visualized under a fluorescence microscope. Skin sections were analysed and graded visually as (i) no, (ii) very weak, (iii) weak, (iv) moderate, (v) strong and (vi) very strong penetration.

2.12 *Ex vivo* gut, trachea and eye penetration studies.

The eye, ileum, colon and trachea were also chosen for *ex vivo* penetration studies. These organs were taken after healthy mice were sacrificed as per "schedule one" cervical dislocation; the organs were carefully excised to avoid accidental damage of the tissues. Following excision, the ileum and colon were cut into small pieces (approximately 2 cm) and then washed thoroughly with 1 x PBS to remove undigested food and faeces. Trachea was separated from lung and washed with PBS. One end of the colon, ileum and trachea was tied with a surgical suture and the investigational compound (5µl) was placed in the centre of the tube from the other open end. Then, the open end was also closed with a surgical suture and the organ was incubated for a required time in complete medium (DMEM with serum and antibiotics) at room temperature. Following treatment with the investigational compound, one suture was removed and the organ was flushed with the PBS to wash the tube thoroughly. The organs were then either fixed in 4% PFA for 3 hours or snap-frozen in liquid nitrogen. The paraformaldehyde fixed organs were embedded and blocked in paraffin and 4µm sections were cut for further analysis; the remaining protocol for deparaffinisation is similar to that in section 2.11. Frozen tissues

were cut as 8µm sections and dried for 1 hour at room temperature. The sections were then mounted in Vectashield and visualised under a fluorescent microscope.

For assessment of penetration of the investigational compounds into the eye, the eyes were excised from the orbit of the euthanased healthy mice. Immediately after excision, the eyes were placed (cornea facing downward) in the respective wells of a round bottom 96-well plate containing 5µl drug and left at room temperature for the required time. Following this the eyes were washed with PBS by transferring them along a series of wells (4-6) containing PBS. After washing, the eyes were either fixed in PFA for 3 hours or snap-frozen in liquid nitrogen. The remaining protocol for deparaffinisation and/or visualisation under fluorescence microscopy was as for the skin (section 2.11) and the other internal organs (see above).

2.13 Western blotting

2.13.1. Protein sample preparation

Cells were grown in T175 flasks until 60-70% confluency was obtained. Cells were washed twice with PBS and detached from the flask using cell dissociation solution (3mls). Cells numbers were adjusted to 1 million cells/ml and pelleted by centrifugation at 800 x g for 5 minutes. The cells were lysed with 100µl lysis buffer (see solutions in appendix) and the protein concentration was estimated using a Bio-Rad Dc protein assay kit (Bio-Rad, Hertfordshire, UK) as per the manufacturer's instructions.

2.13.2 SDS-polyacrylamide gel preparation and electrophoresis

SDS-polyacrylamide gels (10%) were prepared and mixed in the following proportions; 2.5mls of 40% acrylamide (Sigma-Aldrich, Dorset, UK), 2.0mls of separating buffer (2.0 M Tris-HCl, pH 8.9), 100µl of 10% (w/v) SDS and 4.38mls of dH_2O. Polymerisation was initiated by adding 18.75µl TEMED (Sigma-Aldrich, Dorset, UK) and 1ml (50mg/10mls) ammonium persulphate (Sigma-Aldrich, Dorset, UK).

Stacking gels were prepared using 500µl of 40% acrylamide (Sigma-Aldrich, Dorset, UK), 0.5mls of stacking gel buffer (0.5 M Tris-HCl, pH 6.7), 50µl of 10% (w/v) SDS and 3.46mls of dH_2O. The stacking gels were polymerised by adding 12.5µl TEMED (Sigma-Aldrich, Dorset, UK) and 500µl of 50mg/10mls (w/v) ammonium persulphate (Sigma-Aldrich, Dorset, UK). 50µl of denatured loading buffer (see solutions section in appendix) was added to the 100µl protein samples, heated at 100^{o}C for 5 minutes and then the samples were loaded into the wells; pre-stained full range Rainbow molecular weight markers (GE Healthcare, Bukinghamshire, UK) were also loaded into one well for estimation of molecular size of positive bands on the subsequent Western blot. Gels were subjected to electrophoresis at 0.02A for 60-90 minutes until the dye front reached the bottom of the gel.

2.13.3 Immunoblotting

Following electrophoresis, the semi-dry samples were electrotransferred (at 25V and 0.18A for 30 minutes) from SDS-PAGE gels onto hybond ECL nitrocellulose membrane (GE Healthcare, Bukinghamshire, UK). After transfer the membrane was washed with Tris-buffer saline (TBS) (0.02M tris, 0.5M NaCl, pH 7.5) for 5 minutes and subsequently

in 20mls 5% (w/v) dried milk powder (Marvel) in TBS containing 0.05% Tween 20™ (GE Healthcare, Bukinghamshire, UK) for 1 hour at room temperature with gentle agitation. Membranes were incubated with the primary antibody in 20mls of TBS containing 0.05% Tween 20™ and 5% (w/v) milk powder at room temperature for approximately 1 hour with gentle agitation. Membranes were then washed three times for 5 minutes each in TTBS (TBS containing 0.05% Tween 20) and then incubated with the appropriate secondary antibody conjugated with horseradish peroxidase. Following secondary antibody incubation, the membrane was washed three times for 5 minutes each in TTBS and kept moist until detection.

The membrane was incubated with freshly prepared ECL plus western blotting reaction mixture (GE healthcare, Buckinghamshire, UK), which causes a light signal from the reporter molecule when in contact with the horseradish peroxidise on the secondary antibody. Photographic film was used to detect the light; this detection system resulted in dark bands on the photographic film at the site of light production (i.e. at the site adjacent to the secondary antibody/primary antibody/protein complex).

2.14 Tyrosinase assay

This protocol is adapted from Dutkiewicz R *et al* (Dutkiewicz *et al.* 2000). Tyrosinase actvity was measured spectrophotometrically based on its DOPA oxidase activity which caused the oxidation of L-DOPA to dopaquinone. In the presence of 3-methyl-benzothiazolinonehydazone (MBTH) (Sigma-Aldrich, Dorset, UK), dopaquinone forms a pink product with absorbance at 505nm.

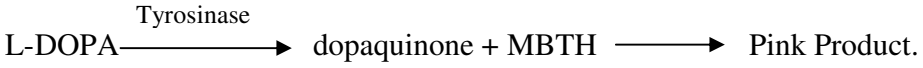

For this assay, cells were seeded at 5 x 10^3 per well in 96-well plates. Test compounds were added to the respective triplicate wells and the plate was left in the incubator for the required time point. Cells were then washed twice with PBS and lysed with 20µl of 50mM sodium phosphate buffer (Na_2HPO_4 + NaH_2PO_4, pH 6.9) containing 0.05% Triton X-100. The cells lysates were frozen at -80^{0}C until further analysis. In order to determine tyrosinase activity, the cell lysates were thawed at room temperature for 25 minutes, then incubated at 37^{0}C for 5 minutes. 180µl of freshly prepared reaction mixture (6.3mM MBTH, 1.1 mM L-DOPA in 48mM sodium phosphate buffer at pH 7.1) containing 4% v/v N,N'-dimethylformamide was added to 20µl of cell lysate. The kinetic study of tyrosinase activity was performed spectrophometrically by measuring absorbance at 508nm over 60 minutes at a constant temperature of 37^{0}C. A final absorbance value at 1 hour was used to compare tyrosinase activity between samples and also to compare against the activity of standard mushroom tyrosinase (Sigma-aldrich, Dorset, UK).

2.15 Anti-microbial activity measurement

S. aureus (all strains) were grown on supplemented proteose-peptone agar (see appendix section) incubated at 37^{0}C in air containing 5% (vol/vol) CO_2. The next day "a loop of bacterial colony" was taken from the subculture plate and dissolved in 1ml of PBS to make a bacterial suspension for spectrophotometric reading. Spectrophotometric readings allowed the estimation of the bacterial concentratioin and were taken to enable a

suspension of 1 x 10^7/ml colony forming units (cfu) of bacteria to be made. In each well of a 12 well plate, 100µl of 1 x 10^7/ml cfu were added to 900µl of proteose-peptone broth containing the different investigational compounds. The plates (with the bacteria and investigational compounds) were then put in an incubator maintained at 37^0C with 5% CO_2 for various time points. Following this, 15µl of the bacterial suspension from each well was spread onto three separate proteose-peptone agar plates and incubated further at 37^0C with 5% CO_2 until colonies become visible. Colonies were counted using a ProtoCol automated bacterial colony counter.

2.16 Haematoxylin and Eosin (H & E) staining

For H & E staining of PFA-fixed paraffin embedded sections, the tissue section/slide was passed through 2 changes of 100% xylene and one further change in 100% and 70% alcohol to water respectively in order to deparaffinise the sections. For H & E staining of un-fixed frozen tissue sections, the tissues were fixed in ice cold acetone before the staining steps. Samples were then stained in Mayer's Haematoxylin solution (Sigma-Aldrich, Dorset, UK) for 5 minutes followed by washing in running tap water for 5 minutes. Following haematoxylin staining, the sections were dipped in 1% acid alcohol (see solutions in appendix) for 5 seconds and washed in running tap water for 5 minutes. The sections were then immersed in Eosin solution (Sigma-Aldrich, Dorset, UK; see appendix) for 5 minutes followed by two changes in 100% alcohol (3-5 minutes each) and 100% xylene (3-5 minutes each). The samples were then mounted under glass coverslips and looked at using bright field microscopy.

2.17 Statistical analysis – Standard deviation was employed for experiments performed once or twice, whereas standard error of the mean was used to for experiments which were performed three or more times. Graph pad prism was used to depict the data in graph form and to analyse the difference between groups using a variety of parametric and non-parametric statistical tests, including paired t-test, One Way ANOVA and Fisher's exact tests where appropriate. In this study paired t-test was employed when there is one measurement variable in two different treatment groups. One way ANOVA was used to test the significant difference in the mean of two or more treatment groups, analysed by using variance. Fisher exact test was used to see if there are non random associations between two treatment groups.

Chapter 3; PPL-αMSH and skin

3.1 Introduction

The delivery of many therapeutics compounds (like hydrophilic drugs, peptides and oligonucleotides) through the skin is restricted by the stratum corneum. However, many classes of topical agents are available to treat skin disorders. These include topical local anaesthetics, topical antipruritics, topical corticosteroids and other topical preparations for eczema and psoriasis, topical preparations for acne, warts, calluses and topical anti-infective preparations such as antibacterial, antifungal, antiviral and parasiticidal preparations (British National Formulary 50th edition). Many drugs (e.g. azathioprine, methotrexate, ciclosporin, efalizumab), which are poorly absorbed through the stratum corneum, are given systemically to treat cutaneous disorders, however, this can result in a number of adverse effects (Lebwohl & Ali 2001). The main limiting factors of drug penetration into skin include the chemical nature of the compound (its hydrophobic or hydrophilic nature) and its molecular size. The molecular weight of the compound is a critical factor for penetration into skin. According to the "500 dalton hypothesis", molecules less than 500 daltons generally penetrate the stratum corneum of normal skin (Bos & Meinardi 2000), although, in some disease conditions, such as atopic dermatitis, where the integrity of skin is compromised, molecules larger then 500 dalton can permeate the stratum corneum (Jakasa *et al.* 2007). Furthermore some comounds such as neomycin sulphate and tacrolimus whose molecular weight are greater than 500 dalton can penetrate the stratum corneum (Bos & Meinardi 2000). Neomycin sulphate consists of two neomycine molecules, therefore penetrate the stratum corneum, however the mechanisms of penetration of tacrolimus is not clear yet.

To assist the penetration of larger drugs through the stratum corneum, several techniques including ultrasonication, microinjection, electroporation, iontophoresis and the use of cell-penetrable peptides (CPPs), have been developed (Kondo *et al.* 1987; Tsai *et al.* 1996; Prausnitz 2004; Mehier-Humbert & Guy 2005). Sonication (20kHz frequency) generates cavities within the stratum corneum thus allowing the diffusion of drugs (Kost *et al.* 2000). Recent advancements in microinjection techniques have allowed the delivery of oligonucleotides, DNA and protein vaccines into the skin. In the "poke with patch" technique, a microneedle (poke) makes a hole in the skin and then the oligonucleotide is applied to the skin surface (Lin *et al.* 2001). Whereas the "dip and scrape" method the microneedle is first dipped into a DNA vaccine solution and scraped across skin surface (Mikszta *et al.* 2002). In the "coat and poke" method the needle is coated with the protein vaccine and then inserted into skin (Matriano *et al.* 2002). Electroporation has also proved to be an effective method for the delivery of DNA across phospholipid bilayers, and it has been demonstrated that the application of 100-1500V of electrical current sufficiently perturbs the intercellular lipid layer of the stratum corneum, allowing the delivery of many agents into the skin (Denet & Preat 2003; Sung *et al.* 2003). The main limitation of these physical techniques (ultrasonication, electroporation and microinjection) is that many skin conditions affect large areas of the body, thereby requiring multiple injections or electrical currents to deliver the compounds, and this may be poorly tolerated by the patient.

CPPs have also been reported to transport drugs into skin, such as the delivery of cyclosporine by polyarginine (Rothbard *et al.* 2000), interferon-γ by penetratin (Lee *et al.* 2005) and superoxide dismutase by tat and polylysine (Park *et al.* 2002). At present there

is a paucity of data describing the use of CPP-based carrier molecules for the efficient delivery of drugs into skin, and it is possible that some existing CPPs may not be able to transport drugs into this organ as failures tend to go unreported. In addition, there are potential drawbacks associated with the use of certain CPPs that seem capable of carrying cargo molecules into skin. For example, it has been reported that tat (derived from HIV) can upregulate some pro-inflammatory cytokines (Zauli *et al.* 1993), polylysine can cause degranulation of mast cells (Church *et al.* 1991) and penetratin (part of the antennapedia transcription factor) may interfere with endogenous biological processes. Furthermore, in a recent study, polyarginine failed to release its cargo sufficiently rapidly to be effective in a phase II clinical trial (presented by Paul Wender at the Society for Investigative Dermatology conference 2007).

In this study, we investigated the ability of a new cell-penetrable peptide, polypseudolysine (PPL), to deliver αMSH into cells and skin. αMSH is a 13 amino acid hormone, which is reported to play an important role in pigmentation and immunomodulation (Lerner & Mcguire 1961; Ichiyama *et al.* 2000; Cooper *et al.* 2005). The pigmentary action of αMSH is thought to be mediated through the binding of this compound to the melanocortin 1 receptor (*MC1R*) on the cell surface of the melanocyte (Mountjoy *et al.* 1992; Robbins *et al.* 1993). In addition, αMSH has been reported to have anti-inflammatory activity and to have antimicrobial activity particularly to *S. aureus*, a bacterium which is found in certain skin conditions such as impetigo and impetiginised eczema (Cutuli *et al.* 2000; Cooper *et al.* 2005). Therefore, αMSH could be a useful agent to use topically either as a possible tanning agent or as an effective treatment for inflammatory skin disorders, especially where infection with *S. aureus* and inflammation

co-exist. Therefore, in this study the ability of PPL to deliver αMSH into cells and skin was investigated.

3.2 Materials and Methods

3.2.1 Melanin assay: The cloudmann mouse melanoma (S91) cell line was used for the melanin assay, in which intracellular melanin was measured spectrophotometrically at absorbance 450nm and 492nm against standard mushroom melanin (as per section 2.4).

3.2.2. Ligand Binding assay: Competitive ligand binding assays were performed on *MC1R* transfected B16G4F cells to compare the surface receptor (*MC1R*) binding characteristics of αMSH, NDP-αMSH and PPL[98]-conjugated αMSH as described in section 2.5.

3.2.3. Lymphocyte transformation test (LTT): The LTT assay was performed on peripheral blood mononuclear cells (PBMCs), to investigate the immunosuppressive properties of αMSH, αMSH-PPL[98] and αMSH-PPL[99] following challenge with PHA and separately with streptokinase/streptodornase (see section 2.10).

3.2.4. Flow cytometry: B16G4F, B16UWT-3 and HEK-293 cell lines were analysed by flow cytometry in order to investigate the penetration of αMSH and αMSH-PPL[98], and to investigate toxicity using the cell death marker dye propidium iodide as per materials and methods sections 2.7.2 and 2.9.

3.2.5 Fluorescence Microscopy: Fluorescence microscopy was performed on various cell lines (B16G4F, B16UWT-3, HEK-293, HT1080, HaCaT, RPMI-7951 and S91) with fluorescein conjugated αMSH, αMSH-PPL[98] and αMSH-PPL[99] using a Leica fluorescence microscope as per material and methods section 2.6.

3.2.6. Confocal microscopy: Confocal microscopy was used to investigate the pattern of intracellular staining of fluorescence labelled αMSH, and αMSH-PPL[98] and αMSH-PPL[99] in cells to determine whether penetration by the compound had occurred. The SP2 Leica laser scanning confocal microscope was used to obtain a central Z plane image at the midpoint of the cells; see section 2.6 for details.

3.2.7. *Ex vivo* skin penetration assay: Franz's diffusion chambers were employed for detection of *ex-vivo* skin penetration by compounds αMSH-PPL[99]-Fluo and Fluo-αMSH into mouse, pig and human skin as per section 2.11.

3.2.8. LDH assay: Toxicity of the investigational compounds on B16G4F, B16UWT-3 and HEK-293 cells was investigated using a lactate dehydrogenase (LDH) kit following treatment of the cells with αMSH and αMSH-PPL[98] as per materials and methods 2.7.1.

3.2.9 Effects of compounds on *S aureus* viability: *S. aureus* was obtained from the Health Protection Agency, Southampton. Bacteria were grown on proteose-peptone agar plates (recipe in appendix) and the effect of αMSH, αMSH analogues (SHU9119, NDP-αMSH and MTII) and αMSH-PPL[98] on bacterial colony forming units was determined

after 6 and 24 hours treatment.

3.2.10 Haematoxylin and Eosin staining: The Fluo-αMSH and αMSH-PPL[99]-Fluo treated skin sections were stained for haematoxylin and eosin as per section 2.16.

3.3 Results

3.3.1 Functional studies

To investigate the pigmentation efficiency of PPL-linked αMSH, a melanin assay was performed on S91 cells. Two different concentrations (10^{-6}M and 10^{-8}M) of αMSH, αMSH–PPL[98], αMSH–PPL[99] and fluorescein-linked αMSH–PPL (i.e. Fluo-αMSH-PPL) were tested for their ability to induce melanin production. All of these compounds caused an significant increase in melanin pigmentation at 10^{-8}M and 10^{-6}M ($p = 0.014$, αMSH; $p = 0.021$, αMSH-PPL[98]; $p = 0.024$, αMSH-PPL[99]; $p = 0.015$, fluorescein-linked αMSH; $p = 0.018$, fluorescein-linked αMSH-PPL[98] and $p = 0.026$, fluorescein-linked αMSH-PPL[99]; One way ANOVA), indicating that all four PPL conjugated αMSH compounds could stimulate melanogenesis (figure 3.1). Additionally, with the exception of Fluo-αMSH there was no significant difference in pigmentation with any of the compounds as compared to αMSH alone.

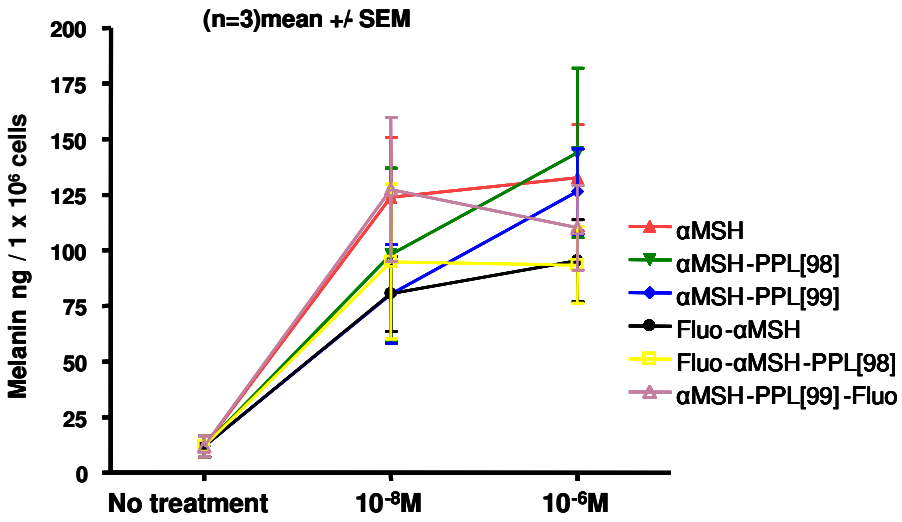

Figure 3.1. **Melanin synthesis in S91 cells following treatment with different compounds.** An increase in intracellular melanin was observed on day 5th following treatment with αMSH and Fluo and / or PPL linked αMSH compounds (10^{-8}M and 10^{-6}M). The data shown are the mean value of ratio + SEM of three experiments performed each in triplicates

S91 cell pigmentation was also clearly visualised using phase contrast microscopy on the 5th day of the melanin assay following treatment with the compounds. Representative images of αMSH and αMSH-PPL[98] treated S91 cells are shown in figure 3.2. The αMSH-PPL[98] treated S91 cells pigmented to a similar extent as the αMSH treated cells.

A B C

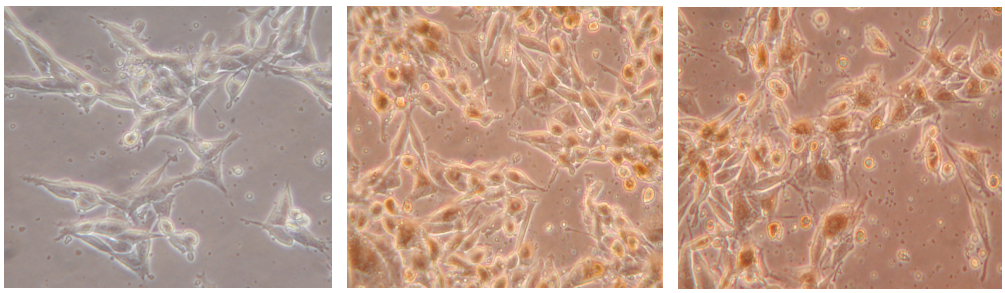

Figure 3.2. Pigmented and non-pigmented S91 cells. Images of S91 cells (on day 5) without treatment (A), treated with αMSH 10^{-6}M (B) and αMSH-PPL[98] 10^{-6}M (C).

The pigmentary action of αMSH is mediated through its binding to the MC1R on the cell surface of melanocytes and melanoma cells. Previously, it has been shown that NDP-αMSH (a very potent αMSH analogue) binds to MC1R more efficiently than αMSH (Sawyer *et al.* 1980). A competitive ligand binding assay was performed to investigate the receptor binding efficiency of αMSH alone and αMSH in conjugation with PPL (αMSH-PPL[98]). In this experiment, the binding affinity of a single concentration of radiolabeled ligand (^{125}I-NDP-αMSH) was compared against various concentrations of unlabeled ligand (NDP-αMSH, αMSH, Fluo-αMSH-PPL[98] and αMSH-PPL[98]) on *MC1R* transfected B16G4F cells. The results shown in figure 3.3 suggest that the NDP-αMSH binds to MC1R more efficiently than the other compounds. αMSH–PPL[98] also binds to the receptor and its binding affinity is slightly greater than that observed for αMSH alone.

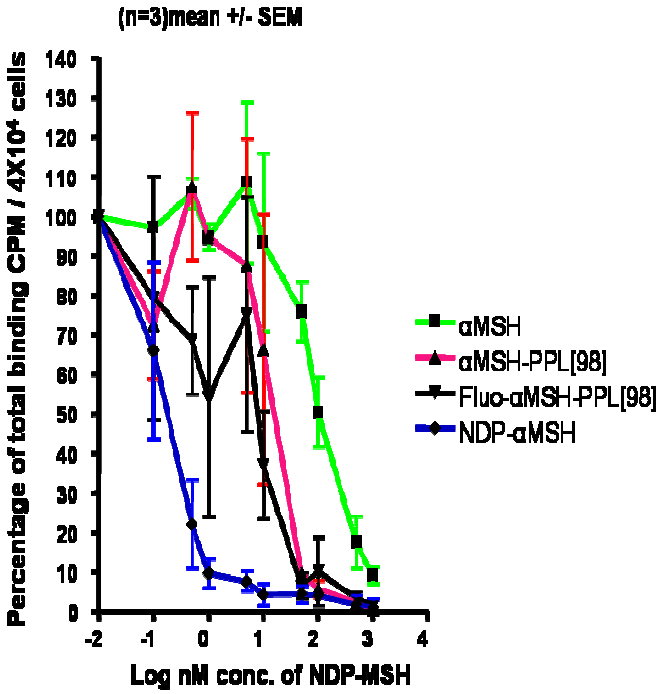

Figure 3.3 Receptor (*MC1R*) binding affinity of αMSH and PPL linked αMSH. Competitive ligand binding experiments performed on *MC1R* transfected B16G4F melanoma cells. The results show that each of the compounds (αMSH, NDP-αMSH, αMSH-PPL[98] and Fluo-αMSH-PPL[98]) bind to MC1R and that the binding of αMSH-PPL[98] is intermediate to that of αMSH and NDP-αMSH. The data shown are the mean value of ratio + SEM of three experiments performed each in triplicates.

Apart from its main role in pigmentation, αMSH has also been reported to have an immunomodulatory role in mice and humans (Raap *et al.* 2003; Cooper *et al.* 2005). The immunomodulatory effect of αMSH and αMSH-PPL[98] and separately αMSH-PPL[99] was investigated using a lymphocyte transformation (LTT) assay where the incorporation of [^{3}H] thymidine into the DNA of dividing cells is a widely used technique to assess cell proliferation. Briefly, PBMCs were isolated, and challenged with either the mitogen phytohemagglutinin (PHA-P) or the antigen streptokinase/streptodornase (SK/SD) to induce lymphocyte proliferation. αMSH and separately αMSH-PPL were added to the

culture at various concentrations and on day 6 after challenge with SK/SD or on day 3 after challenge with PHA-P, proliferation was assessed in triplicate wells. There was a slight inhibition of PHA-P stimulated lymphocyte proliferation with all tested concentrations of αMSH and αMSH-PPL[99], whereas there seemed to be a greater effect of αMSH and αMSH-PPL[98] on SK/SD stimulated lymphocyte proliferation (although these varied according to the concentration of the compounds within the same experiment and between the experiments) (figure 3.4).

A.

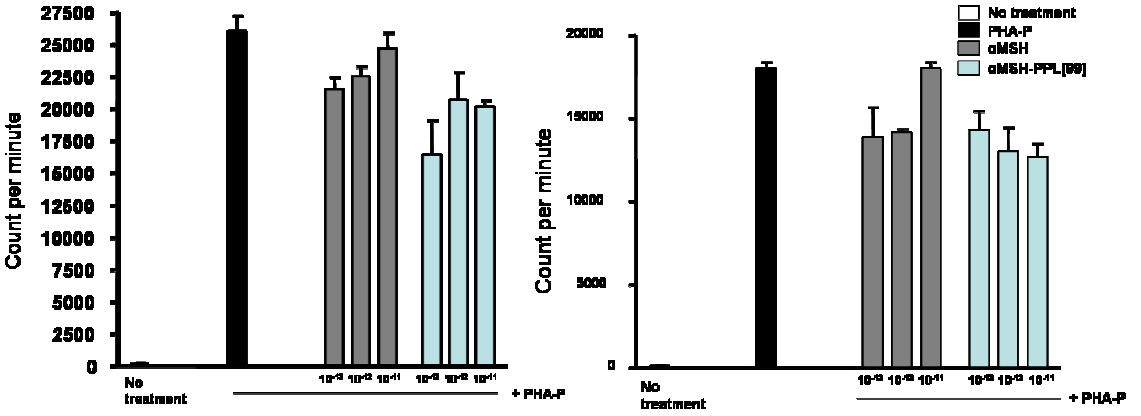

B.

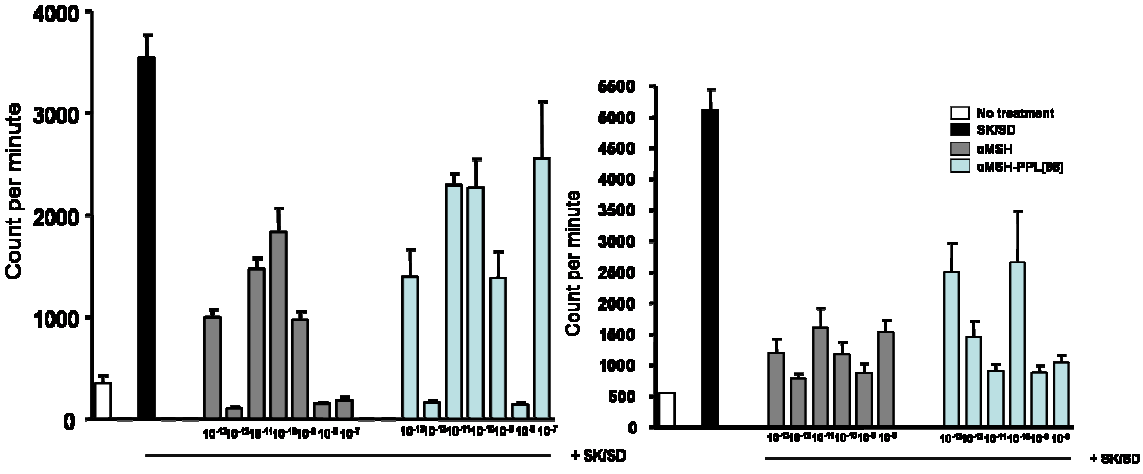

Figure 3.4 – Efeect of αMSH and αMSH-PPL[99] on lymphocytes proliferation. Results of LTT assay performed in the presence of various concentrations of αMSH and αMSH-PPL[99] following challenge with PHA-P (4µg/ml) (A) and with αMSH and αMSH-PPL[98] after challenge with SK/SD (0.5/0.125U/ml) (B). Each graph represents

a single experiment performed in triplicate wells and presented as standard deviation of the mean.

3.3.2 *In vitro* penetration studies

In vitro cell penetration studies were carried out with Fluo-αMSH-PPL[98] and αMSH–PPL[99]-Fluo to investigate the ability of PPL to deliver αMSH into cells. HEK-293 (no MC1R receptor) cells and two subtypes of B16G4F melanoma cell lines were selected for investigation; one B16G4F line that had been transfected with wild type MC1R (B16UWT-3) and the original parental line lacked the MC1R receptor (B16G4F). Cell penetration was determined by confocal microscopy, but flow cytometry and fluorescence microscopy were used initially to assess the concentrations of the investigational compounds which might penetrate into the cells and which would be subsequently examined with confocal microscopy. Therefore, cells were treated with various concentrations (10^{-5}M to 10^{-15}M) of the Fluo-αMSH and Fluo-αMSH–PPL[98] for 3 hours and analysed by flow cytometry for a shift in fluorescence intensity as compared to control cells which had not received any investigational compound. The FACS results showed a log shift in fluorescence at 10^{-5}M of Fluo-αMSH–PPL[98] in all cell lines (B16G4F, B16UWT-3 and HEK-293), with HEK-293 demostrating a greater shift as compared to the other two cell lines (figure 3.5).

A. B16G4F

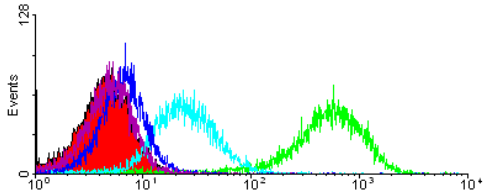

FL-1

B. B16UWT-3

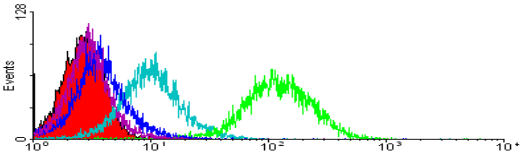

FL-1

C. HEK-293

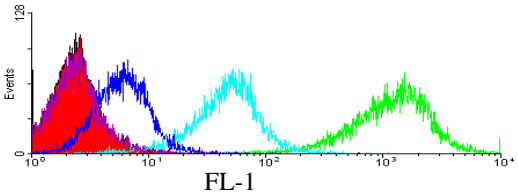

FL-1

Figure 3.5. Flow cytometric (FACS) shift in fluorescence in response to increasing doses of Fluo-αMSH-PPL[98]. FACS analysis results indicating the shift in fluorescence in B16G4F (A), B16UWT-3 (B) and HEK-293 (C) cells following treatment with Fluo-αMSH-PPL[98] at 10^{-5}M (green), 10^{-6}M (light blue), 10^{-7}M (dark blue) and 10^{-8}M (violet) for 3 hours. Red filled histogram represents untreated cells.

There was also a definite increase in fluorescence in each of these lines at 10^{-6}M Fluo-αMSH–PPL[98], but while there was a shift in fluorescence at 10^{-7}M Fluo-αMSH–PPL[98] in the HEK-293, this was less obvious in the B16G4F and B16UWT-3 lines (figure 3.5). For Fluo-αMSH-PPL[98] concentrations lower than 10^{-7}M there was a negligible shift in fluorescence in all three cell lines as compared to the untreated cells (figures 3.5 and 3.6). After 24 hours culture of the HEK-293 and B16G4F cell lines with 10^{-5}M of Fluo-αMSH–PPL[98], the shift in fluorescence was similar to that seen at the 3 hours time point on these cells (see figure 3.7 in comparison with figure 3.5).

A. B16G4F B. B16UWT-3 C. HEK-293

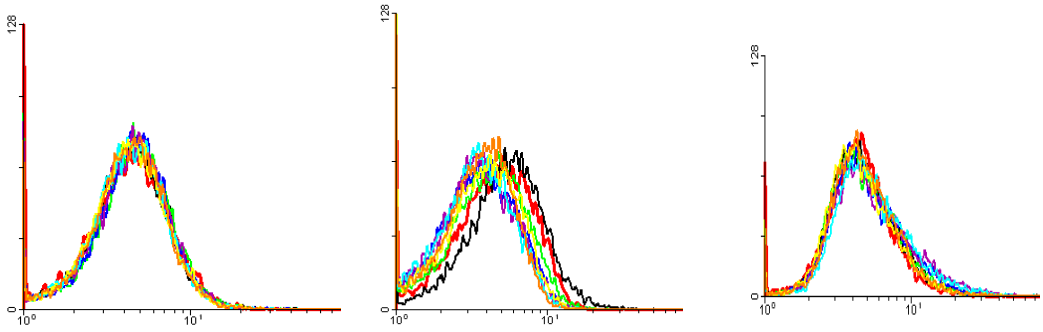

Figure 3.6. Flow cytometric (FACS) shift in fluorescence in response to decreasing doses (less than 10^{-8}M) of Fluo-αMSH-PPL[98]. FACS analysis results showing negligible shift in fluorescence in B16G4F (A), B16UWT-3 (B) and HEK-293 (C) cells treated with Fluo-αMSH-PPL[98] at 10^{-9}M (black), 10^{-10}M (green), 10^{-11}M (dark blue), 10^{-12}M (violet), 10^{-13}M (light blue), 10^{-14}M (yellow) and 10^{-15}M (orange) for 3 hours.

A. B16G4F B. HEK-293

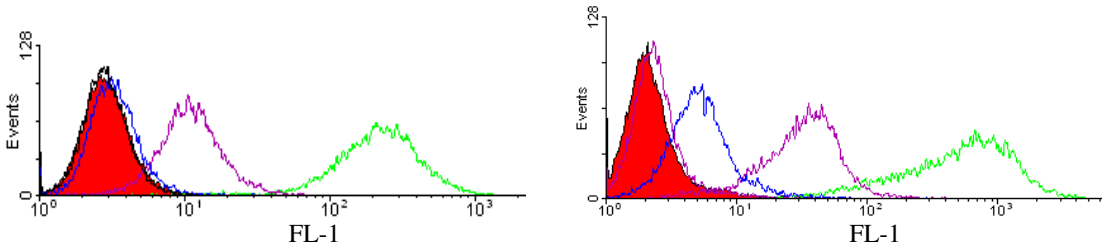

Figure 3.7. **Flow cytometric (FACS) shift in fluorescence after 24 hours treatment.** FACS analysis of the shift in fluorescence in B16G4F (A) and HEK-293 (B) cells following 24 hours treatment with Fluo-αMSH-PPL[98] at 10^{-5}M (green), 10^{-6}M (violet), 10^{-7}M (dark blue) and 10^{-8}M (light purple)

In comparison to Fluo-αMSH, Fluo-αMSH–PPL[98] showed more than a log shift in fluorescence at 10^{-5}M (24 hours incubation) in HEK-293 and B16G4F cell lines (figure 3.8). B16UWT-3 cells were not included in subsequent FACS analysis because of presence of MC1R receptor, which may enhance the intensity of fluorescence.

A. B16G4F

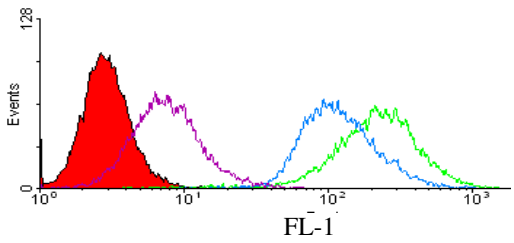

B. HEK-293

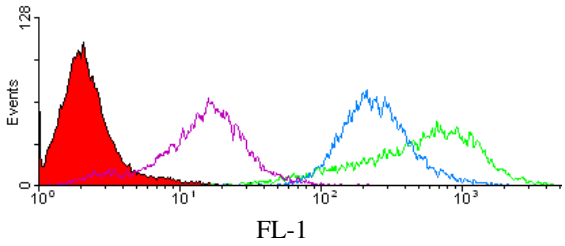

Figure 3.8. Comparison of flow cytometric shift in fluorescence following treatment with Fluo-αMSH, Fluo-PPL[98] and Fluo-αMSH-PPL[98]. FACS analysis for the shift in fluorescence following 24 hours incubation at 10^{-5}M concentration of Fluo-αMSH (violet), Fluo-PPL[98] (light blue) and Fluo-αMSH-PPL[98] (green) on B16G4F (A) and HEK-293 (B) cells.

Based on the FACS results, the 10^{-5}M concentration was chosen for further investigations in fluorescence and confocal microscopy experiments. Following a 3 hour incubation with 10^{-5}M Fluo-αMSH-PPL[98] and separately with 10^{-5}M Fluo-αMSH, there was an enhanced fluorescence signal during fluorescence microscopy from the HEK-293 and B16G4F cells which had received the Fluo-αMSH-PPL[98], whereas cells cultured with fluorescein conjugated αMSH without PPL showed a very weak signal (Figure 3.9). Fluo-αMSH-PPL[98] and Fluo-αMSH treated cells images were taken with identical microscope setting at same session, where experimental conditions were analysed first followed by negative control.

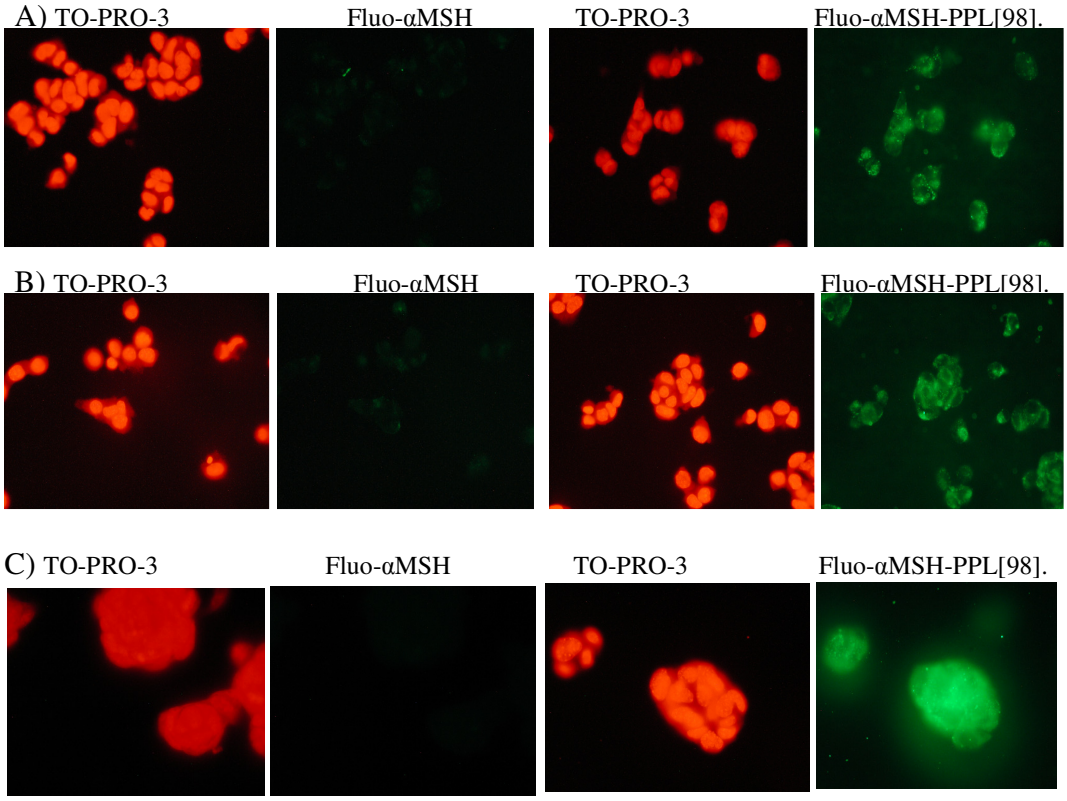

Figure 3.9 Visualisation of Fluo-αMSH and Fluo-αMSH-PPL[98] treated cells under fluorescence microscope. Fluorescence microscopy results obtained from HEK-293 (A) and B16G4F (B) and B16UWT-3 (C) cells following 3 hours incubation with 10^{-5}M concentrations of Fluo-αMSH and Fluo-αMSH-PPL[98]. TO-PRO-3 was used as nuclear counter stain (seen as red) to identify the cells and the TO-PRO-3 cells in the figure indicate where the cells are in the adjacent right panel for each of the investigational compounds.

After visualisation of Fluo-αMSH-PPL[98] fluorescence in B16G4F, B16UWT-3 and HEK-293 cells, various other cell lines were investigated for the penetration/visualisation of fluorescein linked PPL-αMSH. Indeed, at 10^{-5}M, Fluo-αMSH-PPL and αMSH-PPL[99]-Fluo gave a similar fluorescence signal in a range of cell lines (HT1080, S91 and RPMI-7951); see figure 3.10 for results from HT1080 and S91 cells.

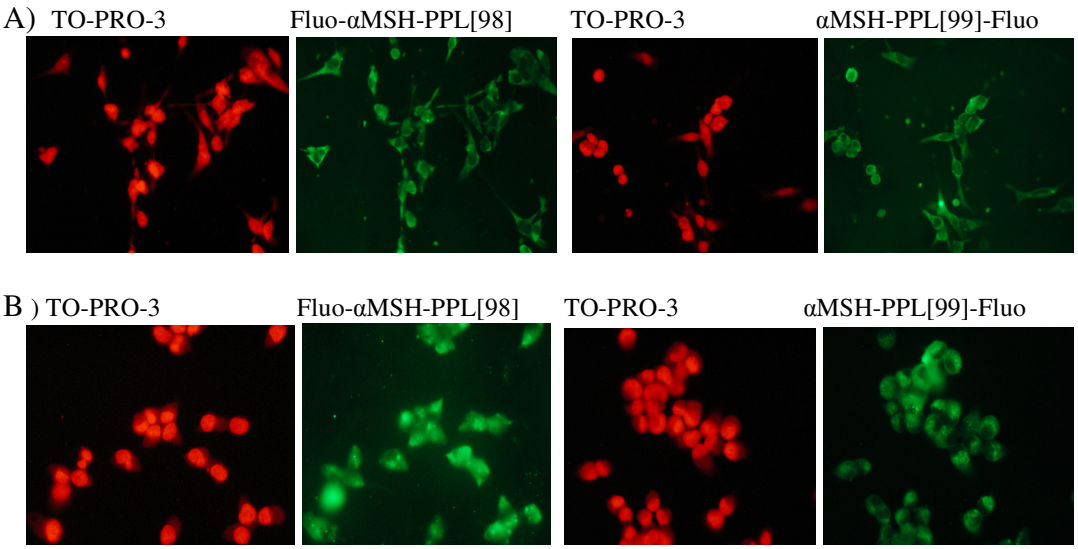

Figure 3.10. Comparison of Fluo-αMSH-PPL and αMSH-PPL[99]-Fluo. Fluorescence microscopy results with Fluo-αMSH-PPL[98] and αMSH-PPL[99]-Fluo (at 10^{-5}M for 3 hours) treated S91 (A) and HT1080 (B) cells. TO-PRO-3 was used as nuclear counter stain (seen as red) and indicates where the cells are in the adjacent right panel for each of the investigational compounds

A similar fluorescence intensity was seen with cells cultured with 10^{-5}M Fluo-PPL as with the cells that had received the αMSH-PPL[99]-Fluo and Fluo-αMSH-PPL[98] compounds at this concentration for 3 hours (see figures 3.11 and 3.10). Cells treated for 3 hours with concentrations lower than 10^{-5}M Fluo-PPL and Fluo-αMSH-PPL[98] demonstrated less visible fluorescence (figures 3.11 and 3.12).

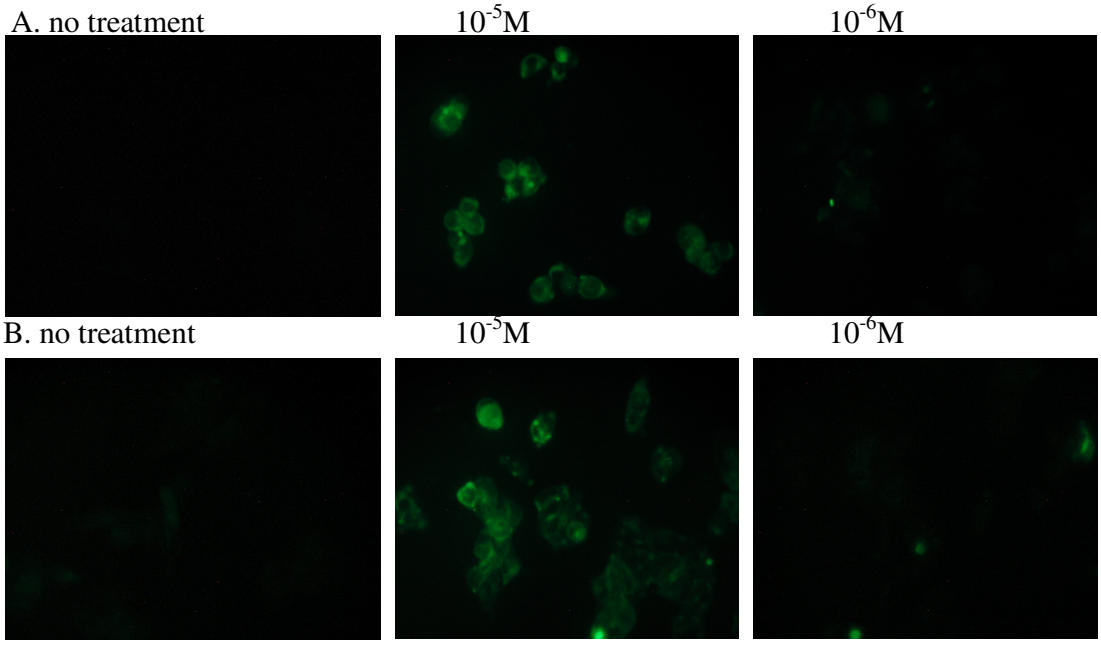

Figure 3.11. Fluorescent microscopy based visualisation of cells following treatment with Fluo-PPL. Results showed that B16G4F (A) and B16UWT-3 (B) cells treated with 10^{-5}M and 10^{-6}M Fluo-PPL for 3 hours exhibits different intensity of fluorescence.

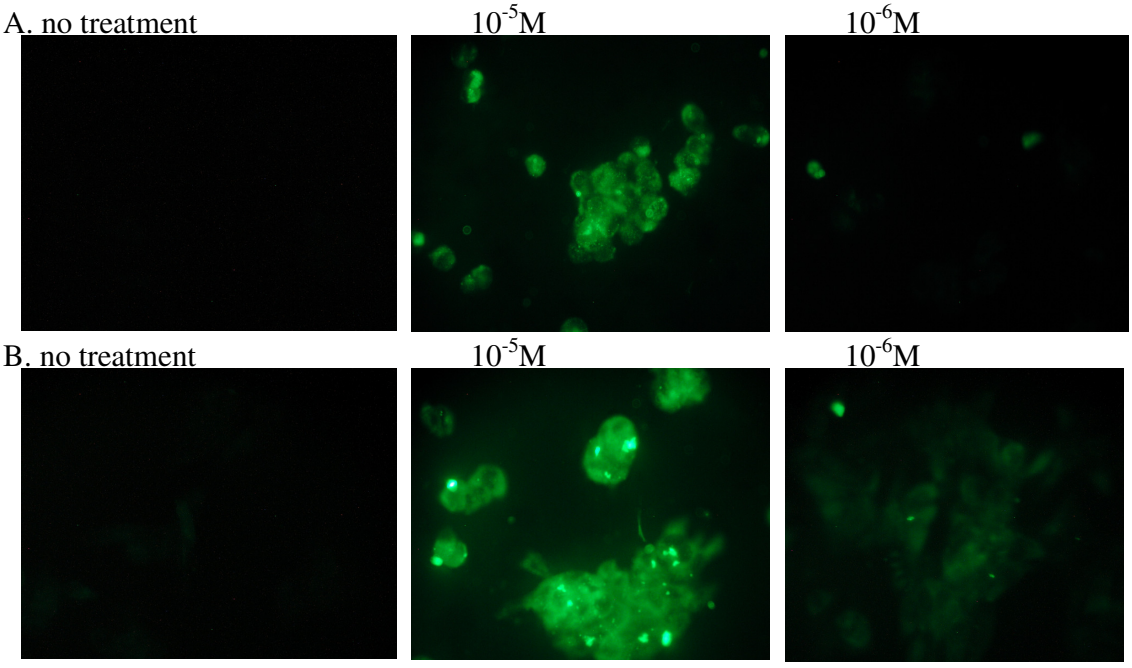

Figure 3.12 Intensity of cell fluorescence following two different doses of Fluo-αMSH-PPL[98]. Fluorescence microscopy results on B16G4F (A) and B16UWT-3 (B) cells treated with Fluo-αMSH-PPL[98] (at 10^{-5}M and 10^{-6}M concentrations for 3 hours).

Because the FACS and fluorescent microscopy results cannot adequately discriminate between surface staining and intracellular staining, confocal microscopy (which provides Z-plane optical sections of cells) was used to examine whether PPL was allowing the penetration of αMSH into the cells. Initially, confocal microscopy experiments were performed on the B16G4F cells, which were incubated with 10^{-5}M Fluo-αMSH-PPL[98] and Fluo-αMSH separately at different time points (10 minutes, 30 minutes, 3 hour and 24 hours). The mid-cell Z-plane results (i.e. the Z-plane section mid way between the top and bottom of the cell) demonstrated that Fluo-αMSH-PPL[98] was present in the cytoplasm of B16G4F cells, especially after 3 hours incubation. In contrast, Fluo-αMSH poorly penetrated into the cells (figure 3.13). The images presented in figure 3.13 were generated from single experiment performed on same day and similar confocal microscopy set up was used for generating the data.

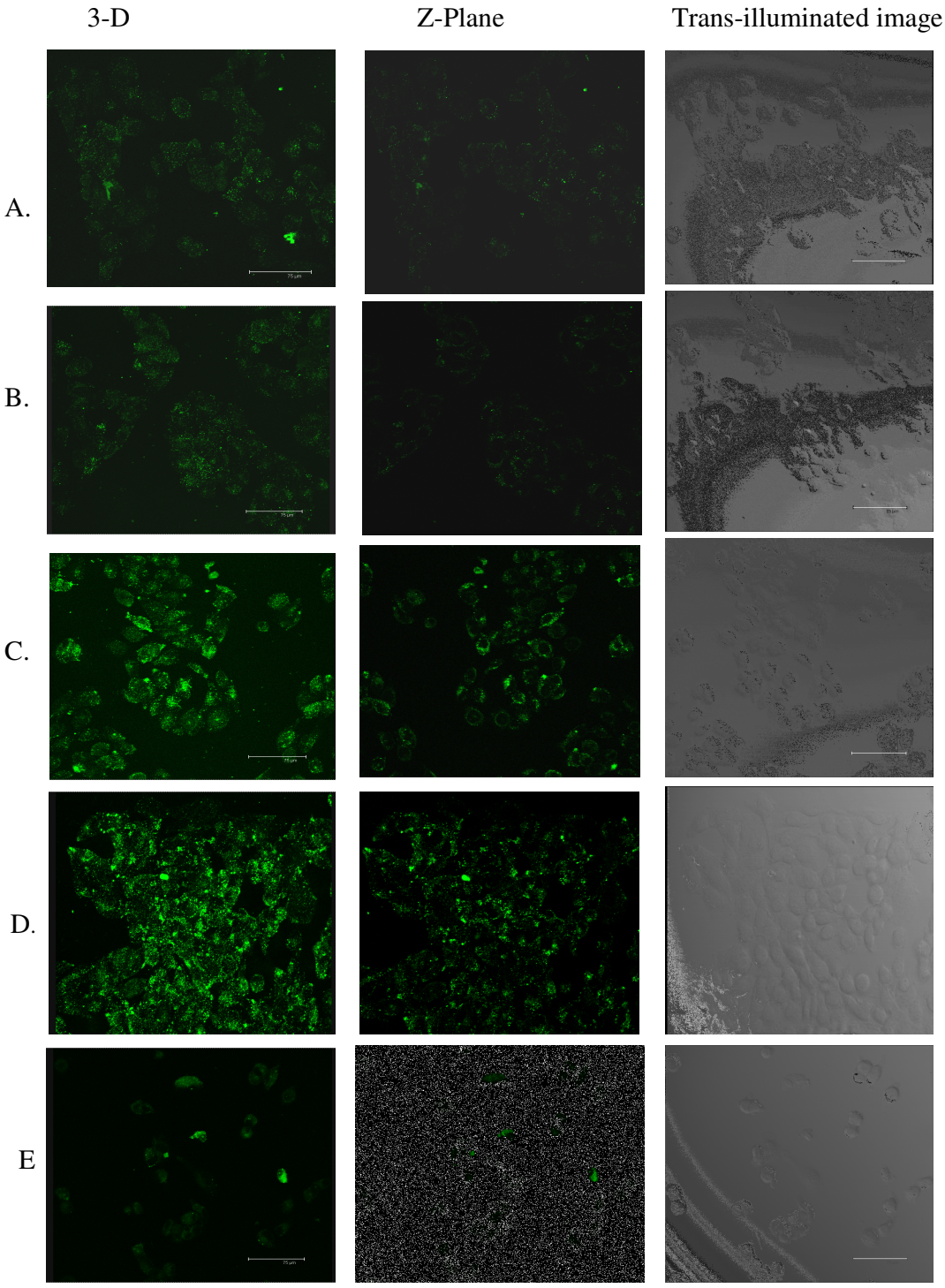

Figure 3.13 Cell penetration of Fluo-αMSH-PPL[98]. Confocal microscopy result on B16G4F cells following treatment with Fluo-αMSH-PPL[98] at 10^{-5}M concentration for 10 minutes (A), 30 minutes (B), 3 hours (C), 24 hours (D) or with Fluo-αMSH at10^{-5}M concentration for 3 hours (E). In each part of the figure 3-D images are on the left hand side, Z-plane images are in the middle and on the right hand side are the trans-illuminated images. Scale bar are 75µm in each image.

As compared to Fluo-αMSH-PPL[98], B16G4F cells following 3 hours incubation with 10^{-5}M Fluo-PPL (without cargo) showed a similar fluorescence intensity to that seen in cells cultured with 10^{-5}M Fluo-αMSH-PPL[98] for 3 hours in B16G4F cell following 3 hours incubation at 10^{-5}M concentration (see figures 3.13 and 3.14).

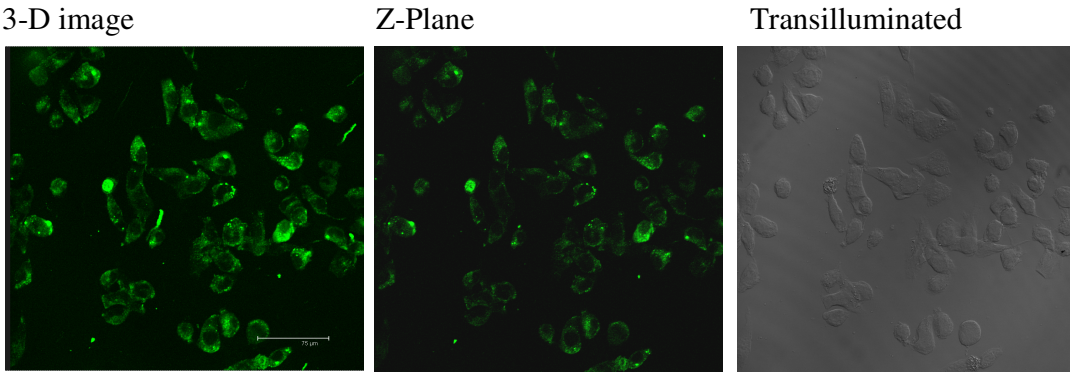

Figure 3.14. **Cell penetration of Fluo-PPL.** Confocal microscopy of B16G4F cells following treatment with Fluo-PPL at 10^{-5}M for 3 hours showed internalisation of compound. Scale bar are 75μm in each image.

Confocal microscopy also demonstrated successful penetration of 10^{-5}M Fluo-αMSH-PPL[98] into B16UWT-3 cells at 3 hours incubation (figure 3.15).

3-D Image+transilluminated Z-Plane

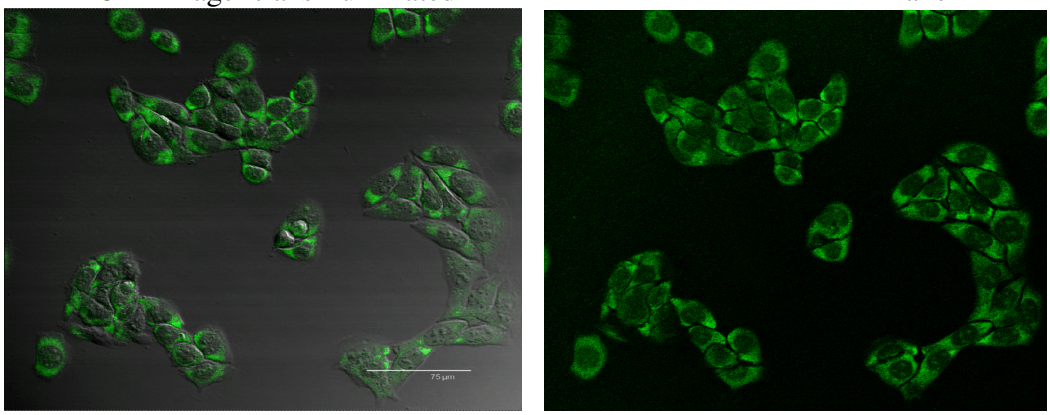

Figure 3.15. Internalisation of Fluo-αMSH-PPL[98] into B16UWT-3 cells. Confocal microscopy results on B16UWT-3 cells treated with 10^{-5}M Fluo-αMSH-PPL[98] indicated penetration of conjugated peptide; left panel shows 3-D and transilluminated images combined and right panel shows mid-cell Z-plane image. Scale bar are 75µm in each image.

Using TO-PRO-3 as a nuclear counterstain indicated that αMSH-PPL[99]-PPL and Fluo-αMSH-PPL[98] had penetrated into the cytoplasm of the cell lines treated with these compounds and that Fluo-αMSH did not penetrate into the cells (figure 3.16).

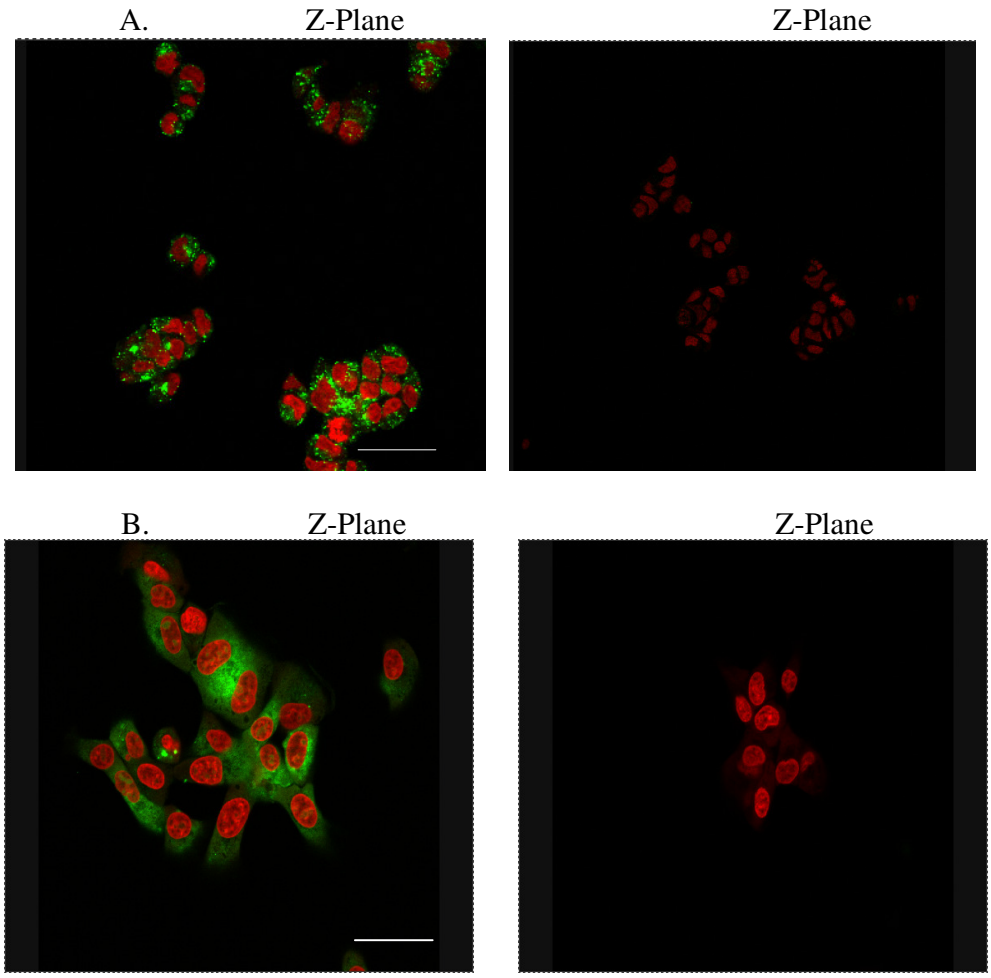

Figure 3.16. Internalisation of αMSH-PPL[99]-Fluo into the cell cytoplasm. Confocal microscope Z-plane results of A) HEK-293 (40x) and B) RPMI -7951 (63x) cell lines treated with αMSH-PPL[99]-Fluo (left panels) and Fluo-αMSH (right panels) at 10^{-5}M for 3 hours showed mainly cytoplasmic staining. TO-PRO-3 has been used as a nuclear counter-stain (seen as red). Scale bar are 75µm in top panel image and 47.3µm in bottom panel.

Similar cell penetration investigations were carried out on a range of cell lines with Fluo-αMSH–PPL[98] or αMSH-PPL[99]-PPL at 10^{-5}M for 3 hours. A summary of all the cell lines used in the penetration studies can be seen in table 3.0.

Table 3.0 List of cell lines used for penetration study. Cell lines/cells used for in *vitro* penetration investigations on fixed cells with Fluo-αMSH, Fluo-αMSH-PPL[98] and αMSH-PPL[99]-Fluo (10^{-5}M for 3 hours).

	Fluo-αMSH	Fluo-αMSH-PPL[98]	αMSH-PPL[99]-Fluo	n*
B16G4F	no*	yes*	yes	n=3
B16UWT-3	no	yes	yes	n=2
HEK-293	no	yes	yes	n=3
HT1080	no	yes	yes	n=2
RPMI-7951	no	yes	yes	n=2
HaCaT	no	yes	yes	n=2
B cells	no	yes	not tested	n=1

*no = not penetrated, yes = penetrated, n is the number of times experiments were performed for each cell type.

The cell penetration investigations were also carried out on live non-fixed cells to ensure that the penetration of the compounds into fixed cells had not been as a result of the fixation process. Live cell confocal microscopy penetration studies were performed in duplicate on HaCaT and B16G4F cell lines which had been incubated for 3 hours with Fluo-αMSH and αMSH-PPL[99]-Fluo at two different concentrations (10^{-5}M and 3x 10^{-5}M). Strong intracellular staining was detected in both cell lines with $3x10^{-5}$M αMSH-PPL[99]-Fluo. The PPL also enhanced the penetration of αMSH at a concentration of 10^{-5}M, but the intracellular fluorescence was not as strong as that seen with $3x10^{-5}$M treatment (figure 3.17). The penetration of Fluo- αMSH was very weak in both cell lines.

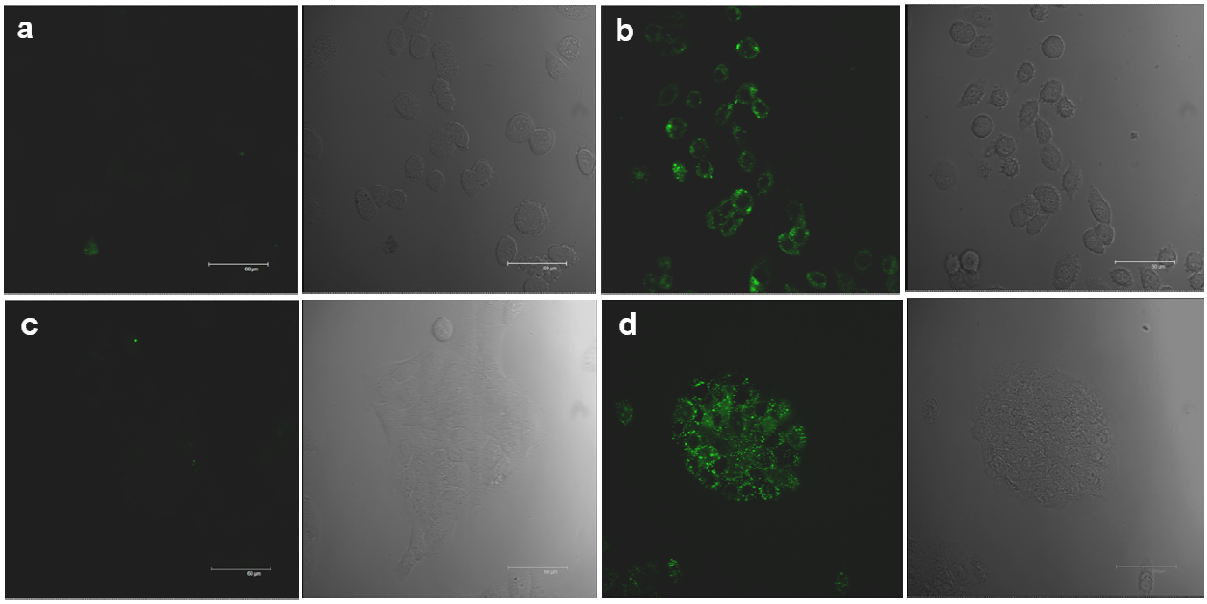

Figure 3.17. Penetration of αMSH-PPL[99]-Fluo into live unfixed cells. Confocal microscopy results showed that PPL conjugation enhances the penetration of αMSH into B16G4F (b) and HaCaT cells (d) at $3x10^{-5}$M, whereas penetration of Fluo-αMSH at similar concentration (a and c) was very weak in both cell lines. The trans-illuminated images are also shown for each treatment. Scale bar are 75μm in each image.

3.3.3 *Ex vivo* skin penetration

To investigate the ability of PPL to transport αMSH into skin, an *ex vivo* skin penetration assay was performed using Franz diffusion chambers. Initially, different concentrations of αMSH–PPL[99]-Fluo were used to determine the optimum concentration of compound required to permeate the stratum corneum. Freshly excised back skin (6mm diameter) from hairless mice was mounted on each Franz diffusion chamber and the investigational compounds were applied topically (epidermal side) via the donor chambers. Fluorescence microscopy visualisation of the skin sections showed that αMSH–PPL[99]-Fluo penetrated the stratum corneum when applied at a concentration of 10^{-3}M. However, the penetration results with αMSH–PPL[99]-Fluo were variable, with the intensity of fluorescence indicating weak penetration in some cases to very strong

staining in other cases, therefore the results of the αMSH–PPL[99]-Fluo and Fluo-αMSH treated skin samples were graded as no penetration, very weak, weak, moderate, strong and very strong penetration according to the different amounts of fluorescence observed (as demonstrated in figure 3.18). The results of all the penetration experiments on mouse skin are listed in figure 3.19. Several batches of αMSH–PPL[99]-Fluo were tested for skin penetration experiments, which may account for the variation in the results. Compare to different batches of αMSH–PPL[99]-Fluo, first batch showed better penetration and reproducibility.

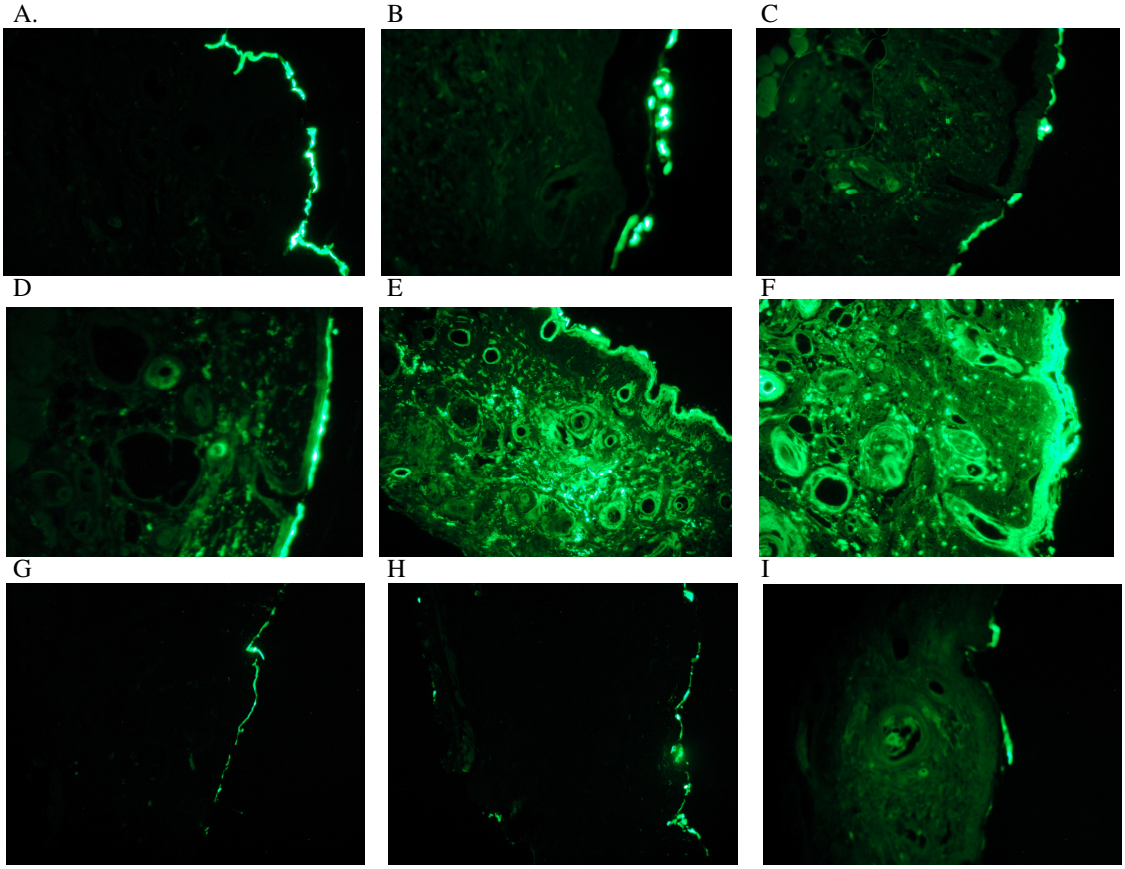

Figure 3.18 Penetration of αMSH-PPL[99]-Fluo and Fluo-αMSH into mouse skin. Fluorescence microscopy based analysis of skin penetration by αMSH-PPL[99]-Fluo showing samples of no penetration (A), very weak (B), weak (C), moderate (D), strong (E) and very strong (F) penetration. Images G – H represent Fluo-αMSH treated skin samples which demonstrate no (G), weak (H) and moderate penetration (I).

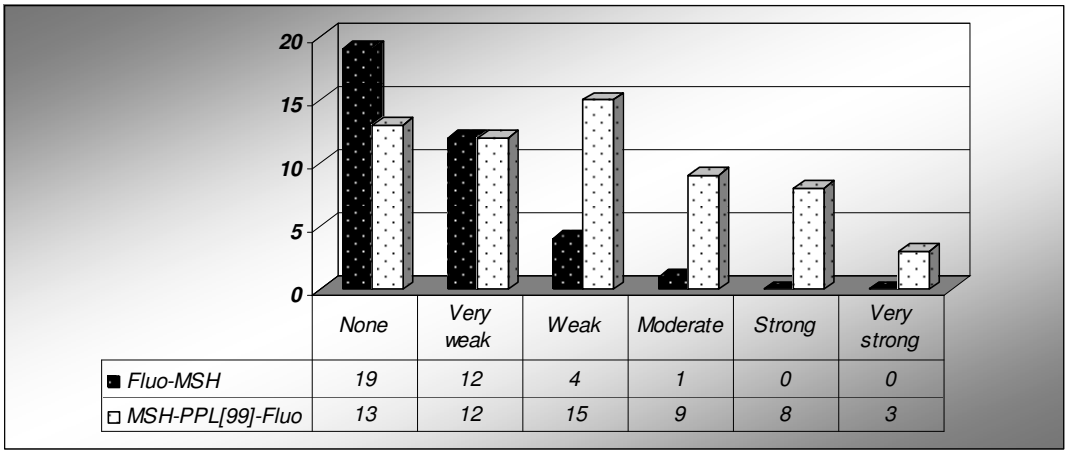

Figure 3.19. Summary of mouse skin penetration with αMSH-PPL[99]-Fluo and Fluo-αMSH. Results of penetration into hairless mouse skin by αMSH-PPL[99]-Fluo and Fluo-αMSH. The table include all the batches of αMSH-PPL[99]-Fluo used for skin penetration analysis. αMSH-PPL[99]-Fluo penetrated into murine skin in 35 of 60 (58.3%) cases, whereas Fluo-αMSH only penetrated in 5 of 36 (13.9%) samples (p = 0.001, Fisher exact test).

Haematoxylin and eosin staining of several αMSH and αMSH–PPL[99]-Fluo treated mouse skin samples demonstrated a normal skin histology with an intact stratum corneum (figure 3.20), suggesting that the penetration of the αMSH–PPL[99]-Fluo compound had not been achieved as a result of a disrupted stratum corneum.

A. B.

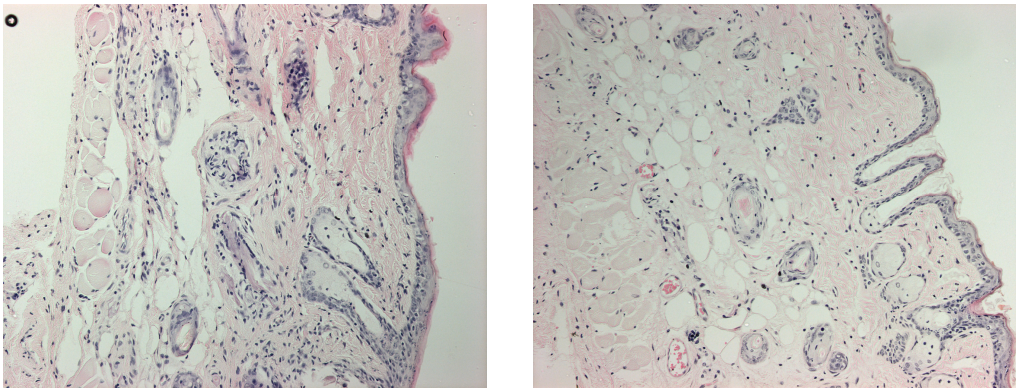

Figure 3.20. Haematoxylin and eosin staining of Fluo-αMSH and αMSH–PPL[99]-Fluo treated mouse skin. Result showed that stratum corneum is not disrupted following treatment with Fluo-αMSH (A) and αMSH–PPL[99]-Fluo (B).

Ex vivo skin penetration studies were also performed on human and pig skin using the

Franz's diffusion chamber system. Although these were carried out on a limited number of specimens, the results demonstrated that PPL was also able to transport αMSH into pig's skin (only in few cases, see table 3.2) at a concentration of 10^{-3}M following 3 hours incubation (figures 3.21 and 3.22).

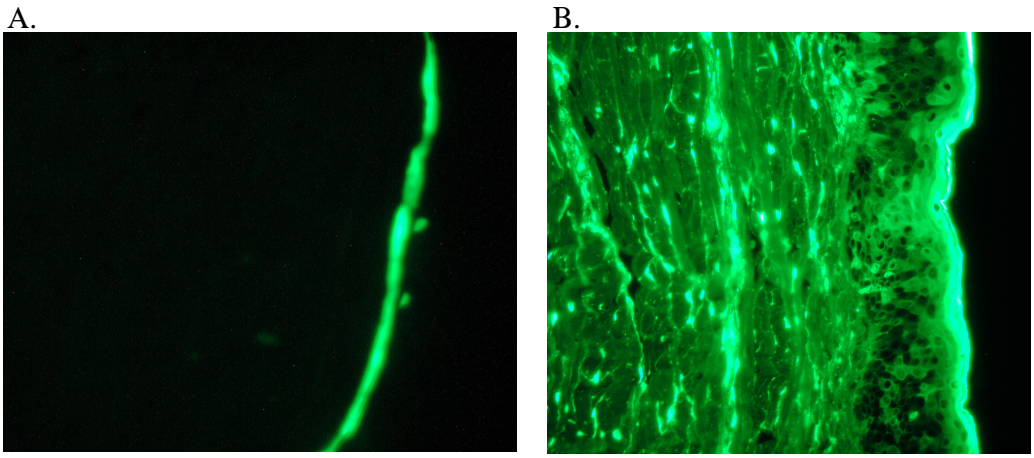

Figure 3.21 Penetration of αMSH-PPL[99]-Fluo and Fluo-αMSH into pig skin. Fluorescence microscopy shows penetration of 10^{-3}M αMSH-PPL[99]-Fluo (B) visualisation into pig's skin following 3 hours culture with this compound but no visible penetration by 10^{-3}M Fluo-αMSH (A).

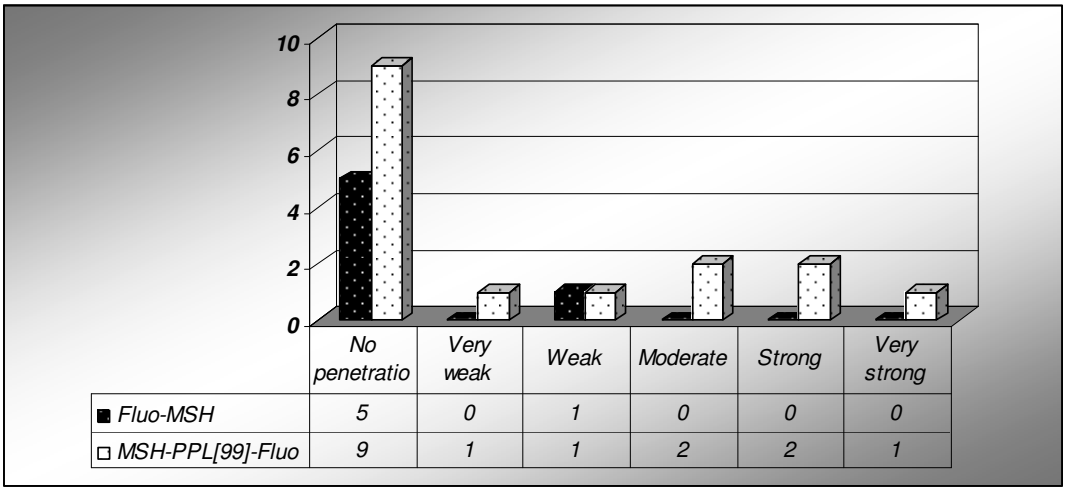

Figure 3.22. Summary of pig skin penetration with αMSH-PPL[99]-Fluo and Fluo-αMSH. Results of penetration into pig's skin by αMSH-PPL[99]-Fluo and Fluo-αMSH. αMSH-PPL[99]-Fluo penetrated into pig skin in 6 of 16 (37.5%) cases, whereas Fluo-αMSH only penetrated in 1 of 6 (16.2%) samples (p=0.6158, Fisher exact test).

Similarly, fluorescein labelled αMSH-PPL[99] penetrated into human skin, whereas fluorescein labelled αMSH did not penetrate to the same extent (figures 3.23 and 3.24).

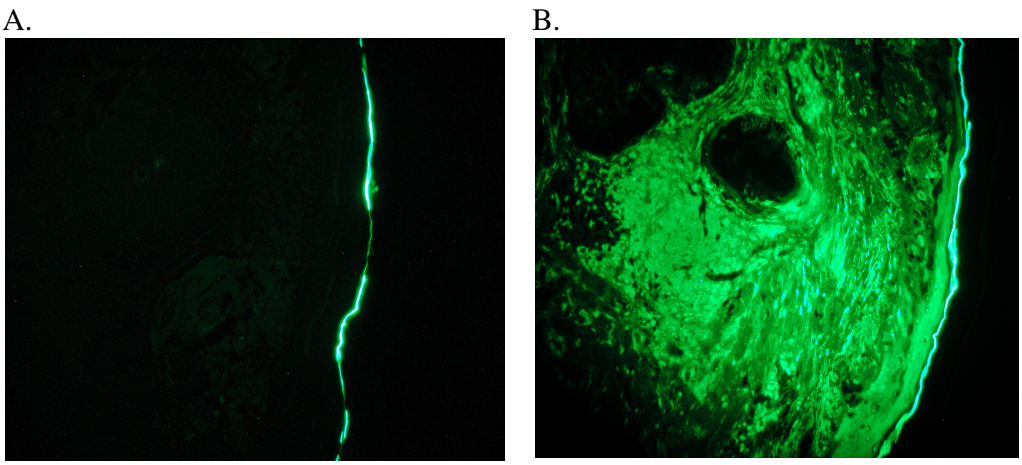

Figure 3.23 Penetration of αMSH-PPL[99]-Fluo and Fluo-αMSH into human skin. Fluorescence microscopy demonstrates poor penetration of 10^{-3}M Fluo-αMSH (A) into human skin following 3 hours incubation but good penetration by 10^{-3}M αMSH–PPL[99]-Fluo (B).

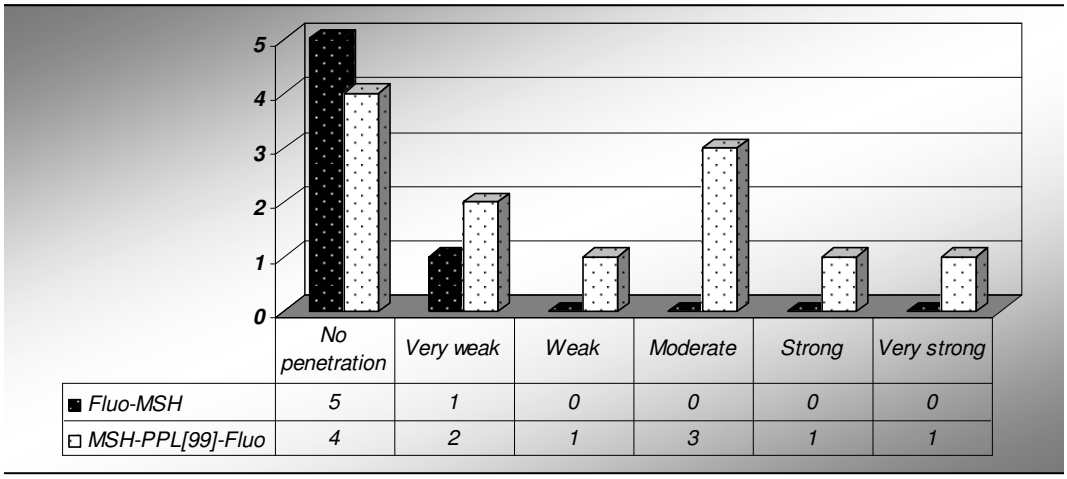

.

Figure 3.24 Summary of human skin penetration with αMSH-PPL[99]-Fluo and Fluo-αMSH. Results of overall skin penetration into human skin by Fluo-αMSH and by αMSH-PPL[99]-Fluo. αMSH-PPL[99]-Fluo entered into human skin in 6 of 12 (50%) cases whereas Fluo-αMSH did not penetrate into the human skin samples (0 of 6 cases; p = 0.0498, Fisher exact test).

The skin penetration was also investigated by fluorescence microscopy using mouse skin which was frozen instead of fixed in paraformaldehyde following treatment with Fluo-αMSH and separately αMSH-PPL[99]-Fluo in order to confirm that the previous skin penetration results were not due to a fixation artefact. The results in the frozen skin sections showed that the αMSH-PPL[99]-Fluo penetrated into the epidermis and the dermis at 10^{-3}M concentration, whereas Fluo-αMSH did not penetrate (Figure 3.25).

A) B)

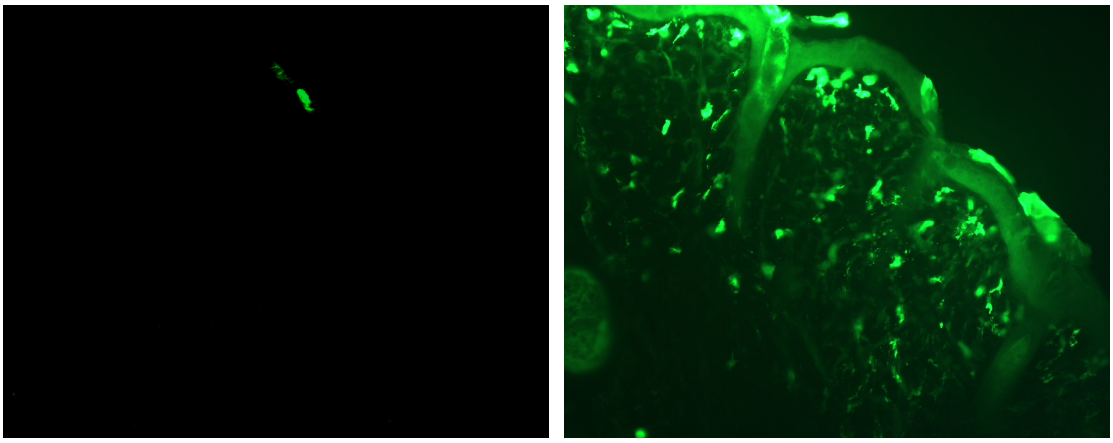

Figure 3.25. Penetration of fluoresceinated αMSH with or without PPL into mouse skin. Following treatment with investigational compounds mouse skin was frozen prior to the sections being cut. αMSH-PPL[99]-Fluo (B) penetrated into mouse skin which had not been fixed following culture with the investigational compound, whereas Fluo-αMSH (A) did not penetrate.

In fact, the skin penetration results obtained from frozen skin sections indicated that 7 of 12 skin samples were positive with weak to moderate staining for αMSH-PPL[99]-Fluo, whereas Fluo-αMSH did not penetrate into the skin except in one case which exhibited very weak staining.

For statistical analysis, a fluorescence intensity of weak or greater taken to indicate entry of the substance into the skin. Investigations on murine and human skin demonstrated that the PPL-conjugated αMSH penetrated to a greater extent than the αMSH in the

absence of the PPL carrier. Specifically, αMSH-PPL[99]-Fluo penetrated into murine skin in 35 of 60 (58.3%) cases, whereas Fluo-αMSH only penetrated in 5 of 36 (13.9%) samples (p = 0.001, Fisher exact test). Similarly, αMSH-PPL[99]-Fluo entered into human skin in 6 of 12 (50%) cases whereas Fluo-αMSH did not penetrate into the human skin samples (0 of 6 cases; p = 0.0498, Fisher exact test). However, data obtained from pig's skin penetration were not statistically significant (p=0.6158, Fisher exact test).

3.3.4 Cytotoxicity analysis

3.3.4.1.LDH assay

To investigate the cytotoxicity of the test compounds a lactate dehydogenase (LDH) assay was performed; this assay measures the activity of LDH released from any sick or damaged cells. The assay was performed on B16G4F, HEK-293 and B16UWT-3 cell lines following 3 hours treatment with different concentrations of Fluo-αMSH–PPL[98], αMSH–PPL[98], αMSH, Fluo-PPL and Fluo-αMSH.

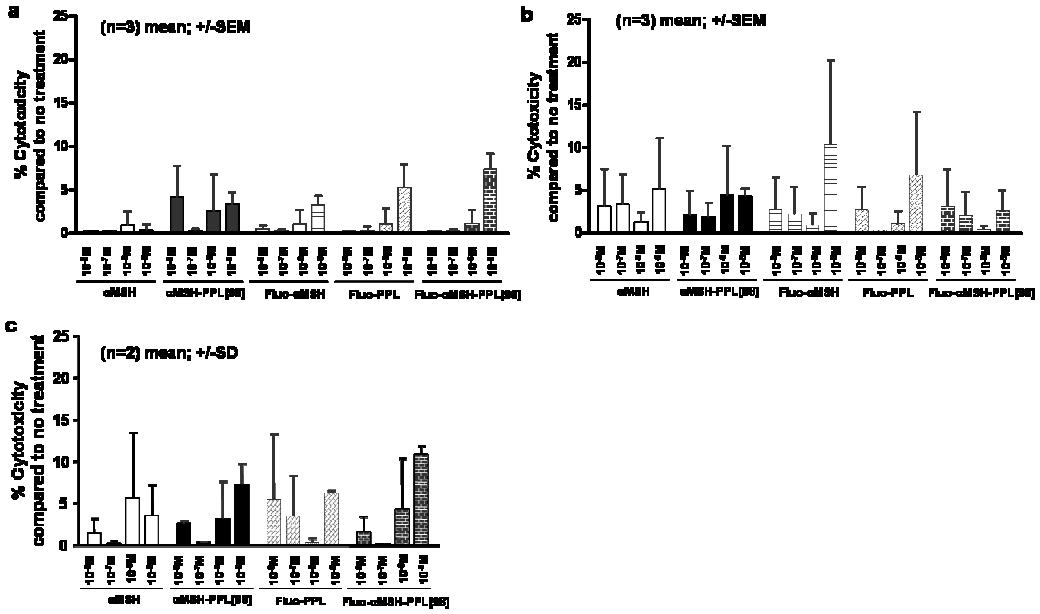

Figure 3.26. Cytotoxicity analysis. LDH assay on A) B16UWT-3, B) HEK-293 and C) B16G4F cells following treatment with αMSH alone, αMSH-PPL[98], Fluo-αMSH (except B16G4F), Fluo-PPL and Fluo-αMSH–PPL. The assay was performed following 3 hours incubation with the compounds at concentrations ranging from 10^{-5}M to 10^{-8}M. The data shown are the mean value of ratio + SEM of three experiments performed each in triplicates for B16UWT-3 and HEK-293, whereas in case of B16G4F data shown are mean value of ratio + SD of two experiments performed each in triplicates.

Minimal toxicity was observed on all three cell lines with each of the compounds at 10^{-6}M to 10^{-8}M, with slightly more cytotoxicity at 10^{-5}M with some of the fluoresceinated compounds, however, there was no significant difference between the PPL-linked and the unconjugated αMSH compounds at this concentration ($p = 0.184$ and $p=0.717$, paired t-test, for 10^{-5}M αMSH-PPL[98] versus 10^{-5}M αMSH alone in the case of the B16CWT-3 and HEK-293 cells respectively (figure 3.26).

3.3.4.2 Cells death analysis with propidium iodide (PI)

Cell death was also determined with propidium iodide which is an exclusion dye

commonly used to stain dead cells, where it binds to DNA and after binding its fluorescence increases by 20-30 fold and can be detected by flow cytometry. B16G4F and HEK-293 cells were incubated with various concentrations (10^{-7}M to10^{-5}M) of αMSH or αMSH-PPL[99] for 4 hours and 24 hours. Total 10,000 events were analysed and cell death was measured by the number of PI positive cells (figure 3.27).

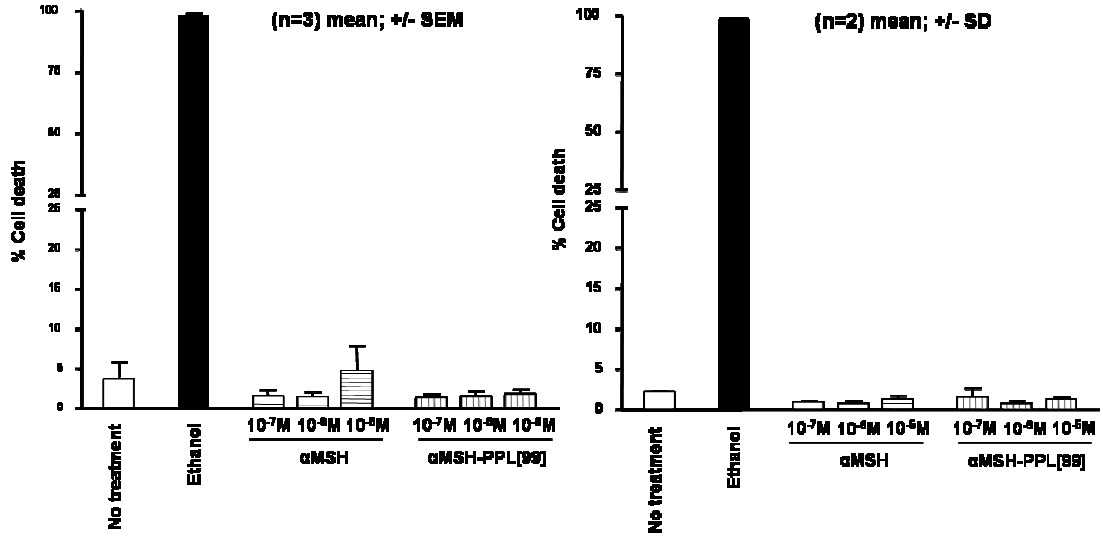

Figure 3.27. Flow cytometry based toxicity investigation in B16G4F cells. Percentage of dead cells (propidium iodide positive cells) in cultures of B16G4F cells treated for 4 hours (A) or 24 hours (B) with αMSH or αMSH-PPL[99] at concentrations ranging from 10^{-5}M to 10^{-7}M. Ethanol was used as a positive control. The data shown are the mean value of ratio + SEM of three (right panel figure) or two (left panel figure) independent experiments performed each in duplicate.

Following 4 hours treatment with the various concentration of αMSH-PPL[99] (n=3 experiments), there was no significant increase in cell death as compared to αMSH ($p = 0.366$, one way anova) (figure 3.27). In addition, after 24 hours treatment no obvious difference in cell death was observed between the αMSH-PPL[99] and αMSH treated B16G4F cells; statistical analysis could not be performed because of the low number of repeats at this time point (n=2). HEK-293 cells showed a comparatively higher percentage of dead cells at 10^{-5}M concentration of αMSH compared to αMSH-PPL[99];

again statistical analysis was not possible because of the low number of repeats (figure 3.28).

A. B.

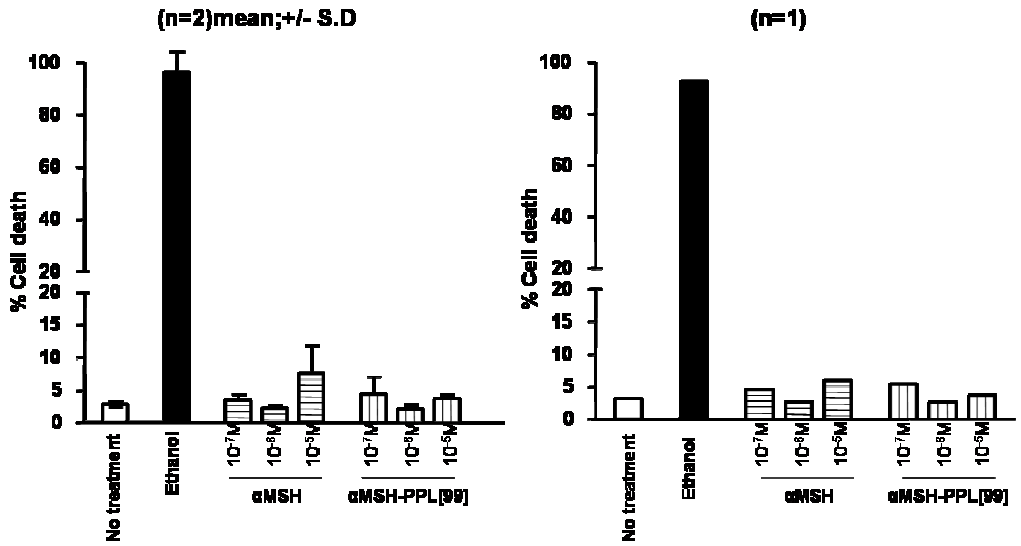

Figure 3.28. **Flow cytometry based toxicity investigation in HEK-293 cells.** Percentage of dead cells (propidium iodide positive cells) in cultures of HEK-293 cells treated for 4 hours (A) or 24 hours (B) with αMSH or αMSH-PPL[99] at concentrations ranging from 10^{-5}M to 10^{-7}M. Ethanol was used as a positive control. The data shown are the mean value of ratio + SEM of two (right panel figure) or one (left panel figure) experiment performed each in duplicates.

3.3.4.3 Cell death analysis after ultraviolet (UV) irradiation

Skin can be exposed to UVR in sunshine and UVR can have various effects in the skin depending upon the dose/lenght of exposure. Because PPL may have the potential to deliver compounds into skin; it was considered useful to know whether UVR exposure would increase the toxicity of the test compounds. The effect of different concentration of αMSH or αMSH-PPL[99] on B16G4F cell viability following UVR treatment (TL-12 lamp, 15 minutes ~ 735mJ/cm^2 a moderate UVR dose, chosen after a series of different doses) was assessed by flow cytometry. B16G4F cells were treated with αMSH or

αMSH-PPL[99] at a concentration ranging from 10^{-5}M - 10^{-7}M for 3 hours, followed by irradiation with UVB for 15 minutes in PBS. After UVB irradiation, the αMSH or αMSH-PPL [99] containing culture media was then added back and the cells were further incubated for 24 hours. The percentage of cell death was determined by the number of propidium iodide positive cells detected by flow cytometry. The results showed no obvious increase in toxicity following UV irradiation in αMSH- or αMSH-PPL[99]-treated B16G4F cells (figure 3.29); statistical analysis was not performed because of low number of repeats. Cells were incubated with ethanol (as a positive control) for 5 minutes following detachment.

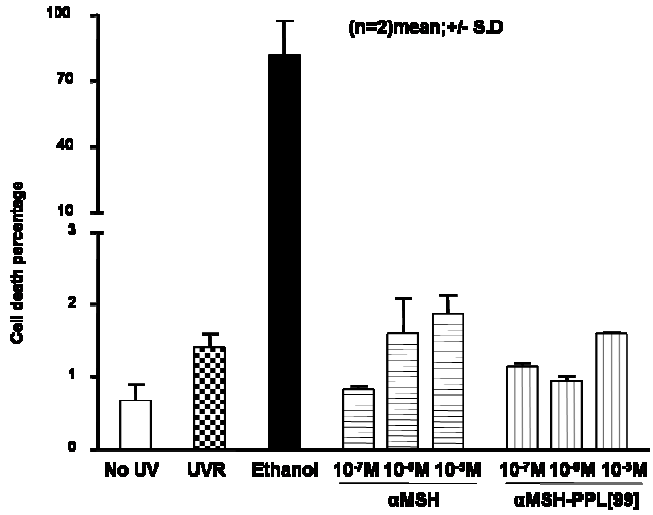

Figure 3.29. Flow cytometry based toxicity investigation in B16G4F cells following UVR irradiation. Percentage of B16G4F cell death as measured by PI positive cells in the presence of various concentrations of αMSH or αMSH-PPL[99]. The data shown are the mean value of ratio + SEM of two experiments performed each in duplicates.

3.3.5 Quantification of half life of fluorecsceinated compounds in vitro / "pulse chase" experiment

The half life of the fluoresceinated compounds was assessed *in vitro.* Briefly, B16G4F cells were treated with αMSH-PPL[99]-Fluo for 3 hours, the cells were then washed and

left in fresh culture media (without test compound) for 1, 3, 5 and 24 hours and cells were analysed on FACS for intensity of fluorescence. The results based on shift in fluorescence suggested that approximately 60% of the compound was degraded or lost from the cell at 24 hours (half life approximately 18 hours) after removal of compound from the medium (figure 3.30).

A. B. **(n=2) mean; +/- SD.**

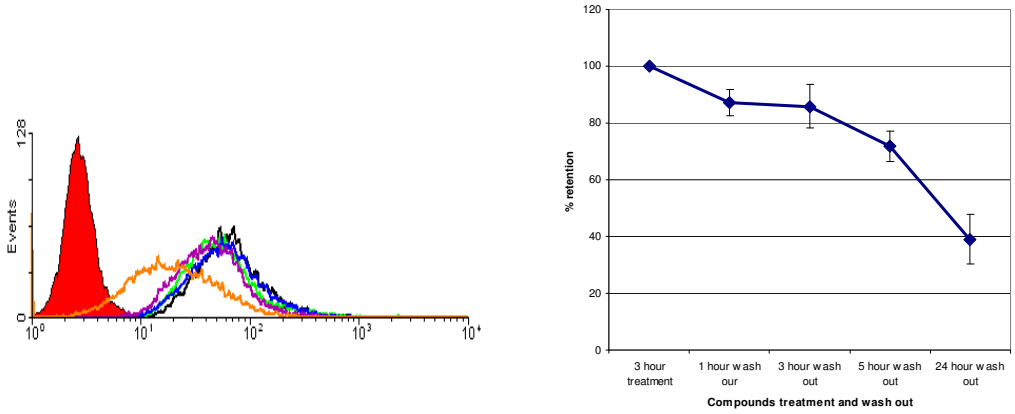

Figure 3.30. Pulse chase/ half life quantification of αMSH-PPL[99]-Fluo. A) B16G4F cells were treated with αMSH-PPL[99]-Fluo for 3 hours then mean fluorescence intensity of cells was measured following 1 hour (green empty histogram), 3 hour (blue empty histogram), 5 hour (violet empty histogram) and 24 hour (orange empty histogram) after removal of the compound from the medium and compared against 3 hours treatment (black empty histogram) with αMSH-PPL[99]-Fluo but without a washout period. Red filled histogram shows the untreated cells. B) Graph showing the percentage mean fluorescence intensity of cells following various periods after washout of compound in comparison with 3 hour treatment without washout (which was considered as 100%).

3.3.6 Anti-staphylococcal activity of αMSH, αMSH analogues and αMSH-PPL[99]

S aureus can infect skin and cause impetigo and staphylococcal scalded skin syndrome. αMSH is reported to have anti-staphylococcal activity (Cutuli *et al.* 2000), therefore PPL might be useful to deliver αMSH into skin to target this organism and might even have greater anti-staphylococcal activity if the toxicity against *S aureus* is dependent on the ability of αMSH to get inside the organism. For comparison, the anti-staphylococcal

properties of αMSH and αMSH analogues (SHU9119, NDP-αMSH and MTII) were investigated as well as αMSH-PPL[99]. Briefly, one million colony forming unit (CFU) of bacteria were incubated with 10^{-5}M concentration of the appropriate compounds for 6 hours and 24 hours in proteose-peptone broth.

With the exception of αMSH and 6 hours treatment with NDP-αMSH, all compounds significantly (one way anova) inhibited the growth of *S aureus* at 6 hours and 24 hours; αMSH-PPL[99] had a greater effect than αMSH alone but did not seem any more effective than some of the other compounds (e.g. SHU9119 at 24 hours) (figure 3.31).

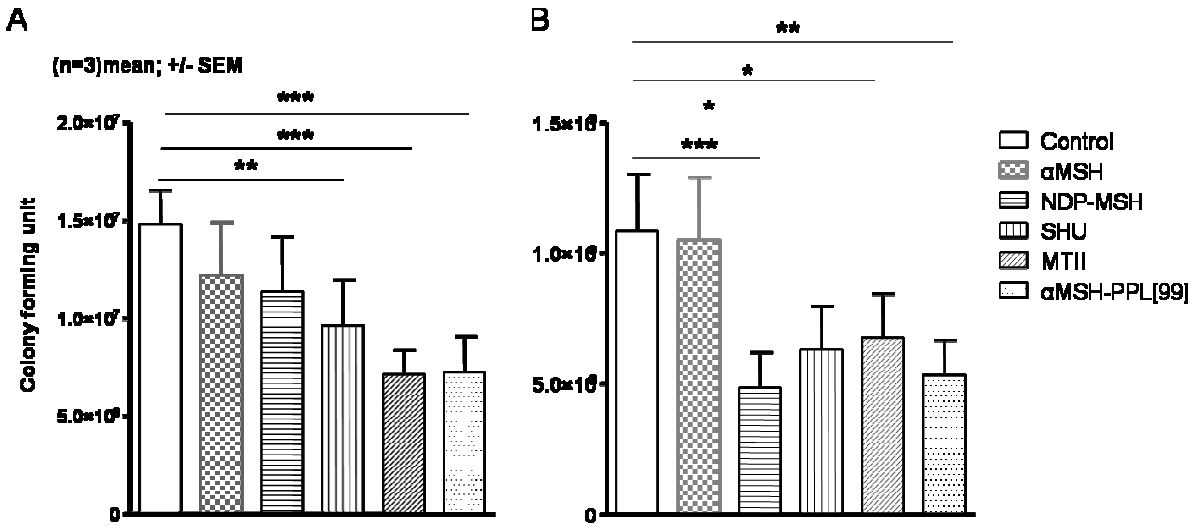

Figure 3.31. Anti-staphylococcal activity of various compounds. Effects of αMSH, its analogues and αMSH-PPL[99] on *Staphylococcal aureus* viability (measured as number of colony forming units) at 6 hours (A) and 24 hours (B). The data shown are the mean value of ratio + SEM of three experiments performed each in triplicates (*p≤0.05, ** p≤0.001,*** p≤0.0001).

3.4 Discussion

In this chapter the ability of a new carrier molecule, polypseudolysine (PPL), to deliver the neuropeptide αMSH into cells and skin was investigated. The results suggest that PPL

can deliver αMSH into various cells and skin and the limited toxicity investigations imply that PPL is not particularly toxic. Initially, in the skin penetration studies both Fluo-αMSH-PPL[98] and αMSH-PPL[99]-Fluo were used, however, αMSH-PPL[99]-Fluo was found to be more efficient at entering into the skin. Co-localisation studies with different cell markers would be necessary to confirm which cell types of the skin it gets in. Thus it is possible that the structure of the linked compounds, in particular the way the compound is attached to the cargo molecule, plays an important role in the efficiency of the transport of the cargo molecule. It is notable that the concentrations of the compounds required for the skin penetration studies were higher than the concentrations in the cell penetration investigations. However, many existing commercially available topical formulations contain concentrations of drugs which are likely to be in the 10^{-1}M to 10^{-3}M range. For example, pimecrolimus which is used to treat atopic eczema is available as a 1% cream (trade name Elidel as listed in the British National Formulary 50th edition). In addition, a landmark paper on CPP based skin delivery using polyarginine as a carrier molecule also reported the delivery of cyclosporine into mouse skin at 10^{-3}M concentration (Rothbard *et al.* 2000). It is possible that concentrations lower than 10^{-3}M of αMSH-PPL[99]-Fluo may also penetrate the skin, however, the detection methods used in this study were not sensitive enough to measure this. In most of the previous published work on CPP based topical delivery, an immunohistochemical detection method was used for the detection of the conjugate within skin (Rothbard *et al* 2000, Park *et al* 2002, Robbins *et al* 2002, Lim *et al* 2003, Lee *et al* 2005, Lopes *et al* 2005). By contrast, in this study a fluorescence signal was used for the detection of the compounds, however, fluorescein (molecular weight 332 Daltons) itself is an additional

molecule which might also have an effect on the structure of the compound. Because of the reliance on a fluorescence signal and the limitations of detection by microscopy, it was difficult to know in cases where very weak or no fluorescence was observed if the compound had penetrated, so it is possible that this might explain some of the variability in the skin penetration results. Additional investigations such as mass spectrometric examination of epidermal and dermal skin sections for the presence of the compound or immunohistochemical detection of the compounds using specific antibodies against the cargo molecule might increase the sensitivity. The variation in the skin penetration results observed in the mouse, pig and human skin studies was unlikely to be due to experimental error because measures were taken to minimise variation (such as using the same set-up, including pre-incubation of the skin in the chamber with PBS before adding the investigational compound and incubating at the same temperature in each experiment). Another source of variation could be because a few different batches of PPL compounds were used in this project, and the penetration observed with the first batch of PPL was better than that seen with the remaining batches. According to the chemist who was involved in the synthesis and purification of the PPL compound, each time the PPL conjugated compound was synthesised differently (because the synthesis formed part of a PhD thesis for the chemist). However, while that might explain some of the differences in penetration between the mouse, pig and human skin studies (the pig and human skin work was performed later than the mouse skin experiments), it would not explain much of the variability within the same experiment and between successive experiments.

One potential obstacle in CPP mediated delivery is the fact that the peptide should ideally transport the cargo into the cell and/or skin before they are metabolically

cleaved/degraded and the active (cargo) molecule should ideally remain in the cell/skin long enough to reduce the requirement for multiple daily dosing (Trehin *et al.* 2004). There are few studies published examining the metabolic stability of CPPs and their half-lives. Shen and Ryser have shown that poly-D-lysine is more stable than poly-L-lysine in respect of methotrexate delivery (Shen & Ryser 1979). Lindgren *et al* showed metabolic stability of peptides in the following order transportan>transportan10 (a analogue of transporter)>penetratin (Lindgren *et al.* 2004). Recently another investigation of the half-life of Tat, penetratin and human calcitonin derived sequences (hCT) was performed by Trehin *et al* on epithelial models (MDCK, Calu-3 and the TR146) using mass spectrometry (Trehin *et al.* 2004). In their study the half life of the compounds varied (Tat = 9-20 hours, penetratin= 1-8 hours and hCT= 30 minutes – 6 hours) depending on the epithelial model used. The fluorescence results of the αMSH-PPL[99]-Fluo compound in the B16G4F cell line in this study suggests that the compound was fairly stable with a half-life estimated to be approximately 17 hours. However, this assumes that the decrease in the intracellular fluorescence following wash-out of the compound is an indicator of the degradation of the full compound, but it is possible that only the fluorescein degrades and the αMSH-PPL remains stable for a longer period or alternatively that the αMSH was cleaved from the carrier at an earlier stage and has or has not already been degraded. Therefore, more studies would be required to test this, for example mass spectrometry of cell lysates following wash-out of the compound to determine the amount of αMSH, αMSH-PPL and αMSH-PPL-Fluo remaining in the cell. In addition, the stability of the investigational compounds in skin has not yet been examined; it could be assumed that, once the compounds penetrate the stratum corneum

barrier, the half-life of the compounds within the skin cells would be similar to the *in vitro* cell results, but it is possible that this would not be the case.

The preliminary toxicity results based on the LDH assay and PI staining of cells indicated that the PPL conjugated compound has little or no toxicity greater than that of αMSH alone. Although the skin penetration of Fluo-linked αMSH-PPL[99] was evident at 10^{-3}M, the toxicity analysis of the compound at this concentration was not performed because it was thought that only a small fraction of the compound actually penetrated the stratum corneum and translocated into the epidermis and dermis; this assumption was based on the fact that the intensity of fluorescence observed with 10^{-5}M of the compound in the cells was comparable to that seen with 10^{-3}M in the skin. However, in order to investigate the toxicity of the compound in greater detail, *in vivo* studies (e.g. applying the test compounds topically to mouse skin *in vivo*) will be required.

Several studies has been published on the anti-staphylococcal and anti-candidal activity of αMSH (Catania *et al.* 2000; Cutuli *et al.* 2000; Grieco *et al.* 2003). Because of the poor ability of αMSH to cross the stratum corneum, experiments were performed to investigate whether a PPL based approach might be useful to target *S. aureus* within the skin. Despite the observation that αMSH-PPL has more anti-staphylococcal activity compared to αMSH alone, the anti-staphylococcal activity was probably not sufficient to make it useful as a therapeutic compound.

In summary, the work in this chapter indicates that PPL can transport αMSH into cells and skin, suggesting that PPL may also have the potential to enable the topical delivery of other molecules and compounds. Investigations using another cargo molecule attached to PPL (as outlined in the next chapter) could determine whether the ability of PPL to

transport αMSH into cells and skin was based on the unique chemistry / structure of the αMSH-PPL compounds or due to a more universal ability of PPL to deliver cargo molecules across cell membranes and the stratum corneum.

Chapter 4: PPL-PNA targeted against tyrosinase

4.1 Introduction

It was shown in the previous chapter (chapter 3) that the novel CPP-based carrier molecule, PPL, delivered αMSH into cells and skin. The aim of the work presented in this chapter is to investigate the ability of PPL to transport another type of cargo molecule, i.e. an antisense agent, into cells and skin. Topical delivery of an antisense agent could be a useful approach to treat many skin diseases. For example, Citro *et al* have shown that a combination of cisplatin (a chemotherapeutic drug) and an antisense targeting *c-myc* led to a profound inhibition of the growth of melanoma cells *in vitro*, thus the topical treatment of secondary melanomas with antisense agents such as this might be an effective treatment in the longer term future (Citro *et al.* 1998). Interestingly, Mehta *et al* showed that the topical application of an oligonucleotide (ON) antisense to human skin which had been grafted onto SCID mice downregulated the expression of its target gene, intercellular adhesion molecule-1 (Mehta *et al.* 2000). Sakamoto *et al* also demonstrated that iontophoretic delivery of an oligonucleotide (ON) targeted to the IL-10 mRNA improved the skin lesions in a murine atopic dermatitis model (Sakamoto *et al.* 2004).

The advantages of the cutaneous delivery of ONs over systemic delivery include direct access to the target cells within the skin and the potential for less toxicity. Amongst the many functions of skin, one function is to generate melanin pigmentation to protect the skin from UVR. Tyrosinase is one of the main enzymes responsible for melanin pigmentation and is encoded by the tyrosinase (*Tyr, TYR)* gene. The benefits of targeting the *Tyr* gene in an assessment of the ability of PPL to transport an antisense compound into cells and skin include the fact that, in the adult, this gene is not thought to be

involved in controlling any other vital cell functions, its activity is restricted to the skin and an antisense effect could be observed directly as a decrease in cell pigmentation. It is also possible that an anti-tyrosinase agent could be useful to treat hyperpigmentation and skin disorders like melasma in the clinic or as a skin lightening agent for cosmetic reasons. Therefore tyrosinase mRNA was selected as the target to assess the efficacy of PPL to deliver an antisense peptide nucleic acid (PNA) into melanoma cells and into skin. In most of the antisense investigations in the literature to date, the translational start site is the most frequently targeted site for optimum gene inhibition. For example, in one study, 11mer PNA that targeted the translational start region of the death-signalling p75 neutrotrophin receptor (p75NTR) mRNA significantly downregulated its expression (Bonham *et al.* 1995). Another study by Mologni *et al* showed an 80% and 54% inhibition of *bcl-2* gene expression with PNA targeting the start codon and the 5' untranslated region (UTR) respectively (Mologni *et al.* 1999). The translational start site was also used by Boonanuntanasarn *et al* (2004) to target tyrosinase mRNA for the successful inhibition of pigmentation in a fish model. Although CPPs (such as penetratin, transportan and Tat) have been shown to deliver antisense agents into cells, no one has reported on a CPP-based delivery of an antisense agent into the skin. However, more efficient delivery of antisense molecules into skin might be possible with the use of a CPP-based approach, therefore a PPL-conjugated antisense ON and a PPL-conjugated antisense PNA were generated with the aim of switching off tyrosinase gene function.

4.2 Materials and Methods

4.2.1 Antisense compounds: The compounds used in this study to target the translational start site of the mouse tyrosinase mRNA are listed in chapter 2 under section 2.1, and include a 19mer-antisense ON (with and without PPL) and 9mer-, 12mer- and 15mer-antisense PNAs (with and without PPL, and with and without fluorescein to visualise the compound as required). The antisense sequences were complementary to the sense strand of the murine *Tyr* gene so that it would target the *Tyr* mRNA sequence (see figure 4.1) because the work in chapter 3 suggested that PPL carries its cargo into the cytoplasm (where it would meet the mature mRNA going to the ribosome) but not into the nucleus or only to a limited extent into the nucleus.

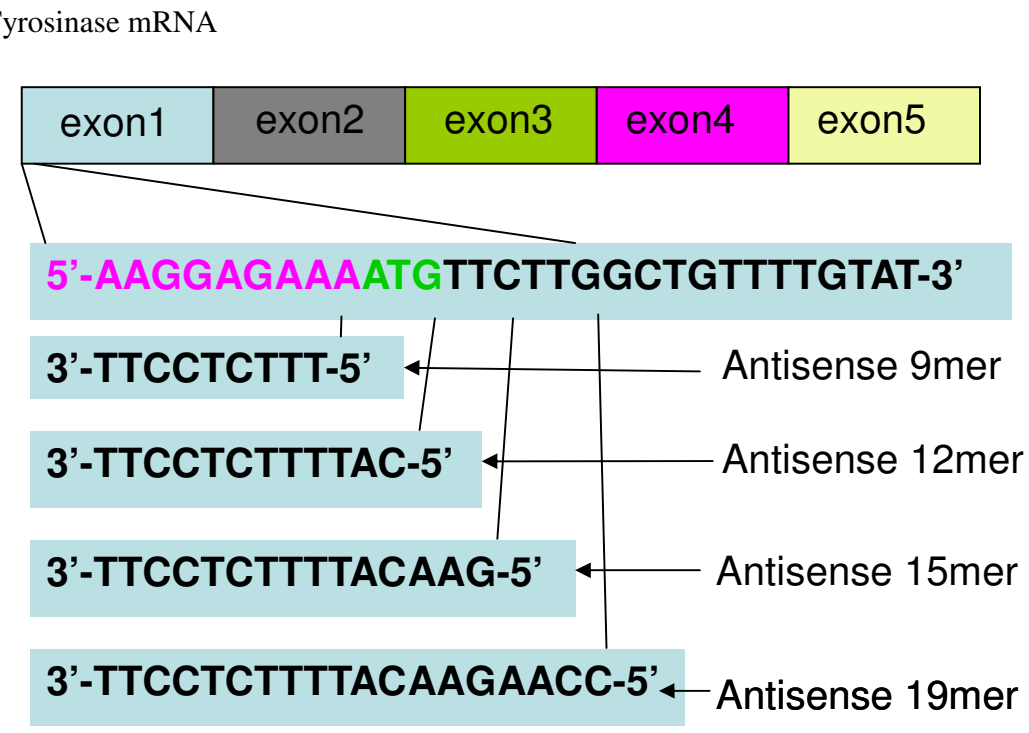

Figure 4.1. Target sequence within tyrosinase mRNA. Sequence within the 1st exon of tyrosinase mRNA targeted by the 9merPNA, 12merPNA, 15merPNA and 19merON complementary sequences.

4.2.2 Melanin assay: The intracellular melanin content of B16F10 cells was measured spectrophotometrically and compared against standard synthetic mushroom melanin as per sections 2.4 and 2.4.1. The effects of the 12merPNA, 15merPNA, 12merPNA-PPL and 15merPNA-PPL on melanin synthesis were measured after 48 hours of culture with these compounds.

4.2.3 Tyrosinase assay: Tyrosinase enzyme activity was measured spectrophotometrically and compared against standard mushroom tyrosinase. The effects of the 15merPNA and 19merON (with and without PPL) were measured after 48 hours and 96 hours of culture with these compounds on B16F10 and S91 cell lines respectively (as per material and methods section 2.14).

4.2.4 Western Blotting: B16F10 and S91 cells were analysed for the presence of tyrosinase protein using western blotting. For detailed protocol, see material and methods section 2.13.

4.2.5 Confocal microscopy: Confocal microscopy was used for the detection of the penetration of fluorescein-conjugated PNA-PPL into a B16F10 cell line *in vitro* (as per material and methods section 2.6).

4.2.6 Franz diffusion chamber / Fluorescence microscopy: Franz diffusion chamber was employed for the detection of *ex vivo* skin penetration of fluorescein-conjugated PNA-PPL into mouse and human skin (as outlined in material and methods section 2.11).

4.3 Results

4.3.1 Design of antisense compounds

In the designing of an antisense compound, it is critical to choose a sequence that binds efficiently to the target mRNA sequence of interest and to make sure that the sequence has no significant homology or complimentarity with other DNA/mRNA sequences. As outlined above in the introduction to this chapter, literature searches indicated that the translational start site of an mRNA is the most commonly used target for optimum inhibition by an antisense agent. However, the length of an antisense sequence is also a critical factor for efficient inhibition, for example, a 20merPNA complementary to the SV40 large T antigen mRNA showed 50% inhibition in its expression compared to 40% for a 15merPNA and no inhibition for a 10mer PNA (Hanvey *et al* 1992). Another parameter which was also considered in designing an effective antisense agent included the avoidance of four contiguous guanosine residues in the sequence because these might form an G-quartet and result in undesirable side effects (Matveeva *et al.* 2000). In addition, CG dinucleotides are frequently found in viral and bacterial DNA, therefore CpG motifs were avoided,in the sequence because the CG motif might stimulate immune responses during later *in vivo* experiments (Krieg *et al.* 1995; Cowdery *et al.* 1996). Furthermore, PNAs rich in GC (purine) motifs should be avoided because it might adversely affect its solubility (Koppelhus & Nielsen 2003). Following consideration of all these points, several antisense sequences were designed to target the translational start site of the tyrosinase mRNA and a BLAST database search was carried out on each sequence to avoid significant similarity with other known mRNA / DNA sequences.

4.3.2 Tyrosinase activity of melanoma cell lines

In order to develop a suitable system to measure the antisense activity of the PPL-conjugated compounds, initially the tyrosinase activity of two mouse melanoma (S91 and B16F10) cell lines was investigated in the presence of various pigmentation stimuli, including αMSH, forskolin, 3-isobutyl -1-methylxanthine (IBMX); forskolin activates cAMP by interacting with its catalytic subunit (Seamon *et al.* 1981), whereas IBMX is an inhibitor of phosphodiesterase which degrades cAMP (Fuller *et al.* 1993). Higher basal tyrosinase activity was observed in the B16F10 cells than in the S91 cells. An increase in tyrosinase activity was observed in the presense of the various stimuli in both these cell lines, with higher increases observed in the B16F10 cells. Moreover, 10^{-6}M αMSH stimulated tyrosinase more than 10^{-3}M IBMX and 10^{-6}M forskolin in the B16F10 line; tyrosinase activity was also greater in the S91 cell line after treatment with 10^{-6}M αMSH than following 10^{-3}M IBMX but was equipotent to 10^{-6}M forskolin in these cells (figure 4.2). A HaCaT keratinocyte cell line was included as a negative control and, as expected, did not show any tyrosinase activity. Because of greater tyrosinase activity, initially B16F10 cells were chosen for further antisense investigation.

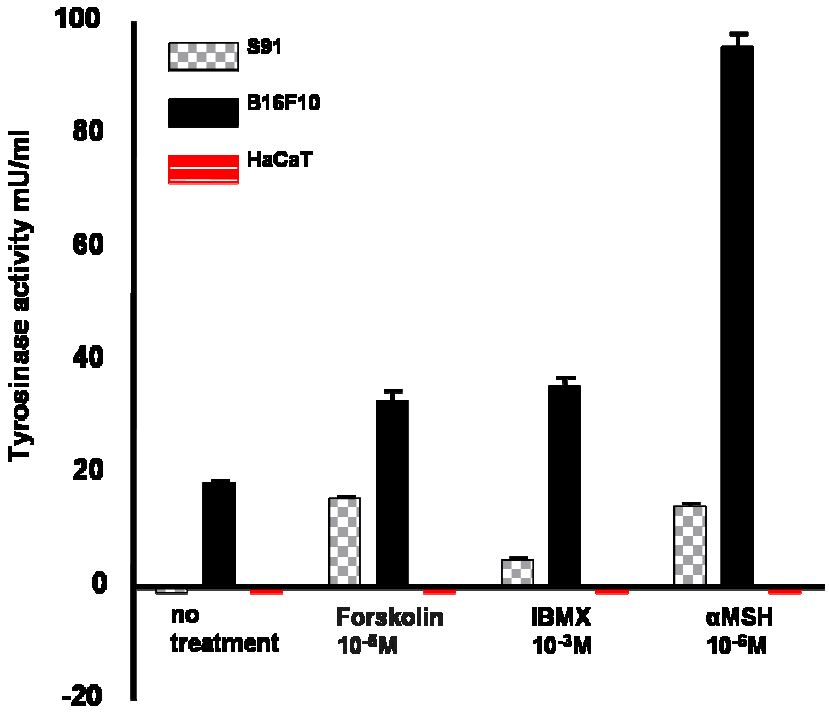

Figure 4.2. Tyrosinase activity in different cell lines. Tyrosinase activity (basal and following addition of 10^{-5}M forskolin, 10^{-3}M IBMX and 10^{-6}M αMSH) in S91, B16F10 and HaCaT cells. B16F10 and HaCaT cells were stimulated for 48 hours, whereas S91 cells were incubated for 5 days. Datas are the mean of tripicates well from a single experiment.

Western blotting with an anti–tyrosinase primary antibody (α-PEP7) at a dilution of 1:2000 was also used to detect the presence of tyrosinase protein in the B16F10 and S91 cells. Tyrosinase was easily detected in the B16F10 cells after 2 days culture, but S91 cells are less pigmented than B16F10 cells and it was difficult to detect a basal level of tyrosinase in the S91 cells after 5 days in culture. Therefore 10^{-6}M αMSH was added to stimulate the production of tyrosinase in the S91 cells, but despite the presence of a tyrosinase band in the αMSH-treated S91 cells, more tyrosinase protein was observed in the unstimulated B16F10 cells than in the αMSH-stimulated S91 cells (figure 4.3).

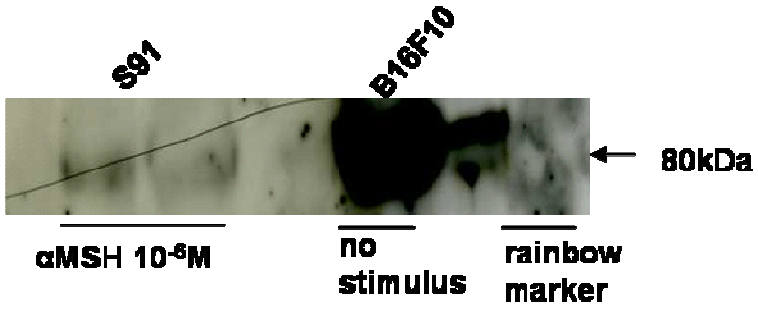

Figure 4.3. Detection of tyrosinase protein in melanoma cells. Western blot demonstrating the presence of tyrosinase in αMSH treated S91 cells and in B16F10 cells following 5 days and 2 days culture respectively. α-PEP-7 antobody at a dilution of 1:2000 was used to detect the presence of tyrosinase protein and representative image from one of the three independent experiments are shown.

Based on the levels of tyrosinase protein / activity, and the ease of inducing tyrosinase activity in these lines, it was considered that the B16F10 and S91 cell lines were likely to be appropriate for the study of the antisense activity of the PPL-conjugated compounds. However, it was thought best to avoid testing the antisense effects in cells with too little tyrosinase activity and also in cells in which the tyrosinase was over-stimulated, thus a dose response study with a range of concentrations of αMSH was performed on B16F10 cells in order to select a suitable level of tyrosinase activity for future studies. An increase in tyrosinase activity was observed for concentrations higher than 10^{-10}M αMSH (figure 4.4) in each of the three separate experiments.

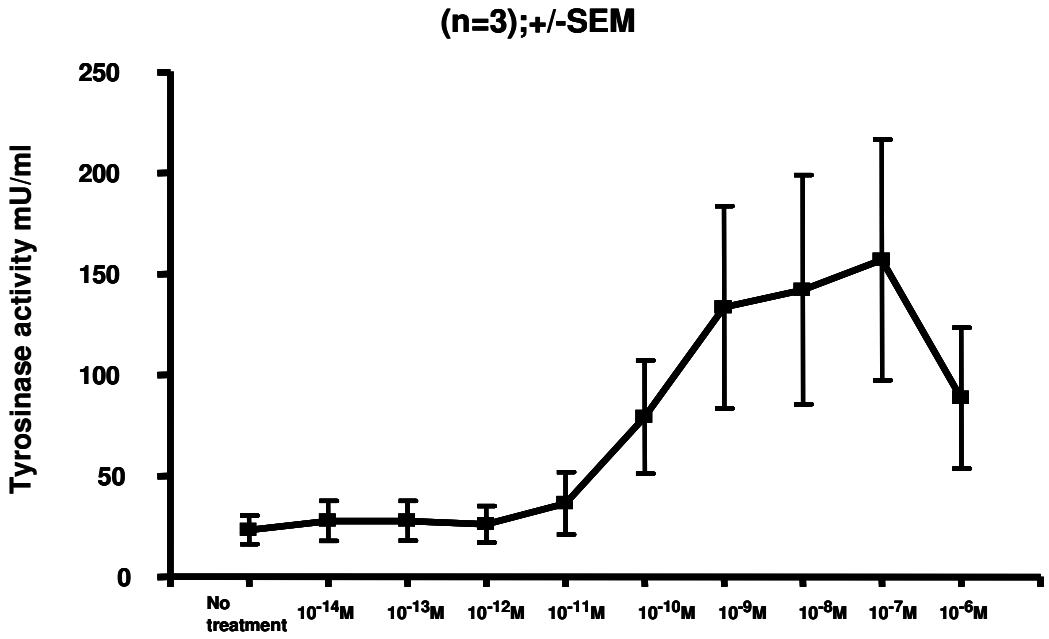

Figure 4.4. Tyrosinase activity in B16F10 cells following increasing doses of αMSH. Tyrosinase activity in B16F10 cells treated with a range of doses of αMSH in comparison with no treatment. Note that there is an increase in tyrosinase activity at αMSH concentrations of 10^{-10}M and above; the decrease in tyrosinase activity at 10^{-6}M in comparison with 10^{-9}M to 10^{-7}M might be due to growth inhibition of B16F10 cells by 10^{-6}M αMSH (as per the greater inhibition of proliferation of wild type *MC1R* transfected B16G4F cells by 10^{-6}M αMSH in Robinson & Healy, 2002). The data shown are the mean ± SEM of three experiments performed each in triplicate.

A dose response melanin assay was also performed in B16F10 cells following stimulation with different concentrations (10^{-12}M to 10^{-8}M) of αMSH. A dose dependent increase in melanin pigmentation was observed in each of three separate experiments (figure 4.5). Based on the results of the melanin and tyrosinase dose response assays, 10^{-10}M αMSH was selected to stimulate tyrosinase activity / melanin pigmentation in subsequent experiments on B16F10 cells.

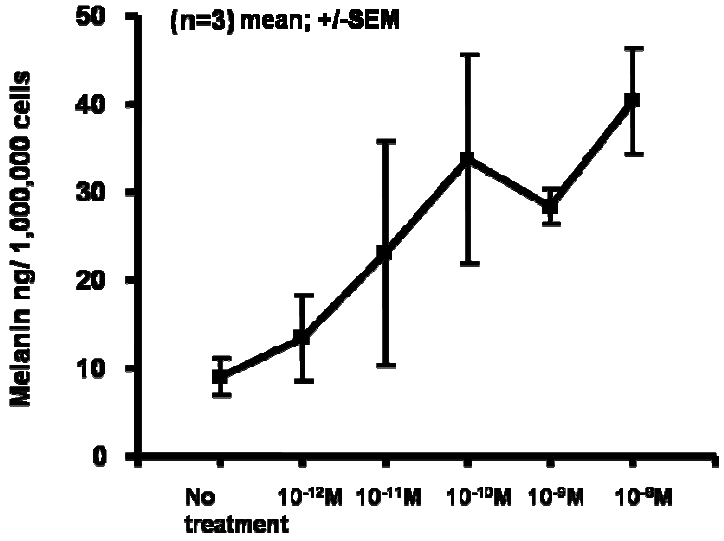

Figure 4.5. Meanin synthesis in B16F10 cells follwing increasing doses of αMSH. Melanin assay showing an increase in pigmentation of B16F10 cells in a dose dependent manner (except 10^{-9}M) following treatment with different concentrations (10^{-8}M to 10^{-12}M) of αMSH. The data shown are the mean ± SEM of three experiments performed each in triplicate.

4.3.3 Antisense activity of 15merPNA-PPL targeted against mouse tyrosinase

The ability of the 15merPNA-SS-PPL to inhibit tyrosinase activity was investigated. Briefly, B16F10 cells were cultured in 96-well plates with or without 10^{-10}M αMSH, and different concentrations (10^{-7} to 10^{-5}M) of 15merPNA-SS-PPL. Analysing the group overall, αMSH-stimulated tyrosinase activity was significantly inhibited by 15merPNA-SS-PPL ($p \leq 0.05$, One Way ANOVA, figure 4.6), however individual concentration did not appear significant compare to αMSH stimulation but a reduction in tyrosinase activity was observed in each of three separate experiments (figure 4.6). No inhibition of

tyrosinase activity was seen with PNA plus αMSH treatment (i.e. PNA which had not been conjugated to PPL). A paired t-test was also performed to analyse the data, which showed significant ($p \leq 0.003$, paired t-test, fig 4.6) reduction in tyrosinase activity by 15merPNA-SS-PPL when compared to PNA plus αMSH (but not with αMSH alone).

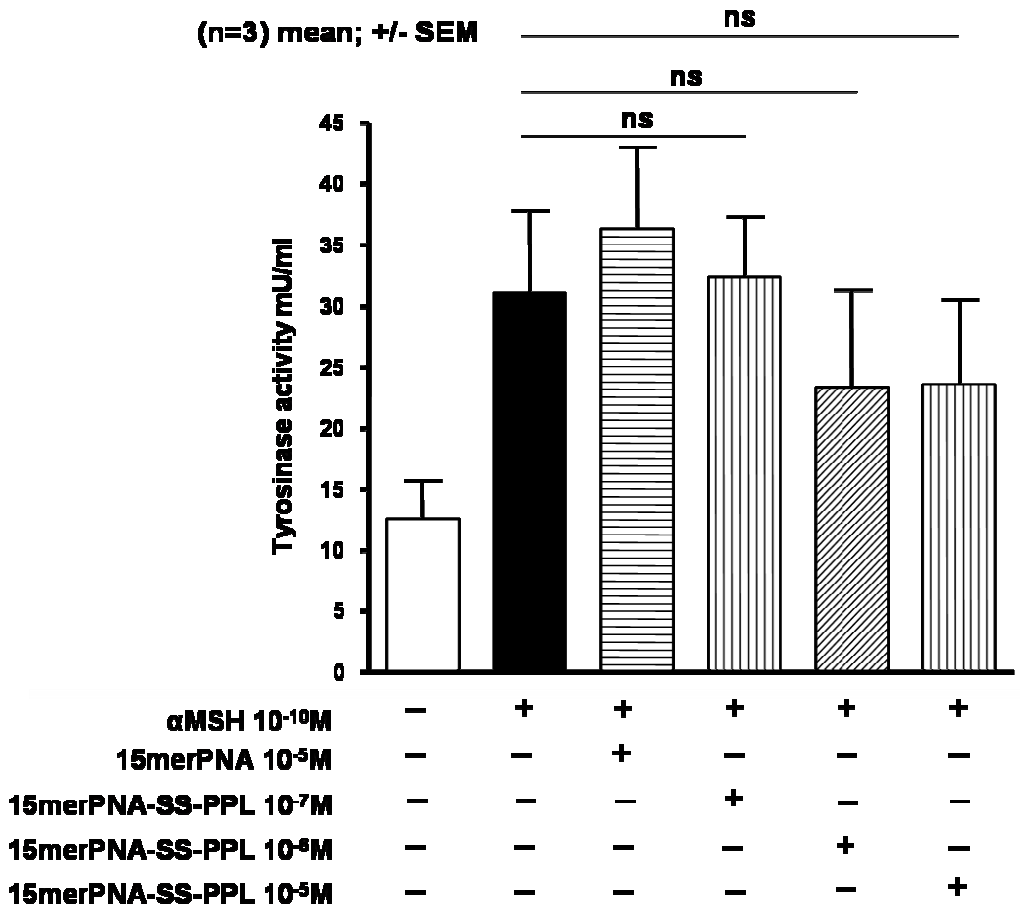

Figure 4.6. Effect of 15merPNA-SS-PPL on αMSH-induced tyrosinase activity in B16F10 cells. Different doses (10^{-5}M to 10^{-7}M) of In contrast to PNA alone, 15merPNA-SS-PPL were analysed for the reduction in tyrosinase activity in B16F10 cells. The results showed a reduction in αMSH-stimulated tyrosinase activity following treatment with 15merPNA-SS-PPL. The data shown are the mean ± SEM of three experiments performed each in duplicate.

The ability of 15merPNA-SS-PPL to inhibit αMSH-induced melanin synthesis in the B16F10 cell line was investigated. Intracellular melanin was measured after 48 hours following the addition of 10^{-5}M 15merPNA-SS-PPL and separately 15merPNA. Compared to αMSH alone or PNA plus αMSH treatment, the 15merPNA-SS-PPL significantly inhibited the αMSH stimulated melanin production ($p \leq 0.001$, One Way ANOVA, $p \leq 0.001$ and $p \leq 0.009$, paired t-test compare to αMSH alone or PNA plus αMSH treatment respectively, figure 4.7).

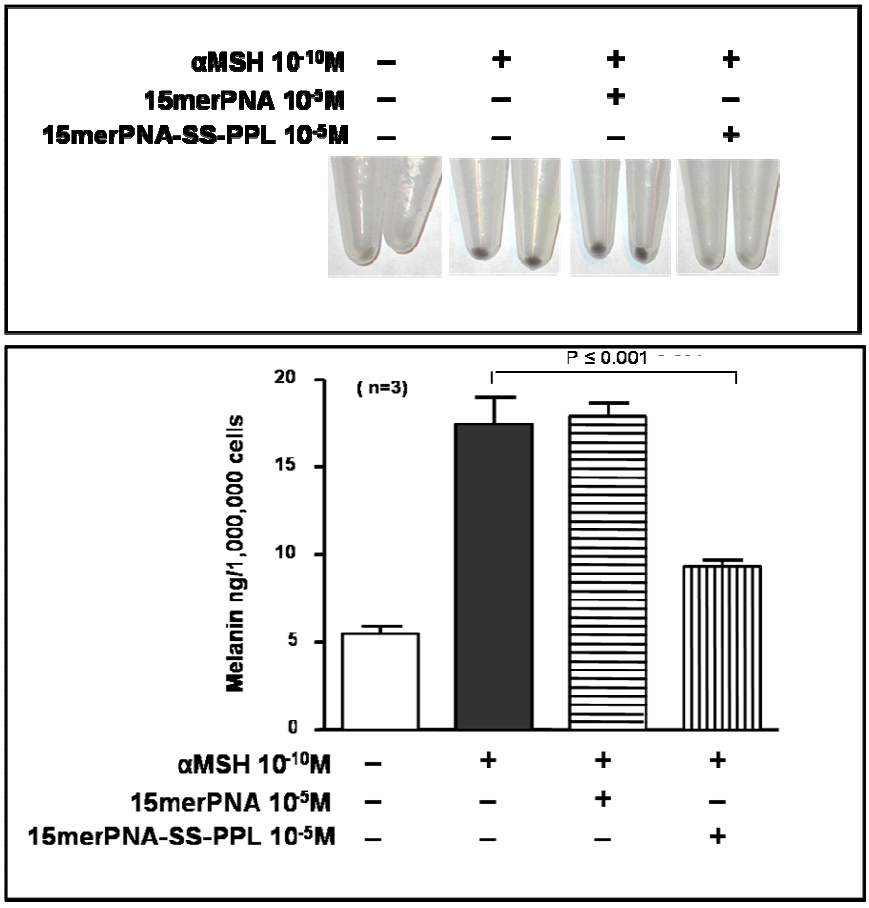

Figure 4.7. **Effect of 15merPNA-SS-PPL on αMSH-induced melanin synthesis in B16F10 cells.** 15merPNA-SS-PPL at 10^{-5}M significantly inhibited αMSH-induced pigmentation of B16F10 melanoma cells whereas 15merPNA in the absence of the PPL carrier did not. Upper panel shows cells pellet from a single representative experiment after culture for 48 hours. The data shown in lower panel are the mean ± SEM of three experiments performed each in duplicate.

The antisense activity of 15merPNA-SS-PPL was also investigated on S91 cells using the melanin assay readout. 10^{-9}M αMSH was used as a stimulus in this case because the S91 cells are less pigmented than B16F10 cells. Compared to αMSH alone or PNA plus aMSH treatment, a decrease in αMSH-induced pigmentation was seen with the 15merPNA-SS-PPL in each of three separate experiments, although the overall reduction from the three experiments was not statistically significant ($p>0.05$, One Way ANOVA, $p\leq0.09$ and $p\leq0.11$, paired t-test compare to αMSH alone or PNA plus αMSH treatment respectively, figure 4.8). PNA alone did not have an inhibitory effect on αMSH stimulated S91 cells pigmentation.

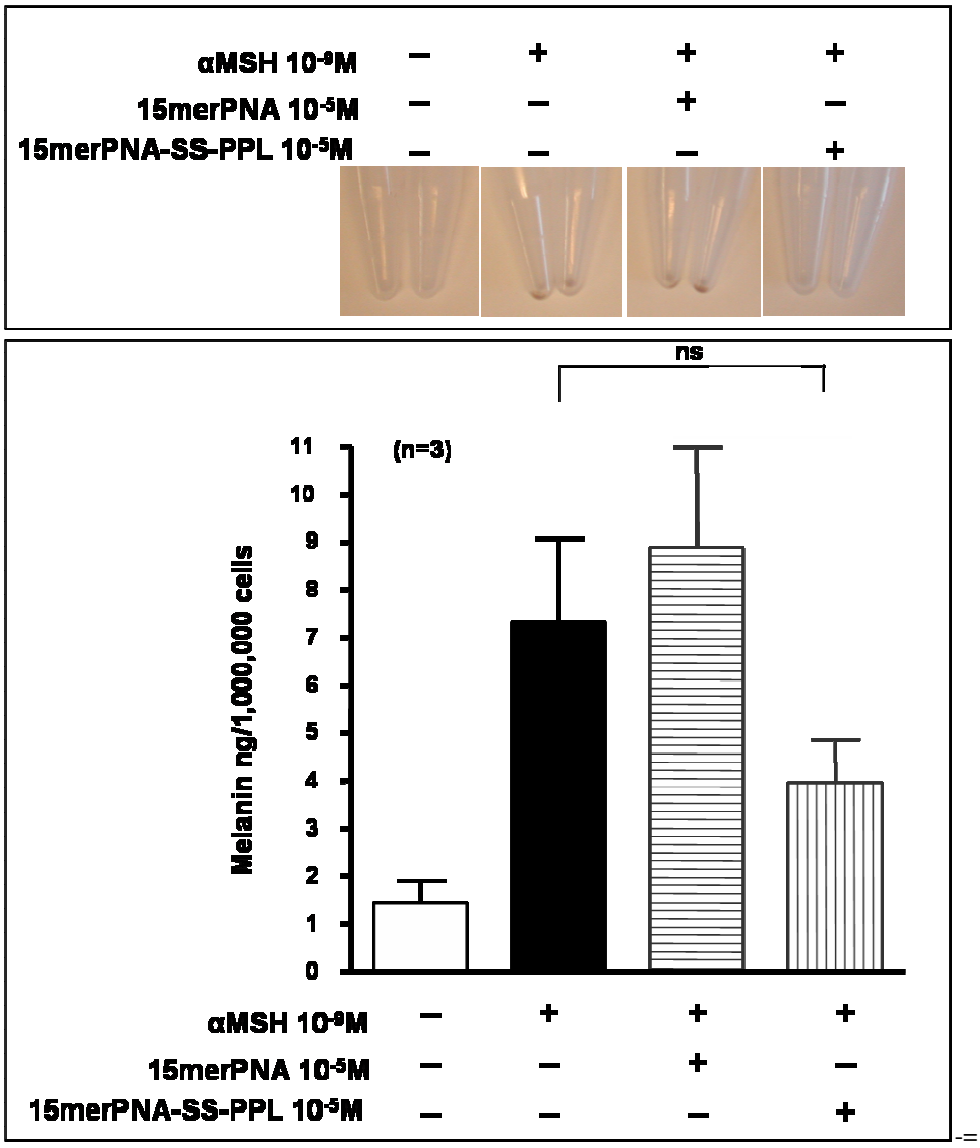

Figure 4.8. Effect of 15merPNA-SS-PPL and 15merPNA on αMSH-stimulated pigmentation in S91 cells. 15merPNA-SS-PPL at 10^{-5}M inhibited αMSH-induced pigmentation from each of three separate experiments, whereas 15merPNA in the absence of the PPL carrier did not. Upper panel shows cells pellet from a single representative experiment after culture for 96 hours. The data shown are the mean ± SEM of three experiments performed each in duplicate.

A version of the 15merPNA linked to PPL by a maleimide linker (15merPNA-M-PPL) was also generated by the chemists. To investigate the antisense activity of the 15merPNA-M-PPL compound, an αMSH-stimulated melanin assay was performed using the B16F10 cell line. Compared to αMSH alone or PNA plus aMSH treatment, a

reduction in αMSH-stimulated pigmentation was observed in each of three separate experiments with 10^{-5}M 15merPNA-M-PPL, but the overall results of the three experiments were not statistically significant ($p>0.05$ or paired t-test, figure 4.9). 15merPNA alone had no effect on αMSH-stimulated pigmentation (figure 4.9).

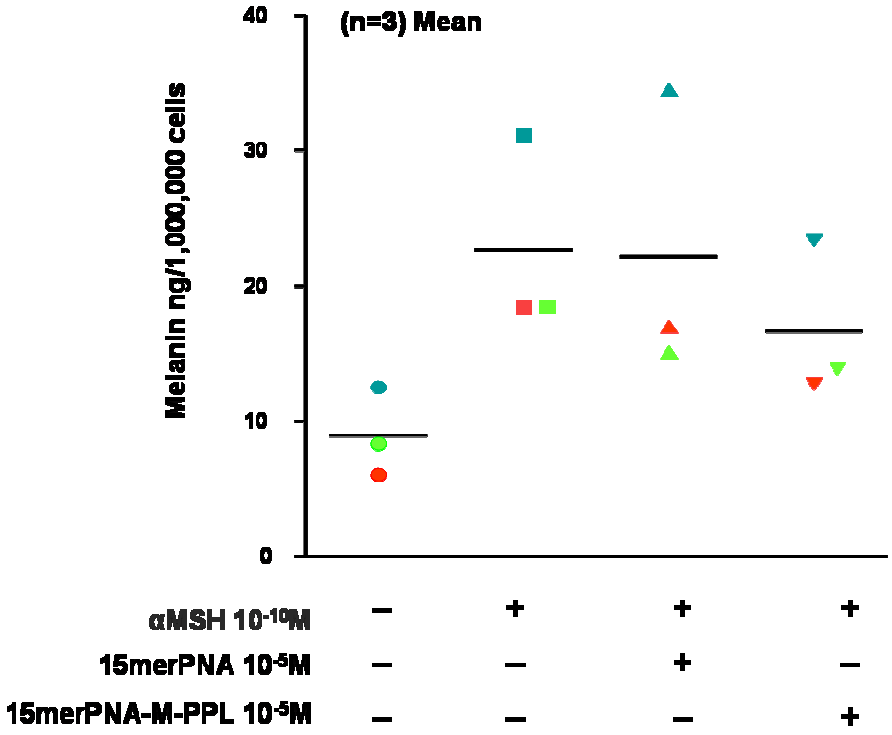

Figure 4.9. Effect of 15merPNA-M-PPL and 15merPNA on αMSH-stimulated pigmentation in B16F10 cells. Melanin assay results of αMSH-induced melanin pigmentation in B16F10 cells with 10^{-5}M 15merPNA-M-PPL and 10^{-5}M 15merPNA. Each of three separate experiments is represented by different coloured symbols and mean of three experiments (performed each in duplicate) is shown as black line.

4.3.4 Antisense activity of 12merPNA-PPL targeted against mouse tyrosinase

To examine whether a 12merPNA conjugated to PPL (12merPNA-PPL) could inhibit tyrosinase activity/melanin pigmentation, a melanin assay was performed on both B16F10 and S91 cells following stimulation with αMSH. The results showed that 10^{-5}M

12merPNA-PPL significantly inhibited 10^{-10}M αMSH-induced melanin synthesis by B16F10 cells as compared to αMSH alone or PNA plus αMSH ($p \leq 0.05$, One Way ANOVA, $p \leq 0.004$, paired t-test compare PNA plus αMSH treatment, figure 4.10).

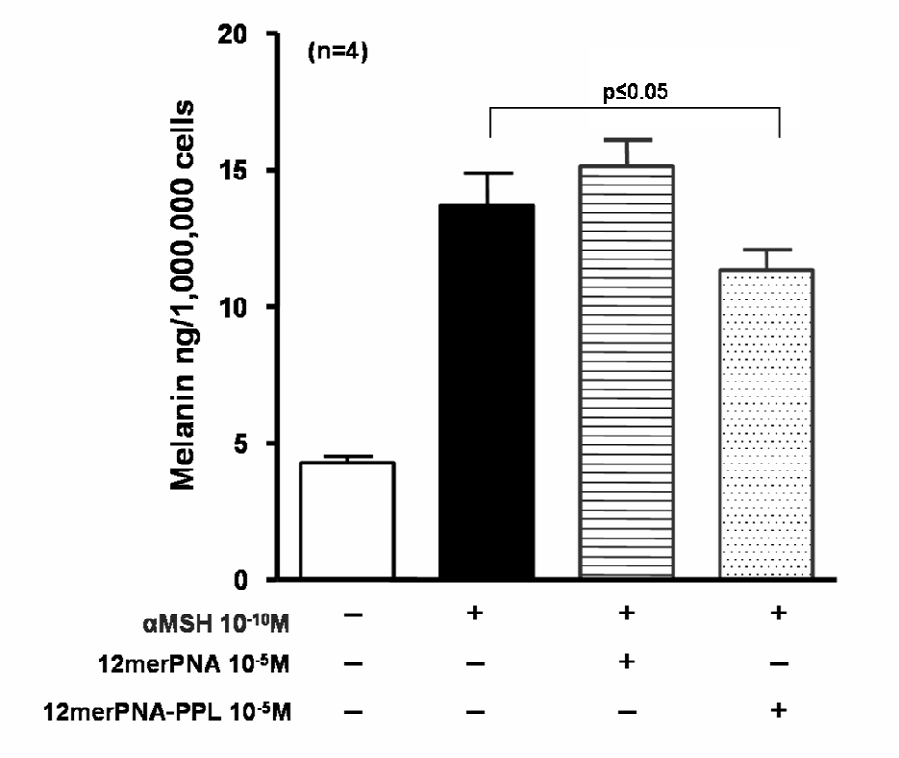

Figure 4.10. **Effect of 12merPNA-PPL and 12merPNA on αMSH-stimulated pigmentation in B16F10 cells.** A melanin assay was performed to investigate the antisense activity of 12merPNA-PPL on αMSH-stimulated B16F10 cells. As compared to αMSH treated cells, αMSH stimulated pigmentation of B16F10 cells was significantly inhibited by the 12merPNA-PPL. The data shown are the mean ± SEM of four experiments performed each in duplicate.

As compared to PNA alone, the αMSH-stimulated S91 cell pigmentation was inhibited by 12merPNA-PPL at $3x10^{-5}$M concentration ($p \leq 0.05$, One Way Anova and $p \leq 0.018$ paired t-test, figure 4.11) however in comparison to αMSH alone the inhibition of αMSH-stimulated pigmentation were not significant but a reduction in melanin was observed in each of three separate experiments. A reduction in pigmentation was also observed at a

10^{-5}M concentration of 12merPNA-PPL in each of three separate experiments, but this was not statistically significant (figure 4.11).

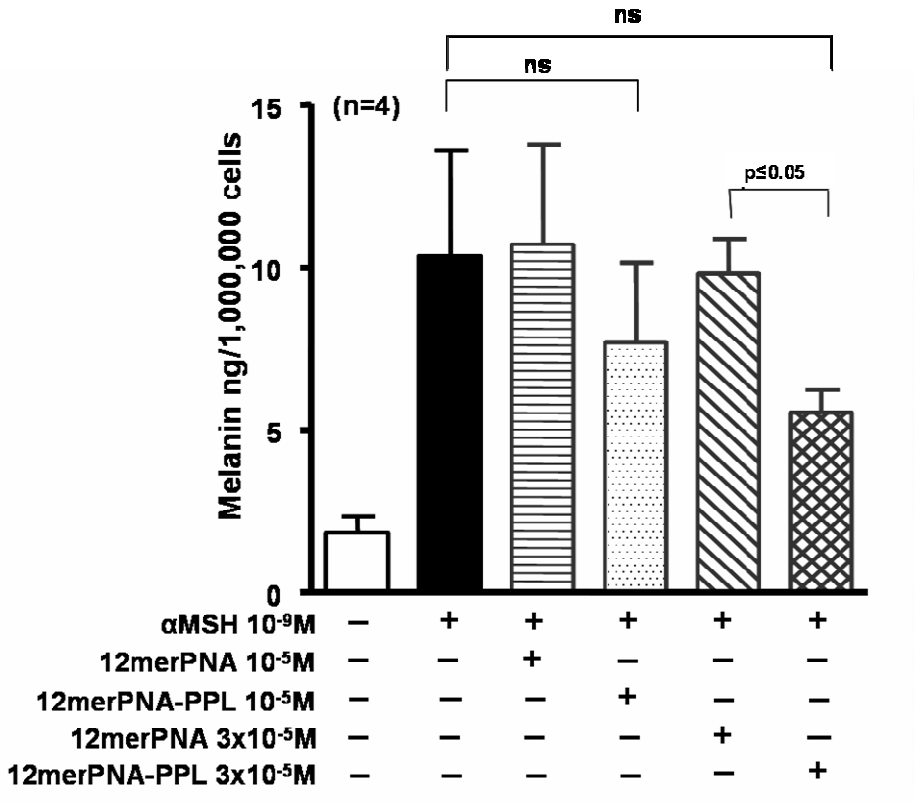

Figure 4.11. Effect of 12merPNA-PPL and 12merPNA on αMSH-stimulated pigmentation in S91 cells. Two different concentrations (10^{-5}M and 3 x10^{-5}M) of 12merPNA and 12merPNA-PPL were investigated for antisense activity in a melanin assay on S91 cells. As compared to 12merPNA alone but not with αMSH, the αMSH-stimulated S91 cell pigmentation was significantly inhibited by 12merPNA-PPL at 3x10^{-5}M concentration. The data shown are the mean ± SEM of four experiments performed each in duplicate.

4.3.5 Cytotoxicity investigation

The LDH assay was performed on S91 cells to determine cytotoxicity following treatment with 10^{-5}M and 3 X 10^{-5}M of 12merPNA, 15merPNA, 12merPNA-PPL, and 15merPNA-PPL for 3 hours. The results suggest that PPL conjugated PNA and PNA alone were minimally or non toxic (figure 4.12).

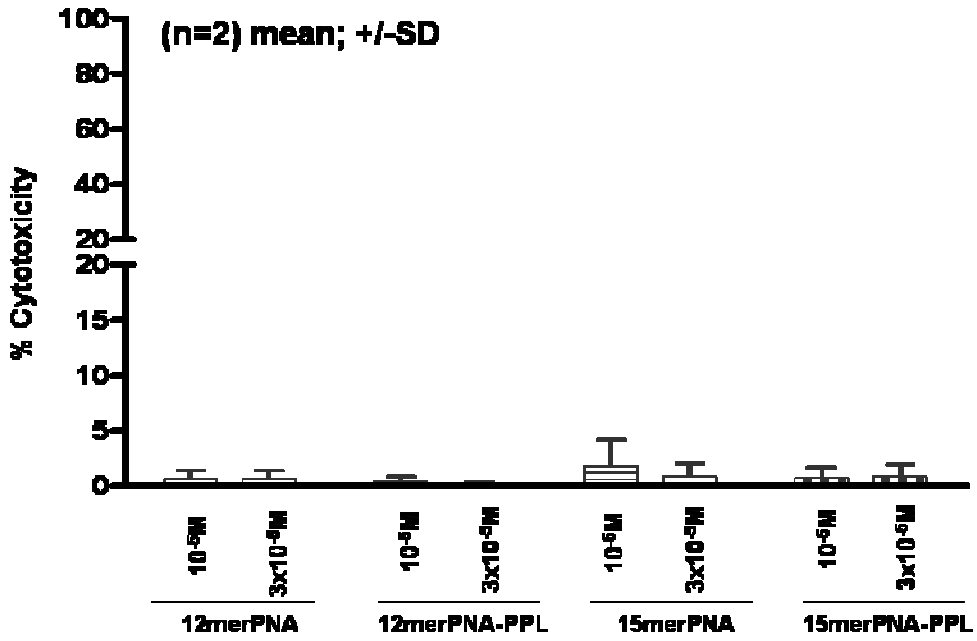

Figure 4.12. Toxicity investigation. Results of LDH assay which was performed to investigate the cytotoxicity of S91 cells following treatment with 12merPNA, 15merPNA, 12merPNA-PPL and 15merPNA-PPL. S91 cells showed minimal or no toxicity at the two different concentrations of the 12merPNA, 15merPNA, 12merPNA-PPL and 15merPNA-PPL which were tested. The data shown are the mean ± SEM of two experiments performed each in triplicate.

4.3.6 *In vitro* cells penetration investigation

Although fluorescein-conjugated 15merPNA-SS-PPL and 15merPNA-M-PPL had been synthesised by the chemists, these compounds would not dissolve completely and could not be used for cell (and skin) penetration studies. Therefore, cell penetration investigations were carried out with fluoresceinated PNA-PPL, in which the PNA was directly coupled to PPL instead of using a disulfide or a maleimide linker. B16F10 cells were used to investigate the *in vitro* penetration with fluorescein-linked 9mer/12mer/15merPNA-PPL. The confocal microscopy results showed that PPL can deliver PNA (irrespective of its length) into B16F10 cells (n=2 in duplicates), but this

was at a concentration of 10^{-4}M (figure 4.13). Fluorescein-conjugated PNA without PPL penetrated poorly into the cells (n=2 in duplicates).

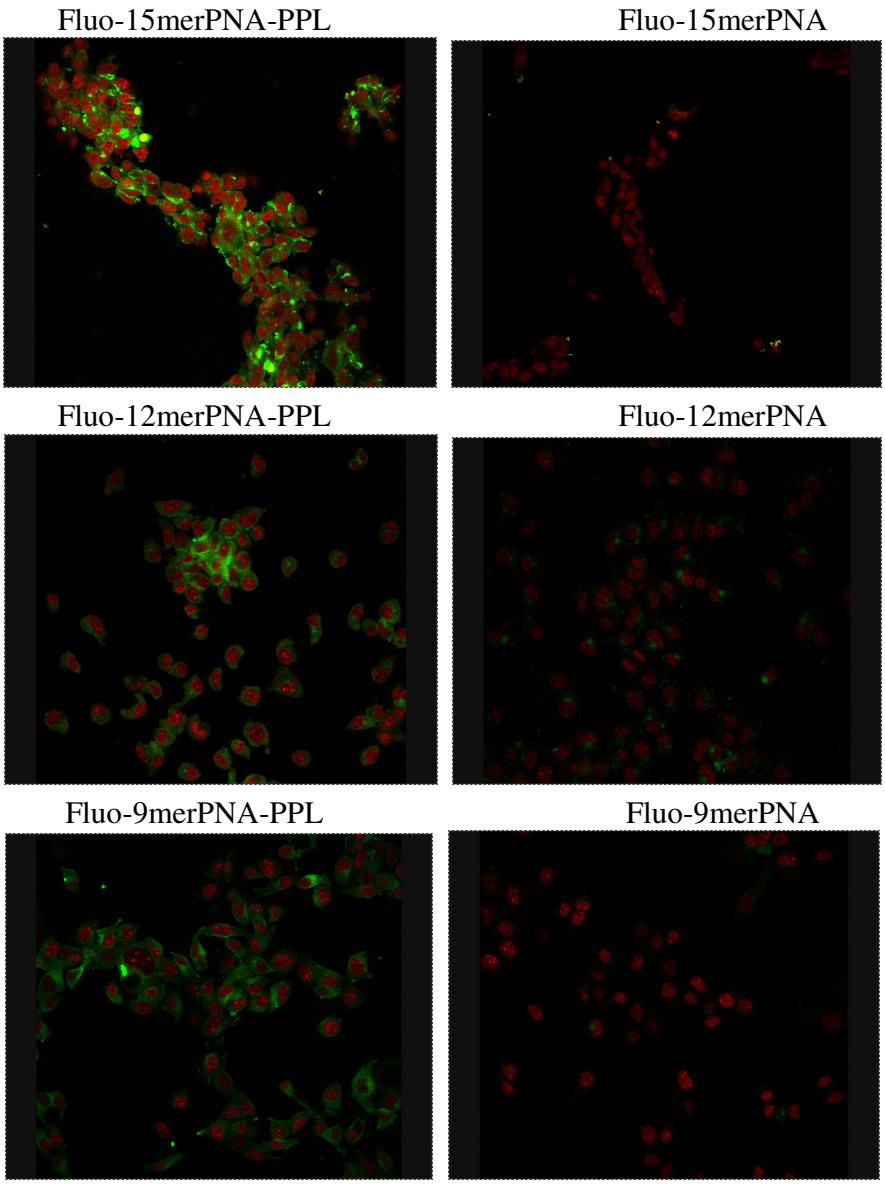

Figure 4.13. Cell penetration of 9mer, 12mer, 15merPNA with or without PPL in live B16F10 cells, subsequently fixed in PFA. Confocal microscopy (Z-plane) indicates that fluorescein-conjugated PNA-PPL compounds (10^{-4}M for 3 hours) can penetrate into B16F10 cells. TO-PRO-3 counterstaining of nuclei (seen as red) shows that the PPL-conjugated compounds have entered into most cells. Fluorescein conjugated PNA did not penetrate into the cells. Images were taken at 40x magnification with a scale bar of 75µm.

Cell penetration investigations were also performed on live unfixed B16F10 cells with

12merPNA-PPL and 15merPNA-PPL. The results demonstrated that the 12merPNA-PPL and 15merPNA-PPL penetrated into live cells (n=2 in duplicates) following 3 hours incubation at 10^{-4}M (figure 4.14).

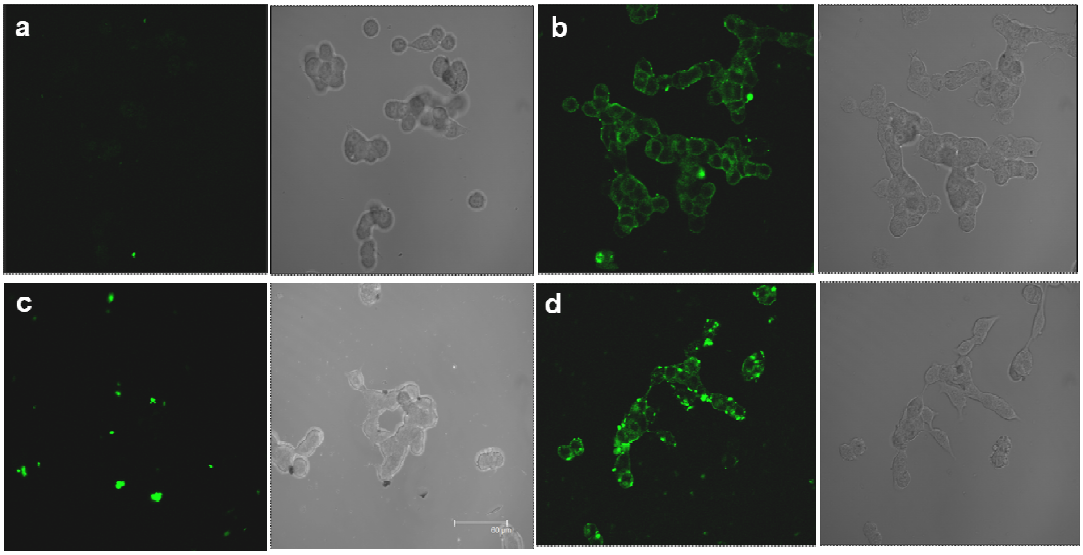

Figure 4.14. **Cell penetration of 9mer, 12mer, 15merPNA with or without PPL in live unfixed B16F10 cells.** Confocal microscopy demonstrated that fluorescein-conjugated 12merPNA-PPL (b) and 15merPNA-PPL (d) penetrated into the majority of live unfixed B16F10 cells, whereas fluorescein-conjugated 12mer PNA (a) or 15merPNA (c) without PPL did not internalise. Trans-illuminated images (for each treatment) indicate the presence of the cells in the field of view. Microscopy was performed after the cells were incubated with 10^{-4}M of the compounds for 3 hours. Images were taken at 40x magnification with a scale bar of 75µm.

4.3.7 *Ex vivo* skin penetration investigations

To examine the ability of PPL to carry PNA into the skin, *ex vivo* skin penetration studies in a Franz diffusion chamber were performed. The results demonstrated that fluoresceinated PNA-PPL compounds (10^{-3}M for 3 hours) penetrated into the mouse skin whereas fluorescein-conjugated PNA did not (figure 4.15).

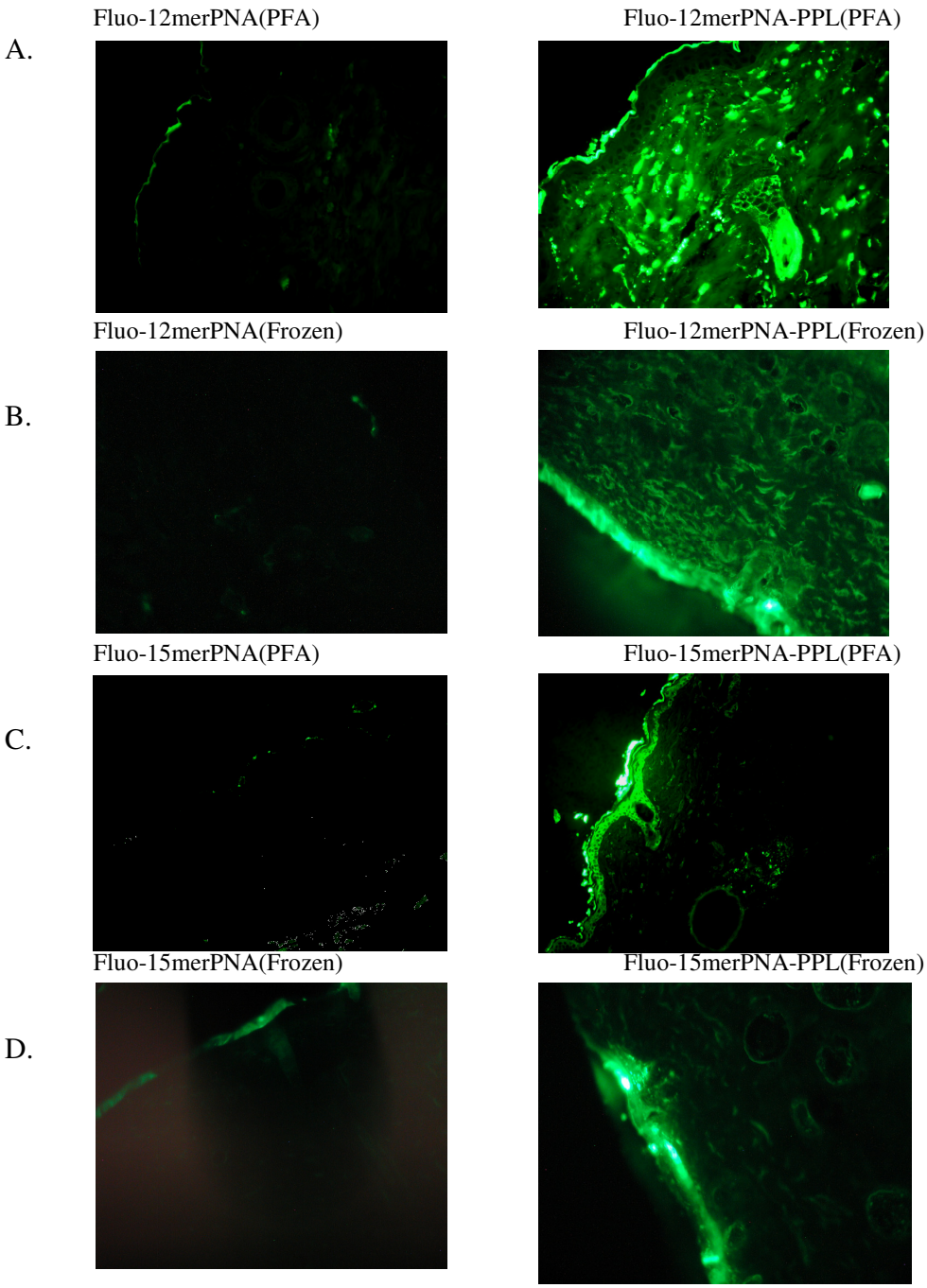

Figure 4.15. **Penetration of 12mer and 15merPNA with or without PPL into mouse skin.** After treatment skin was either fixed in PFA or frozen prior to sections being cut. Results indicated that fluorescein labelled 12merPNA-PPL penetrated into the epidermis and dermis of mouse skin (A and C), whereas 15merPNA-PPL penetrated mainly into the epidermis (B and D). Fluorescein labelled PNA without PPL did not penetrate appreciably into the epidermis or dermis.

Interestingly, the skin penetration of the Fluo-15merPNA-PPL seemed to be mainly confined to the epidermis whereas the Fluo-12merPNA-PPL was observed in both the epidermis and dermis. The overall *ex vivo* topical penetration events in mouse skin are summarised in figure 4.17. Weak to moderate penetration of PPL conjugated 15merPNA was evident in both paraformaldehyde and frozen unfixed mouse skin, however, strong or very strong penetration of 15merPNA-PPL was seen only in paraformaldehyde-fixed tissues. In a few cases the pattern of fluorescence suggested that the PPL-conjugated compounds may have entered into/by the skin's appendages. The *ex vivo* skin penetration studies were also carried out in human skin. As compared to fluoresceinated-PNA alone, fluoresceinated-12merPNA-PPL penetrated into human skin (n=2) at a concentration of 10^{-3}M after 3 hours incubation time. In contrast to the skin penetration of this compound in mouse skin (figure 4.15), the 12merPNA-PPL mainly localised into the epidermis (figure 4.16).

A) B)

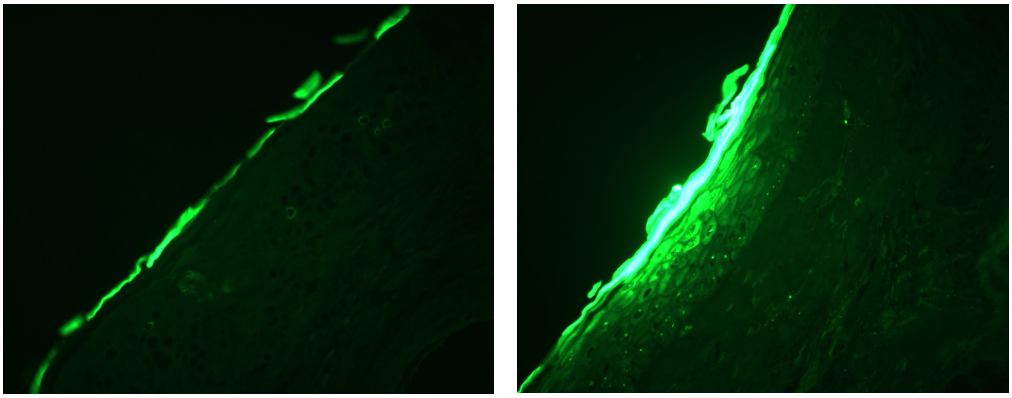

Figure 4.16. **Penetration of 12mer with or without PPL into human skin, subsequently fixed in PFA.** PPL-conjugation enhances the penetration of 12merPNA (B) into human skin, whereas 12merPNA alone (A) did not penetrate to the same extent.

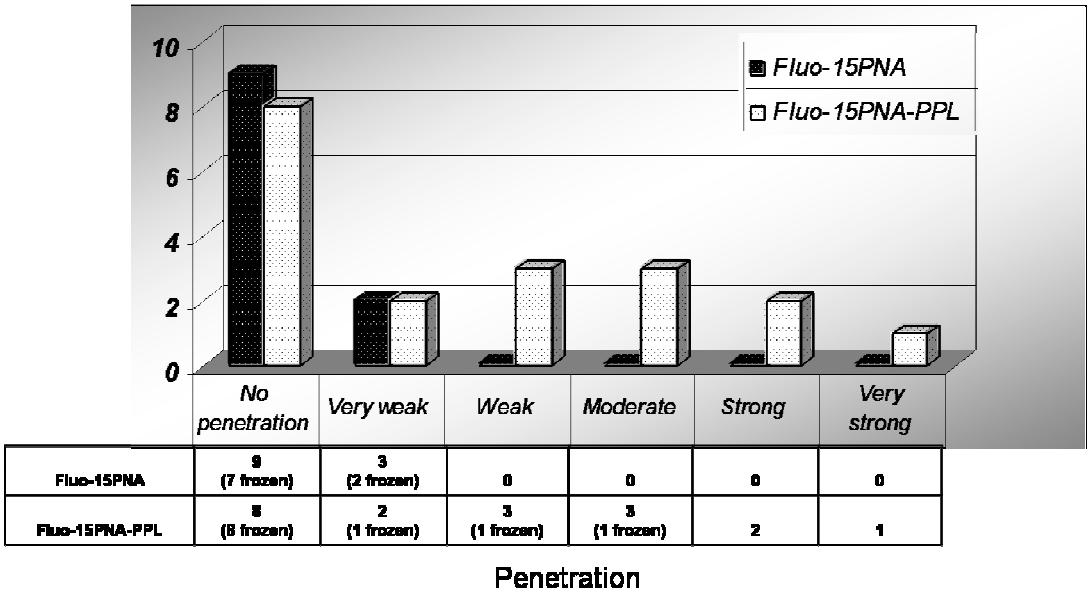

Figure 4.17. Penetration of 15merPNA or 15merPNA-PPL into mouse skin. Summary of penetration skin events of fluoreceinated 15merPNA or 15merPNA-PPL on both fixed and frozen mouse skin.

4.4.8 Antisense oligonucleotide targeted against the mouse tyrosinase

During the synthesis of the PNA-PPL compounds, a limited amount of a PPL-linked 19mer antisense oligonucleotide (ON) was generated by the chemists because it was considered worthwhile conjugating the PPL to commercially synthesised ON as a proof of concept for being able to attach PPL to antisense molecules generated by other companies. The ON was linked to the PPL in two ways, i.e. via a single sulfide linker and via a disulfide linker. To investigate the basal and αMSH (10^{-10}M) stimulated antisense activity of 19merON-S-PPL / 19merON-SS-PPL, a tyrosinase assay was performed on the B16F10 cell line (n=3 in duplicates wells). Although a mild reduction in B16F10 basal tyrosinase activity was seen at 48 hours incubation with 10^{-5}M 19merON-SS-PPL (and less reduction with 19merON-S-PPL) in each of three separate experiments, this

reduction was not statistically significant (figure 4.18). Unexpectedly, the ON alone seemed to increase "basal" tyrosinase activity.

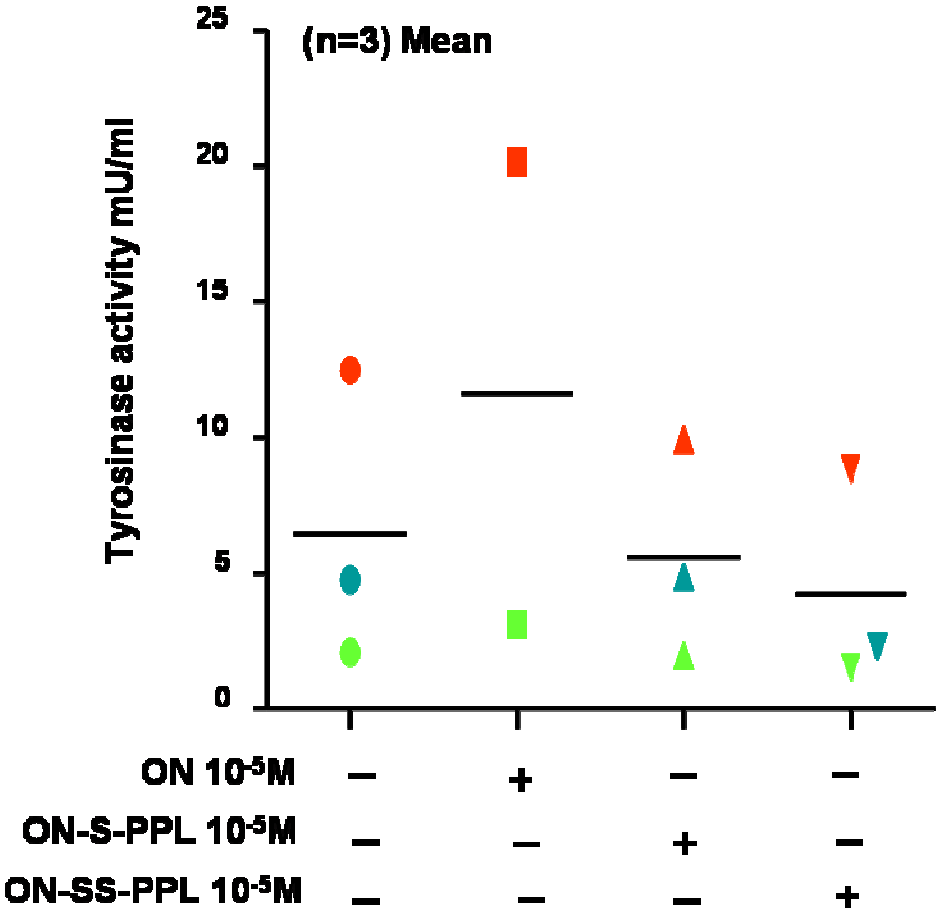

Figure 4.18. Effect of 19merON-S/SS-PPL on basal tyrosinase activity in B16F10 cells. Both 19merON-S-PPL and 19merON-SS-PLL at 10^{-5}M inhibited the basal tyrosinase activity of B16F10 cells in each of three independent experiments. The tyrosinase activity in each of three separate experiments are represented by different coloured symbols. One preliminary experiment was performed without ON control, therefore missing one square in the figure.

In the αMSH-stimulated tyrosinase experiment, the ON alone also seemed to enhance tyrosinase activity. However, as compared to, the 19merON-SS-PPL significantly

inhibited the tyrosinase activity following stimulation by 10^{-10}M αMSH ($p \leq 0.05$, One way ANOVA, figure 4.19). The effect on αMSH-induced tyrosinase activity by 10^{-5}M 19merON-S-PPL was not statistically significant (figure 4.19). A melanin assay was not performed with the 19merON-SS-PPL and 19merON-S-PPL because of the shortage of these compounds. Interestingly, ON significantly enhance the melanin production as compare to αMSH alone.

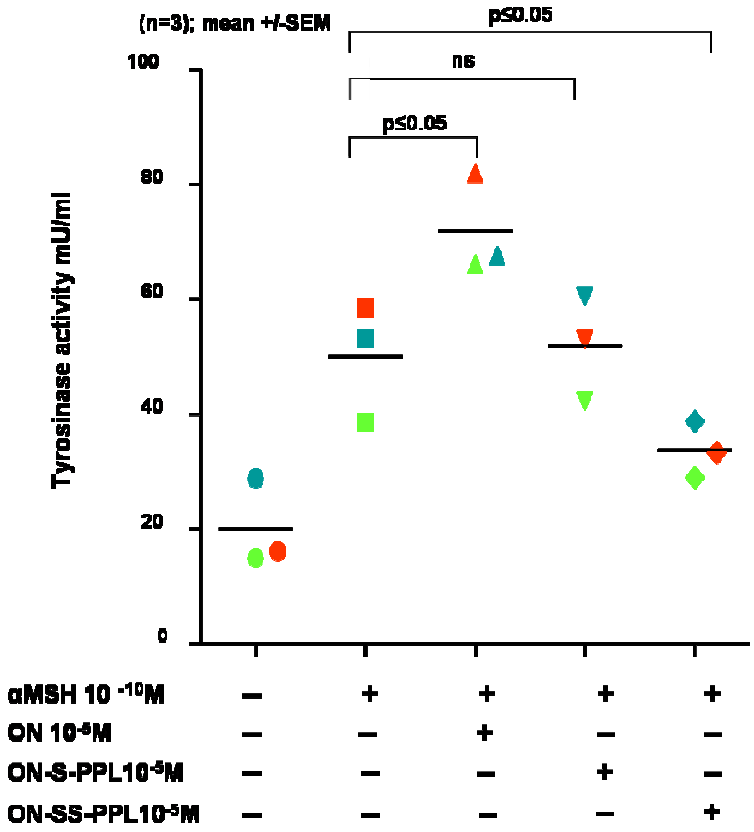

Figure 4.19. Effect of 19merON and 19merON-S/SS-PPL on αMSH-induced tyrosinase activity in B16F10 cells. 19merON-SS-PLL at 10^{-5}M concentration significantly inhibited the αMSH stimulated tyrosinase activity of B16F10 cells The black lines in the figure are the mean value of ratio + SEM of three experiments (shown in three different colours) performed each in triplicates.

4.4 Discussion

The physical nature of skin and cells makes them impermeable to ONs and PNAs. However, Vlassov *et al* reported that a 15merON in a solution of glycerol and Tween 80 was able to penetrate into mouse ear skin and also reported on the usefulness of electroporation for greater bioavailability of the ON (Vlassov *et al.* 1993). A study by Dokka *et al* also showed the importance of the follicular route for the transport of an ON (not targeted to any gene) in the presence of chemical enhancers (glyceryl monostearate, hydroxylpropyl methylcellulose, isopropyl myristate, paraben and water). (Dokka *et al.* 2005).

One of the aims of the studies in this chapter was to examine whether PPL could transport an anti-tyrosinase PNA (and ON) into the cytoplasm of cells, where it would bind to the complementary tyrosinase mRNA sequence, thereby inhibiting its translation. The *in vitro* inhibition of pigmentation in S91 and/or B16F10 cells by the 15merPNA-SS-PPL, 15merPNA-PPL and 12merPNA-PPL suggested that PPL successfully delivered its cargo into the cytoplasm. Although *in vitr*o cell penetration studies were not performed with the fluoresceinated disulfide- and maleimide-linked PNA-PPL compounds, the confocal microscopy results indicated that PNA directly conjugated to PPL was able to enter into B16F10 cells. Interestingly, data obtained from the melanin assays imply that the different types of linker can affect the antisense activity of the compounds because the PNA-PPL conjugate with a disulfide linker seemed to show a better antisense activity compared to that with a maleimide linker. This effect of linker type has also been reported in a study performed by Bendifallah *et al*, where a maleimide linker impaired the antisense activity of a trasportan-M-18merPNA conjugate as compared to a disulfide or

an ester linker (Bendifallah *et al.* 2006). The altered effect as a result of different linkers may be due to the fact that the linker might influence the three-dimensional structure of the conjugate, which might affect its activity, or the ability of the cargo to dissociate from the carrier once inside the cell/tissue. The results in the present study with the ON also suggest that a disulfide linker may be better than a single sulfide linker as a means of conjugating PPL to an ON (or PNA).

In human skin, melanocytes are situated in the basal part of the epidermis. In order to inhibit skin pigmentation, PPL would need to carry the PNA or the ON across the stratum corneum into the epidermis so that it can then enter the melanocytes in the basal layer. The results in the skin penetration assays indicated that the PPL delivered the 12merPNA into both the epidermis and dermis and delivered the 15merPNA mainly into the epidermis. Furthermore, the pattern of staining suggested localization of the 15merPNA in all cell types of the epidermis, whereas the 12mer PNA mainly accumulated in the dermis, suggesting that the length of the PNA may be a critical factor for its localization after its delivery into skin. Further work on the preferential accumulation by PNA-PPL compounds of various lengths will be necessary with other PNA sequences, but this observation may ultimately be useful for the design of a PNA-PPL conjugate which will target a specific cell type within the epidermis or the dermis. For example, to target a gene in the keratinocytes, a PNA with longer chain length may be preferred over the shorter one. Related to this, Oldenburg *et al* have reported that the iontophoretic transport of an ON into hairless mouse skin was inversely related to the ON size (Oldenburg *et al.* 1995). However, the human skin penetration results in this chapter showed that the 12merPNA-PPL penetrated mainly into the epidermis, but the numbers

of experiments on human skin are not enough to confirm the exact pattern of penetration. The presence of 15merPNA-PPL in the mouse keratinocytes is clearly visible by fluorescence microscopy and it is likely, based on the pattern of staining, that the compound also went into the epidermal melanocytes (which are present in this mouse model; E Healy, personal communication); if necessary, this could be confirmed in future work examining for colocalisation with a tyrosinase antibody which is specific to the melanocytes.

Tyrosinase inhibition is the most commonly used approach to achieve skin hypopigmentation because of its prime role in the melanin biosynthesis pathway. Targeting tyrosinase is a useful approach for the removal of undesirable pigmented patches due to the accumulation of melanin in many skin conditions and this approach can also be used to lighten skin colour. Hydroquinone is a well known topical depigmenting agent, which inhibits tyrosinase through its interaction with copper at the active enzymatic site (Arndt & Fitzpatrick 1965; Jimbow *et al.* 1974). Potential undesirable side effects of hydroquinone (especially above 4% concentrations) include hyperpigmentation (ochronosis) and permanent hypomelanosis as a result of melanocyte cytotoxicity, thus limiting its use as a depigmenting agent (Findlay & Moores 1980). In addition, the human use of hydroquinone (over a certain concentration) now comes under legal restrictions and is banned in Europe since December 2000 (Solano *et al.* 2006). A PPL-based approach to deliver an antisense against tyrosinase mRNA into the skin, might be a useful alternative way to lighten skin colour. However, one potential disadvantage of targeting tyrosinase and reducing the melanin content in skin includes a possible increase in skin cancer susceptibility because of sun protective role that melanin provides

(Kobayashi *et al.* 1998). In addition, tyrosinase seems to have a role in retinal development, an observation which is supported by the fact that the re-introduction of a functional tyrosinase gene into tyrosinase-negative albino mice corrects these abnormalities (Jeffery *et al.* 1997). Therefore, although unlikely to be a problem for adults, the use of an anti-tyrosinase compound during pregnancy might result in abnormal retinal development of the embryo if the antisense compound reached the systemic circulation.

The results indicate that PPL might be a useful way of using other antisenses topically for diseases such as psoriasis, melanoma, Merkel cell carcinoma, etc. For example, in a mouse model (human psoriatic lesional skin grafted onto nude mice) Wraight *et al* have shown that epidermal hyperproliferation in psoriasis can be reversed by repeated injection of antisense oligonuleotide targeted against insulin growth factor-1 receptor (Wraight *et al* 2000). Other potential target genes in psoriasis include ICAM-1, IL-2 and IL-8, which play an important role in inflammation (White and Wraight 2004). Furthermore, targeting c-myc and bcl-2 genes may have a huge potential to treat melanoma and Merkel cell carcinoma (target bcl-2) (Citro *et al* 1998, Schlagbauer-Wadi *et al* 2000; White and Wraight 2004). White *et al* have been reported that, aquous solution of oligonucleotiode antisense did not penetrate into viable human skin grafted onto nude mice over a 24 hour period (White *et al* 1999). Therefore, PPL conjugation may have the potential to act as a molecular carrier for the delivery of drugs, antisense and therapeutic molecules in the skin *in vivo*.

Chapter 5: PPL and other epithelial barriers

5.1 Introduction

Systemic delivery of drugs is used for the treatment of a wide variety of diseases which affect the internal organs of the body, however, it would be beneficial if drugs could be targeted in their distribution within the body so that they only go to the site of interest. While this is unlikely to be possible for the foreseeable future, there are some organs within the body where drug delivery approaches have been used to try to get most of the drug into the diseased organ, for example in the gastrointestinal tract, the respiratory tract and the eye. Thus, to target diseases in the gut such as ulcerative colitis, Crohn's disease and irritable bowel syndrome, drug delivery through the oral route is considered convenient but the modification/degradation of drugs by gastric juices and absorption resulting in restricted delivery of low molecular weight compounds to the distal ileum and colon are the major drawbacks of this route (Pillay & Fassihi 1999). In addition, physiological changes associated with intestinal disease conditions, such as alteration of luminal pH, modification of intestinal epithelium, decrease in enzymatic activity, increase of non-specific proteolysis, motility and fluid content may affect the efficacy of drugs at the target site (Yang *et al.* 2002; Siccardi *et al.* 2005). Various techniques such as a prodrug approach and nano-particulate, multiparticulate, microsphere and mucoadhesive delivery systems have been developed to enhance the delivery and efficacy of drugs targeted to the gut (Chourasia & Jain 2003). In the prodrug approach, a pharmacologically inactive molecule is converted into an active molecule following enzymatic modification upon reaching the appropriate biological environment and/or the diseased site (Friend & Chang 1985). For instance, the drug is covalently conjugated

with a carrier using either an azo bond or cyclodextrin / glycoside / glucornate / dextran / poly(aspartic acid) or polymer conjugate, which on internalisation is reduced/cleaved by the common inhabitant microflora of the intestine, thus releasing the active free drug (Chourasia & Jain 2003). Thus, sulphasalazine (which is used for inflammatory bowel disorders) chemically consists of sulfapyridine and salicylate linked by an azo bond, which following oral administration reaches the colon where it is cleaved by the colonic microflora to liberate sulphapyridine and an active 5'-aminosalicylic acid (Azad Khan & Truelove 1980). The coating of a drug molecule with various polymers has also been successively used to deliver intact molecules into the intestine. The pH of the human gut increases progressively from the stomach to the distal ileum (Nugent *et al.* 2001), therefore the coating of a tablet or capsule with a pH sensitive polymer provides delayed release of the active drug . Methacrylic acid copolymers are the most commonly used pH sensitive polymers and have been shown to deliver insulin, prednisolone and cyclosporine in the colon (Lowman *et al.* 1999; Carelli *et al.* 2000; Dai *et al.* 2004). Drug molecules can also be embedded in a biodegradable polymer matrix, such as polysaccharide matrices (amylose, chitosan, chondriotin sulphate, dextran and pectin) which are resistant to degradation by gastric enzymes and low pH but are easily degraded by the bacterial polysaccharidases in the colon, thus allowing the release of the core molecules (Harboe *et al.* 1989; Rubinstein *et al.* 1992; Milojevic *et al.* 1996; Tozaki *et al.* 1997). For optimum therapeutic effects at a specific site of the intestine, the drug must be available at high concentration locally, so bioadhesion techniques in which various polymers (such as polycarbophils, polyurethanes and polyethylene oxide-polypropylene oxide copolymers) allow adhesion to a specific site in the intestine, therefore extending

the time for the release of the drugs (Tamburic & Craig 1996). In addition, nanoparticle technology has recently emerged as new method for the delivery of drugs or therapeutic agents to a variety of systems, including the gut. Essentially, nanoparticles are a derivative of the microparticulate system, in which natural (gelatine, starch, ethyl cellulose) or synthetic (poly lactic acid, poly hydoxybutrate) microparticles containing dispersed drug particles in crystalline or solution form have been used successfully to deliver treatments by various systemic routes (Dandagi *et al.* 2006). The nanoparticles can be either encapsulated with drugs or layered by polymeric covering, and have shown to deliver therapeutic agents to the gut (McClean *et al.* 1998; Hariharan *et al.* 2006).

The eye is another organ where it would seem relatively easy to direct the administration of a drug to that site. Many forms of eye-drops exist to treat diseases such as glaucoma, and recent advances in the understanding of molecular biology based therapies (including monoclonal antibodies, gene knockdown/gene therapy and growth factors) open up the possibility to treat a variety of ocular disorders. However, the delivery of these agents are hampered by the outer epithelial barrier (cornea and sclera) of the eye. Intravitreal injection, viral based delivery, chemical and physical methods have been tested for the delivery of genes into laboratory animals. For example, Takahashi *et al* have shown in a mouse model that the subretinal injection of a bovine immunodeficiency lentivirus vector coding for endostatin (an endogenous inhibitor of tumour angiogenesis and chorodial neovascularisation) significantly reduced retinal vascular permeability and suggested that similar injections for endostatin gene transfer might be useful for patients with diabetic retinopathy (Takahashi *et al.* 2003). At the present time, intravitreal injection is now commonly used in the clinic to deliver anti-VEGF therapy into the eye to treat

proliferative diabetic retinopathy and age related macular degeneration in humans but this required repeated injections on a monthly basis (Ferrara *et al.* 2006). Other viral vectors such as adenovirus, adeno-associated virus and herpes simplex virus have also been explored for the delivery of genes into the eye tissue of various animals (Liu *et al.* 1999; Liu *et al.* 2005). However, the risks of viral based gene delivery such as insertional mutagenesis, cytotoxicity and limited duration of transgene expression means that more investigations will be necessary before this type of eye-therapy becomes routine in humans. Non-viral gene delivery methods (electroporation, naked DNA injection, liposomes) are less efficient in gene expression but offer great promise in terms of easy production, low toxicity and immunogenicity (Bul-Hassan *et al.* 2000, Stechschulte *et al* 2001, Jiang *et al* 2007).

Delivery of drugs into the lungs via inhalation offer many advantages over the oral-ingestion (Edwards *et al.* 1998). Aerosolized delivery of therapeutic compounds into the lungs greatly inhances the treatment of many respiratory disorders, particularly asthma and chronic obstructive pulmonary disease (Acerbi *et al* 2007). The devices frequently used to deliver medications into lung are inhalar, spacer and nebulizer (O'Callaghan & Barry 2000). Metered-dose inhalers (which use chemical propellants to expel medication) and dry powder inhalers (which rely on rapid inhalation instead of a chemical propellant) are two of the most commonly used inhalers for drug delivery. Additional devices, such as spacers (which avoid the chemical propellant depositing most of the dose onto the nasopharynx) and nebulisers (in which medication is given through a face mask in the form of a mist) are also helpful in assisting delivery of the medication directly to the lung (O'Callaghan & Barry 2000).

Thus, although a number of mechanisms or potential mechanisms exist for the delivery of therapeutic agents into the gut, eye and lungs, there is the possibility to deliver novel therapies (e.g. antisense molecules) into these organs using a combination of conventional delivery methods and a cell penetrable carrier approach. Based on the work in the previous chapters (chapters 3 and 4), where PPL was able to transport a peptide and an antisense compound into cells and skin, it was hypothesised that PPL might also be able to transport antisense molecules and other therapeutic agents into the intestine, the eye and/or the respiratory tract.

5.2 Materials and methods

5.2.1 Ileum and colon delivery – The ileum and colon were carefully removed from healthy euthanased mice, and cut into small tubes (approximately 3 cm in length). The test compound, diluted in culture medium, was added into the middle part of the ileal or colonic tube (as per section 2.12 in Chapter 2, Materials and Methods) and the tube was then tied at that end with a suture and incubated for the required length of time. Each experiment was set up in duplicate and following the incubation with the test compound, frozen sections and/or paraformaldehyde-fixed paraffin-embedded sections were used for fluorescence microscopy to assess penetration.

5.2.2 Eye delivery - Both eyes were carefully removed from the orbit from euthanased mice and then immediately transfered into the wells of a 96 well-plate containing 5µl of compound. Following treatment, eyes were washed in PBS and either snap frozen in liquid nitrogen or fix in PFA for further analysis (as per Materials and Methods, section 2.12).

5.2.3 Lung delivery – The trachea was carefully excised from healthy euthanased mice and ligated at one end with a surgical suture. The investigational compound was added into the tracheal tube from the other open end and the tube sealed shut with another suture at that end. After incubation for the required time, paraformaldehyde or frozen sections were used to assess penetration (for detail protocol, see material and method section 2.12).

5.2.4 Haematoxylin and Eosin (H&E) stain – H & E staining was performed on ileum, colon and eyes for the histology of the tissues, in which PFA fixed tissues were used for H&E staining according to the method described in Materials and Methods, section 2.16.

5.3 Results

5.3.1 Delivery of PNA

Haematoxylin and eosin (H&E) staining of the ileum, colon, eyes and trachea were carried out to allow comparison of fluorescence staining in the penetration experiments with the histology of the tissue because the structural features were useful to define the extent of penetration of PNA-PPL and αMSH-PPL into these organs. PFA fixed tissue was selected for H&E because it produces a better morphology under microscopy. As expected, the H&E sections of the ileum and colon showed four major layers: the mucosa, the submucosa, the muscularis layer and the adventitia (also known as serosa) arranged from the lumen to the outside; histologically the mucosa is further subdivided into the epithelial lining, lamina propria and muscularis mucosae. The colon has a wider lumen than the ileum and whereas the mucosa in the ileum contains villi and crypts, the

mucosa of the colon consists of tubular glands (also called crypts) which are lined by absorptive cells and mucus-secreting goblet cells (figure 5.1). The muscularis externa is the prominent structure of the colon which enhances the expulsion of mucus and the movement of intestinal contents (peristalsis). H&E of the eye showed is composed of three layers: the outer corneal layer, the corneal stroma layer and the iris layer (figure 5.1).

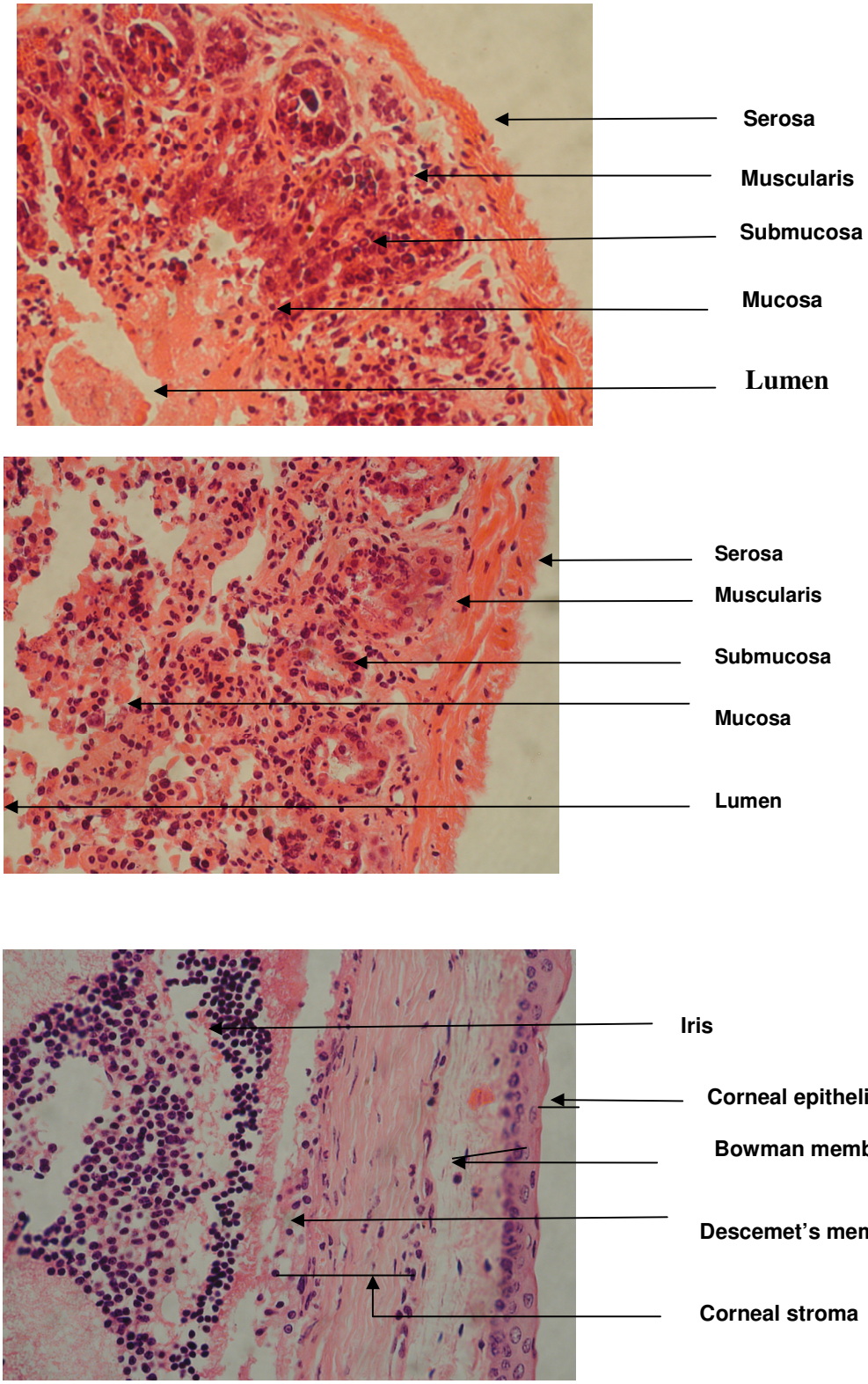

Figure 5.1. H&E staining of mouse organs. Transverse sections of the mouse ileum (A) colon (B) and eye (C), demonstrating the major structural layers.

The ability of PPL to deliver PNA into the ileum and the colon was investigated in an *in vitro* system in which 10^{-3}M of the fluoresceinated 15merPNA, with or without PPL, was applied to the lumen of these tubes. The results showed that the PPL conjugated fluoresceinated PNA penetrated into most of the cells types in the ileum, whereas fluorescein-PNA alone did not penetrate to the same extent (figure 5.2).

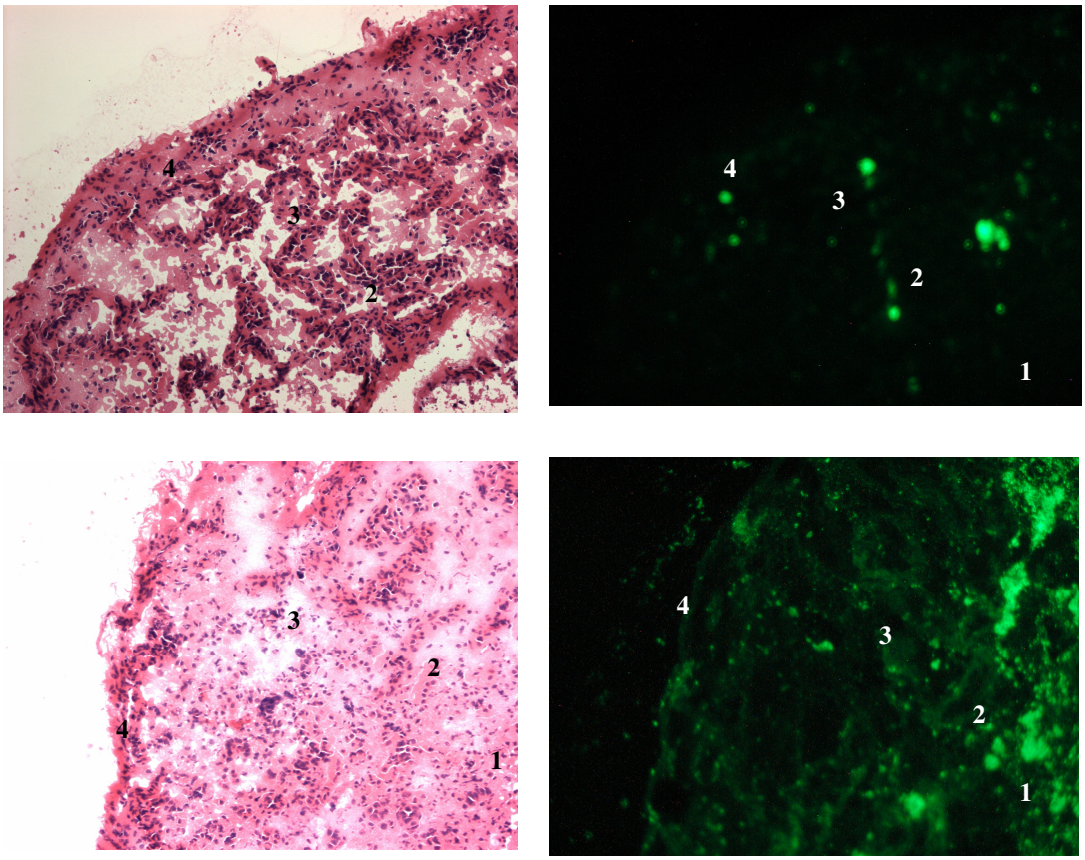

Figure 5.2. Delivery of PNA into ileum. Fluorescent microscopy results showed that PPL conjugation enhanced the delivery of 15merPNA (10^{-3}M)into the ileum (lowerpanel, right), whereas the 15merPNA alone at similar concentration did not penetrate into the ileum to the same extent (upperpanel, right). H&E staining in left panels represent adjacent tissue sections to show morphology in more detail. The numbers in the image correspond to mucosa (1), submucosa (2), muscularis (3) and serosa (4).

Similar to the penetration into the ileum, PPL strongly enhanced the penetration of

15merPNA into the colon at similar concentration and time points, whereas penetration of PNA alone was minimal (figure 5.3).

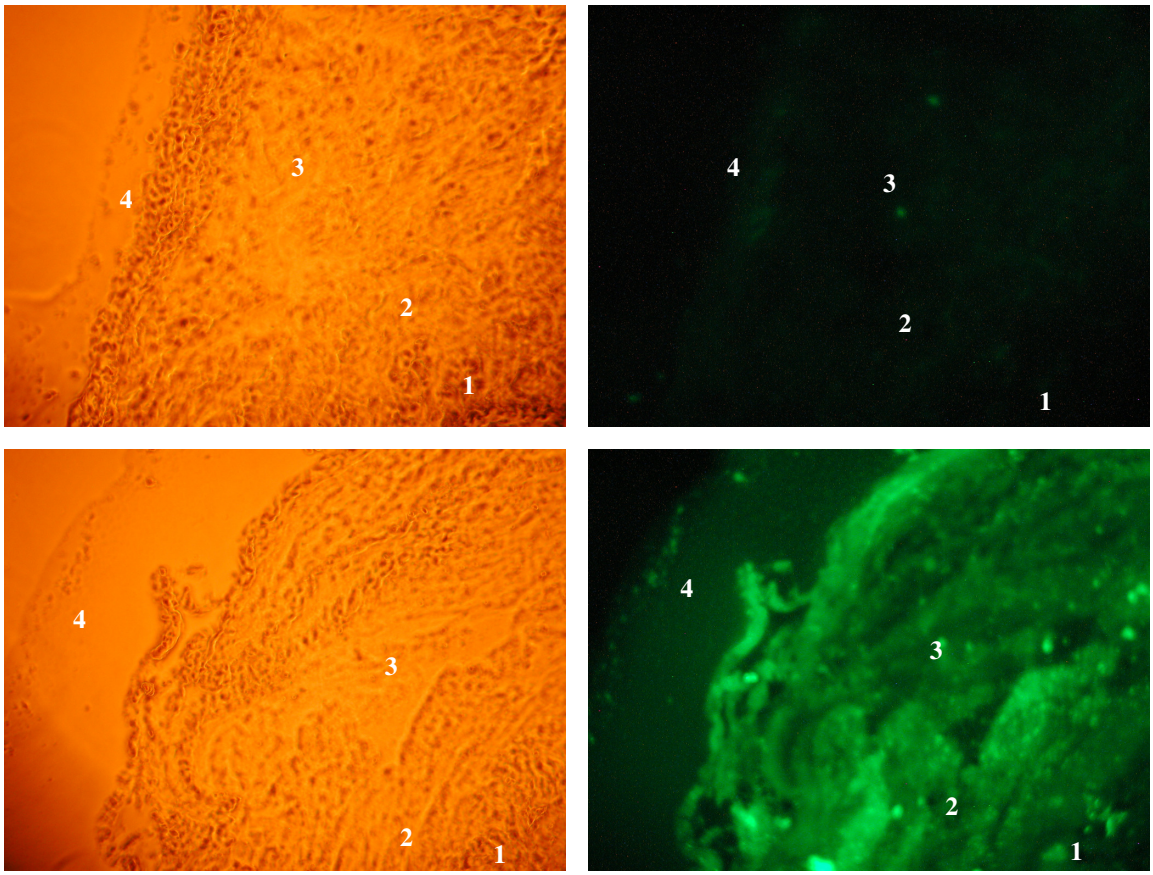

Figure 5.3. **Delivery of PNA into colon.** Fluorescent microscopy results showed that PPL conjugation enhanced the delivery of 15merPNA (at 10^{-3}M) into the colon (lowerpanel, right), whereas the penetration of 15merPNA alone at similar concentration was poor (upperpanel, right). Trans-illuminated image of corresponding section shown in left panels. The numbers in the images correspond to mucosa (1), submucosa (2), muscularis (3) and serosa (4).

PPL was also investigated for the delivery of the 12mer and 15merPNAs into the eye. The eyes were carefully excised from the orbit and placed (with the optic nerve up and therefore outside of solution) into the wells of a 96 well plate containing 5µl of fluoresceinated form of 10^{-3}M PNA or PNA-PPL; this meant that approximately one tenth of the surface area of the eye was immersed in the compound. The eyes that had

received 12merPNA-PPL and 15merPNA-PPL were brightly fluorescent with some of the retinal cells exhibiting fluorescence, indicating that the compound had penetrated to this level, whereas little or no fluorescence was observed with Fluo-PNA alone (figure 5.4).

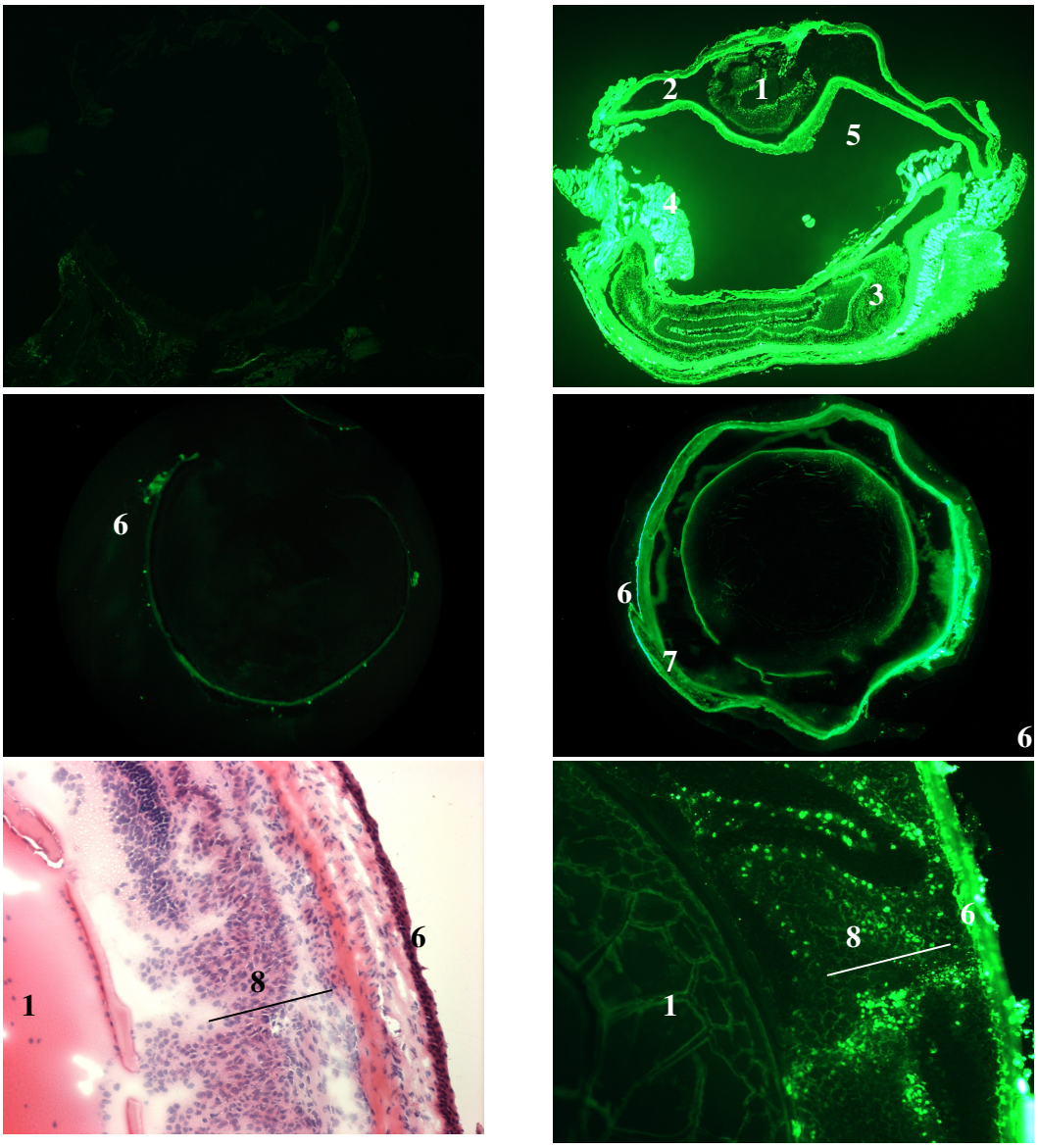

Figure 5.4. **Delivery of PNA into mouse eye.** Fluoresceinated 12merPNA-PPL (upper panel, right) and 15merPNA-PPL (middle panel, right) penetrated into mouse eyes following 3 hours treatment at 10^{-3}M concentration, whereas fluorescein-PNA alone (upper and middle panel, left) did not penetrate to the same extent. Lower panel shows higher magnification of Fluo-15merPNA-PPL (right) indicating that the compound had penetrated deep into the sclera; for comparison a H&E image from the same eye is shown in the lower left panel. The numbers in the image correspond to lens (1), cornea (2), retina (3), vitrous chamber (4), iris (5), sclera (6), lens fibre (7) and ciliary body (8) layers.

The penetration of 12merPNA-PPL was also investigated in a rat eye, which is bigger than a mouse eye. Similar to what had been observed with the mouse eyes, 10^{-3}M Fluo-12merPNA-PPL had penetrated into the rat eye at 3 hours, whereas the Fluo-12merPNA showed no visible penetration (figure 5.5).

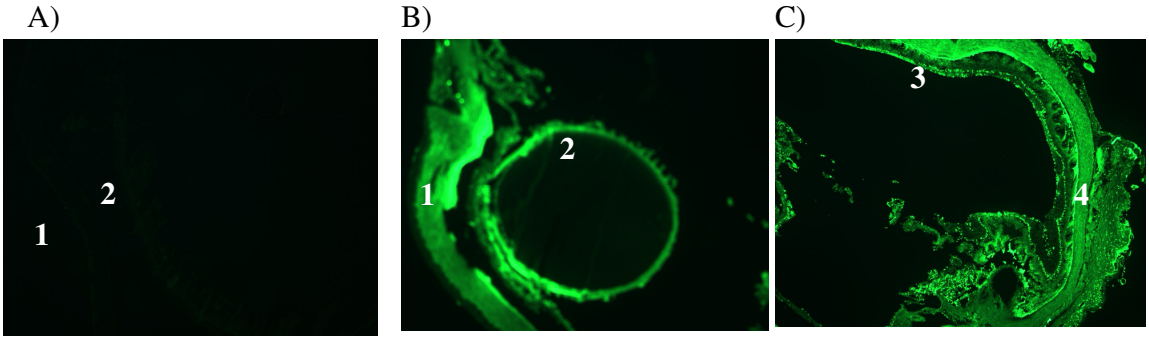

Figure 5.5. **Delivery of PNA into rat eye.** Photographs of rat eyes treated with 10^{-3}M fluoresceinated-12merPNA (A) and 10^{-3}M fluoresceinated-12merPNA-PPL (B and C from same eye) for 3 hours showed penetration into different layers. The numerics in the image correspond to cornea (1), lens (2) retina (3) and sclerea (4).

Following the successful delivery of PNA-PPL into the ileum, colon and eye, the delivery of PNA by PPL was also investigated in the trachea of mice. Successful penetration of Fluo-15merPNA-PPL was evident in the trachea of mice at 10^{-3}M concentration following 3 hours incubation, whereas Fluo-15merPNA penetrated poorly (figure 5.6).

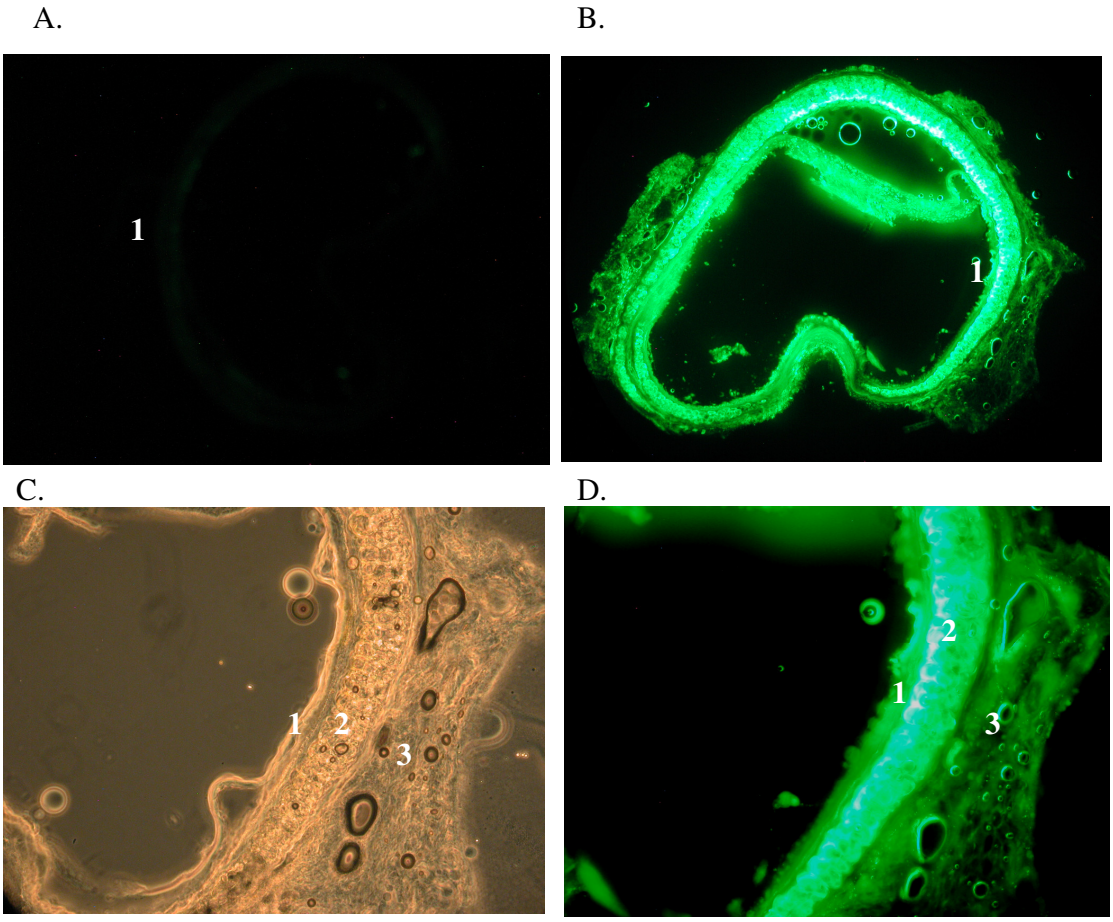

Figure 5.6. Delivery of PNA into mouse trachea. Fluorescein conjugated PPL enhanced the delivery of 15merPNA into the trachea at 10^{-3}M concentration (B), whereas the penetration of fluoresceinated15merPNA alone at similar concentration was poor (A). Lower panel shows higher magnification of Fluo-15merPNA-PPL image (D) and corresponding transilluminating image (C). The numbers in the image correspond to tracheal epithelium (1), hyaline cartilage (2), and smooth muscle (3) layers.

The overall results of the penetration experiments with Fluo-15merPNA, Fluo-15merPNA-PPL, Fluo-12merPNA and Fluo-12merPNA-PPL in the different mouse organs are summarised in table 5.1.

Table 5.1. Total penetration events. Summary of the number of times where fluorescein-15merPNA-PPL and fluorescein-15merPNA penetrated into various organs of the mouse.

	Fluo-15merPNA-PPL		**Fluo-15merPNA**	
	*yes	*no	yes	no
Ileum	8 of 8 (*7 frozen)	0 of 8	1 of 6 (Weakly stained)	5 of 6 (4 frozen)
Colon	5 of 5(2 frozen) (1 weakly stained)	0 of 5	2 of 5 (Weakly stained)	3 of 5 (3 frozen)
Eye	7 of 7 (5 frozen)	0 of 7	1 of 4 (Weakly stained)	3 of 4 (1 frozen)
Trachea	2 of 2 (2 frozen)	0 of 2	0 of 2	2 of 2
	Fluo-12merPNA-PPL		**Fluo-12merPNA**	
	yes	no	yes	no
Ileum	3 of 3 (all fixed)	0 of 3	0 of 3	3 of 3 (all fixed)
Eye	2 of 2 (all fixed)	0 of 3	0 of 2	2 of 2 (all fixed)

*Both paraformaldehyde-fixed and frozen section results were included in this table. "Yes" indicates that the compound had penetrated into most structures in the organ, whereas "no" represents little or no penetration.

5.3.2 Delivery of αMSH

PPL-mediated delivery of αMSH into the different organs of mice was also investigated *ex vivo*. Similar to the PNA delivery investigations, the tissues were exposed to a 10^{-3}M concentration of the αMSH-PPL[99]-Fluo and Fluo-αMSH compounds for 3 hours. PPL mediated penetration of αMSH was detected in the ileum and colon, whereas the Fluo-αMSH penetrated less well into these organs (figure 5.7).

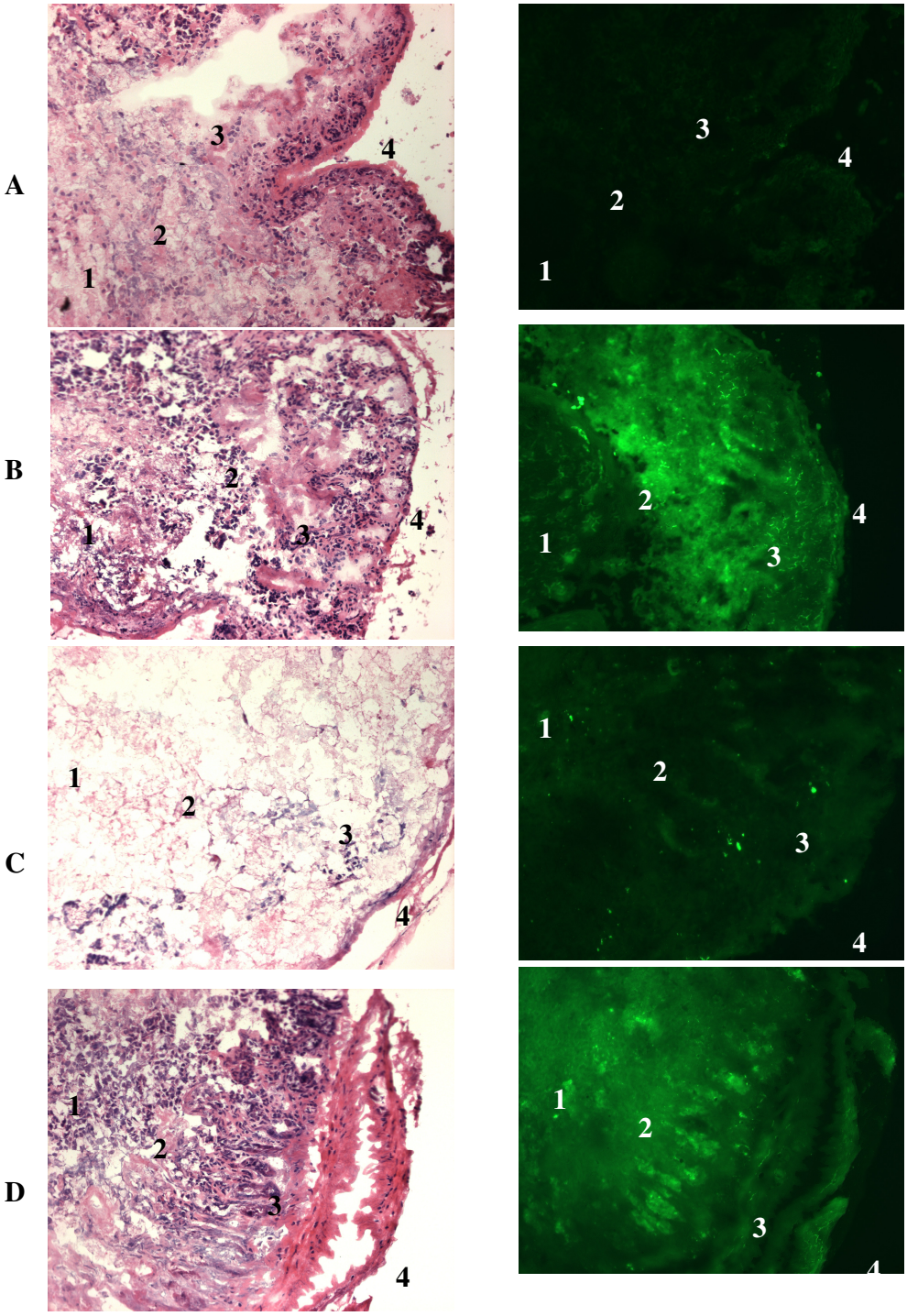

Figure 5.7. Delivery of αMSH into mouse ileum and colon. Fluorescein conjugated PPL- enhanced the delivery of αMSH into the ileum (B, right) and colon (D, right) at 10^{-3}M after 3 hours treatment, whereas fluoresceinated αMSH alone was poorly penetrated into the ileum (A, right) and the colon (C, right). H&E staining of corresponding images shown in left. The numbers in the images correspond to mucosa (1), submucosa (2), muscularis (3) and serosa (4).

The same experimental protocol as was used in the investigations on the delivery of PNA into the eye was used to examine the transport of αMSH into the eye. Interestingly, both 10^{-3}M αMSH and 10^{-3}M αMSH-PPL[99]-Fluo seemed to penetrate into all layers of the mouse eyes, however, the fluorescence intensity of PPL-conjugated αMSH was greater than that of αMSH alone (figure 5.8).

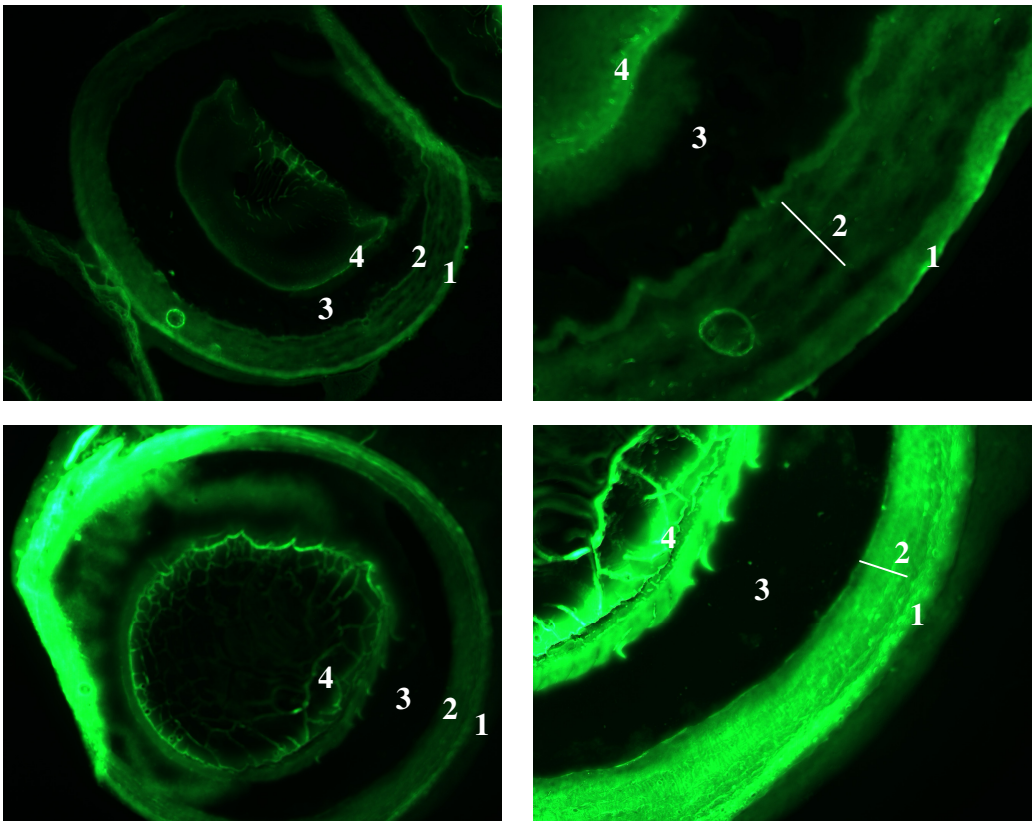

Figure 5.8. **Delivery of αMSH into mouse eye.** The fluorescein microscopy results shows the penetration of Fluo-αMSH and αMSH-PPL[99]-Fluo into mouse eyes following 3 hours treatment with the compounds at a concentration of 10^{-3}M. The numbers in the image correspond to the sclera (1) ciliary body (2) posterior chamber (3) and lens fibres (4); right panels 5X magnification and left panels 20X magnification.

The overall penetration results of fluoresceinated-αMSH or fluoresceinated-αMSH-PPL[99] into the different organs are shown in table 5.2. Penetration of fluoresceinated-

αMSH was seen in the ileum and colon in occasional cases; however, it penetrated into the eye in every instance. The PPL-mediated penetration of αMSH was evident in each of these organs, although it failed to penetrate the ileum in some cases.

Table 5.2 Total penetration events of fluoresceinated-αMSH or fluoresceinated-αMSH-PPL[99]. Summary of *ex vivo* penetration events following treatment with fluoresceinated-αMSH or fluoresceinated-αMSH-PPL[99] into various organs of the mouse. Tissue sections (frozen) were analysed and the results are presented in this table; yes indicates that the compound penetrated into the organ, whereas no means little or no penetration.

	αMSH-PPL[99]-Fluo		**Fluo-αMSH**	
	yes	no	yes	no
Ileum	4 of 6	2 of 6	2 of 6 (1 Weakly stained)	4 of 6
Colon	4 of 4	0 of 4	2 of 4	2 of 4
Eye	4 of 4	0 of 4	3 of 3 (2 Weakly stained)	0 of 3

5.4 Discussion

The delivery of molecules or therapeutic agents into the intestingal wall and the eye is restricted to compounds with a molecular weight of less then 600 daltons (Artursson *et al.* 1993; Prausnitz & Noonan 1998; Bos & Meinardi 2000). To date, the delivery of a PNA via the lumen of the intestine and to the eye using a cell-penetrable peptide approach has not being investigated. However, plasmid DNA and siRNA has been delivered to eye using cell-penetrable peptide approach (Johnson *et al* 2008). Using the Tat protein as a carrier, Fawell *et al* delivered a β-galactosidase into various tissues of mice *in vivo* following an intravenous injection (Fawell *et al.* 1994). Later Schwarze *et al* showed that intraperitoneal injection of a Tat-β-galactosidase-conjugate into mice leads to a strong detection of β-galactosidase enzymatic activity in the liver, the kidney, the lung, the brain

and the heart muscle (Schwarze *et al.* 1999). The first *in vivo* intracellular delivery of an PNA was performed by Tyler *et al*, who gave multiple microinjections of PNAs targeted against opoid and neurotensin receptors into rat periaqueductral grey matter, which led to a loss of normal behaviour responses to morphine and neurotensin (Tyler *et al.* 1998). Later, the same group showed delivery of PNA into the brain and the small intestine following intraperitoneal injection of 12merPNA (Tyler *et al.* 1999). Pooga *et al* showed that multiple intrathecal injections of PNA, conjugated to a CPP (penetratin or transportan) targeted against the rat galanin receptor regulated the levels of this receptor and modified the pain transmission signal (Pooga *et al.* 1998).

In the current chapter, the ability of PPL to deliver PNA and αMSH across the intestine and trachea and into the eye was investigated in an *ex vivo* system. For the gut penetration investigations the ileum and the colon were preferred over other parts because the terminal ileum and the colon are the major sites for inflammatory disorders such as Crohns disease and ulcerative colitis (Farmer *et al.* 2000). In the present study, mouse (and occasionally rat) tissues were used for investigating the PPL-mediated transport of PNA and αMSH, because these animal models have been used frequently for drug/therapeutic agent delivery studies (Fawell *et al.* 1994; Morishita *et al.* 2007). For example, Morishita *et al* recently performed an *in situ* absorption experiment for insulin delivery by polyarginine into rat intestine, in which the ileum was exposed and cannulated at both end following a small incision in the abdomen (Morishita *et al.* 2007). The polyarginine and insulin mixed solution (un-conjugated) was then administered directly into the ileal loop and the absorption of insulin was monitored in the blood at several time points. Intestinal drug delivery has also been assessed *in vitro* using a

chamber method, in which excised rat tissue was mounted in a donor chamber and the test sample collected from an acceptor chamber for penetration analysis (Foger *et al.* 2006). However, the surface area of mouse intestinal tissue was not large enough to examine delivery using a Franz diffusion chamber as was used in the skin penetration studies in chapters 3 and 4, therefore the gut penetration investigations were carried out using a protocol where tissues were excised and ligated at both ends after placing the test compound inside. The surface area was similarly an issue for the investigations on the eye and trachea, hence the approach that was taken in this chapter. The penetration of PPL-PNA and/or PPL-αMSH into the gut, eye and trachea was evident at 10^{-3}M, which is similar to the concentration (2.6×10^{-3}M) used by Morishita *et al* (2007) for polyarginine mediated delivery of insulin. In the present study, the delivery into each organ was confirmed visibly by fluorescence under microscopy and compared to a non-PPL-linked fluoresceinated-compound. It is unlikely that the fluorescein dissociated from the compound before penetration and thus it is likely that the positive fluorescence represents delivery of the entire compound, however, future work using *in situ* hybridisation with the complementary sequence could be done to confirm the presence of the PNA compound in cells of these organs. Although the low gastric pH might degrade PPL-linked compounds following oral delivery, this could be prevented by coating the PPL-PNA (or other PPL-linked) compounds with a pH sensitive polymer which facilitates release of the compound at a specific site in the intestine.

The ability to deliver αMSH into the ileum, colon, eye and lung could have benefits for a variety of diseases. Work has shown that αMSH can inhibit inflammation in the intestines and lungs in mouse models of colitis and allergic lung inflammation (Rajora *et*

al. 1997; Raap *et al.* 2003), therefore a PPL-αMSH approach might be useful here. In addition, the benefits of using PPL to transport PNAs into cells within the gut, lungs and eyes could have huge potential. For example, PPL could deliver PNAs to switch off the function of various genes in each of these organs. The TNF-α gene could be an interesting target in inflammatory bowel diseases such as ulcerative colitis and Crohn's disease (Wirtz & Neurath 2003). Other targets in the gut to modulate inflammatory conditions include Nod2 and the IL-12 receptor whereas the SKP2 (overexpressed in small cell lung cancer) and gob-5 (responsible for mucous hypersecretion) genes could be targets in the lung (Nakanishi *et al.* 2001; Yokoi *et al.* 2002; Wirtz & Neurath 2003). An obvious target in the eye is VEGF, because at the present time patients with diabetic retinopathy require monthly injections of an anti-VEGF monoclonal antibody to treat this condition (Caldwell *et al.* 2003).

Chapter 6.0 - Discussion

Many cutaneous therapeutic compounds such as steroids, retinoids and tacrolimus are applied topically, on account of their ability to penetrate the stratum corneum, to treat various skin conditions. By contrast, a large number of other drugs (methotrexate, azathioprine, dapsone, hydroxycarbamide and proteins such as biologics) for skin disease must be given by the systemic route due to poor permeability through the skin barrier (McCullough *et al.* 1976; Helton *et al.* 2000). In addition, antisense/oligonucleotide (ON) therapies may have the potential to treat many skin disorders but they need to get into cells and their topical use is limited by the stratum corneum barrier (White *et al.* 2002). Various delivery technologies have been attempted, however, it is still difficult to get many drugs and therapeutic molecules into skin by a topical approach. Over the last decade, cell-penetrable peptide (CPP) technology has emerged as a new tool for the intracellular delivery of larger molecules such as oligonucleotides, peptides and proteins into cells (listed in table 1.2). In order to deliver compounds into epithelial tissues (and intracellularly as required), one hurdle is that the CPPs must cross the relevant epithelial barriers, otherwise they will need to be delivered by a systemic route. To date, the vast majority of CPP-based approaches to deliver compounds into cells have used tat, penetratin, polyarginine and polylysine (see table 1.2), however, it is difficult to know from the limited literature whether these carrier molecules are going to be useful in the treatment of skin diseases and whether these carrier molecules will be able to transport all kinds of drugs or molecules across this and other epithelial barriers.

It is for these reasons that a novel cell-penetrable peptide, polypseudolysine (PPL), was designed and tested in this thesis for its ability to deliver a short peptide, αMSH, and a

peptide nucleic acid (PNA) into skin and into other organs such as the gut, eye and trachea. Polylysine has been used for efficient intracellular delivery of various drugs, for example, polylysine can improve the transport of methotrexate into cells (Ryser & Shen 1980) and can allow superoxide dismutase to penetrate into skin (Park *et al.* 2002). Similarly, Lemaitre *et al* reported on the antiviral activity of a poly-L-lysine conjugated oligodeoxyribonucleotide targeted against the N-protein of the vesicular stomatitis virus; this antiviral activity indicated successful cellular internalisation (Lemaitre *et al.* 1987). To enhance the cellular delivery of polylysine-oligonucleotide conjugates, the compound can be linked to a ligand involved in endocytosis, such as by linking it to the hepatocyte specific receptor asialoglycoprotein (Bunnell *et al.* 1992). The carrier molecule PPL used in this thesis was designed as a derivative of polylysine, because (with personnel communication with Prof. Mark Bradley) it is comparatively easy to synthesise and also has a net positive charge, which seems important in order to be a successful CPP, because the positive charge allows the CPP to form ionic bonds (electrostatic interaction) with the negatively charged groups of cell membrane phospholipids (Smith 2005). Histidine also carries a positive charge but it is partly positive at physiological pH (7.0) because of low affinity of its side chain to H^+ ion (Smith 2005). The side chains of both lysine and arginine carry a net positive charge at physiological pH (Smith 2005), however, because of the presence of a guanidium group, the synthesis of polyarginine is comparatively more difficult than polylysine as being told by chemist. In addition, the cellular penetration of lysine and related peptides seem independent of the stereochemistry of the compound and also seem to resistant from proteolytic degradation (Peretto *et al.* 2003).

After consideration of various potential molecules/agents as cargo, αMSH and peptide

nucleic acid targeted against tyrosinase gene were selected as cargo to link with PPL. In addition to its pigmentary role, αMSH is reported to have anti inflammatory effects in various animal models (colitis and allergic lung inflammation) and also shown to inhibit antigen induced lymphocytes proliferation (Rajora *et al.* 1997; Raap *et al.* 2003; Cooper *et al.* 2005), therefore localised delivery to specific sites such as the skin, trachea and gut might have therapeutic potential. The PNA targeted against tyrosinase was chosen as another cargo because PNAs are resistant to nuclease degradation (Knudsen & Nielsen 1996) and it was considered that an anti-tyrosinase PNA that would inhibit pigmentation might serve as a suitable prototype to test the ability of PPL to deliver antisense agents topically.

Prior to this thesis, a single cell penetration study of PPL had been conducted on two different cell lines (HEK-293 and B16F10), in which an energy dependent endocytotic mode of entry was suggested (Peretto *et al.* 2003). In that study, there was no "drug" or "therapeutic agent" employed as a cargo, however, it did show that a 6 carbon (aminohexinoic acid) spacer could be used to link a fluorescein group to the PPL for a efficient coupling and transport into these cells. In the present study, the same linker (aminohexanoic acid) and separately lysine were used to link αMSH and PNA was either directly linked to PPL or through a maleimide or a single sulfide or a disulfide linkers. As per the published literature and the results in chapter 4, the type of linker may influence the translocation efficiency of the compound, and thereafter the efficacy of the antisense molecules (Bendifallah *et al.* 2006). Direct conjugation and coupling through a maleimide linker may prevent separation of the cargo from the carrier and result in retention of the carrier-cargo complex in negatively charged cellular components whereas

a covalently bound disulfide linker is reduced within the cell membrane by glutathione and the cargo is released from the carrier, however, in one study both maleimide-linked and disulfide-linked ONs showed similar antisense actvity (Moulton *et al.* 2004). In another study, a maleimide-linked PNA appeared to have less antisense activity compared to a disulfide linked PNA (Bendifallah *et al.* 2006). In the functional studies with PNA-PPL in this thesis, a significant inhibition of pigmentation was observed with a disulfide linked 15merPNA-SS-PPL. Although the antisense activity of 15merPNA-M-PPL was investigated in separate experiments, there was less inhibition of αMSH stimulated pigmentation than that seen with the disulfide linker. The 19merON-SS-PPL also appeared to have greater antisense effects than the 19merON-S-PPL. A number of studies have also suggested that the antisense activity of ON-CPP conjugates primarily depends on the length of the antisense component and the position of the target sequence within the mRNA (Bonham *et al.* 1995; Flanagan *et al.* 1996). In the studies on pigmentation in this thesis, a higher concentration of 12merPNA-PPL than 15merPNA-SS-PPL was required to inhibit melanin synthesis, which may be due to the shorter chain length antisense being less effective or because of direct conjugation of the PNA to the PPL in the 12mer compound, or possibly a combination of both.

Following the functional studies with αMSH-PPL and separately with PNA-PPL, the cell and tissue penetration efficiencies of PPL were carried out in *in vitro* and *ex vivo* systems. In a similar way, CPPs based cellular delivery of proteins and peptides with Tat, penetratin and polyarginine has previously been investigated using *in vitro* models. In those studies, Tat successfully delivered β-galactosidase, horseradish peroxidase and ovalbumin into cells (Fawell *et al.* 1994; Moy *et al.* 1996). Likewise, penetratin has been

shown to deliver many peptides, such as Stat6BP, BH3 fusion peptide and Grb10-SH2 domain, into cells (Holinger *et al.* 1999; Stolzenberger *et al.* 2001). Similarly polyarginine has delivered ovalbumin and the p53 protein into cells in culture (Michiue *et al.* 2005; Mitsui *et al.* 2006). In this thesis, both Fluo-PPL, Fluo-αMSH-PPL[98] and αMSH-PPL[99]-Fluo have shown a similar cell penetration efficiency in a range of cell lines. However, the cell penetration of PPL-conjugated PNAs was evident at a higher concentration than that seen with the αMSH-PPL compounds, which may be due to the larger molecular weight of the PNA molecule or the presence of different linkers or a combination of both. In the cell penetration studies, diffuse and punctuate cytoplasmic fluorescence was observed with the fluoresceinated PPL conjugated compounds. Punctate staining may suggest an endocytotic mode of entry of these peptides, however diffuse staining in some cell types may indicate a non-endocytotic mechanism of internalisation or release into the cytoplasm following an endocytotic entry. Furthermore, the anti-pigmentation results with the 15merPNA-SS-PPL suggest that the PNA got into the cells, and taken in conjunction with the fluorescence results, suggests that PNA bound to the complementary tyrosinase mRNA sequence in the cytoplasm to inhibit pigmentation. To identify the mechanism of translocation of the PPL-associated compounds into the cells, additional work such as colocalisation studies with endosome markers, and separately in the presence of endocytosis inhibitors, might be helpful (but this may not be the same way that the PPL compounds enter through the stratum corneum).

Cell-penetrable peptides have also been investigated as molecular carriers for the delivery of protein and peptides into tissues. Rothbard *et al* firstly showed that the transdermal delivery of ciclosporin can be achieved by this approach (Rothbard *et al.* 2000). Later the

skin penetration potential of Tat, penetratin and polylysine, as well as polyarginine, were investigated in which penetratin-INF-γ, tat-superoxide dismutase, polylysine-superoxide dismutase and hemagglutinin epitope-polyarginine constructs penetrated into skin (not human) (Rothbard *et al.* 2000; Park *et al.* 2002; Robbins *et al.* 2002; Lim *et al.* 2003; Lee *et al.* 2005; Lopes *et al.* 2005). Moreover, skin delivery of antisense agents in the form of cream or patch would be a attractive approach to target many genes such as TNF-α for inflammatory disorders, Rho-C and Bcl-2 to target melanoma (Jansen *et al.* 2000; Carr *et al.* 2003). In this thesis, PPL has been investigated for the delivery of the peptide αMSH and antisense PNA into skin and various other organs. The skin penetration results showed that PPL-conjugated compounds penetrated in approximately 60% of analysed samples. Image analysis would be one approach to quantifying the accuracy of the extent of penetration. These results were based on a single application of the PPL-onjugated compounds where PBS was used as a solvent, and the penetration might be improved if the PPL-conjugated compounds were applied twice or thrice or applied in combination with a chemical penetration enhancer. There is a lack of published data on the efficiency of a diffusion chamber system for *ex vivo* skin penetration studies. In addition, as per as my knowledge none of the reports on CPP-based skin penetration in the published literature included information on the total number of times that the carrier-cargo conjugates entered/did not enter into the skin. The delivery of larger molecules into organs such as the eye and into the distal bowel, and into the cells of these organs and of the airways, is not a simple task. Polyarginine have been shown to be able to transport fluorescein isothiocyanate-dextran and pyridoxamine into the cornea, conjuctiva and conjuctiva/sclera of rabbit eyes (Nemoto *et al.* 2006), however, in another study,

polyarginine has been shown to promote apoptosis and necrosis of cultured airway epithelial cells (Shahana *et al.* 2002). It has also been reported that polylysine can damage tracheal epithelium (Yu *et al.* 1994). This indicates that an extensive toxicity analysis of these compounds (and of all CPPs relevant to future use in humans) will be essential before they can be used as carriers for the treatment of diseases. Although in the present study, the results suggest that PPL is capable of transporting αMSH and PNA into skin, gut, eyes and trachea, additional work will be required to test the stability and half-life of PPL in these environments as well as the *in vivo* efficacy.

Indeed, one limitation of this present study is the lack of *in vivo* investigations. However, it is necessary to generate enough initial *in vitro*/*ex vivo* results to comply with the 3Rs of replacement, reduction and refinement in order to avoid administering a very toxic compound to animals and to ensure that only the bare minimum number of experiments that need to be carried out on animals are performed. At the present time, based on the results in this thesis, there is probably enough background data to allow submission of an application to the Home Office to conduct some *in vivo* efficacy and toxicity experiments. For example, a topical anti-tyrosinase antisense investigation with PNA-SS-PPL applied *in vivo* to the skin of a pigmented mouse model would provide data on the ability of this compound to depigment skin and on toxicity from topical application. Subsequent studies could use a pig model (because of its thicker epidermis and stratum corneum barrier) or pigmented human skin grafted onto SCID/nude mice. Other *in vivo* studies could be performed on the eye and gut, for example it is interesting to investigate the delivery of therapeutic agents into mouse and primate eyes by instillating PPL-peptide/PNA compound. For gut delivery, PPL-peptide/PNA conjugated can be

incorporated into a biodegradable polymer matrix or pH sensitive polymers (methacrylic acid copolymers) to release compound to specific target site. In summary, the results in this thesis suggest that PPL can transport αMSH and PNA into cells, skin, eye and gut, and that the PPL-linked compounds retain their biological activity. Thus, PPL may have the potential to act as a molecular carrier for the delivery of drugs and therapeutic molecules into skin and other epithelial organs in humans *in vivo*.

A.1.0 APPENDIX

A.1.1 Structure of the compounds

A.1.1 αMSH

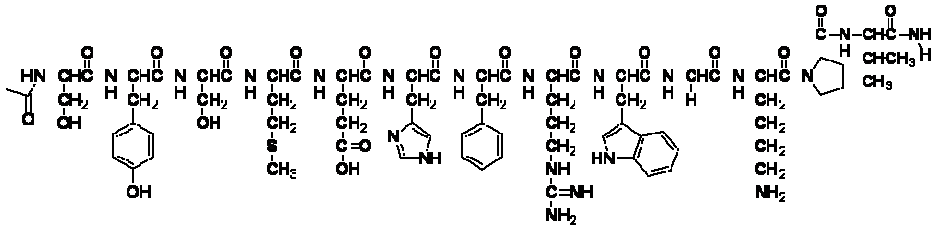

Ser-Tyr –Ser -Met-Glu-His-Phe- Arg -Trp- Gly- Lys- Pro- Val

A.1.2 Fluo-αMSH

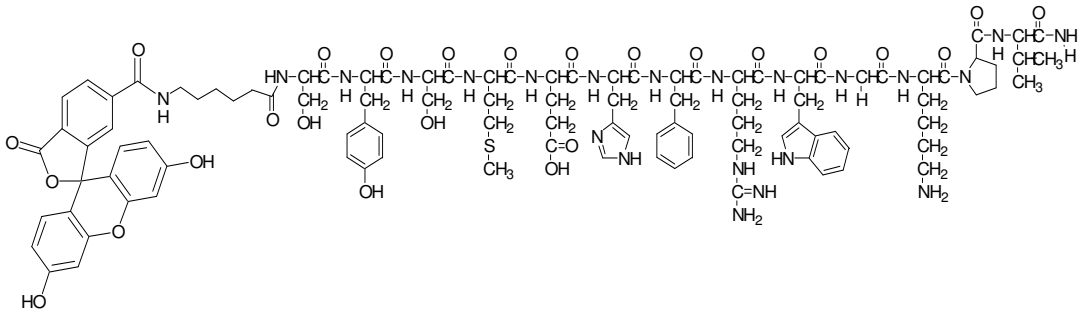

A.1.3 NDP-αMSH

Ac-Ser-Tyr-Ser-Nle-Glu-His-D-Phe-Arg-Trp-Gly-Lys-Pro-Val-NH2

A.1.4 MTII

Ac-Nle-c[Asp-His-d-Phe-Arg-Trp-Lys]-NH2

A.1.5 SHU

Ac-Nle-c[Asp-His-*D*Nal(2′)-Arg-Trp-Lys]-NH2

A.1.6 αMSH-PPL[98]

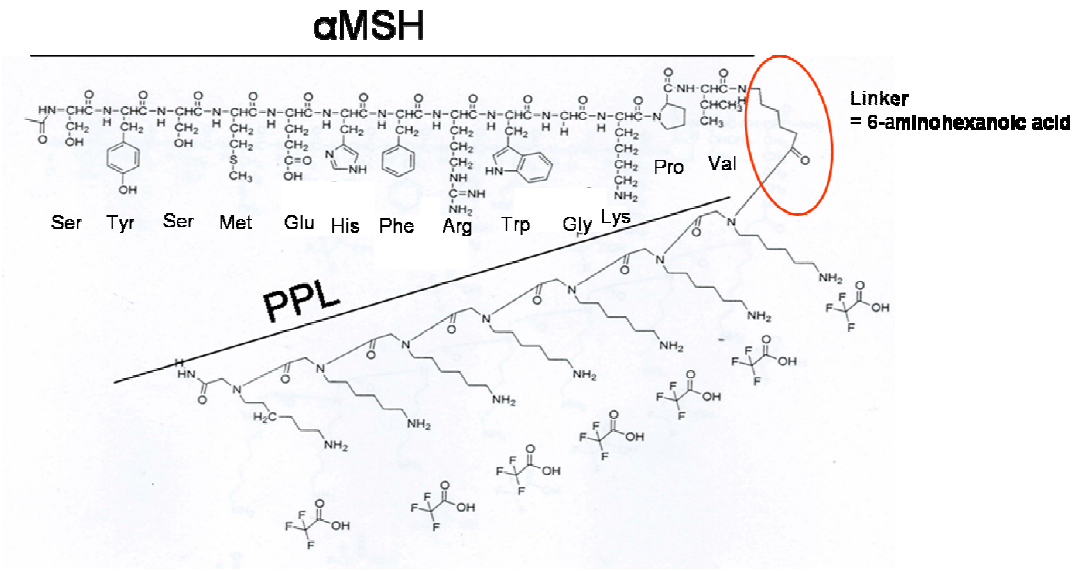

A.1.7 Fluo-αMSH-PPL[98]

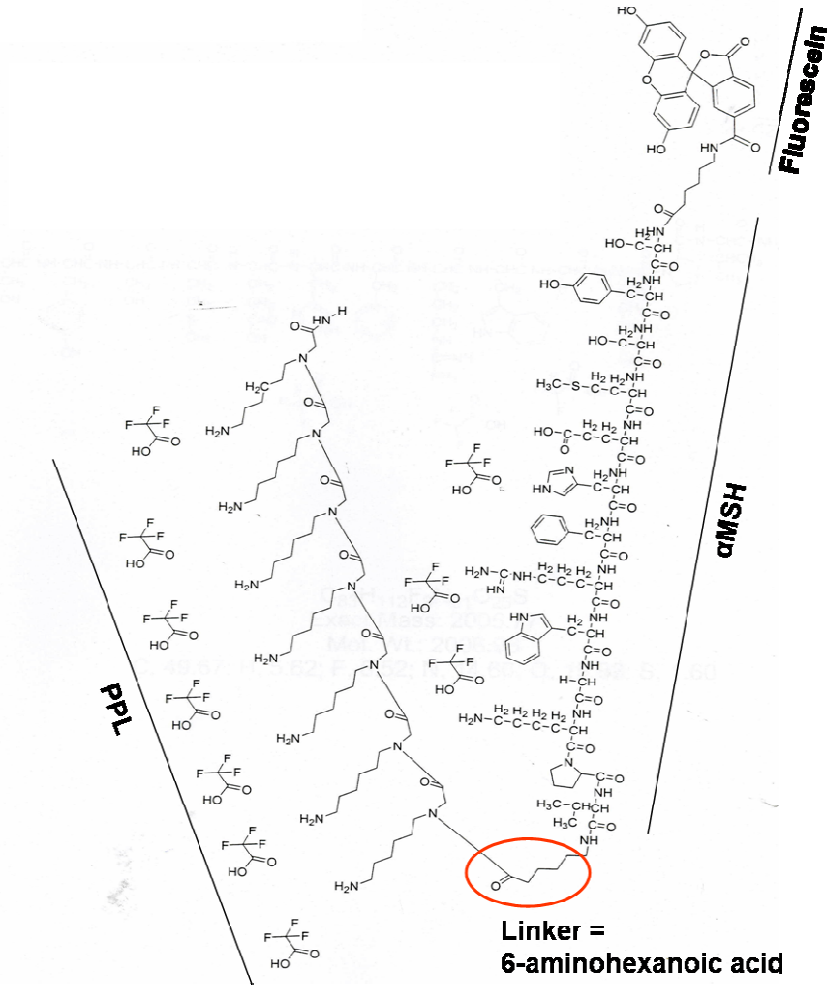

A.1.8 αMSH-PPL[99]

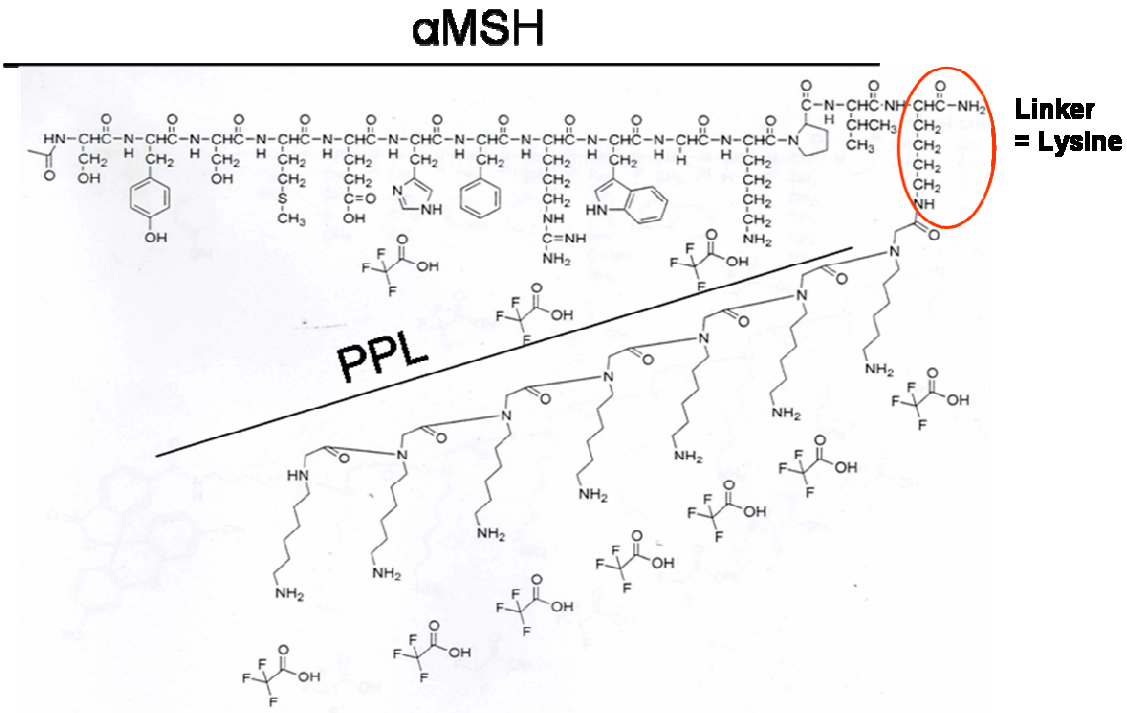

A.1.9 αMSH-PPL[99]-Fluo

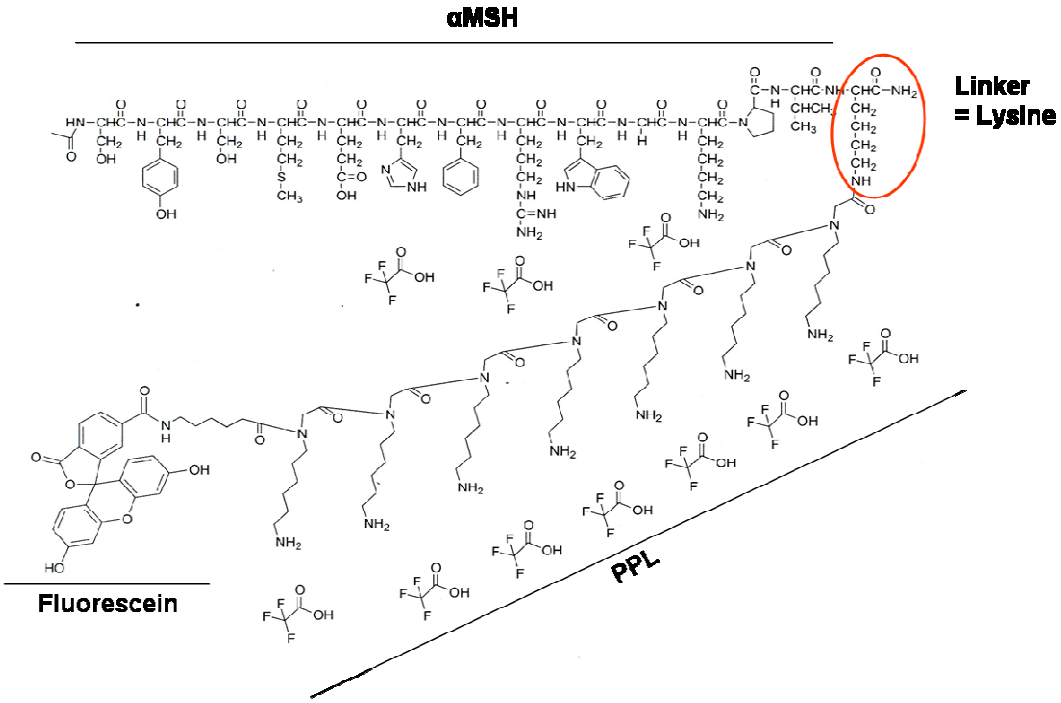

A.1.10 19merON-SS-PPL

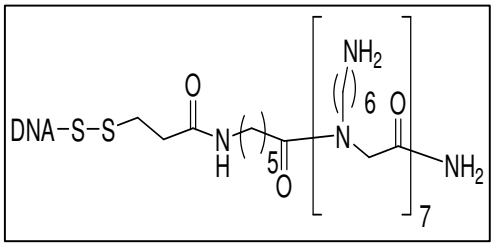

A.1.11 19merON-S-PPL

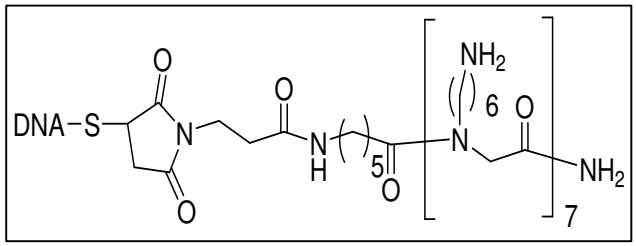

A.1.12 PNA

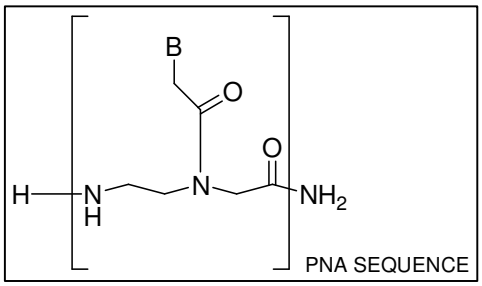

A.1.13 Fluo-PNA

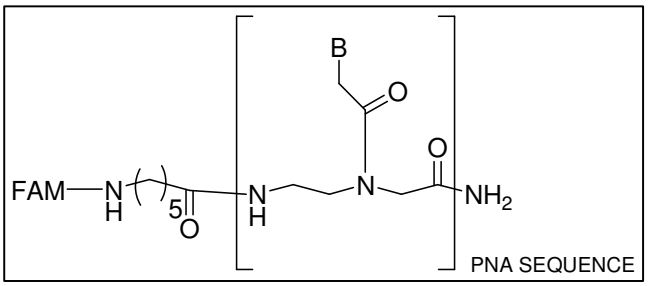

A.1.14 PNA-PPL

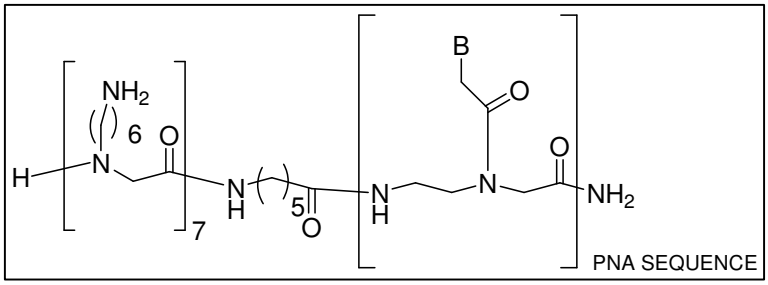

A.1.15 Fluo-PNA-PPL

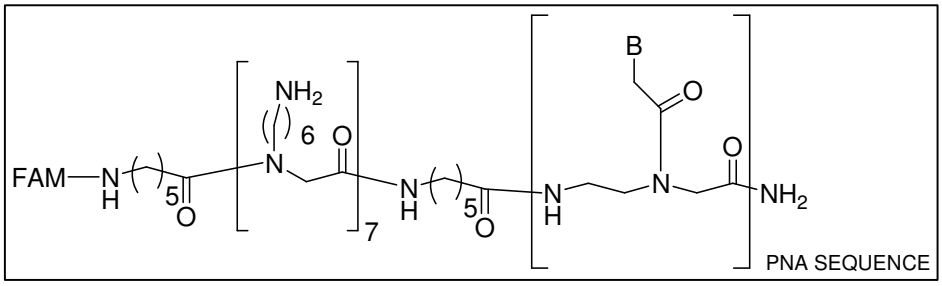

A.1.16 DNA Bases

Thymine Cytosine Adenine Guanine

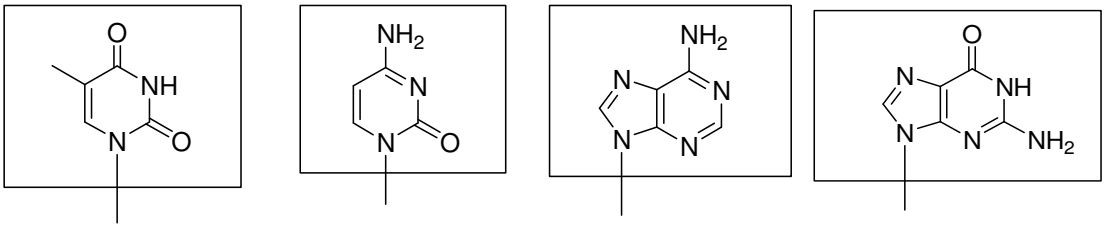

A.1.17 15merPNA-SS-PPL

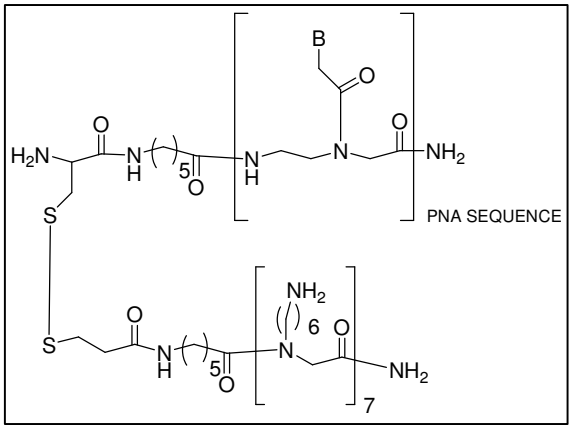

A.1.18 PNA-S-PPL

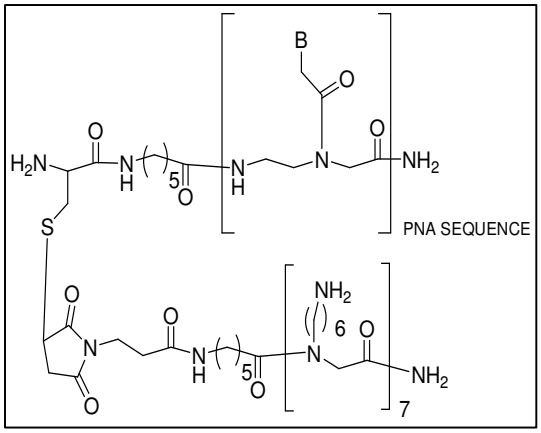

A.1.19 Fluo-15merPNA-SS-PPL

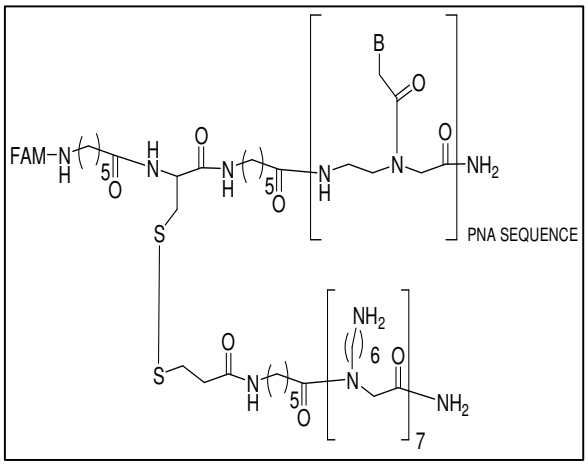

A.1.20 Fluo-PNA-S-PPL

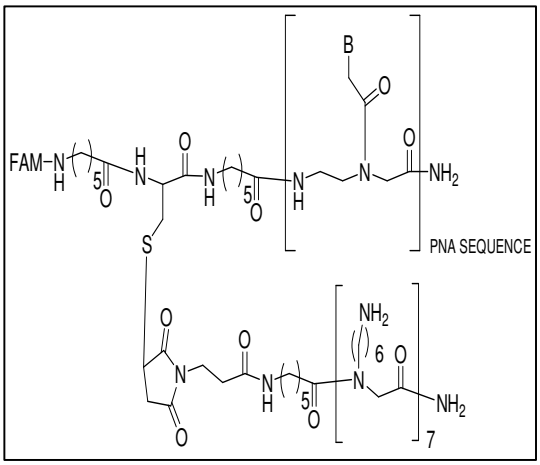

A.1.2 Cell culture reagents

A.1.2.1 Complete Dulbecco's Modified Eagle Medium (DMEM):

To 500mls of DMEM (Cat. No. 21969-035, Gibco-Invitrogen, Paisley, UK), containing: Sodium Pyruvate, Pyroxidine and without L-Glutamine add:

50ml (10%) EU approved heat inactivated FBS (Gibco-Invitrogen, Paisley, UK)

2mM L-Glutamine (Gibco-Invitrogen, Paisley, UK)

A.1.2.2 Cell Dissociation Solution (Sigma, Poole, UK)

1x Non enzymatic sterile filtered Cell Dissociation Solution, prepared in Hank's buffered salt solution (HBSS) without calcium and magnesium.

A.1.2.3 Geneticin solution (in water)

Contain 50mg/mls active geniticin (Sigma, Poole, UK)

A.1.2.4 Cell storage medium

EU approved Heat inactivated FBS (Gibco-Invitrogen, Paisley, UK)

10% DMSO

1.3 Flow cytometry

A.1.3.1 FACS Buffer

0.1% Sodium azide (Sigma, Poole, UK)

1% BSA (Sigma, Poole, UK)

Prepared in 500mls PBS.

1.4 Ligand Binding

A.1.4.1 Ligand Binding Buffer

To 500mls Minimal Essential Medium (Gibco-Invitrogen, Paisley, UK) with Earle's salt, with 25mM HEPES (pH 7.0), and without L-Glutamine add:

0.2% BSA (Sigma, Poole, UK)

1mM 1,10-Phenanthrolin (Sigma, Poole, UK)

0.5 mg/litre Leupeptin (Sigma, Poole, UK)

200mg/litre Bacitracin (Sigma, Poole, UK)

A.1.5 Cell lysis buffer for western blotting

100µl (1%) Triton x-100 and

One proteinase inhibitor cocktail tablet in 10mls dH_2O

A.1.6 SDS-PAGE gel running buffer

2.12g Tris

10.25g glycine

7mls 10% SDS in 690 mls dH_2O

A.1.7 SDS-PAGE separating buffer

2.0 M Tris-HCl in dH_2O pH 8.9

A.1.8 PAGE -separating gels (10%)

2.5 mls 40% acrylamide (Sigma-Aldrich, Dorset, UK)

2.0 mls separating buffer

100 µl 10% (w/v) SDS

4.38 mls dH_2O

18.75 µl TEMED (Sigma-Aldrich, Dorset, UK)

1ml (50mg/10mls) ammonium persulphate (Sigma-Aldrich, Dorset, UK)

A.1.9 Stacking gel buffer

0.5 M Tris-HCl in dH_2O pH 6.7

A.1.10 Stacking gels

500ul 40% acrylamide (Sigma-Aldrich, Dorset, UK)

0.5 mls stacking gel buffer

10% (w/v) SDS

3.46 mls dH_2O

12.5ul TEMED (Sigma-Aldrich, Dorset, UK)

500ul of 50mg/10mls (w/v) ammonium persulphate (Sigma-Aldrich, Dorset, UK)

A.1.11 Loading buffer

2mls stacking buffer

20% (v/v) glycerol

25% (w/v) 10% SDS

0.2mls of 0.1% bromophenol blue

10%(v/v) β-mercaptoethanol

A.1.12 TTBS

0.02M Tris

0.5M NaCl pH 7.5 containing

0.05% Tween 20™ (Amersham Bioscience Ltd) in dH_2O

A.1.13 Bacteria growth medium and solution

Proteose-peptone (PP) agar

PP agar, prepared according to the method of Zak and colleagues (Zak *et al*., 1984)

Material:	**Amount per litre (dH_2O)**
Proteose peptone (BD Bioscience)	10g
Bacto-agar (N.1 Oxoid)	10g
Starch	1g
$K_2HPO_4.3H_2O$ (Fisher)	5.24g
$K_2H_2PO_4$	1g
Sodium Chloride (Fisher)	5g
Supplement A	8mls
Supplement B	2mls

All components except supplement A and B were sterlised by autoclaving at 1.05kg cm^{-2} for 15 min. Supplement A and B were added to the autoclaved solution after cooling to 50^0C.

Supplement A:	**Amount per 800ml (dH2O)**
Glucose	100g

L-glutamine	10g
Para-amino-benzoic acid (Sigma)	13mg
Nicotinamide adenine dinucleotide (Sigma)	250mg
Thiamine hydrochloride (Sigma)	3mg
Co-carboxylase (Sigma)	100mg
Cyanocobalamin (Sigma)	10mg
Ferric nitrate	20mg

The components of supplement A were dissolved in dH_20, filter sterilised, and stored at 20^0C.

Supplement B:	**Amount per 200ml**
L-cysteine hydrochloride (Sigma)	26g
Adenine (Sigma)	1g
Guanidine hydrochloride (Sigma)	30mg
Uracil (Sigma)	800mg
Hypoxanthine (Sigma)	320mg

A.1.14 1% Acid alcohol

Ethanol – 350ml

dH2O – 150ml

Concentrated HCl– 5ml

A.1.15 Eosin solution

Eosin – 5g

Calcium chloride – 5g

Tap water – 500ml

8.0 References

Acerbi D, Brambilla G, Kottakis I. (2007) Advances in asthma and COPD management: delivering CFC-free inhaled therapy using Modulite technology. *Pulm Pharmacol Ther.* **20(3)** 290-303.

Agar N & Young AR (2005) Melanogenesis: a photoprotective response to DNA damage? *Mutat Res.* **571** 121-132.

Agrawal S, Temsamani J, Galbraith W & Tang J (1995) Pharmacokinetics of antisense oligonucleotides. *Clin Pharmacokinet.* **28** 7-16.

Agrawal S, Temsamani J & Tang JY (1991) Pharmacokinetics, biodistribution, and stability of oligodeoxynucleotide phosphorothioates in mice. *Proc.Natl.Acad Sci U.S.A.* **88** 7595-7599.

Al Taei S, Penning NA, Simpson JC, Futaki S, Takeuchi T, Nakase I & Jones AT (2006) Intracellular traffic and fate of protein transduction domains HIV-1 TAT peptide and octaarginine. Implications for their utilization as drug delivery vectors. *Bioconjug.Chem.* **17** 90-100.

Arndt KA & Fitzpatrick TB (1965) Topical use of hydroquinone as a depigmenting agent. *JAMA.* **194** 965-967.

Arora A, Hakim I, Baxter J, Rathnasingham R, Srinivasan R, Fletcher DA & Mitragotri S (2007) Needle-free delivery of macromolecules across the skin by nanoliter-volume pulsed microjets. *Proc.Natl.Acad Sci U.S.A.* **104** 4255-4260.

Artursson P, Ungell AL & Lofroth JE (1993) Selective paracellular permeability in two models of intestinal absorption: cultured monolayers of human intestinal epithelial cells and rat intestinal segments. *Pharm.Res* **10** 1123-1129.

Asbill C, Kim N, El-Kattan A, Creek K, Wertz P, Michniak B (2000) Evaluation of a human bio-engineered skin equivalent for drug permeation studies. *Pharm Res.* **17(9)**:1092-7.

Astriab-Fisher A, Sergueev DS, Fisher M, Shaw BR & Juliano RL (2000) Antisense inhibition of P-glycoprotein expression using peptide-oligonucleotide conjugates. *Biochem Pharmacol.* **60** 83-90.

Azad Khan AK & Truelove SC (1980) Circulating levels of sulphasalazine and its metabolites and their relation to the clinical efficacy of the drug in ulcerative colitis. *Gut* **21** 706-710.

Baker BS, Ovigne JM, Powles AV, Corcoran S & Fry L (2003) Normal keratinocytes express Toll-like receptors (TLRs) 1, 2 and 5: modulation of TLR expression in chronic

plaque psoriasis. *Br J Dermatol.* **148** 670-679.

Barnetson RS, Ooi TK, Zhuang L, Halliday GM, Reid CM, Walker PC, Humphrey SM & Kleinig MJ (2006) [Nle4-D-Phe7]-alpha-melanocyte-stimulating hormone significantly increased pigmentation and decreased UV damage in fair-skinned Caucasian volunteers. *J Invest Dermatol.* **126** 1869-1878.

Bartlett A, Brown M, Marriott C, Whitfield PJ. (2000) The infection of human skin by schistosome cercariae: studies using Franz cells. *Parasitology*. **121 (Pt 1)** 49-54

Barry BW (2002) Drug delivery routes in skin: a novel approach. *Adv Drug Deliv Rev.* **54** S31-S40.

Barton DE, Kwon BS & Francke U (1988) Human tyrosinase gene, mapped to chromosome 11 (q14----q21), defines second region of homology with mouse chromosome 7. *Genomics* **3** 17-24.

Beermann F, Ruppert S, Hummler E, Bosch FX, Muller G, Ruther U & Schutz G (1990) Rescue of the albino phenotype by introduction of a functional tyrosinase gene into mice. *EMBO J.* **9** 2819-2826.

Bendifallah N, Rasmussen FW, Zachar V, Ebbesen P, Nielsen PE & Koppelhus U (2006) Evaluation of cell-penetrating peptides (CPPs) as vehicles for intracellular delivery of antisense peptide nucleic acid (PNA). *Bioconjug Chem.* **17** 750-758.

Bhardwaj RS, Schwarz A, Becher E, Mahnke K, Aragane Y, Schwarz T, Luger TA (1996) Pro-opiomelanocortin-derived peptides induce IL-10 production in human monocytes. *J Immunol.* **156**: 2517–2521.

Bhorade R, Weissleder R, Nakakoshi T, Moore A & Tung CH (2000) Macrocyclic chelators with paramagnetic cations are internalized into mammalian cells via a HIV-tat derived membrane translocation peptide. *Bioconjug Chem.* **11** 301-305.

Bliss JM, Ford D, Swerdlow AJ, Armstrong BK, Cristofolini M, Elwood JM, Green A, Holly EA, Mack T, MacKie RM, *et al* (1995) Risk of cutaneous melanoma associated with pigmentation characteristics and freckling: systematic overview of 10 case-control studies. The International Melanoma Analysis Group (IMAGE). *Int J Cancer.* **9** 367-76.

Bonham MA, Brown S, Boyd AL, Brown PH, Bruckenstein DA, Hanvey JC, Thomson SA, Pipe A, Hassman F, Bisi JE *et al*. (1995) An assessment of the antisense properties of RNase H-competent and steric-blocking oligomers. *Nucleic Acids Res.* **23** 1197-1203.

Boonanuntanasarn S, Yoshizaki G, Iwai K & Takeuchi T (2004) Molecular cloning, gene expression in albino mutants and gene knockdown studies of tyrosinase mRNA in rainbow trout. *Pigment Cell Res.* **17** 413-421.

Bos JD & Meinardi (2000) The 500 Dalton rule for the skin penetration of chemical compounds and drugs. *Exp Dermatol*. **9** 165-169.

Braasch DA & Corey DR (2002) Novel antisense and peptide nucleic acid strategies for controlling gene expression. *Biochemistry* **41** 4503-4510.

Joint formulary committee. Skin. British national formulary, Edn 50th, pp 560-603. Ed. Mehta DK *et al* BMJ Publishing group, London, U.K.

Bronaugh RL & Maibach HI (1985) Percutaneous absorption of nitroaromatic compounds: In vivo and in vitro studies in the human and monkey. *J Invest Dermatol.* **84** 180-183.

Brown MB, Martin GP, Jones SA & Akomeah FK (2006) Dermal and transdermal drug delivery systems: current and future prospects. *Drug Deliv.* **13** 175-187.

Bul-Hassan K, Walmsley R & Boulton M (2000) Optimization of non-viral gene transfer to human primary retinal pigment epithelial cells. *Curr Eye Res.* **20** 361-366.

Bunnell BA, Askari FK & Wilson JM (1992) Targeted delivery of antisense oligonucleotides by molecular conjugates. *Somat Cell Mol Genet.* **18** 559-569.

Caldwell RB, Bartoli M, Behzadian MA, El-Remessy AE, Al-Shabrawey M, Platt DH & Caldwell RW (2003) Vascular endothelial growth factor and diabetic retinopathy: pathophysiological mechanisms and treatment perspectives. *Diabetes Metab Res Rev.* **19** 442-455.

Candille SI, Kaelin CB, Cattanach BM, Yu B, Thompson DA, Nix MA, Kerns JA, Schmutz SM, Millhauser GL, Barsh GS (2007) A beta -defensin mutation causes black coat color in domestic dogs. *Science* **318** 1418-23.

Carelli V, Di Colo G, Nannipieri E, Poli B & Serafini MF (2000) Polyoxyethylene-poly(methacrylic acid-co-methyl methacrylate) compounds for site-specific peroral delivery. *Int J Pharm* **202** 103-112.

Carr KM, Bittner M, Trent JM (2003) Gene-expression profiling in human cutaneous melanoma. O*ncogene* **22(20)** 3076-80

Catania A, Colombo G, Rossi C, Carlin A, Sordi A, Lonati C, Turcatti F, Leonardi P, Grieco P & Gatti S (2006) Antimicrobial properties of alpha-MSH and related synthetic melanocortins. *ScientificWorldJournal.* **6** 1241-1246.

Catania A, Cutuli M, Garofalo L, Carlin A, Airaghi L, Barcellini W & Lipton JM (2000) The neuropeptide alpha-MSH in host defense. *Ann N Y Acad Sci.* **917** 227-231.

Catania A & Lipton JM (1993) Alpha-melanocyte-stimulating hormone peptides in host responses. From basic evidence to human research. *Ann N Y Acad Sci.* **680** 412-423.

Chan JH, Lim S & Wong WF (2006) Antisense oligonucleotides: from design to therapeutic application. *Clin Exp Pharmacol Physiol.* **33** 533-540.

Chen L, Wright LR, Chen CH, Oliver SF, Wender PA & Mochly-Rosen D (2001) Molecular transporters for peptides: delivery of a cardioprotective [epsilon]PKC agonist peptide into cells and intact ischemic heart using a transport system, R7. *Chemistry & Biology* **8** 1123-1129.

Chhajlani V, Wikberg JE (1992) Molecular cloning and expression of the human melanocyte stimulating hormone receptor cDNA. *FEBS Lett*. **14** 417-20.

Chourasia MK & Jain SK (2003) Pharmaceutical approaches to colon targeted drug delivery systems. *J Pharm Pharm Sci.* **6** 33-66.

Church MK, Okayama Y & el Lati S (1991) Mediator secretion from human skin mast cells provoked by immunological and non-immunological stimulation. *Skin Pharmacol* **4** Suppl 1 15-24.

Citro G, D'Agnano I, Leonetti C, Perini R, Bucci B, Zon G, Calabretta B & Zupi G (1998) c-myc antisense oligodeoxynucleotides enhance the efficacy of cisplatin in melanoma chemotherapy in vitro and in nude mice. *Cancer Res.* **58** 283-289.

Clark RA, Chong B, Mirchandani N, Brinster NK, Yamanaka Ki, Dowgiert RK & Kupper TS (2006) The vast majority of CLA+ T Cells are resident in normal skin. *J Immunol.* **176** 4431-4439.

Colleen M.Smith (2005) Amino acids in proteins. In *Marks' Basic Medical Biochemistry: A clinical approach*, edn 1st, pp 72-92. Ed AD Colleen M.Smith. Lippincott Williams & Wilkins.

Cooper A, Robinson SJ, Pickard C, Jackson CL, Friedmann PS & Healy E (2005) Alpha-melanocyte-stimulating hormone suppresses antigen-induced lymphocyte proliferation in humans independently of melanocortin 1 receptor gene status. *J Immunol.* **175** 4806-4813.

Cowdery JS, Chace JH, Yi AK & Krieg AM (1996) Bacterial DNA induces NK cells to produce IFN-gamma in vivo and increases the toxicity of lipopolysaccharides. *J Immunol.* **156** 4570-4575.

Cruz DP (2001) The epidermis: an outpost of the immune system. In *The biology of the skin*, edn 1st, pp 255-263. Eds KR Freinkel & TD Woodley. The Parathenon Publishing Group.

Cutuli M, Cristiani S, Lipton JM & Catania A (2000) Antimicrobial effects of alpha-MSH peptides. *J Leukoc.Biol.* **67** 233-239.

Dai J, Nagai T, Wang X, Zhang T, Meng M & Zhang Q (2004) pH-sensitive nanoparticles for improving the oral bioavailability of cyclosporine A. *Int J Pharm.* **280** 229-240.

Dandagi PM, Mastiholimath VS, Patil MB & Gupta MK (2006) Biodegradable

microparticulate system of captopril. *Int J Pharm.* **307** 83-88.

Del Marmol V, Beermann F (1996) Tyrosinase and related proteins in mammalian pigmentation. *FEBS Lett.* **381(3)** 165-8

Denet AR & Preat V (2003) Transdermal delivery of timolol by electroporation through human skin. *J Control Release.* **88** 253-262.

Derer W, Easwaran HP, Knopf CW, Leonhardt H & Cardoso MC (1999) Direct protein transfer to terminally differentiated muscle cells. *J Mol Med.* **77** 609-613.

Derossi D, Joliot AH, Chassaing G & Prochiantz A (1994) The third helix of the Antennapedia homeodomain translocates through biological membranes. *J Biol Chem.* **269** 10444-10450.

Derossi D, Calvet S, Trembleau A, Brunissen A, Chassaing G & Prochiantz A (1996) Cell internalization of the third helix of the antennapedia homeodomain is receptor-independent. *J Biol Chem.* **271** 18188-18193.

Dick IP & Scott RC (1992) Pig ear skin as an in-vitro model for human skin permeability. *J Pharm Pharmacol.* **44** 640-645.

Diffey BL (1991) Solar ultraviolet radiation effects on biological systems. *Phys Med Biol.* **36** 299-328.

Diffey B (2004) Climate change, ozone depletion and the impact on ultraviolet exposure of human skin. *Phys Med Biol.* **49** R1-R11.

Diffey BL (2002) Sources and measurement of ultraviolet radiation. *Methods* **28** 4-13.

Dingwall C, Ernberg I, Gait MJ, Green SM, Heaphy S, Karn J, Lowe AD, Singh M, Skinner MA & Valerio R (1989) Human immunodeficiency virus 1 tat protein binds trans-activation-responsive region (TAR) RNA in vitro. *Proc Natl Acad Sci U.S.A.* **86** 6925-6929.

Dokka S, Cooper SR, Kelly S, Hardee GE & Karras JG (2005) Dermal delivery of topically applied oligonucleotides via follicular transport in mouse Skin. *J Invest Dermatol.* **124** 971-975.

Donnarumma G, Paoletti I, Buommino E, Antonietta Tufano M & Baroni A (2004) alpha-MSH reduces the internalization of Staphylococcus aureus and down-regulates HSP 70, integrins and cytokine expression in human keratinocyte cell lines. *Exp Dermatol.* **13** 748-754.

Dorr RT, Dvorakova K, Brooks C, Lines R, Levine N, Schram K, Miketova P, Hruby V & Alberts DS (2000) Increased eumelanin expression and tanning is induced by a superpotent melanotropin [Nle4-D-Phe7]-alpha-MSH in humans. *Photochem Photobiol.* **72** 526-532.

Drin G, Cottin S, Blanc E, Rees AR & Temsamani J (2003) Studies on the internalization mechanism of cationic cell-penetrating peptides. *J Biol Chem.* **278** 31192-31201.

Dubin N, Moseson M, Pasternack BS (1989) Sun exposure and malignant melanoma among susceptible individuals. *Environ Health Perspect.* **81** 139-51.

Dutkiewicz R, Albert DM & Levin LA (2000) Effects of latanoprost on tyrosinase activity and mitotic index of cultured melanoma lines. *Exp Eye Res.* **70** 563-569.

Edwards DA, Ben-Jebria A & Langer R (1998) Recent advances in pulmonary drug delivery using large, porous inhaled particles. *J Appl Physiol.* **85** 379-385.

Eller MS, Maeda T, Magnoni C, Atwal D & Gilchrest BA (1997) Enhancement of DNA repair in human skin cells by thymidine dinucleotides: Evidence for a p53-mediated mammalian SOSáresponse. *Proc Natl Acad Sci.U.S.A.* **94** 12627-12632.

Eves PC, MacNeil S & Haycock JW (2006) [alpha]-Melanocyte stimulating hormone, inflammation and human melanoma. *Peptides* **27** 444-452.

Faller C & Bracher M (2002) Reconstructed skin kits: reproducibility of cutaneous irritancy testing. *Skin Pharmacol Appl Skin Physiol* **15 Suppl 1** 74-91.

Farmer M, Petras RE, Hunt LE, Janosky JE & Galandiuk S (2000) The importance of diagnostic accuracy in colonic inflammatory bowel disease. *Am J Gastroenterol.* **95** 3184-3188.

Fawell S, Seery J, Daikh Y, Moore C, Chen LL, Pepinsky B & Barsoum J (1994) Tat-mediated delivery of heterologous proteins into cells. *Proc Natl Acad Sci U.S.A.* **91** 664-668.

Ferrara N, Damico L, Shams N, Lowman H & Kim R (2006) Development of ranibizumab, an anti-vascular endothelial growth factor antigen binding fragment, as therapy for neovascular age-related macular degeneration. *Retina* **26** 859-870.

Findlay GH & Moores PP (1980) Pigment anomalies of the skin in the human chimaera: their relation to systematized naevi. *Br J Dermatol.* **103** 489-498.

Finnin BC & Morgan TM (1999) Transdermal penetration enhancers: applications, limitations, and potential. *J Pharm Sci.* **88** 955-958.

Fisher L, Soomets U, Cortes T, V, Chilton L, Jiang Y, Langel U & Iverfeldt K (2004) Cellular delivery of a double-stranded oligonucleotide NFkappaB decoy by hybridization to complementary PNA linked to a cell-penetrating peptide. *Gene Ther.* **11** 1264-1272.

Fitzpatrick TB (1988) The validity and practicality of sun-reactive skin types I through VI. *Arch Dermatol.* **124** 869-871.

FitzpatrickTB (1965) Mammalian melanin biosynthesis. *Trans St Johns Hosp Dermatol*

Soc. **51** 1-26.

Fitzpatrick TB & Breathnach AS (1963) The epidermal melanin unit system. *Dermatol Wochenschr.* **147** 481-489.

Flanagan WM, Kothavale A & Wagner RW (1996) Effects of oligonucleotide length, mismatches and mRNA levels on C-5 propyne-modified antisense potency. *Nucleic Acids Res.* **24** 2936-2941.

Foger F, Schmitz T & Bernkop-Schnurch A (2006) In vivo evaluation of an oral delivery system for P-gp substrates based on thiolated chitosan. *Biomaterials* **27** 4250-4255.

Frankel AD & Pabo CO (1988) Cellular uptake of the tat protein from human immunodeficiency virus. *Cell* **55** 1189-1193.

Freeman SE, Ley RD & Ley KD (1988) Sunscreen protection against UV-induced pyrimidine dimers in DNA of human skin in situ. *Photodermatol.* **5** 243-247.

Friedmann PS & Gilchrest BA (1987) Ultraviolet radiation directly induces pigment production by cultured human melanocytes. *J Cell Physiol.* **133** 88-94.

Friend DR & Chang GW (1985) Drug glycosides: potential prodrugs for colon-specific drug delivery. *J Med Chem.* **28** 51-57.

Fuller BB, Rungta D, Iozumi K, Hoganson GE, Corn TD, Cao VA, Ramadan ST & Owens KC (1993) Hormonal regulation of melanogenesis in mouse melanoma and in human melanocytes. *Ann N Y Acad Sci.* **680** 302-319.

Futaki S (2005) Membrane-permeable arginine-rich peptides and the translocation mechanisms. *Adv Drug Deliv Rev.* **57** 547-558.

Futaki S, Suzuki T, Ohashi W, Yagami T, Tanaka S, Ueda K & Sugiura Y (2001) Arginine-rich Peptides. An abundant source of membrane-permeable peptides having potential as carriers for intracellular protein delivery. *J Biol Chem.* **276** 5836-5840.

Gantz I, Miwa H, Konda Y, Shimoto Y, Tashiro T, Watson SJ, DelValle J & Yamada T (1993) Molecular cloning, expression, and gene localization of a fourth melanocortin receptor. *J Biol Chem.* **268** 15174-15179.

Gantz I, Shimoto Y, Konda Y, Miwa H, Dickinson CJ & Yamada T (1994) Molecular cloning, expression, and characterization of a fifth melanocortin receptor. *Biochem Biophys Res Commun.* **200** 1214-1220.

Gantz I & Fong TM (2003) The melanocortin system. *Am J Physiol Endocrinol Metab.* **284** E468-E474.

Gehring WJ, Muller M, Affolter M, Percival-Smith A, Billeter M, Qian YQ, Otting G & Wuthrich K (1990) The structure of the homeodomain and its functional implications.

Trends Genet. **6** 323-329.

Getting SJ (2002) Melanocortin peptides and their receptors: new targets for anti-inflammatory therapy. *Trends Pharmacol Sci.* **23** 447-449.

Giebel LB, Tripathi RK, King RA & Spritz RA (1991) A tyrosinase gene missense mutation in temperature-sensitive type I oculocutaneous albinism. A human homologue to the Siamese cat and the Himalayan mouse. *J Clin Invest.* **87** 1119-1122.

Giebel LB, Tripathi RK, Strunk KM, Hanifin JM, Jackson CE, King RA & Spritz RA (1991) Tyrosinase gene mutations associated with type IB ("yellow") oculocutaneous albinism. *Am J Hum Genet.* **48** 1159-1167.

Gilchrest BA, Eller MS, Geller AC & Yaar M (1999) The pathogenesis of melanoma induced by ultraviolet radiation. *N Engl J Med.* **340** 1341-1348.

Gimenez E, Lavado A, Giraldo P, Cozar P, Jeffery G & Montoliu L (2004) A transgenic mouse model with inducible Tyrosinase gene expression using the tetracycline (Tet-on) system allows regulated rescue of abnormal chiasmatic projections found in albinism. *Pigment Cell Res.* **17** 363-370.

Gordon BK, Chan SL & . (2001) Inflammation and immunity. In edn 1st, pp 239-254. TD Freinkel. The Parathenon Publishing Group.

Gordon JW, Scangos GA, Plotkin DJ, Barbosa JA & Ruddle FH (1980) Genetic transformation of mouse embryos by microinjection of purified DNA. *Proc Natl Acad Sci U.S.A.* **77** 7380-7384.

Green M & Loewenstein PM (1988) Autonomous functional domains of chemically synthesized human immunodeficiency virus tat trans-activator protein. *Cell* **55** 1179-1188.

Greenwood J, Amos CL, Walters CE, Couraud PO, Lyck R, Engelhardt B & Adamson P (2003) Intracellular domain of brain endothelial intercellular adhesion molecule-1 is essential for T lymphocyte-mediated signaling and migration. *J Immunol.* **171** 2099-2108.

Grieco P, Rossi C, Colombo G, Gatti S, Novellino E, Lipton JM & Catania A (2003) Novel alpha-melanocyte stimulating hormone peptide analogues with high candidacidal activity. *J Med Chem.* **46** 850-855.

Grubauer G, Feingold KR, Harris RM & Elias PM (1989) Lipid content and lipid type as determinants of the epidermal permeability barrier. *J Lipid Res.* **30** 89-96.

Haake A, Scott AG & Holbrook AK (2001) Structure and function of the skin: overview of the epidermis and dermis. In the biology of the skin, Edn 1st, pp 19-45. Ed KR Freinkel. The Parthenon Publishing Group Limited, U.K.

Hadley ME & Haskell-Luevano C (1999) The proopiomelanocortin system. *Ann N Y Acad Sci.* **885** 1-21.

Hadley ME, Wood SH, Lemus-Wilson AM, Dawson BV, Levine N, Dorr RT & Hruby VJ (1987) Topical application of a melanotropic peptide induces systemic follicular melanogenesis. *Life Sci.* **40** 1889-1895.

Halaban R, Svedine S, Cheng E, Smicun Y, Aron R & Hebert DN (2000) Endoplasmic reticulum retention is a common defect associated with tyrosinase-negative albinism. *Proc Natl Acad Sci U.S.A.* **97** 5889-5894.

Hamilton SE, Simmons CG, Kathiriya IS & Corey DR (1999) Cellular delivery of peptide nucleic acids and inhibition of human telomerase. *Chemistry & Biology* **6** 343-351.

Hancock RE & Scott MG (2000) The role of antimicrobial peptides in animal defenses. *Proc Natl Acad Sci U.S.A.* **97** 8856-8861.

Hancock RE (2001) Cationic peptides: effectors in innate immunity and novel antimicrobials. *Lancet Infect Dis.* **1** 156-164.

Hanvey JC, Peffer NJ, Bisi JE, Thomson SA, Cadilla R, Josey JA, Ricca DJ, Hassman CF, Bonham MA, Au KG, et al. (1992) Antisense and antigene properties of peptide nucleic acid. *Science* **258(5087)** 1481-5.

Harboe E, Larsen C, Johansen M & Olesen HP (1989) Macromolecular Prodrugs. XV. Colon-targeted delivery Bioavailability of naproxen from orally administered dextran–naproxen ester prodrugs varying in molecular size in the pig. *Pharml Res.* **6** 919-923.

Harder J, Bartels J, Christophers E & Schroder JM (1997) A peptide antibiotic from human skin. *Nature* **387** 861.

Hariharan S, Bhardwaj V, Bala I, Sitterberg J, Bakowsky U & Ravi Kumar M (2006) Design of estradiol loaded PLGA nanoparticulate formulations: A potential oral delivery system for hormone therapy. *Pharm Res.* **23** 184-195.

Haycock JW, Rowe SJ, Cartledge S, Wyatt A, Ghanem G, Morandini R, Rennie IG & MacNeil S (2000) alpha-melanocyte-stimulating hormone reduces impact of proinflammatory cytokine and peroxide-generated oxidative stress on keratinocyte and melanoma cell lines. *J Biol Chem.* **275** 15629-15636.

Hedley, Gawkrodger, Weetman, Morandini, Boeynaems, Ghanem & Mac N (1998) alpha-melanocyte stimulating hormone inhibits tumour necrosis factor-alpha stimulated intercellular adhesion molecule-1 expression in normal cutaneous human melanocytes and in melanoma cell lines. *Br J Dermatol.* **138** 536-543.

Helton DR, Osborne DW, Pierson SK, Buonarati MH & Bethem RA (2000) Pharmacokinetic profiles in rats after intravenous, oral, or dermal administration of

dapsone. *Drug Metab Dispos.* **28** 925-929.

Holinger EP, Chittenden T & Lutz RJ (1999) Bak BH3 Peptides Antagonize Bcl-xL function and induce apoptosis through cytochrome c-independent activation of caspases. *J Biol Chem.* **274** 13298-13304.

Hunt G, Kyne S, Ito S, Wakamatsu K, Todd C & Thody A (1995) Eumelanin and phaeomelanin contents of human epidermis and cultured melanocytes. *Pigment Cell Res.* **8** 202-208.

Ichiyama T, Sato S, Okada K, Catania A & Lipton JM (2000) The neuroimmunomodulatory peptide alpha-MSH. *Ann N Y Acad Sci* **917** 221-226.

Jacobi U, Kaiser M, Toll R, Mangelsdorf S, Audring H, Otberg N, Sterry W & Lademann J (2007) Porcine ear skin: an in vitro model for human skin. *Skin Res Technol.* **13** 19-24.

Jakasa I, Verberk MM, Esposito M, Bos JD & Kezic S (2007) Altered penetration of polyethylene glycols into uninvolved skin of atopic dermatitis patients. *J Invest Dermatol.* **127** 129-134.

Jansen B, Wacheck V, Heere-Ress E, Schlagbauer-Wadl H, Hoeller C, Lucas T, Hoermann M, Hollenstein U, Wolff K, Pehamberger H (2000) Chemosensitisation of malignant melanoma by BCL2 antisense therapy. *Lancet* **356(9243)**:1728-33

Jeffery G, Brem G & Montoliu L (1997) Correction of retinal abnormalities found in albinism by introduction of a functional tyrosinase gene in transgenic mice and rabbits. *Brain Res Dev Brain Res* **99** 95-102.

Jiang J, Gill HS, Ghate D, McCarey BE, Patel SR, Edelhauser HF, Prausnitz MR (2007) Coated microneedles for drug delivery to eye. *Invest Opthalmol Vis Sci* **48** 4038-43

Jimbow K, Obata H, Pathak MA & Fitzpatrick TB 1974 Mechanism of depigmentation by hydroquinone. *J Invest Dermatol.* **62** 436-449.

Jin LH, Bahn JH, Eum WS, Kwon HY, Jang SH, Han KH, Kang TC, Won MH, Kang JH, Cho SW, Park J, Choi SY (2001) Transduction of human catalase mediated by an HIV-1 TAT protein basic domain and arginine-rich peptides into mammalian cells. *Free Radic Biol Med.* **31** 1509-1519.

Johnson LN, Cashman SM, Kumar-Singh R (2008) Cell-penetrating peptide for enhanced delivery of nucleic acids and drugs to ocular tissues including retina and cornea. *Mol Ther* **16(1)**-107-14.

Joliot A, Pernelle C, Deagostini-Bazin H & Prochiantz A (1991) Antennapedia homeobox peptide regulates neural morphogenesis. *Proc Natl Acad Sci U.S.A.* **88** 1864-1868.

Jones SW, Christison R, Bundell K, Voyce CJ, Brockbank SMV, Newham P & Lindsay

MA (2005) Characterisation of cell-penetrating peptide-mediated peptide delivery. *Br J Pharmacol.* **145** 1093-1102.

Jungbauer FHW, Coenraads PJ & Kardaun SH (2001) Toxic hygroscopic contact reaction to N-methyl-2-pyrrolidone. *Contact Dermatitis* **45** 303-304.

Kabouridis PS, Hasan M, Newson J, Gilroy DW & Lawrence T (2002) Inhibition of NF-kappa B activity by a membrane-transducing mutant of I kappa B alpha. *J Immunol.* **169** 2587-2593.

Kadekaro AL, Kavanagh RJ, Wakamatsu K, Ito S, Pipitone MA & Abdel-Malek ZA (2003) Cutaneous photobiology. The melanocyte vs. the sun: who will win the final round? *Pigment Cell Res.* **16** 434-447.

Kanetsky PA, Swoyer J, Panossian S, Holmes R, Guerry D & Rebbeck TR (2002) A polymorphism in the agouti signaling protein gene is associated with human pigmentation. *Am J Hum Genet.* **70** 770-775.

Kask K, Berthold M & Bartfai T (1997) Galanin receptors: Involvement in feeding, pain, depression and Alzheimer's disease. *Life Sciences* **60** 1523-1533.

Kasraee B, Hugin A, Tran C, Sorg O & Saurat JH (2004) Methimazole is an inhibitor of melanin synthesis in cultured B16 melanocytes. *J Invest Dermatol.* **122** 1338-1341.

Kim DW, Eum WS, Jang SH, Yoon CS, Choi HS, Choi SH, Kim YH, Kim SY, Lee ES, Baek NI, Kwon HY, Choi JH, Choi YC, Kwon OS, Cho SW, Han K, Lee KS, Park J, Choi SY (2003) Ginsenosides enhance the transduction of tat-superoxide dismutase into mammalian cells and skin. *Mol Cells.* **16** 402-406.

Kligman AM (1965) Topical pharmacology and toxicology of dimethyl sulfoxide. 1. *JAMA.* **193** 796-804.

Knudsen H & Nielsen PE (1996) Antisense properties of duplex- and triplex-forming PNAs. *Nucleic Acids Res.* **24(3)** 494-500.

Kobayashi N, Nakagawa A, Muramatsu T, Yamashina Y, Shirai T, Hashimoto MW, Ishigaki Y, Ohnishi T & Mori T (1998) Supranuclear melanin caps reduce ultraviolet induced DNA photoproducts in human epidermis. *J Invest Dermatol***. 110** 806-810.

Kondo S, Yamanaka C & Sugimoto I (1987) Enhancement of transdermal delivery by superfluous thermodynamic potential. III. Percutaneous absorption of nifedipine in rats. *J Pharmacobiodyn.* **10** 743-749.

Kono R, Jimbow K & Takahashi H (1984) Ultrasonic comparison of two morphologically distinct melanosomes in malignant melanomas. *Experientia* **40** 571-572.

Koppelhus U & Nielsen PE (2003) Cellular delivery of peptide nucleic acid (PNA). *Adv Drug Deliv Rev.* **55** 267-280.

Kost J, Mitragotri S, Gabbay RA, Pishko M & Langer R (2000) Transdermal monitoring of glucose and other analytes using ultrasound. *Nat Med.* **6** 347-350.

Kretz A, Wybranietz WA, Hermening S, Lauer UM & Isenmann S (2003) HSV-1 VP22 augments adenoviral gene transfer to CNS neurons in the retina and striatum in vivo. *Mol Ther.* **7** 659-669.

Krieg AM, Yi AK, Matson S, Waldschmidt TJ, Bishop GA, Teasdale R, Koretzky GA & Klinman DM (1995) CpG motifs in bacterial DNA trigger direct B-cell activation. *Nature* **374** 546-549.

Kurreck J (2003) Antisense technologies. Improvement through novel chemical modifications. *Eur J Biochem.* **270** 1628-1644.

Kwon BS, Haq AK, Pomerantz SH & Halaban R 1987a Isolation and sequence of a cDNA clone for human tyrosinase that maps at the mouse c-albino locus. *Proc Natl Acad Sci U.S.A.* **84** 7473-7477.

Kwon BS, Wakulchik M, Haq AK, Halaban R & Kestler D (1988) Sequence analysis of mouse tyrosinase cDNA and the effect of melanotropin on its gene expression. *Biochem Biophys Res Commun.* **153** 1301-1309.

Lamason RL, Mohideen MA, Mest JR, Wong AC, Norton HL, Aros MC, Jurynec MJ, Mao X, Humphreville VR, Humbert JE, Sinha S, Moore JL, Jagadeeswaran P, Zhao W, Ning G, Makalowska I, McKeigue PM, O'donnell D, Kittles R, Parra EJ, Mangini NJ, Grunwald DJ, Shriver MD, Canfield VA & Cheng KC (2005) SLC24A5, a putative cation exchanger, affects pigmentation in zebrafish and humans. *Science* **310** 1782-1786.

Lautenschlager S, Wulf HC & Pittelkow MR (2007) Photoprotection. *The Lancet* **370** 528-537.

Lebwohl M & Ali S (2001) Treatment of psoriasis. Part 2. Systemic therapies. *J Am Acad Dermatol.* **45** 649-661.

Lebwohl M, Menter A, Koo J & Feldman SR (2004) Combination therapy to treat moderate to severe psoriasis. *J Am Acad Dermatol.* **50** 416-430.

Lee J, Jung E, Park J & Park D (2005) Transdermal delivery of interferon-gamma (IFN-gamma) mediated by penetratin, a cell-permeable peptide. *Biotechnol Appl Biochem.* **42** 169-173.

Lemaitre M, Bayard B & Lebleu B (1987) Specific antiviral activity of a Poly(L-lysine)-conjugated oligodeoxyribonucleotide sequence complementary to vesicular stomatitis virus N protein mRNA initiation site. *Proc Natl Acad Sci U.S.A.* **84** 648-652.

Lerner AB & McGuire JS (1961) Effect of alpha- and beta-Melanocyte stimulating hormones on the skin colour of man. *Nature* **189** 176-179.

Letoha T, Gaal S, Somlai C, Venkei Z, Glavinas H, Kusz E, Duda E, Czajlik A, Petak F & Penke B (2005) Investigation of penetratin peptides. Part 2. In vitro uptake of penetratin and two of its derivatives. *J Pept Sci.* **11** 805-811.

Lim JM, Chang MY, Park SG, Kang NG, Song YS, Lee YH, Yoo YC, Cho WG, Choi SY & Kang SH (2003) Penetration enhancement in mouse skin and lipolysis in adipocytes by TAT-GKH, a new cosmetic ingredient. *J Cosmet Sci.* **54** 483-491.

Lin W, Cormier M, Samiee A, Griffin A, Johnson B, Teng CL, Hardee GE & Daddona PE (2001) Transdermal delivery of antisense oligonucleotides with microprojection patch (macroflux) technology. *Pharm Research.* **18** 1789-1793.

Lindgren M, Gallet X, Soomets U, Hallbrink M, Brakenhielm E, Pooga M, Brasseur R & Langel U (2000) Translocation properties of novel cell penetrating transportan and penetratin analogues. *Bioconjug Chem.* **11** 619-626.

Lindgren ME, Hallbrink MM, Elmquist AM & Langel U (2004) Passage of cell-penetrating peptides across a human epithelial cell layer in vitro. *Biochem J.* **377** 69-76.

Lotte C, Patouillet C, Zanini M, Messager A & Roguet R (2002) Permeation and skin absorption: reproducibility of various industrial reconstructed human skin models. *Skin Pharmacol Appl Skin Physiol* **15 Suppl 1** 18-30.

Lipton JM & Catania A (1997) Anti-inflammatory actions of the neuroimmunomodulator [alpha]-MSH. *Immunology Today.* **18** 140-145.

Liu X, Hu Y, Filla MS, Gabelt BT, Peters DM, Brandt CR & Kaufman PL (2005) The effect of C3 transgene expression on actin and cellular adhesions in cultured human trabecular meshwork cells and on outflow facility in organ cultured monkey eyes. *Mol Vis.* **11** 1112-1121.

Liu X, Brandt CR, Gabelt BT, Bryar PJ, Smith ME & Kaufman PL (1999) Herpes simplex virus mediated gene transfer to primate ocular tissues. *Exp Eye Res.* **69** 385-395.

Lopes LB, Brophy CM, Furnish E, Flynn CR, Sparks O, Komalavilas P, Joshi L, Panitch A & Bentley MV (2005) Comparative study of the skin penetration of protein transduction domains and a conjugated peptide. *Pharm Res.* **22** 750-757.

Lore K, Sonnerborg A, Spetz AL, Andersson U & Andersson J (1998) Immunocytochemical detection of cytokines and chemokines in Langerhans cells and in vitro derived dendritic cells. *J Immunol Methods.* **214** 97-111.

Lowes MA, Bowcock AM & Krueger JG (2007) Pathogenesis and therapy of psoriasis. *Nature* **445** 866-873.

Lowman AM, Morishita M, Kajita M, Nagai T & Peppas NA (1999) Oral delivery of insulin using pH-responsive complexation gels. *J Pharm Sci.* **88** 933-937.

Lundberg M, Wikstrom S & Johansson M (2003) Cell surface adherence and endocytosis of protein transduction domains. *Molecular Therapy* **8** 143-150.

Lundberg P & Langel U (2003) A brief introduction to cell-penetrating peptides. *J Mol Recognit.* **16** 227-233.

Lv H, Zhang S, Wang B, Cui S, Yan J (2006) Toxicity of cationic lipids and cationic polymers in gene delivery. *J Control Release*. **10** 100-9

Madison KC (2003) Barrier function of the skin: "la raison d'etre" of the epidermis. *J Invest Dermatol.* **121** 231-241.

Mai JC, Shen H, Watkins SC, Cheng T & Robbins PD (2002) Efficiency of Protein transduction is cell type-dependent and is enhanced by dextran sulfate. *J Biol Chem.* **277** 30208-30218.

Manabe M & O'Guin WM (1992) Keratohyalin, trichohyalin and keratohyalin-trichohyalin hybrid granules: an overview. *J Dermatol.* **19** 749-755.

Manna SK & Aggarwal BB (1998) Alpha-melanocyte-stimulating hormone inhibits the nuclear transcription factor NF-kappa B activation induced by various inflammatory agents. *J Immunol.* **161** 2873-2880.

Fara MA, Díaz-Mochón JJ & Bradley M (2006). Microwave-assisted coupling with DIC/HOBt for the synthesis of difficult peptoids and fluorescently labelled peptides a gentle heat goes a long way *Tetrahedron Letter* **47** 1011-1014.

Marjukka Suhonen T, Bouwstra A & Urtti A (1999) Chemical enhancement of percutaneous absorption in relation to stratum corneum structural alterations. *J Controlled Release.* **59** 149-161.

Martin LW, Catania A, Hiltz ME, Lipton JM (1991) Neuropeptide alpha-MSH antagonizes IL-6- and TNF-induced fever. *Peptides.* **12(2)** 297-9

Matriano JA, Cormier M, Johnson J, Young WA, Buttery M, Nyam K & Daddona PE (2002) Macroflux microprojection array patch technology: A new and efficient approach for intracutaneous immunization. *Pharm Res.* **19** 63-70.

Mattner F, Fleitmann JK, Lingnau K, Schmidt W, Egyed A, Fritz J, Zauner W, Wittmann B, Gorny I, Berger M, Kirlappos H, Otava A, Birnstiel ML & Buschle M (2002) Vaccination with Poly-L-Arginine as immunostimulant for peptide vaccines: induction of potent and long-lasting T-cell responses against cancer antigens. *Cancer Res.* **62** 1477-1480.

Matveeva OV, Tsodikov AD, Giddings M, Freier SM, Wyatt JR, Spiridonov AN, Shabalina SA, Gesteland RF & Atkins JF (2000) Identification of sequence motifs in oligonucleotides whose presence is correlated with antisense activity. *Nucleic Acids Res.* **28** 2862-2865.

Maxton DG, Bjarnason I, Reynolds AP, Catt SD, Peters TJ & Menzies IS (1986) Lactulose, 51Cr-labelled ethylenediaminetetra-acetate, L-rhamnose and polyethyleneglycol 400 [corrected] as probe markers for assessment in vivo of human intestinal permeability. *Clin Sci (Lond).* **71** 71-80.

Mayes S & Ferrone M (2006) Fentanyl HCl patient-controlled iontophoretic transdermal system for the management of acute postoperative pain. *Ann Pharmacother***. 40** 2178-2186.

McCullough JL, Snyder DS, Weinstein GD, Friedland A & Stein B (1976) Factors affecting human percutaneous penetration of methotrexate and its analogues in vitro. *J Invest Dermatol.* **66** 103-107.

McClean S, Prosser E, Meehan E, O'Malley D, Clarke N, Ramtoola Z & Brayden D (1998) Binding and uptake of biodegradable poly-lactide micro- and nanoparticles in intestinal epithelia. *Eur J Pharm Sci.* **6** 153-163.

McEvoy B, Beleza S & Shriver MD (2006) The genetic architecture of normal variation in human pigmentation: an evolutionary perspective and model. *Hum Mol Genet.* **15** R176-R181.

McMahon BM, Mays D, Lipsky J, Stewart JA, Fauq A & Richelson E (2002) Pharmacokinetics and tissue distribution of a peptide nucleic acid after intravenous administration. *Antisense Nucleic Acid Drug Dev.* **12** 65-70.

McShan WM, Rossen RD, Laughter AH, Trial J, Kessler DJ, Zendegui JG, Hogan ME & Orson FM (1992) Inhibition of transcription of HIV-1 in infected human cells by oligodeoxynucleotides designed to form DNA triple helices. *J Biol Chem.* **267** 5712-5721.

Mehier-Humbert S & Guy RH (2005) Physical methods for gene transfer: Improving the kinetics of gene delivery into cells. *Adv Drug Deliv Rev.* **57** 733-753.

Mehta RC, Stecker KK, Cooper SR, Templin MV, Tsai YJ, Condon TP, Bennett CF & Hardee GE (2000) Intercellular adhesion molecule-1 suppression in skin by topical delivery of anti-sense oligonucleotides. *J Invest Dermatol.* **115** 805-812.

Megrab NA, Williams AC & Barry BW (1995) Oestradiol permeation across human skin, silastic and snake skin membranes: The effects of ethanol/water co-solvent systems. *Int J Pharm.* **116** 101-112.

Mempel M, Voelcker V, Kollisch G, Plank C, Rad R, Gerhard M, Schnopp C, Fraunberger P, Walli AK, Ring J, Abeck D & Ollert M (2003) Toll-like receptor expression in human keratinocytes: nuclear factor [kappa]B controlled gene activation by staphylococcus aureus is toll-like receptor 2 but not toll-like receptor 4 or platelet activating factor receptor dependent. *J Invest Dermatol.* **121** 1389-1396.

Michiue H, Tomizawa K, Wei FY, Matsushita M, Lu YF, Ichikawa T, Tamiya T, Date I

& Matsui H (2005) The NH2 terminus of influenza virus hemagglutinin-2 subunit peptides enhances the antitumor potency of polyarginine-mediated p53 protein transduction. *J Biol Chem.* **280** 8285-8289.

Mikszta JA, Alarcon JB, Brittingham JM, Sutter DE, Pettis RJ & Harvey NG (2002) Improved genetic immunization via micromechanical disruption of skin-barrier function and targeted epidermal delivery. *Nat Med.* **8** 415-419.

Milojevic S, Newton JM, Cummings JH, Gibson GR, Louise Botham R, Ring SG, Stockham M & Allwood MC (1996) Amylose as a coating for drug delivery to the colon: Preparation and in vitro evaluation using 5-aminosalicylic acid pellets. *J Controlled Release.* **38** 75-84.

Mitchell DJ, Steinman L, Kim DT, Fathman CG & Rothbard JB (2000) Polyarginine enters cells more efficiently than other polycationic homopolymers. *J Pept Res.* **56** 318-325.

Mitsui H, Inozume T, Kitamura R, Shibagaki N & Shimada S (2006) Polyarginine-mediated protein delivery to dendritic cells presents antigen more efficiently onto MHC class I and class II and elicits superior antitumor immunity. *J Invest Dermatol*. **126** 1804-1812.

Mologni L, Nielsen PE & Gambacorti-Passerini C (1999) In vitro transcriptional and translational block of the bcl-2 gene operated by peptide nucleic acid. *Biochem Biophys.Res Commun.* **264** 537-543.

Monia BP, Johnston JF, Ecker DJ, Zounes MA, Lima WF & Freier SM (1992) Selective inhibition of mutant Ha-ras mRNA expression by antisense oligonucleotides. *JBiol Chem.* **267** (1995)4-(1996)2.

Morishita M, Kamei N, Ehara J, Isowa K & Takayama K (2007) A novel approach using functional peptides for efficient intestinal absorption of insulin. *J Controlled Release.* **118** 177-184.

Morris MC, Depollier J, Mery J, Heitz F & Divita G (2001) A peptide carrier for the delivery of biologically active proteins into mammalian cells. *Nat Biotech.* **19** 1173-1176.

Moss GP, Dearden JC, Patel H & Cronin MT (2002)a Quantitative structure-permeability relationships (QSPRs) for percutaneous absorption. *Toxicol In Vitro.* **16** 299-317.

Moulton HM, Nelson MH, Hatlevig SA, Reddy MT & Iversen PL (2004) Cellular uptake of antisense morpholino oligomers conjugated to arginine-rich peptides. *Bioconjugate Chem.* **15** 290-299.

Mountjoy KG, Robbins LS, Mortrud MT & Cone RD (1992) The cloning of a family of genes that encode the melanocortin receptors. *Science* **257** 1248-1251.

Mouret S, Baudouin C, Charveron M, Favier A, Cadet J & Douki T (2006) Cyclobutane

pyrimidine dimers are predominant DNA lesions in whole human skin exposed to UVA radiation. *Proc Natl Acad Sci U.S.A.* **103** 13765-13770.

Moy P, Daikh Y, Pepinsky B, Thomas D, Fawell S & Barsoum J (1996) Tat-mediated protein delivery can facilitate MHC class I presentation of antigens. *Mol Biotechnol.* **6** 105-113.

Muratovska A & Eccles MR (2004) Conjugate for efficient delivery of short interfering RNA (siRNA) into mammalian cells. *FEBS Letters.* **558** 63-68.

Nakanishi A, Morita S, Iwashita H, Sagiya Y, Ashida Y, Shirafuji H, Fujisawa Y, Nishimura O & Fujino M (2001) Role of gob-5 in mucus overproduction and airway hyperresponsiveness in asthma. *Proc Natl Acad Sci U.S.A.* **98** 5175-5180.

Nemoto E, Takahashi H, Kobayashi D, Ueda H & Morimoto Y (2006) Effects of poly-L-arginine on the permeation of hydrophilic compounds through surface ocular tissues. *Biol Pharm Bull.* **29** 155-160.

Netzlaff F, Lehr CM, Wertz PW & Schaefer UF (2005) The human epidermis models EpiSkin(R), SkinEthic(R) and EpiDerm(R): An evaluation of morphology and their suitability for testing phototoxicity, irritancy, corrosivity, and substance transport. *Eur J Pharm Biopharm.* **60** 167-178.

Nielsen PE, Egholm M, Berg RH & Buchardt O (1991) Sequence-selective recognition of DNA by strand displacement with a thymine-substituted polyamide. *Science* **254** 1497-1500.

Nordlund JJ & Boissy ER (2001) The biology of melanocytes. In *the biology of the skin*, edn 1ST, pp 113-131. Eds KR Freinkel & TD Woody. The Parthenon Publishing Group.

Nugent SG, Kumar D, Rampton DS & Evans DF (2001) Intestinal luminal pH in inflammatory bowel disease: possible determinants and implications for therapy with aminosalicylates and other drugs. *Gut* **48** 571-577.

O'Callaghan CHRI & Barry PW (2000) How to choose delivery devices for asthma. *Arch Dis Child.* **82** 185-187.

Oehlke J, Scheller A, Wiesner B, Krause E, Beyermann M, Klauschenz E, Melzig M & Bienert M (1998) Cellular uptake of an [alpha]-helical amphipathic model peptide with the potential to deliver polar compounds into the cell interior non-endocytically. *Biochim Biophys Acta.* **1414** 127-139.

Ohtake K, Maeno T, Ueda H, Natsume H & Morimoto Y (2003) Poly-L-arginine predominantly increases the paracellular permeability of hydrophilic macromolecules across rabbit nasal epithelium in vitro. *Pharm Res.* **20** 153-160.

Oldenburg KR, Vo KT, Smith GA & Selick HE (1995) Iontophoretic delivery of oligonucleotides across full thickness hairless mouse skin. *J Pharm Sci.* **84** 915-921.

Orlow SJ & Brilliant MH (1999) The pink-eyed dilution locus controls the biogenesis of melanosomes and levels of melanosomal proteins in the eye. *Exp Eye Res.* **68** 147-154.

Park J, Ryu J, Jin LH, Bahn JH, Kim JA, Yoon CS, Kim DW, Han KH, Eum WS, Kwon HY, Kang TC, Won MH, Kang JH, Cho SW & Choi SY (2002) 9-polylysine protein transduction domain: enhanced penetration efficiency of superoxide dismutase into mammalian cells and skin. *Mol Cells.* **13** 202-208.

Peck D & Isacke CM (1998) Hyaluronan-dependent cell migration can be blocked by a CD44 cytoplasmic domain peptide containing a phosphoserine at position 325. *J Cell Sci.* **111** 1595-1601.

Peretto I, Sanchez-Martin RM, Wang XH, Ellard J, Mittoo S & Bradley M (2003) Cell penetrable peptoid carrier vehicles: synthesis and evaluation. *Chem Commun (Camb.).* 2312-2313.

Perez F, Joliot A, Bloch-Gallego E, Zahraoui A, Triller A & Prochiantz A (1992) Antennapedia homeobox as a signal for the cellular internalization and nuclear addressing of a small exogenous peptide. *J Cell Sci.* **102** 717-722.

Pfeifer A & Verma IM (2001) Gene Therapy: Promises and Problems. *Annu Rev Genomics Hum Genet.* **2** 177-211.

Pillay V & Fassihi R (1999) In vitro release modulation from crosslinked pellets for site-specific drug delivery to the gastrointestinal tract: I. Comparison of pH-responsive drug release and associated kinetics. *J Controlled Release.* **59** 229-242.

Pivarcsi A, Bodai L, Rethi B, Kenderessy-Szabo A, Koreck A, Szell M, Beer Z, Bata-Csorgoo Z, Magocsi M, Rajnavolgyi E, Dobozy A & Kemeny L (2003) Expression and function of Toll-like receptors 2 and 4 in human keratinocytes. *Int Immunol.* **15** 721-730.

Pomerantz SH & Ances IG (1975) Tyrosinase activity in human skin. Influence of race and age in newborns. *J Clin Invest.* **55** 1127-1131.

Ponec M, Boelsma E, Weerheim A, Mulder A, Bouwstra J & Mommaas M (2000) Lipid and ultrastructural characterization of reconstructed skin models. *Int J Pharm.* **203** 211-225.

Pooga M, Hallbrink M, Zorko M & Langel U (1998) Cell penetration by transportan. *FASEB J.* **12** 67-77.

Pooga M, Kut C, Kihlmark M, Hallbrink M, Fernaeus S, Raid R, Land T, Hallberg E, Bartfai T & Langel U (2001) Cellular translocation of proteins by transportan. *FASEB J.* **15** 1451-1453.

Pooga M, Soomets U, Hallbrink M, Valkna A, Saar K, Rezaei K, Kahl U, Hao JX, Xu XJ, Wiesenfeld-Hallin Z, Hokfelt T, Bartfai T & Langel U (1998) Cell penetrating PNA constructs regulate galanin receptor levels and modify pain transmission in vivo. *Nat*

Biotechnol. **16** 857-861.

Pouny Y, Rapaport D, Mor A, Nicolas P, Shai Y (1992) Interaction of antimicrobial dermaseptin and its fluorescently labeled analogues with phospholipid membranes. *Biochemistry*. **15** 12416-23

Prausnitz MR, Bose VG, Langer R & Weaver JC (1993) Electroporation of mammalian skin: a mechanism to enhance transdermal drug delivery. *Proc Natl Acad Sci U.S.A.* **90** 10504-10508.

Prausnitz MR & Noonan JS (1998) Permeability of cornea, sclera, and conjunctiva: a literature analysis for drug delivery to the eye. *J Pharm Sci.* **87** 1479-1488.

Prausnitz MR (2004) Microneedles for transdermal drug delivery. *Adv Drug Deliv Rev.* **56** 581-587.

Prota G & Thomson RH (1976) Melanin pigmentation in mammals. *Endeavour* **35** 32-38.

Raap U, Brzoska T, Sohl S, Path G, Emmel J, Herz U, Braun A, Luger T & Renz H (2003) {alpha}-melanocyte-stimulating hormone inhibits allergic airway inflammation. *J Immunol.* **171** 353-359.

Rajora N, Boccoli G, Catania A & Lipton JM (1997) alpha-MSH modulates experimental inflammatory bowel disease. *Peptides* **18** 381-385.

Ranade VV (1991) Drug delivery systems. 6. Transdermal drug delivery. *J Clin Pharmacol.* **31** 401-418.

Rao NM & Gopal V (2006) Cell biological and biophysical aspects of lipid-mediated gene delivery. *Biosci Rep.* **26** 301-324.

Robbins PB, Oliver SF, Sheu SM, Goodnough JB, Wender P & Khavari PA (2002) Peptide delivery to tissues via reversibly linked protein transduction sequences. *Biotechniques* **33** 190-2, 194.

Robinson SJ, Healy E (2002) Human melanocortin 1 receptor (MC1R) gene variants alter melanoma cell growth and adhesion to extracellular matrix. *Oncogene.* **14;21(52)** 8037-46

Roselli-Rehfuss L, Mountjoy KG, Robbins LS, Mortrud MT, Low MJ, Tatro JB, Entwistle ML, Simerly RB & Cone RD (1993) Identification of a receptor for gamma melanotropin and other proopiomelanocortin peptides in the hypothalamus and limbic system. *Proc Natl Acad Sci U.S.A.* **90** 8856-8860.

Rosen CF (1999) Photoprotection. *Seminars in Cutaneous Medicine and Surgery* **18** 307-314.

Ross MF & Murphy MP (2004) Cell-penetrating peptides are excluded from the

mitochondrial matrix. *Biochem Soc Trans.* **32** 1072-1074.

Rothbard JB, Garlington S, Lin Q, Kirschberg T, Kreider E, McGrane PL, Wender PA & Khavari PA (2000) Conjugation of arginine oligomers to cyclosporin A facilitates topical delivery and inhibition of inflammation. *Nat Med.* **6** 1253-1257.

Rubinstein A, Nakar D & Sintov A (1992) Colonic drug delivery: enhanced release of indomethacin from cross-linked chondroitin matrix in rat cecal content. *Pharm Res.* **9** 276-278.

Rusnati M, Taraboletti G, Urbinati C, Tulipano G, Giuliani R, Molinari-Tosatti MP, Sennino B, Giacca M, Tyagi M, Albini A, Noonan D, Giavazzi R & Presta M (2000) Thrombospondin-1/HIV-1 tat protein interaction: modulation of the biological activity of extracellular Tat. *FASEB J.* **14** 1917-1930.

Ryser HJ, Drummond I & Shen WC 1982 The cellular uptake of horseradish peroxidase and its poly(lysine) conjugate by cultured fibroblasts is qualitatively similar despite a 900-fold difference in rate. *J Cell Physiol.* **113** 167-178.

Ryser HJ & Shen WC (1978) Conjugation of methotrexate to poly(L-lysine) increases drug transport and overcomes drug resistance in cultured cells. *Proc Natl Acad Sci U.S.A.* **75** 3867-3870.

Ryser HJ & Shen WC (1980) Conjugation of methotrexate to poly (L-lysine) as a potential way to overcome drug resistance. *Cancer* **45** 1207-1211.

Ryser HJP (1967) Studies on protein uptake by isolated tumor cells: III. Apparent stimulations due to pH, hypertonicity, polycations, or dehydration and their relation to the enhanced penetration of infectious nucleic acids. *J Cell Biol.* **32** 737-750.

Sakamoto T, Miyazaki E, Aramaki Y, Arima H, Takahashi M, Kato Y, Koga M & Tsuchiya S (2004) Improvement of dermatitis by iontophoretically delivered antisense oligonucleotides for interleukin-10 in NC/Nga mice. *Gene Ther.* **11** 317-324.

Salmon JK, Armstrong CA & Ansel JC (1994) The skin as an immune organ. *West J Med.* **160** 146-152.

Sauder DN, Dinarello CA & Morhenn VB (1984) Langerhans cell production of interleukin-1. *J Invest Dermatol.* **82** 605-607.

Sawyer TK, Sanfilippo PJ, Hruby VJ, Engel MH, Heward CB, Burnett JB & Hadley ME (1980) 4-Norleucine, 7-D-phenylalanine-alpha-melanocyte-stimulating hormone: a highly potent alpha-melanotropin with ultralong biological activity. *Proc Natl Acad Sci U.S.A.* **77** 5754-5758.

Scala G, Ruocco MR, Ambrosino C, Mallardo M, Giordano V, Baldassarre F, Dragonetti E, Quinto I & Venuta S (1994) The expression of the interleukin 6 gene is induced by the human immunodeficiency virus 1 TAT protein. *J Exp Med.* **179** 961-971.

Scheuplein RJ (1967) Mechanism of percutaneous absorption. II. Transient diffusion and the relative importance of various routes of skin penetration. *J Invest Dermatol.* **48** 79-88.

Stechschulte SU, Joussen AM, von Recum HA, Poulaki V, Moromizato Y, Yuan J, D'Amato RJ, Kuo C, Adamis AP (2001) Rapid ocular angiogenic control via naked DNA delivery into cornea. *Invest Opthalmol Vis Sci* **42** 1975-79.

Schlagbauer-Wadl H, Klosner G, Heere-Ress E, Waltering S, Moll I, Wolff K, Pehamberger H, Jansen B (2000) Bcl-2 antisense oligonucleotides (G3139) inhibit Merkel cell carcinoma growth in SCID mice. *J Invest Dermatol.* **114(4)** 725-30.

Schmook FP, Meingassner JG & Billich A (2001) Comparison of human skin or epidermis models with human and animal skin in in-vitro percutaneous absorption. *Int J Pharm.* **215** 51-56.

Schutze-Redelmeier MP, Kong S, Bally MB & Dutz JP (2004) Antennapedia transduction sequence promotes anti tumour immunity to epicutaneously administered CTL epitopes. *Vaccine* **22** 1985-(1991).

Schwarze SR, Ho A, Vocero-Akbani A & Dowdy SF (1999) In Vivo Protein Transduction: Delivery of a Biologically Active Protein into the Mouse. *Science* **285** 1569-1572.

Scott RC., Walker M., & Dugard PH (1986) A comparaison of the in vitro permeability properties of human and some laboratory animal skins. *Int J Cosmet Sci***. 8** 189-194.

Seamon KB, Padgett W & Daly JW (1981) Forskolin: unique diterpene activator of adenylate cyclase in membranes and in intact cells. *Proc Natl Acad Sci U.S.A.* **78** 3363-3367.

Seiji M, Fitzpatrick TB, Simpson RT & Birbeck MS (1963) Chemical composition and terminology of specialized organelles (melanosomes and melanin granules) in mammalian melanocytes. *Nature* **197** 1082-1084.

Sekkat N, Kalia YN & Guy RH (2002) Biophysical study of porcine ear skin in vitro and its comparison to human skin in vivo. *J Pharm Sci.* **91** 2376-2381.

Setlow RB, Grist E, Thompson K & Woodhead AD (1993) Wavelengths effective in induction of malignant melanoma. *Proc Natl Acad Sci U.S.A.* **90** 6666-6670.

Shahana S, Kampf C & Roomans GM (2002) Effects of the cationic protein poly-L-arginine on airway epithelial cells in vitro. *Mediators Inflamm.* **11** 141-148.

Shammas MA, Simmons CG, Corey DR & Shmookler Reis RJ (1999) Telomerase inhibition by peptide nucleic acids reverses 'immortality' of transformed human cells. *Oncogene* **18** 6191-6200.

Shen WC & Ryser HJ (1978) Conjugation of poly-L-lysine to albumin and horseradish

peroxidase: a novel method of enhancing the cellular uptake of proteins. *Proc Natl Acad Sci U.S.A.* **75** 1872-1876.

Shen WC & Ryser HJ (1979) Poly (L-lysine) and poly (D-lysine) conjugates of methotrexate: different inhibitory effect on drug resistant cells. *Mol Pharmacol.* **16** 614-622.

Shibagaki N & Udey MC (2003) Dendritic cells transduced with TAT protein transduction domain-containing tyrosinase-related protein 2 vaccinate against murine melanoma. *Eur J Immunol.* **33** 850-860.

Siccardi D, Turner JR & Mrsny RJ (2005) Regulation of intestinal epithelial function: a link between opportunities for macromolecular drug delivery and inflammatory bowel disease. *Adv Drug Deliv Rev.* **57** 219-235.

Solano F, Briganti S, Picardo M & Ghanem G (2006) Hypopigmenting agents: an updated review on biological, chemical and clinical aspects. *Pigment Cell Res.* **19** 550-571.

Song PI, Park YM, Abraham T, Harten B, Zivony A, Neparidze N, Armstrong CA & Ansel JC (2002) Human keratinocytes express functional CD14 and toll-like receptor 4. *J Invest Dermatol.* **119** 424-432.

Sosnowski BA, Gonzalez AM, Chandler LA, Buechler YJ, Pierce GF & Baird A (1996) Targeting DNA to cells with basic fibroblast growth factor (FGF2). *J Biol Chem.* **271** 33647-33653.

Stenberg P, Luthman K & Artursson P (2000) Virtual screening of intestinal drug permeability. *J Control Release.* **65** 231-243.

Stephenson ML & Zamecnik PC (1978) Inhibition of Rous sarcoma viral RNA translation by a specific oligodeoxyribonucleotide. *Proc Natl Acad Sci U.S.A.* **75** 285-288.

Stolzenberger S, Haake M & Duschl A (2001) Specific inhibition of interleukin-4-dependent Stat6 activation by an intracellularly delivered peptide. *Eur J Biochem.* **268** 4809-4814.

Sulzberger MB & Witten VH (1952) The effect of topically applied compound F in selected dermatoses. *J Invest Dermatol.* **19** 101-102.

Sun L, Fuselier JA, Murphy WA & Coy DH (2002) Antisense peptide nucleic acids conjugated to somatostatin analogs and targeted at the n-myc oncogene display enhanced cytotoxity to human neuroblastoma IMR32 cells expressing somatostatin receptors. *Peptides* **23** 1557-1565.

Sung KC, Fang JY, Wang JJ & Hu OY-P (2003) Transdermal delivery of nalbuphine and its prodrugs by electroporation. *Eur J Pharm Sci.* **18** 63-70.

Suzuki I, Cone RD, Im S, Nordlund J, Abdel-Malek ZA (1996) Binding of melanotropic hormones to the melanocortin receptor MC1R on human melanocytes stimulates proliferation and melanogenesis. *Endocrinology* **137** 1627-33.

Suzuki T, Futaki S, Niwa M, Tanaka S, Ueda K & Sugiura Y (2002) Possible existence of common internalization mechanisms among arginine-rich peptides. *J Biol Chem.* **277** 2437-2443.

Szabo G (1954) The number of melanocytes in human epidermis. *Br Med J.* **1** 1016-1017.

Szabo G, Gerald AB, Pathak MA & Fitzpatrick TB (1969) Racial differences in the fate of melanosomes in human epidermis. *Nature* **222** 1081-1082.

Tadokoro T, Kobayashi N, Zmudzka BZ, Ito S, Wakamatsu K, Yamaguchi Y, Korossy KS, Miller SA, Beer JZ & Hearing VJ (2003) UV-induced DNA damage and melanin content in human skin differing in racial/ethnic origin. *FASEB J.* **17(9)** 1177-9.

Takahashi K, Saishin Y, Saishin Y, Silva RL, Oshima Y, Oshima S, Melia M, Paszkiet B, Zerby D, Kadan MJ, Liau G, Kaleko M, Connelly S, Luo T & Campochiaro PA (2003) Intraocular expression of endostatin reduces VEGF-induced retinal vascular permeability, neovascularization, and retinal detachment. *FASEB J.* 02-0824fje.

Tamburic S and Craig Q.M.D (1996) The use of bioadhesive polymers as a means of improve drug delivery. In chemical aspects of drug delivery systems, edn 1st, pp 11-40. Eds D.R.Karsa & R.A.Stephenson. Royal Society of Chemistry.

Tamilvanan S, Benita S (2004) The potential of lipid emulsion for ocular delivery of lipophilic drugs. *Eur J Pharm Biopharm.* **58(2)**:357-68.

Temsamani J, Tang JY & Agrawal S (1992) Capped oligodeoxynucleotide phosphorothioates. pharmacokinetics and stability in mice. *Ann N Y Acad Sci.* **660** 318-320.

Thody AJ, Higgins EM, Wakamatsu K, Ito S, Burchill SA & Marks JM (1991) Pheomelanin as well as eumelanin is present in human epidermis. *J Invest Dermatol.* **97** 340-344.

Thoren PEG, Persson D, Isakson P, Goksor M, Onfelt A & Norden B (2003) Uptake of analogs of penetratin, Tat (48-60) and oligoarginine in live cells. *Biochem Biophys Res Comm.* **307** 100-107.

Tozaki H, Komoike J, Tada C, Maruyama T, Terabe A, Suzuki T, Yamamoto A & Muranishi S (1997) Chitosan capsules for colon-specific drug delivery: improvement of insulin absorption from the rat colon. *J Pharm Sci.* **86** 1016-1021.

Trehin R, Nielsen HM, Jahnke HG, Krauss U, Beck-Sickinger AG & Merkle HP (2004) Metabolic cleavage of cell-penetrating peptides in contact with epithelial models: human calcitonin (hCT)-derived peptides, Tat(47-57) and penetratin(43-58). *Biochem J.* **382**

945-956.

Tsai JC, Guy RH, Thornfeldt CR, Gao WN, Feingold KR & Elias PM (1996) Metabolic approaches to enhance transdermal drug delivery. 1. Effect of lipid synthesis inhibitors. *J Pharm Sci.* **85** 643-648.

Turner BJ, Cheah IK, Macfarlane KJ, Lopes EC, Petratos S, Langford SJ, Cheema SS (2003) Antisense peptide nucleic acid-mediated knockdown of the p75 neurotrophin receptor delays motor neuron disease in mutant SOD1 transgenic mice. *J Neurochem* 87(3) 752-63

Tyler BM, Jansen K, McCormick DJ, Douglas CL, Boules M, Stewart JA, Zhao L, Lacy B, Cusack B, Fauq A & Richelson E (1999) Peptide nucleic acids targeted to the neurotensin receptor and administered i.p. cross the blood-brain barrier and specifically reduce gene expression. *Proc Natl Acad Sci U.S.A.* **96** 7053-7058.

Tyler BM, McCormick DJ, Hoshall CV, Douglas CL, Jansen K, Lacy BW, Cusack B & Richelson E (1998) Specific gene blockade shows that peptide nucleic acids readily enter neuronal cells in vivo. *FEBS Letters* **421** 280-284.

Uchenna Agu R, Ikechukwu Ugwoke M, Armand M, Kinget R & Verbeke N (2001) The lung as a route for systemic delivery of therapeutic proteins and peptides. *Respiratory Research.* **2** 198-209.

Urtti A (2006) Challenges and obstacles of ocular pharmacokinetics and drug delivery. *Adv Drug Deliv Rev.* **58** 1131-1135.

Valladeau J & Saeland S (2005) Cutaneous dendritic cells. *Semin Immunol.* **17** 273-283.

Valverde P, Healy E, Jackson I, Rees JL & Thody AJ (1995) Variants of the melanocyte-stimulating hormone receptor gene are associated with red hair and fair skin in humans. *Nat Genet.* **11** 328-330.

Vamvakopoulos NC, Rojas K, Overhauser J, Durkin AS, Nierman WC & Chrousos GP (1993) Mapping the human melanocortin 2 receptor (Adrenocorticotropic hormone receptor; ACTHR) gene (MC2R) to the small arm of chromosome 18 (18p11.21-pter). *Genomics* **18** 454-455.

Virador VM, Muller J, Wu X, Abdel-malek ZA, Yu ZX, Ferrans VJ, Kobayashi N, Wakamatsu K, Ito S, Hammer JA & Hearing VJ (2002) Influence of {alpha}-melanocyte-stimulating hormone and ultraviolet radiation on the transfer of melanosomes to keratinocytes. *The FASEB J.* **16** 105-107.

Vives E (2003) Cellular uptake [correction of utake] of the Tat peptide: an endocytosis mechanism following ionic interactions. *J Mol Recognit.* **16** 265-271.

Vives E, Brodin P & Lebleu B (1997) A truncated HIV-1 Tat protein basic domain rapidly translocates through the plasma membrane and accumulates in the cell nucleus. *J*

Biol Chem. **272** 16010-16017.

Vlassov VV, Karamyshev VN & Yakubov LA (1993) Penetration of oligonucleotides into mouse organism through mucosa and skin. *FEBS Letters* **327** 271-274.

Wagner H, Kostka KH, Lehr CM & Schaefer UF (2001) Interrelation of permeation and penetration parameters obtained from in vitro experiments with human skin and skin equivalents. *J Controlled Release.* **75** 283-295.

Wender PA, Mitchell DJ, Pattabiraman K, Pelkey ET, Steinman L & Rothbard JB (2000) The design, synthesis, and evaluation of molecules that enable or enhance cellular uptake: Peptoid molecular transporters. *Proc Natl Acad Sci U.S.A.* **97** 13003-13008.

Wertz PW & Downing DT (1982) Glycolipids in mammalian epidermis: structure and function in the water barrier. *Science* **217** 1261-1262.

Westendorp MO, Li-Weber M, Frank RW & Krammer PH (1994) Human immunodeficiency virus type 1 Tat upregulates interleukin-2 secretion in activated T cells. *J Virol.* **68** 4177-4185.

Westendorp MO, Shatrov VA, Schulze-Osthoff K, Frank R, Kraft M, Los M, Krammer PH, Droge W & Lehmann V (1995) HIV-1 Tat potentiates TNF-induced NF-kappa B activation and cytotoxicity by altering the cellular redox state. *EMBO J.* **14** 546-554.

White PJ, Fogarty RD, Liepe IJ, Delaney PM, Werther GA, Wraight CJ (1999) Live confocal microscopy of oligonucleotide uptake by keratinocytes in human skin grafts on nude mice. *J Invest Dermatol.* **112(6)** 887-92

White PJ, Gray AC, Fogarty RD, Sinclair RD, Thumiger SP, Werther GA & Wraight CJ (2002) C-5 Propyne-modified oligonucleotides penetrate the epidermis in psoriatic and not normal human skin after topical application. *J Invest Dermatol.* **118** 1003-1007.

White PJ, Atley LM, Wraight CJ (2004) Antisense oligonucleotide treatments for psoriasis. *Expert Opin Biol Ther.* **4(1)**:75-81

Williams AC & Barry BW (2004) Penetration enhancers. *Adv Drug Deliv Rev.* **56** 603-618.

Wilson BD, Ollmann MM, Kang L, Stoffel M, Bell GI & Barsh GS (1995) Structure and function of ASP, the human homolog of the mouse agouti gene. *Hum Mol Genet.* **4** 223-230.

Wirtz S & Neurath MF (2003) Gene transfer approaches for the treatment of inflammatory bowel disease. *Gene Ther.* **10** 854-860.

Wraight CJ, White PJ, McKean SC, Fogarty RD, Venables DJ, Liepe IJ, Edmondson SR, Werther GA (2000) Reversal of epidermal hyperproliferation in psoriasis by insulin-like growth factor I receptor antisense oligonucleotides. *Nat Biotechnol.* **18(5)** 521-6

Yang L, Chu JS & Fix JA (2002) Colon-specific drug delivery: new approaches and in vitro/in vivo evaluation. *Int J Pharm.* **235** 1-15.

Yarosh D, Klein J, O'Connor A, Hawk J, Rafal E & Wolf P (2001) Effect of topically applied T4 endonuclease V in liposomes on skin cancer in xeroderma pigmentosum: a randomised study. *The Lancet* **357** 926-929.

Yokoi S, Yasui K, Saito-Ohara F, Koshikawa K, Iizasa T, Fujisawa T, Terasaki T, Horii A, Takahashi T, Hirohashi S & Inazawa J (2002) A novel target gene, SKP2, within the 5p13 amplicon that is frequently detected in small cell lung cancers. *Am J Pathol.* **161** 207-216.

Yu RZ, Geary RS, Leeds JM, Watanabe T, Moore M, Fitchett J, Matson J, Burckin T, Templin MV & Levin AA (2001) Comparison of pharmacokinetics and tissue disposition of an antisense phosphorothioate oligonucleotide targeting human Ha-ras mRNA in mouse and monkey. *J Pharm Sci.* **90** 182-193.

Yu XY, Schofield BH, Croxton T, Takahashi N, Gabrielson EW & Spannhake EW (1994) Physiologic modulation of bronchial epithelial cell barrier function by polycationic exposure. *Am J Respir Cell Mol Biol.* **11** 188-198.

Zauli G, Davis BR, Re MC, Visani G, Furlini G & La Placa M (1992) tat protein stimulates production of transforming growth factor-beta 1 by marrow macrophages: a potential mechanism for human immunodeficiency virus-1-induced hematopoietic suppression. *Blood* **80** 3036-3043.

Zauli G, Furlini G, Re MC, Milani D, Capitani S & La Placa M (1993) Human immunodeficiency virus type 1 (HIV-1) tat-protein stimulates the production of interleukin-6 (IL-6) by peripheral blood monocytes. *New Microbiol.* **16** 115-120.

Zhu L, Schwegler-Berry D, Castranova V & He P (2004) Internalization of caveolin-1 scaffolding domain facilitated by Antennapedia homeodomain attenuates PAF-induced increase in microvessel permeability. *Am J Physiol Heart Circ Physiol.* **286** H195-H201.